

INFORMATION TO USERS

This manuscript has been reproduced from the microfilm master. UMI films the text directly from the original or copy submitted. Thus, some thesis and dissertation copies are in typewriter face, while others may be from any type of computer printer.

The quality of this reproduction is dependent upon the quality of the copy submitted. Broken or indistinct print, colored or poor quality illustrations and photographs, print bleedthrough, substandard margins, and improper alignment can adversely affect reproduction.

In the unlikely event that the author did not send UMI a complete manuscript and there are missing pages, these will be noted. Also, if unauthorized copyright material had to be removed, a note will indicate the deletion.

Oversize materials (e.g., maps, drawings, charts) are reproduced by sectioning the original, beginning at the upper left-hand corner and continuing from left to right in equal sections with small overlaps.

ProQuest Information and Learning
300 North Zeeb Road, Ann Arbor, MI 48106-1346 USA
800-521-0600

UMI[®]

UNIVERSITY OF ALBERTA

**Sedimentology, Ichnology and Stratigraphy
of the Lowermost Cretaceous,
Liard Basin, Canada**

by

Jason Heinz Frank

A thesis submitted to the Faculty of Graduate Studies and Research in partial fulfillment
of the requirements for the degree of Master of Science.

Department of Earth and Atmospheric Sciences

Edmonton, Alberta

Fall 2002



National Library
of Canada

Acquisitions and
Bibliographic Services

395 Wellington Street
Ottawa ON K1A 0N4
Canada

Bibliothèque nationale
du Canada

Acquisitions et
services bibliographiques

395, rue Wellington
Ottawa ON K1A 0N4
Canada

Your file Votre référence

Our file Notre référence

The author has granted a non-exclusive licence allowing the National Library of Canada to reproduce, loan, distribute or sell copies of this thesis in microform, paper or electronic formats.

The author retains ownership of the copyright in this thesis. Neither the thesis nor substantial extracts from it may be printed or otherwise reproduced without the author's permission.

L'auteur a accordé une licence non exclusive permettant à la Bibliothèque nationale du Canada de reproduire, prêter, distribuer ou vendre des copies de cette thèse sous la forme de microfiche/film, de reproduction sur papier ou sur format électronique.

L'auteur conserve la propriété du droit d'auteur qui protège cette thèse. Ni la thèse ni des extraits substantiels de celle-ci ne doivent être imprimés ou autrement reproduits sans son autorisation.

0-612-81395-9

UNIVERSITY OF ALBERTA

LIBRARY RELEASE FORM

NAME OF AUTHOR: **Jason Heinz Frank**

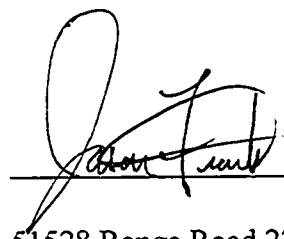
TITLE OF THESIS: **Sedimentology, Ichnology and Stratigraphy of the
Lowermost Cretaceous, Liard Basin, Canada**

DEGREE: **Master of Science**

YEAR THIS DEGREE GRANTED: **2002**

Permission is hereby granted to the University of Alberta Library to reproduce single copies of this thesis and to lend or sell such copies for private, scholarly or scientific research purposes only.

The author reserves all other publication and other rights in association with the copyright in the thesis, and except as herein before provided, neither the thesis nor any substantial portion thereof may be printed or otherwise reproduced in any material form whatever without the author's prior written permission.



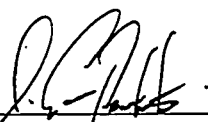
51528 Range Road 221
Sherwood Park, Alberta
T8E 1H1
Canada

August 31st, 2002

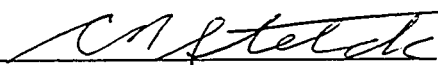
UNIVERSITY OF ALBERTA

FACULTY OF GRADUATE STUDIES AND RESEARCH

The undersigned certify that they have read, and recommend to the Faculty of Graduate studies and Research for acceptance, a thesis entitled **Sedimentology, Ichnology and Stratigraphy of the Lowermost Cretaceous, Liard Basin, Canada** submitted by **Jason Heinz Frank** in partial fulfillment of the requirements for the degree of Master of Science



Dr. S.G. Pemberton (Supervisor)



Dr. C.R. Stelck (Committee Member)



Dr. D.A. Craig (Committee Member)

Date: Sept. 20, 2002

"Do not burn yourselves out. Be as I am – a reluctant enthusiast...a part time crusader, a half-hearted fanatic. Save the other half of yourselves and your lives for pleasure and adventure. It is not enough to fight for the land; it is even more important to enjoy it. While you can. While it is still there. So get out there and hunt and fish and mess around with your friends, ramble out yonder and explore the forests, encounter the grizzly, climb the mountains, bag the peaks. Run the rivers, breathe deep of that yet sweet and lucid air, sit quietly for a while and contemplate the precious stillness, that lovely, mysterious and awesome space. Enjoy yourselves, keep your brain in your head and your head firmly attached to the body, the body active and alive, and I promise you this much: I promise you this one sweet victory over our enemies, over those deskbound people with their hearts in a safe deposit box and their eyes hypnotized by desk calculators. I promise you this: You will outlive the bastards!"

- Edward Abbey

On first examining a new district, nothing can appear more hopeless than the chaos of rocks; but by recording the stratification and nature of the rocks and fossils at many points, always reasoning and predicting what will be found elsewhere, light soon begins to dawn on the district, and the structure of the whole becomes more or less intelligible.

- Charles Darwin

ABSTRACT

The Lowermost Cretaceous within the Liard Basin of northeastern British Columbia has been the target of recent exploration activities. The Lower Cretaceous play has centered around the Maxhamish Lake area, where recoverable reserves are estimated at 400 Bcf. Core and outcrop descriptions have helped determine depositional environments for both the Chinkeh and lowermost member of the Scatter Formation, the Bulwell Member. Sedimentology, Ichnology and stratigraphic analysis has been used to reconstruct depositional environments, predict reservoir distributions, and determine stratigraphic relationships for the Lowermost Cretaceous of the Liard Basin.

At Maxhamish Lake, the reservoir consists of amalgamated storm deposits redistributed parallel to the antecedent topographic high of the Bovie fault scarp. These sediments prograded from the west, and consist of quartzose, glauconite-rich, fine to medium-grained sandstones. Their mineralogy, distribution, and interpreted depositional environment match that of the lowermost Bulwell Member of the Scatter Formation as seen in outcrop exposures.

The quartzose sandstones of the Chinkeh Formation prograded from the North into the Liard Basin. While also highly wave reworked, Chinkeh sandstones originated from point sources entering the basin from both the East and the West. These sandstones became reworked, and distributed along northwest – southeast trending shorelines, that prograded south, however not extending to current day production at Maxhamish Lake.

Acknowledgements

There are a number of people that I would like to thank for helping along the way in completing this thesis. First and foremost I would like to thank George Pemberton. Not only has he been an inspirational figure in my life, but he also believed in me when others (i.e. the University) didn't. I remember talks in your office, where most ideas that I would present were always met with encouragement, no matter how crazy they sounded. Besides giving lessons in Geology, he also gave many life lessons and stories, both I hope to remember always. The environment he helped foster in the Ichnology Research Group was an experience that I will never forget. He brought together people with such passion for Geology and life (in my opinion they go hand-in-hand), that at times you could feel the energy coming from the Lab (if not hear it). Thank-you George!

This project could not have been completed without the initiation from Kathy Aulstead at AEC-West. She somehow picked my name from a stack of resumes, and offered me work after my B.Sc. degree. Near the end of the summer, when I told her my intentions to return to school, and the desire for a fieldwork based project, she initiated the request for approval and funding. Her support was also very much appreciated during CSPG core presentations and talks. Thank-you Kathy for your support throughout this project.

I also had the pleasure to work with Mark Edmonds and Doug Clenchy (AEC-West). Mark accompanied me in the field, and due to bad weather got stuck out a couple of days longer than expected. Thanks for your help at Six Bald Point, and for the other lessons as well like, "pace yourself son, pace your self." Doug Clenchy arranged a second field season into some of the most beautiful country ever imagined – thank-you.

Now for my two field partners Murray Gingras and Jason French. Murray, I can't say enough about you as a friend or as a Geologist. Both helped me out tremendously along the way. Your generosity, kindness, and your overall wonder and excitement for the world around you are qualities that I attempt to emulate in my own life. Thank-you for all your help and guidance! Jason French...they broke the mold with you my friend. I think you're the only guy I know who would pass up the last hot shower in weeks, before heading into the field. Thanks for keeping my sanity in the field, I know Beaver Crow Mountain, and Karma Creek would not have been the same without you.

Dr Stelck, your love for geology has been an inspiration. I love listening to your stories of the 'good old days,' and hope that I have a quarter of the enthusiasm in my work that you show in yours. It was an honor working in your backyard – just wished I found a few more fossils.

The Lab Rats...(in no particular order): Erin Kimball (thanks for the wolf stories at the P.O.), Glenn 'Jäger-Meister' Schmidt, Steve Hubbard (all you need is 3 chords and the truth), Jason Lavigne (for a tough guy, you sure to have a big heart - thanks for keeping me on track), Eric Hanson (thanks for the ideas, edits, and jam sessions), Sue Fleming (thanks for calling my mother, and grandmother), Tom Saunders (you're ideas and creativity inspire everyone around you – I'm glad that I could be part of it. Thanks for the suggestions and ideas), J.P. Zonnefeld (thanks for the drafting material), Carly Barnett (your love and support throughout this whole ordeal have been wonderful – thanks for always believing in me), Chad Harris (nice work two-tone), Jeff Reinprecht (bought the ticket...take the ride), and Tim Loehr (thanks for all your help folding this damn thing!).

My field school partners Ian (Slim) Armitage, and Paul (Sippy) Glombick. Who would have ever guessed the events that would be in store for us, all starting with that fateful trip to Jasper? Thanks for all the good times, and friendship along the way.

Finally my mother and father. I couldn't have asked for a more wonderful set of parents. Their love and support are never-ending. Mom thanks for the creativity and wonderful home cooked meals when I came home. Dad thanks for coming up to the field with me to see what I do, and for asking (although I hated it at the time), "How is your thesis coming?"

Table of Contents

CHAPTER ONE: Introduction

Introductory Remarks	1
Previous Work	1
Cretaceous Stratigraphy of the Liard Basin	3
Paleogeography and Tectonic Setting	5
Study Area and Research Rationale	7
Thesis Layout	11
References	11

CHAPTER TWO: Subsurface Descriptions and Interpretations

Introduction	14
Regional Geology and Stratigraphy	14
The Bovie Fault	16
Reservoir Geology	17
Database and Methodology	19
Cross Sections	19
Maps	22
Facies Descriptions	29
Introduction and Overview	29
Facies A: Triassic Strata	32
Description	32
Interpretation	32
Facies B: Chert-pebble Conglomerate	39
Description	39
Interpretation	39
Facies C: Laminated Sands and Bioturbated Shales	41
Description	41
Interpretation	43
Facies D: Well sorted Quartzose Sands	44
Description	44
Interpretation	47
Facies E: Burrowed Silts with Abundant Wood Fragments	48

<i>Description</i> _____	48
<i>Interpretation</i> _____	51
Facies F: Glauconite-rich, Rooted and Burrowed Siltstone_____	52
<i>Description</i> _____	52
<i>Interpretation</i> _____	52
Facies G: Dark, Fissile Shales_____	54
<i>Description</i> _____	54
<i>Interpretation</i> _____	56
Summary and Discussion_____	56
References_____	61

CHAPTER THREE: Outcrop Descriptions and Interpretations

Introduction_____	65
Methodology_____	67
Outcrop Descriptions_____	68
Introduction_____	68
Lower Cretaceous Chinkeh Formation_____	70
Murky Creek (L18)_____	70
Burnt Timber (L19)_____	72
Six Bald Point (L5)_____	72
Sully Creek (L33)_____	76
Otter Slide (L4)_____	76
Slip Rock Creek (L14)_____	76
Tika Creek (L6)_____	76
Lower Cretaceous Scatter Formation_____	80
Kotaneelee River (L8)_____	80
Sully Creek (L1)_____	80
Facies Descriptions_____	83
Facies A (Permian Strata)_____	83
<i>Description</i> _____	83
<i>Interpretation</i> _____	87
Facies B (Chert pebble to cobble conglomerate)_____	87
<i>Description</i> _____	87

<i>Interpretation</i>	90
Facies C (Laterally continuous shale beds)	91
<i>Description</i>	91
<i>Interpretation</i>	93
Facies D (Large wavelength bedform sandstones)	93
<i>Description</i>	93
<i>Interpretation</i>	100
Facies E (Interbedded sharp based sandstones and bioturbated shales)	103
<i>Description</i>	103
<i>Interpretation</i>	103
Facies F (Carbonaceous-rich bioturbated sandstones)	104
<i>Description</i>	104
<i>Interpretation</i>	105
Facies G (Vertical burrows filled with glauconite-rich sandstones)	107
<i>Description</i>	107
<i>Interpretation</i>	107
Facies H (Wavy to lenticular sandstones capped by shell material)	111
<i>Description</i>	111
<i>Interpretation</i>	111
Facies I (Thinly bedded dark fissile shales)	114
<i>Description</i>	114
<i>Interpretation</i>	114
Relationship between the Chinkeh and Scatter Formations	115
Murky Creek Channel Section	117
<i>Description</i>	117
<i>Interpretation</i>	120
Depositional Synopsis	121
<i>Discussion</i>	121
References	123

CHAPTER FOUR: Depositional relationships of the Lower Cretaceous Scatter and Chinkeh Formations

Introduction_____	126
Objectives_____	126
Outcrop thickness and distribution of the lowermost member within the Scatter Formation_____	126
Definition_____	126
Distribution and thickness_____	128
Mineralogy_____	129
Depositional Model for the Lower Cretaceous Bulwell Member within the Liard Basin_____	133
Introduction_____	133
Regional Cross-sections_____	133
Outcrop Descriptions_____	136
Summary and Conclusions_____	138
References_____	141

CHAPTER FIVE: Conclusions

Conclusions_____	142
------------------	-----

APPENDIX I: Scintillometer Data_____	143
---	------------

List of Tables

CHAPTER TWO: Subsurface Descriptions and Interpretations	Page
Table II-1. Table of facies identified within the subsurface_____	31
CHAPTER THREE: Outcrop Descriptions and Interpretations	
Table III-1. Legend of symbols used within outcrop lithologs and summaries_____	69
Table III-2. Table of facies identified in Lower Cretaceous outcrop exposures within the Liard Basin_____	85

List of Figures

CHAPTER ONE: Introduction	Page
Figure I-1. Location of the Liard Basin_____	2
Figure I-2. Lower Cretaceous Stratigraphy of the Liard Basin_____	4
Figure I-3. Paleogeography and Foredeep location during the Lower Cretaceous_____	6
Figure I-4. Geological Elements within the Study Area_____	8
Figure I-5. Nomenclature scheme_____	10
CHAPTER TWO: Subsurface Descriptions and Interpretations	
Figure II-1. Regional base map_____	15
Figure II-2. Corresponding well logs and core plug analysis_____	18
Figure II-3. Dip oriented cross-section_____	20
Figure II-4. Strike oriented cross-section_____	21
Figure II-5. Top of Lower Cretaceous elevation map_____	24
Figure II-6. Total Lower Cretaceous isopach map_____	26
Figure II-7. Net pay map_____	28
Figure II-8. Well locations within the study area_____	33
Figure II-9. Legend of symbols used within litholog descriptions_____	34
Figure II-10. Gamma-ray and core descriptions for well b-42-J/94-O-14_____	35
Figure II-11. Gamma-ray and core descriptions for well b-53-G/94-O-14_____	36
Figure II-12. Gamma-ray and core descriptions for well b-73-G/94-O-11_____	37
Figure II-13. Photo of Facies A (Triassic Strata)_____	38
Figure II-14. Photo of Facies B (Chert-pebble Conglomerate)_____	40
Figure II-14. Core examples of Facies C (Laminated Sands and Bioturbated Shales)_____	42
Figure II-16. Core examples of Facies D (Well sorted Quartzose sandstones)_____	45
Figure II-17. Detail of carbonate clast within Facies D_____	46
Figure II-18. Gross aspect of Facies E (Burrowed Silts with Abundant Wood Fragments)_____	49
Figure II-19. Detailed photographs of Facies E_____	50
Figure II-20. Detailed photographs of <i>Glossifungites</i> surface_____	53
Figure II-21. Gross aspect of Facies G (Dark, Fissile Shales)_____	55
Figure II-22. Schematic diagram illustrating the depositional setting_____	57

Figure II-23. A typical well within the Maxhamish gas field	59
--	----

CHAPTER THREE: Outcrop Descriptions and Interpretations

Figure III-1. Outcrop base map displaying locations for measured sections	66
Figure III-2. Photomosaic, outcrop litholog, and gamma-ray data for the Chinkeh Formation at Murky Creek (L18)	71
Figure III-3. Photomosaic, outcrop litholog and recorded gamma-ray data for the Chinkeh Formation at Burnt Timber (L19) – Part I	73
Figure III-4. Photomosaic, outcrop litholog and recorded gamma-ray data for the Chinkeh Formation at Burnt Timber (L19) – Part II	74
Figure III-5. Photomosaic, outcrop litholog and recorded gamma-ray data for the Chinkeh Formation at Six Bald Point (L5)	75
Figure III-6. Photomosaic, outcrop litholog and recorded gamma-ray data for the Chinkeh Formation at Sully Creek (L33)	77
Figure III-7. Photomosaic, outcrop litholog and recorded gamma-ray data for the Chinkeh Formation at Otter Slide (L4)	78
Figure III-8. Photomosaic, outcrop litholog and recorded gamma-ray data for the Chinkeh Formation along Slip Rock Creek (L14)	79
Figure III-9. Photomosaic, outcrop litholog and recorded gamma-ray data for the Chinkeh Formation along Tika Creek (L6)	81
Figure III-10. Photomosaic, outcrop litholog and recorded gamma-ray data for the lowermost member of the Scatter Formation along the Kotaneelee River (L8)	82
Figure III-11. Photomosaic, outcrop litholog and recorded gamma-ray data for the lowermost member of the Scatter Formation along Sully Creek	84
Figure III-12. Variability in grain-size within the underlying Permian strata.	86
Figure III-13. Coarse-grained cobble conglomerate of Facies B	88
Figure III-14. Intraformational conglomerates of Facies B	89
Figure III-15. Oblique view of the dark, laterally continuous, fissile shales of Facies C	92
Figure III-16. Bedding plane view of abundant organic debris of Facies D	94
Figure III-17. Amalgamated large wavelength bedforms of Facies D	95
Figure III-18. Shell Fragments within Facies D	97

Figure III-19. Sedimentary structures observed within the middle to upper portions of Facies D_____	98
Figure III-20. Typical Ichnology of Facies D_____	99
Figure III-21. Characteristics typical of Facies E_____	102
Figure III-22. Carbonaceous-rich, highly bioturbated sandstones of Facies F_____	106
Figure III-23. Facies G observed at Six Bald Point (L5)_____	108
Figure III-24. Facies G observed at Burnt Timber (L19)_____	110
Figure III-25. Gross aspect overview of wavy to lenticular bedding of Facies H_____	112
Figure III-26. Details of Facies H_____	113
Figure III-27. Montage of outcrop exposures along Sully Creek_____	116
Figure III-28. Detailed calculations for missing section_____	118
Figure III-29. Murky Creek channel section_____	119
Figure III-30. Interpreted depositional environment for the Lower Cretaceous Chinkeh Formation_____	122

CHAPTER FOUR: Depositional relationships of the Lower Cretaceous Scatter and Chinkeh Formations

Figure IV-1. Stratigraphy of the Lower Cretaceous within the Liard Basin_____	127
Figure IV-2. Bulwell Member isopach map_____	132
Figure IV-3. Locatations of cross-sections, that combine both outcrop and subsurface data_____	134
Figure IV-4. West to East cross-section across the Liard Basin_____	135
Figure IV-5. North-south cross-section constructed from Murky creek outcrop to the Maxhamish gas field_____	137
Figure IV-6. Comparison between Facies E in outcrop and Facies C within the Subsurface_____	139
Figure IV-7. Schematic depositional summary within the Liard Basin_____	140

CHAPTER ONE: Introduction

INTRODUCTORY REMARKS

The depositional history of the lowermost Cretaceous within the Liard Basin is recorded in both cores from the subsurface at the Maxhamish Lake gas field, and in exposed outcrops surrounding the Liard basin to the north (Figure I-1).

Alberta Energy Company Ltd. (as of year 2002) controls the landholding surrounding the Maxhamish Lake area. It was their aim in funding this project, to determine the depositional setting and prediction of producing reservoir intervals. The initial goals for undertaking this project were to combine subsurface data (core, wireline logs, and permeability/porosity data), from Maxhamish Lake, and stratigraphically equivalent outcrop data examined by Leckie *et al.* (1991). The combination of which would lead to a much greater understanding of the geology, both at the reservoir and regional scale. In addition, future exploration targets and prospects could be conceived and tested.

Since completing the core descriptions in the fall and winter of 1998, and subsequent field work in the summer of 1999, the stratigraphy and depositional interpretation of the Lower Cretaceous examined within the study area are more complex than first realized.

PREVIOUS WORK

Although the Liard Basin has been the center of recent drilling and exploration, there is very little literature about the area. Earliest reports concerning the study area are from regional surface mapping programs through the Geological Survey of Canada. Taylor and Stott mapped the Maxhamish Lake area in 1968, wherein they reported basal Cretaceous beds, 11.6 m thick along the Petitot River, just north of the present day Maxhamish gas field. The fine grained, lithic sandstones were described as being thin and somewhat irregular, whose uneven appearance was further intensified by numerous worm burrows. A later report by Williams in 1978, described the subsurface within the Trout Lake, southern Northwest Territories. Using limited well data, he made general correlations and isopach maps of the basal Cretaceous and/or upper Paleozoic sandstones of the areas adjacent to and north of the Bovie Fault. These observations (i.e. Taylor

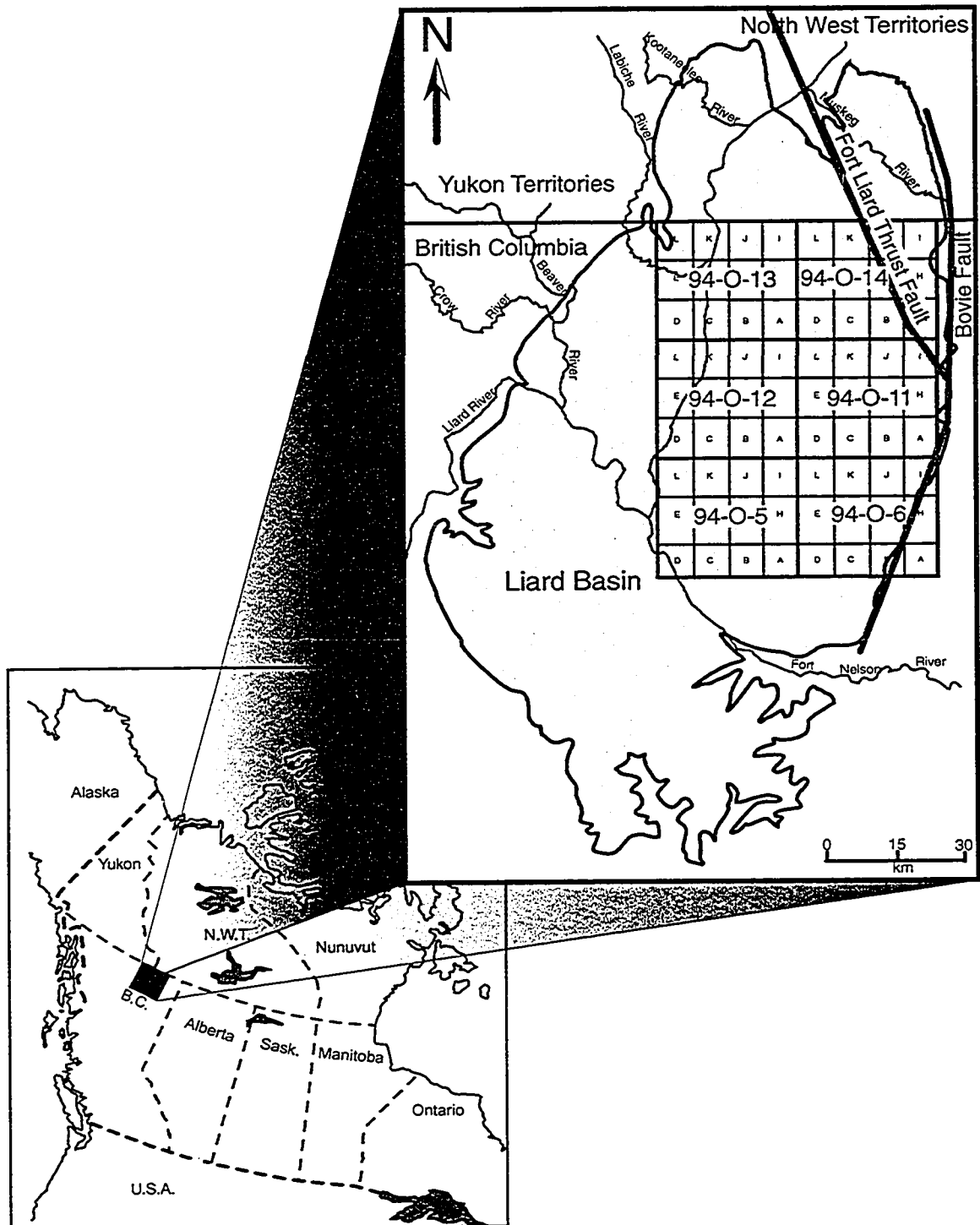


Figure I-1. Location of the Liard Basin. Note the outline of the normal to the west Bovie Fault on the eastern margin of the basin, and the Fort Liard Thrust Fault, which corresponds to Stott's (1982) surface trace.

and Stott, 1968; Williams 1978) were summarized within Stott's 1982 Geological Survey Bulletin on the Lower Cretaceous Fort St. John Group. Wherein Stott made reference to similar basal Cretaceous beds found in outcrop along the Murky and Sully Creeks within the Northwest Territories. This work was followed by the outcrop and limited subsurface chip sample descriptions by Leckie *et al.*, 1991. The report led to the formal creation of a new formation at the base of the Ft. St. John Group. The Chinkeh Formation achieved official formation status, and was created to include strata that was previously described as lower members of the Buckinghorse Formation (Stott, 1960), a unit within the Garbutt Formation (Stott, 1982), and the basal Cretaceous and/or upper Paleozoic sandstone (Williams, 1978).

The newly defined Chinkeh Formation was defined lithostratigraphically as having four major units: 1) conglomeratic breccia, 2) interbedded coal, carbonaceous shale, rooted sandstone, and conglomerate, 3) conglomeratic lag, and 4) upward-coarsening sandstone (Leckie *et al.*, 1991).

CRETACEOUS STRATIGRAPHY OF THE LIARD BASIN

To date very limited biostratigraphic data is available concerning these Lower Cretaceous beds. As a result the ages assigned to them are highly variable ranging from Hauterivian to Albian (Braman and Hills, 1977), Neocomian (Barremian), (Stott, 1982; Leckie *et al.*, 1991), Late Aptian to Early Albian (Dixon, 1986), and earliest Albian (Jeletzky and Stelck, 1981). A stratigraphic table displaying the correlative units south along the Rocky Mountain foothills, and into the Western Canadian Sedimentary Basin is shown in Figure I-2.

Despite the lack of a consensus on the age of the Chinkeh sandstones, they are the oldest Cretaceous deposits within the Liard Basin, resting unconformably on Triassic and older strata. In the subsurface the Lower Cretaceous sandstones rest unconformably on tilted Triassic Toad Formation, while towards the north, the outcrop exposures lie on the Permian Mattson Formation. A southern lateral equivalent of the Chinkeh Formation may be the Cadomin Formation (Stott, 1982), and a northern equivalent may be the Barremian Mount Goodenough Formation and the Aptian to upper Albian Martin House and San Sault Formations (Dixon, 1986). There are no Jurassic aged sediments within the subsurface, or outcrop exposures (Stott, 1982; Williams, 1978).

Sharply overlying the Chinkeh Formation are the marine shales of the Garbutt

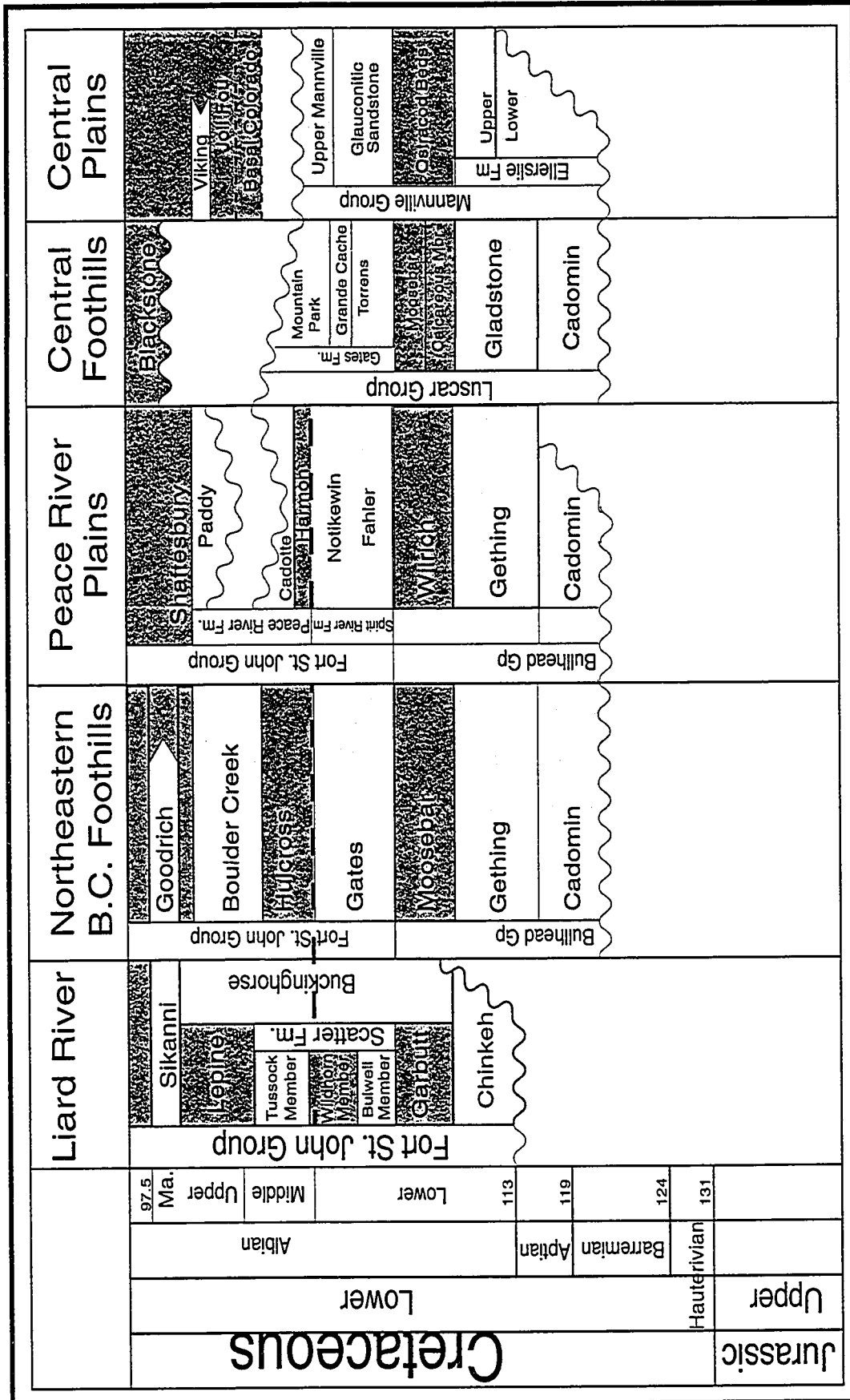


Figure I-2. Lower Cretaceous stratigraphy correlative to the Liard Basin (modified from Smith, 1994).

Formation. The shales are Albian in age and correlate to the Wilrich Member of the Spirit River Formation, and the Moosebar and Gething Formations in the south (Figure I-2) (Stott, 1982). The Garbutt Formation is overlain by the Scatter Formation, that include two sandstone Members, the Bulwell and the Tussock. These sandstones are separated by shales of the Wildhorn Member, all of which encompass the Scatter Formation. Both sandstone members of the Scatter Formation are fine- to very fine-grained and highly glauconite-rich (over 60%) and when observed in outcrop display a distinctive green colour. Southern lateral equivalents of the Bulwell Member include the Falher Member of the Spirit River Formation, and the Gates Formation (Stott, 1982) (Figure I-2). Lateral equivalents of the Tussock Member may be the Boulder Creek and Peace River formations (Leckie *et al.*, 1991).

PALEOGEOGRAPHY AND TECTONIC SETTING

The regional Lower Cretaceous paleogeography of the Western Canada Sedimentary Basin has been extensively documented (Rudkin, 1964; Williams and Stelck, 1975; McLean and Wall, 1981; Jackson, 1984; Smith, 1994) (Figure I-3). Appreciation of these maps must coincide with an understanding of the tectonic elements during these depositional periods. In general, the development of the Canadian Cordillera and related foreland basin (Western Canadian Sedimentary Basin) was controlled by flexural downwarping of the lithosphere beneath the load of the accreting terrains and the developing fold-thrust belt (Price, 1973; Beaumont, 1981; and Jordan, 1981). Stott (1993) has mapped these downwarped foredeeps (Figure I-3), and observed some diachroneity in their distribution throughout the Cretaceous, the result of widespread structural changes along the western margin of North America from the Jurassic to the Cretaceous (Monger and Price, 1979; and Monger *et al.*, 1982).

From the Proterozoic to the Early Jurassic, the western edge of North America was the site of passive margin deposition. Carbonate deposition was dominant in the Paleozoic with sequences that graded westward into shales and cherts. During early Jurassic, carbonate sedimentation ceased, and clastic sediments were deposited in westward thickening wedges. During the middle Jurassic, orogenic activity initiated due to the accretionary plate movements docking allochthonous terrains against ancestral North America (Monger, 1989). The accretion of these terrains, and their associated orogenic activity is known as the Columbian Orogeny, which initiated foreland basin

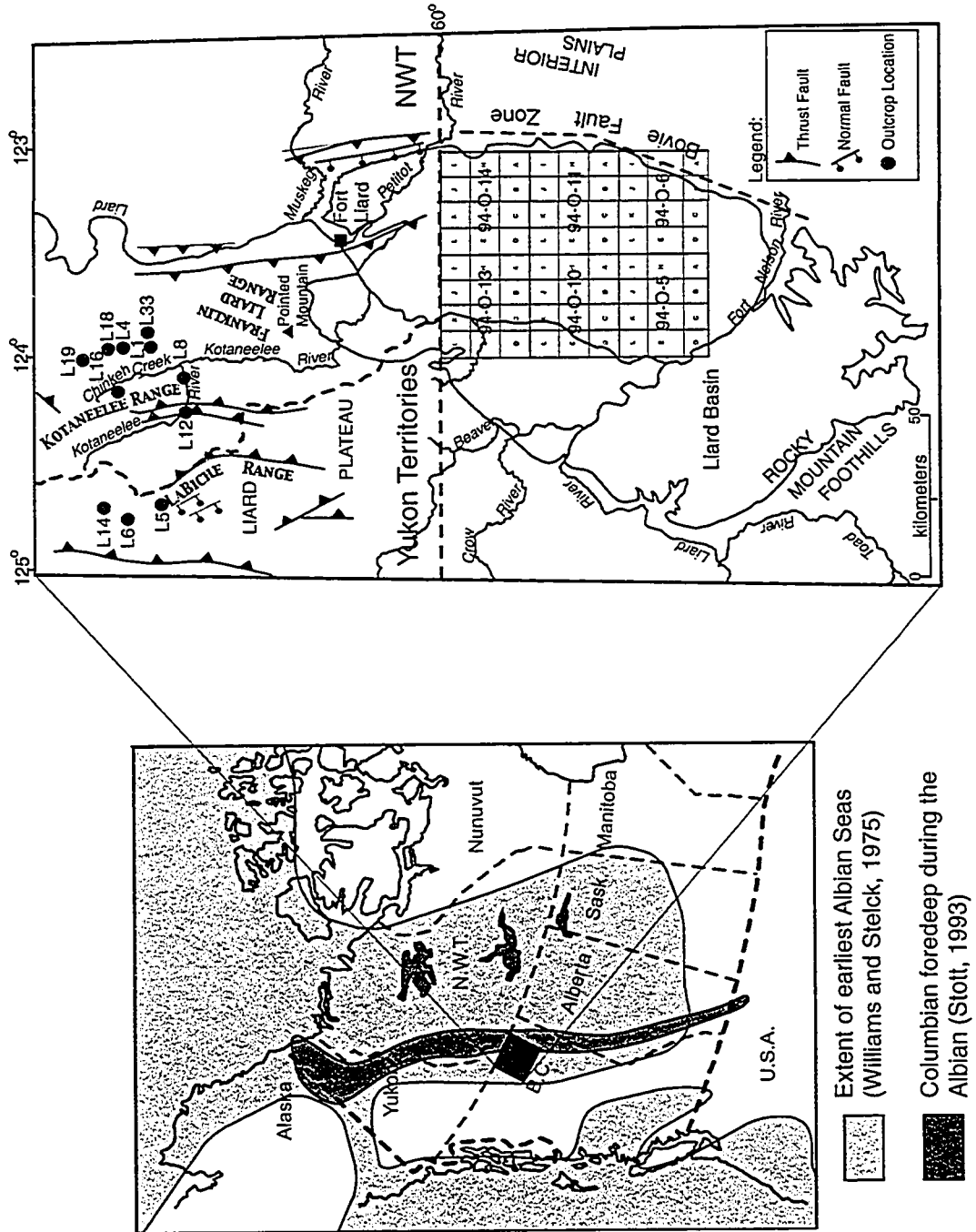


Figure I-3. Paleogeography and foredeep locaion during the Lower Cretaceous (Albian), within the study area.

sedimentation and the development of the Western Canadian Sedimentary Basin and the extension thereof, the Liard Basin.

Further tectonic activity within the cordillera was punctuated with the Laramide orogeny. This Mid-Cretaceous Campanian stage marks the resumption of oblique convergence between ancestral North America and the allochthonous terrains, which continued into the Eocene. This convergent force brought Cretaceous strata to surface around the Liard Basin (Figure I-1), and is responsible for the west verging thrust faults within the study area. Cessation of the Laramide deformation is marked by basinal relaxation and the onset of extensional conditions in the Late Eocene and Oligocene (Price, 1965).

Figure I-4 shows the principal geologic elements of the central part of the western Canadian Cordillera. The Rocky Mountains of the southern Cordillera pass into the Mackenzie Fold Belt of the northern Cordillera, with the Liard Basin situated between the two. The area of study marks a pronounced change of structural style and orientation of structural elements from north-south in the southern Mackenzie Fold Belt to northwest-southeast in the Rocky Mountains (Morrow and Miles, 2000).

The model of the foreland basin proposed by Beaumont (1981), includes an eastern margin that is uplifted due to passive loading by supralithospheric mass loads superimposed during the formation of the fold-thrust belt. Stott (1993) suggested that the faulted structure present associated with the Bovie Lake Fault could be a peripheral bulge associated with the formation of the Liard Basin. Hubbard *et al.* (1999) also observed similar remnant structures further south, believed to be associated with the Columbian Orogeny parallel to the deformational edge of the Rocky Mountains. The role of the Bovie Fault in particular, its influence on the distribution of sediments, and timing of movement will be discussed within Chapter #2.

STUDY AREA AND RESEARCH RATIONALE

The study area is centered on subsurface production at Maxhamish Lake, northeastern British Columbia. Maxhamish Lake is a relatively new sweet gas discovery (the bulk of operations set up between 1997 and 1998), and has estimated initial recoveries of 400 Bcf (British Columbia Ministry of Energy and Mines, 1999). The field itself is located within the Liard Basin (NTS blocks 94-O-11 and 94-O-14), which straddles three geographic borders (Figure I-1).

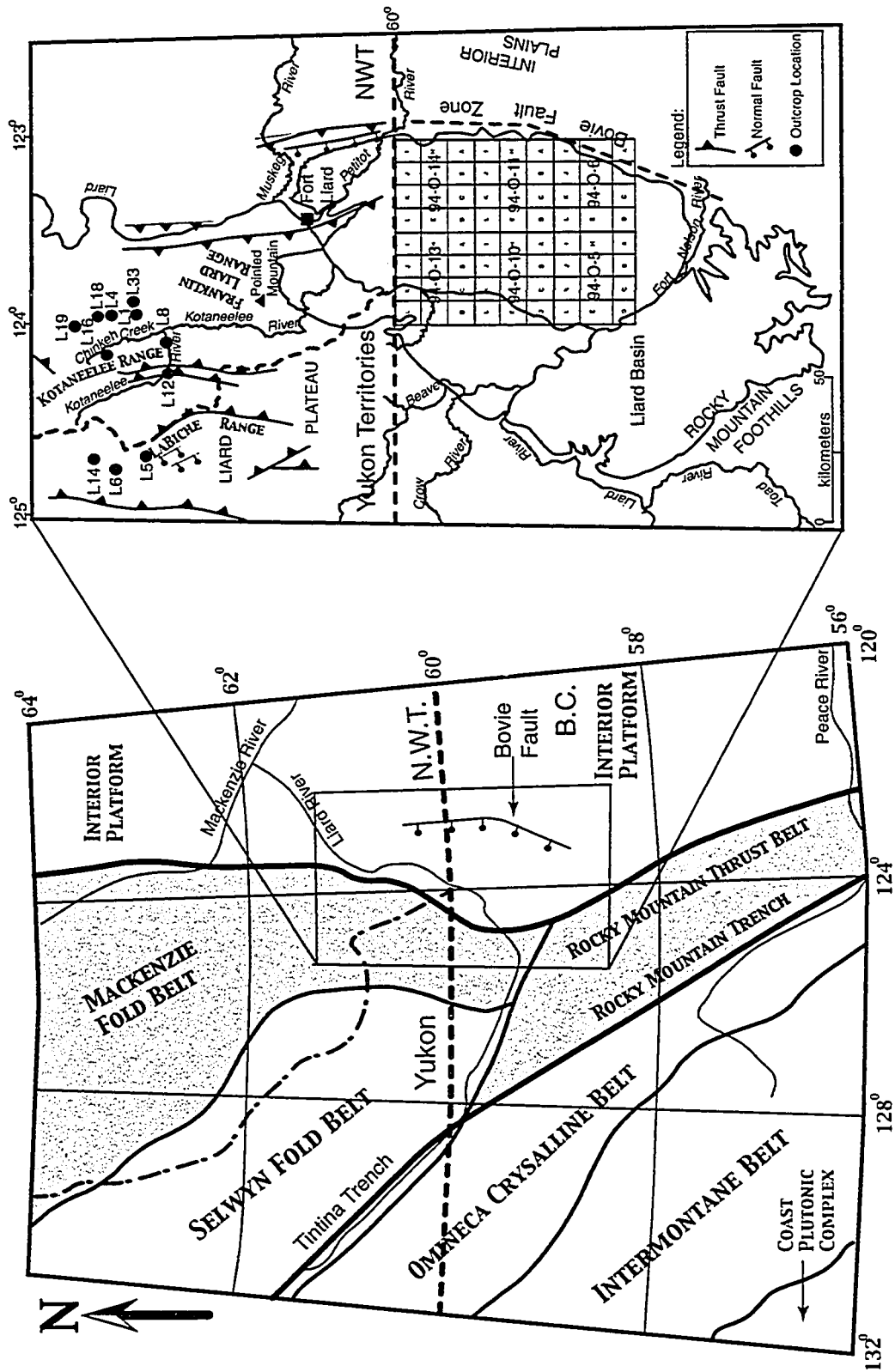


Figure I-4. Geological elements within the study area (modified from Morrow and Miles, 2000).

Descriptions of more than 30 subsurface cores were made during the initial stages of the project. Grain-size measurements, nature of contacts described, sedimentary and ichnological structures were described, photographs taken, and thin-section samples made and analyzed. The descriptions, samples and photographs were compiled into a data base that became the construct upon which chapter two is based. These descriptions were also used from which the comparison of outcrop studies would be based during the summer of 1999.

Outcrop work was complete during the summer of 1999. Eleven outcrop sections were visited, and outcropping sections logged, sampled, photographed and gamma-radiation counts collected. While these sites had been described previously (Leckie *et al.*, 1991), many discrepancies were noted. The author would like to acknowledge that the locations of many of these sites were made possible through the 1991 paper, and this should not be discredited.

Since returning from the field, the fundamental focus of the project shifted. Initially the project entailed combining subsurface and outcrop observations to determine the depositional setting of the sandstones being produced from at Maxhamish, to a more regional project, which was aimed at determining the stratigraphic relationship of the Lower Cretaceous within the Liard Basin. The shift was brought about because it was realized that the paper, which initially described the Chinkeh Formation in outcrop, was in fact describing two Formations: the Chinkeh and the Scatter Formations. While this in itself is not a drastic finding, the similarities between the Scatter Formation and the producing sandstones at Maxhamish Lake are. The result was that the goals of the project had shifted, from being driven by exploration and developmental geology, to a project more focused on understanding the stratigraphy of the Lower Cretaceous within the Liard Basin, in particular the stratigraphic, and depositional relationship between the Chinkeh and Scatter Formations.

In order to avoid further confusion, the following nomenclature scheme has been implemented throughout this thesis (Figure I-5). Any discussion of the sandstones being produced from at Maxhamish will be termed simply, "Lower Cretaceous sandstones." While discussion of outcrop exposures will be referred to by their formal formation names.

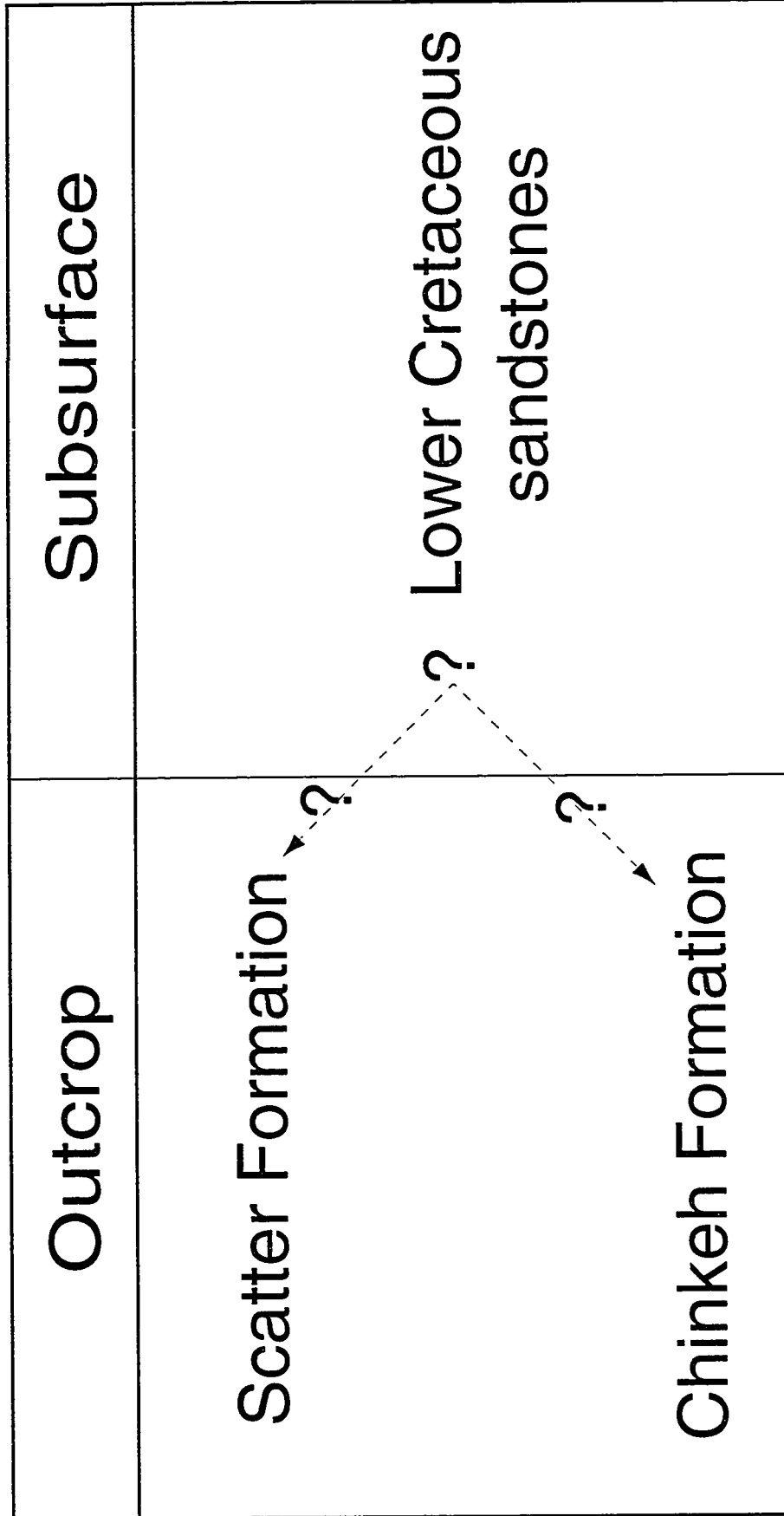


Figure I-5. Nomenclature scheme used to describe the Lower Cretaceous Formations within this thesis. When reference is made to the producing interval within the subsurface the term 'Lower Cretaceous' will be used. Outcrop descriptions will be referred to by their official Formation title.

THESIS LAYOUT

The thesis is organized in the following manner. Subsurface descriptions and interpretations are discussed in chapter two. All outcrop descriptions and their corresponding interpretations are discussed within chapter three. A broad depositional interpretation, based on the data collected to date is summarized in chapter four. It combines the observations from both the subsurface at Maxhamish Lake and outcrop descriptions of the Chinkeh and Scatter formations, with emphasis on the stratigraphic relationship of these Lower Cretaceous formations within the Liard Basin. Finally, conclusions are presented within Chapter five.

REFERENCES

- Beaumont, C., 1981. Foreland basins: *Geophysical Journal of the Royal Astronomical Society*, v. 65, p. 337-381.
- Braman, D.R., and L.V. Hills, 1977. Source of Lower Cretaceous sandstones Jackfish Gap, N.W.T.: *Bulletin of Canadian Petroleum Geology*, v. 25, p. 631-534.
- British Columbia Energy and Mines Division 1999, Hydrocarbon and by-product reserves in British Columbia 1999, Ministry of Energy and Mines.
- Dixon, J., 1986. Cretaceous to Pleistocene stratigraphy and paleogeography, northern Yukon and northwestern District of MacKenzie: *Bulletin of Canadian Petroleum Geology*, v. 34, p. 49-70.
- Hubbard, S.M., S.G. Pemberton, and E.A. Howard, 1999. Regional geology and sedimentology of the basal Cretaceous Peace River oil sand deposit, north-central Alberta: *Bulletin of Canadian Petroleum Geology*, v. 47, p. 270-297.
- Jackson, P.C., 1984. Paleogeography of the Lower Cretaceous Mannville Group of Western Canada. *In: Elmworth – Case study of a Deep Basin Gas Field*. J.A. Masters (ed.). American Association of Petroleum Geologists, Memoir 38, p. 49-77.
- Jordan, T.E., 1981. Thrust loads and foreland basin evolution, Cretaceous western United States: *American Association of Petroleum Geologists, Bulletin*, v. 64, p. 2506-2520.

- Jeletzky, J.A., and C.R. Stelck, 1981. *Pachygyrcia*, a new ammonite from the lower Cretaceous (Earliest Albian?) of northern Canada: Geological Survey of Canada Paper 80-20, 25 p.
- Leckie, D.A., D.J., Potocki, and K., Visser, 1991. The Lower Cretaceous Chinkeh Formation: A Frontier-Type Play in the Liard Basin of Western Canada: American Association of Petroleum Geologists Bulletin, v. 75, p. 1324-1352.
- McLean, J.R., and J.H. Wall, 1981. The early Cretaceous Moosebar Sea in Alberta: Bulletin of Canadian Petroleum Geology, v. 29, p. 334-377.
- Monger, J.W.H., 1989. Cretaceous Tectonics of the North American Cordillera. *In*: W.G.E. Caldwell, and E.G. Kaufman (eds.). Evolution of the Western Interior Basin: Geological Association of Canada, Special Paper 39, p. 31-47.
- Monger, J.W.H., and R.A. Price, 1979. Geodynamic evolution of the Canadian Cordillera – Progress and problems: Canadian Journal of Earth Sciences, v. 16, p. 770-791.
- Monger, J.W.H., R.A. Price, and D.J. Tempelman-Kluit, 1982. Tectonic accretion and the origin of the two major metamorphic and plutonic welts in the Canadian Cordillera: Geology, v. 10, p. 70-75.
- Morrow, D.W., and W.C. Miles, 2000. The Beaver River Structure: a cross-strike discontinuity of possible crustal dimensions in the southern Mackenzie Fold Belt, Yukon and Northwest territories, Canada: Bulletin of Canadian Petroleum Geology, v. 48, p. 19-29.
- Price, R.A., 1965. Flathead map area, British Columbia and Alberta: Geological Survey of Canada, Memoir 336, 221 p.
- Price, R.A., 1973. Large-scale gravitational flow of supracrustal rocks, southern Canadian Rockies. *In*: Gravity and Tectonics. K.A. de Jong, and R. Scholten (eds.). John Wiley, New York, p. 491-502.
- Rudkin, R.A. 1964. Lower Cretaceous. *In*: Geologic History of Western Canada. R.G. McCrossan and R.P. Glaister (eds.). Alberta Society of Petroleum Geologists, p. 156-168.
- Smith, D.G. 1994. Paleogeographic evolution of the Western Canada Foreland Basin. *In*: Geological Atlas of the Western Canada Sedimentary Basin. G.D. Mossop and I. Shetson (comps.). Canadian Society of Petroleum Geologists and Alberta Research Council, p. 277-296.
- Stott, D.F., 1960. Cretaceous rocks in the region of Liard and Mackenzie rivers, Northwest Territories: Geological Survey of Canada Bulletin 63, 36 p.

- Stott, D.F., 1982. Late Cretaceous Fort St. John Group and Upper Cretaceous Dunvegan Formation of the Foothills and Plains of Alberta, British Columbia, District of Mackenzie and Yukon Territory: Geological Survey of Canada Bulletin 328, 124 p.
- Stott, D.F., 1993. Evolution of Cretaceous Foredeeps: A comparative analysis along the length of the Canadian Rocky Mountains. *In*: W.G.E. Caldwell, and E.G. Kaufman (eds.). Evolution of the Western Interior Basin: Geological Association of Canada, Special Paper 39, p. 131-150.
- Taylor, G.C., and D.F. Stott, 1968. Maxhamish British Columbia: Geological Survey of Canada paper 68-12, 23 p.
- Williams, G.K., 1978. An update of subsurface information, Cretaceous rocks, Trout Lake area, southern Northwest Territories: Geological Survey of Canada Paper 78-1A, Report of Activities, Part A, p. 545-553.
- Williams, G.D., and Stelck, C.R. 1975. Speculations on the Cretaceous palaeogeography of North America. *In*: The Cretaceous System in the Western Interior of North America. W.G.E. Caldwell (ed.). The Geological Association of Canada, Special Paper 13, p. 1-20.

CHAPTER TWO: Subsurface Descriptions and Interpretations**INTRODUCTION**

Straddling 3 borders (Figure II-1), the Liard Basin has experienced a recent surge in exploration activity. The recent discovery of the Maxhamish field, with an estimated initial gas recovery of 400 Bcf (British Columbia Ministry of Energy and Mines, 1999) represents the most northerly production from Cretaceous aged strata within British Columbia, and at the time of writing (2002) represents the only producing field within the Liard Basin.

Production at Maxhamish is from Lower Cretaceous sandstones, representing the oldest Cretaceous rocks deposited along the eastern flank of the Liard Basin. At Maxhamish, these sandstones sit unconformably on tilted Triassic shales of the Toad Formation (see Figure II-3), and can be regionally correlated to age equivalent strata within the Western Canadian Sedimentary Basin (see Figure I-2).

The main goal of this paper is to present detailed geological descriptions of the lower Cretaceous sandstones, which are producing at Maxhamish, and to create a depositional model for their reservoir distribution. Other objectives include relating sedimentation to active regional tectonism within the area, particularly the active Bovie Fault, and presenting new exploration strategies for further development within the Lower Cretaceous sandstones at Maxhamish Lake.

Regional Geology and Stratigraphy

The Liard Basin covers approximately 9500 km² whose present day expression formed in response to the late Cretaceous - Early Tertiary Laramide orogeny. The configuration of the Basin is bounded by a number of dominant physiographic features within the study area. The down to the west normal fault of the Bovie creates the eastern margin of the basin (see Figure II-1 and II-3). Bounding the Liard Basin to the southwest are the Rocky Mountain Foothills, and the Liard Plateau to the north and northwest. A structure contour map (see Figure II-5) constructed on top of the Lower Cretaceous sandstones at Maxhamish shows the present day axis along the eastern flank of the Liard Basin. This axis trending northeast-southwest shows a dramatic decrease in structural elevation towards the southwest, and shallows towards the northern portion of the study

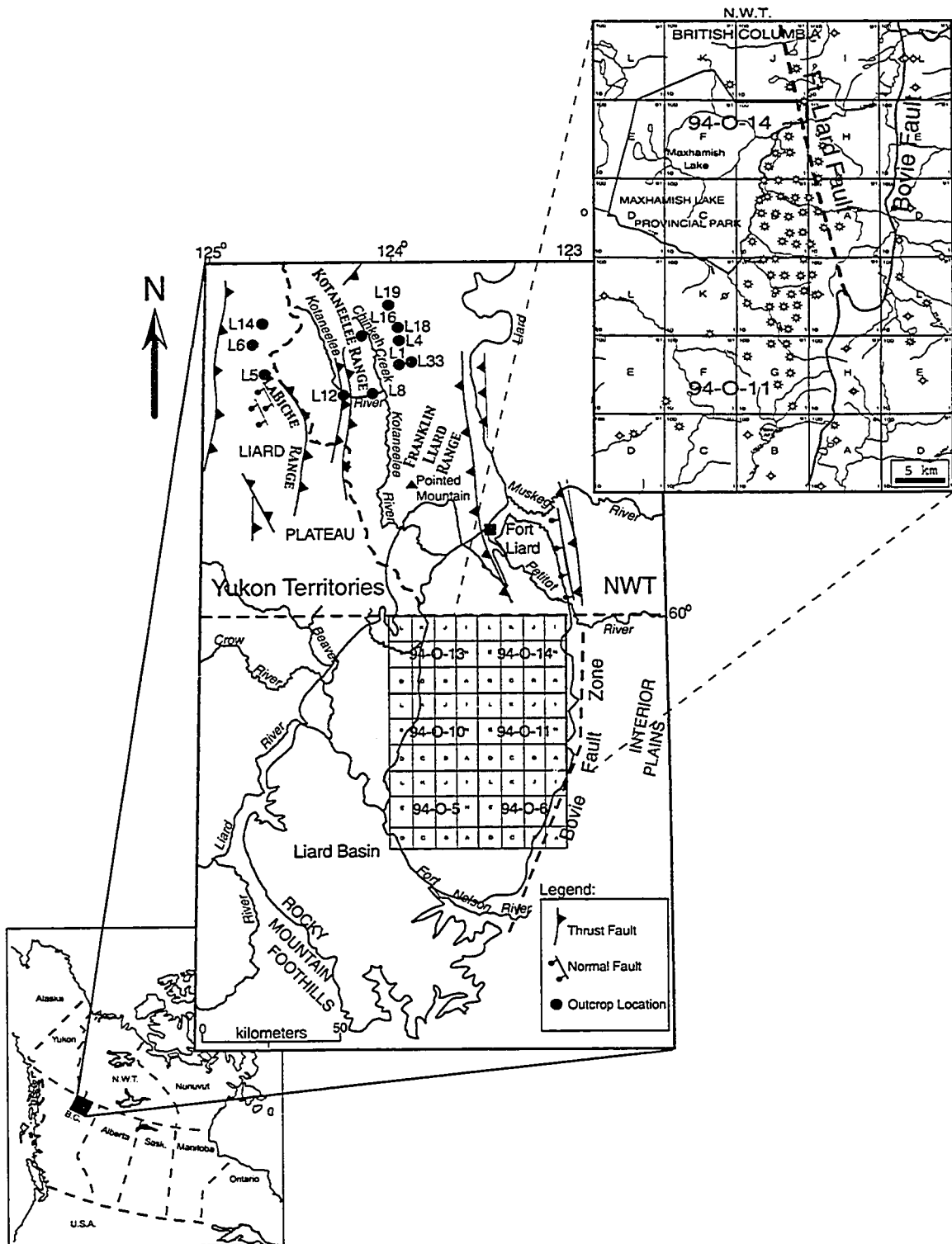


Figure II-1. Regional base map, illustrating the location of the Liard Basin, gross structural geology a surface, and locations of wells within the Maxhamish field. Note the Bowie and Ft. Liard faults.

area. In addition to the structural controls exerted on the basin by the Bovie Fault during deposition of Lower Cretaceous strata, the Ft. Liard thrust fault (informal name) also intersects the present day basin configuration. Passing along the northwest edge of Maxhamish Lake, the thrust cross-cuts the Bovie Fault (see Figure II-1). Its orientation mapped within the subsurface matches the surface trace of the fault mapped by Stott (1982).

Lithostratigraphically, the Lower Cretaceous sandstones were deposited within a complex shoreface to offshore environment, while the overlying shales of the Garbutt Formation were deposited in an offshore marine setting.

The Bovie Fault

The eastern depositional boundary of the Liard Basin is the deep-seated north-south trending Bovie Fault, whose positive physiographic expression can still be observed at surface today. The fault has been active since the early Paleozoic, with the western side consistently structurally lower than the eastern (Taylor and Stott, 1968; Williams, 1977). However, Leckie *et al.*, 1991 has also speculated that there may also exist the possibility of strike-slip motion along the plane of the Bovie Fault. A cross-section constructed across the Bovie fault shows a down to the west normal fault, consistent with previous down to the west, normal fault interpretation (see Figure II-3). Subcrop edges of Pennsylvanian, Permian, and Triassic rocks also form along the Bovie Fault (Williams, 1978; Taylor and Stott, 1968). In addition, prior to the deposition of Triassic sediments, the Mississippian-Pennsylvanian Mattson Formation was eroded from the eastern side of the Bovie Fault (Taylor and Stott, 1968). In wells immediately east of the Bovie fault no Lower Cretaceous sandstones have been found, suggesting that either they were eroded, or simply not deposited. With the Bovie Fault acting as the eastern edge of the Liard Basin, it is envisioned acting as a barrier for eastward prograding sediments. As well if there was movement syndepositional to Lower Cretaceous deposition, the fault would have acted as a strong controlling factor during Cretaceous sedimentation (Stott, 1982).

As mentioned above, the west verging Liard thrust fault cross-cuts the Bovie Fault. Simply put, the timing of the Ft. Liard thrust fault post-dates the timing of the Bovie normal fault. Wherein, the Fort Liard thrust fault is the result of Late Cretaceous compressional tectonics during the Laramide Orogeny. While the thrust fault did not directly impact sandstones at Maxhamish depositionally, the structural flexure across this

feature did alter the sandstones diagenetically. Through thin-section analysis it is observed that leaching of grains, especially glauconite is concentrated along the crest and margins of the Liard thrust fault within facies D (see reservoir geology). The fault acted as a post-depositional conduit for the leaching fluids, through which reservoir porosity and permeability were enhanced. Maps of the Fort Liard thrust within the subsurface are shown in Figure II-5, and discussed within the mapping section of this chapter.

Reservoir Geology

The Maxhamish gas field has an estimated initial gas in place value of 400 billion cubic feet (British Columbia Energy and Mines Division 1999), where sweet gas is contained within shoreface sandstones of Lower Cretaceous age. A well from the heart of the Maxhamish field is illustrated in Figure II-2. Sands are well sorted fine to medium-grained glauconite-rich, quartz arenites, with porosity ranging from 14-20% (averaging of 17%). Permeabilities range from 20-80 millidarcies and wells are fracture stimulated prior to being put on production. The field is intersected by the Ft. Liard thrust fault (see Figure II-1 and II-5), which is believed to be the conduit for fluids into the Lower Cretaceous sandstones, which led to the creation of leached porosity within the reservoir. This leaching effect is evident when looking at the net pay map (Figure II-7), wherein net pay contours deflect to the east reflecting their intersection with the Ft. Liard thrust fault. Although maximum continuous pay thickness of sandstones does not reach more than 6m, they are areally extensive, covering more than 250km². The upper limits of daily production for the field are approximately 100 MMcf/day (during year 2000). A thin oil lag has been encountered in some of the western most wells within the field, however the amount of oil in place is presently non-economic.

The trapping mechanism for the gas produced at Maxhamish is stratigraphic, with an overprint of structural relief and diagenetic enhancement (from the Fort Liard thrust fault). The thick overlying regional shale succession of Garbutt Formation acts as an upper seal for the Lower Cretaceous sandstones. These sandstones pinch out against the Bovie Fault towards the east (see Figure II-3), and towards the south (see Figure II-4). Towards the north there is evidence to suggest that recent freshwater influx is influencing the reservoir, and creating lower pressure gradients. Thus suggesting that the producing sandstones outcrop along strike of the Maxhamish field. The field is underlain by non-permeable Triassic shales of the Liard/Toad Formations that create an effective

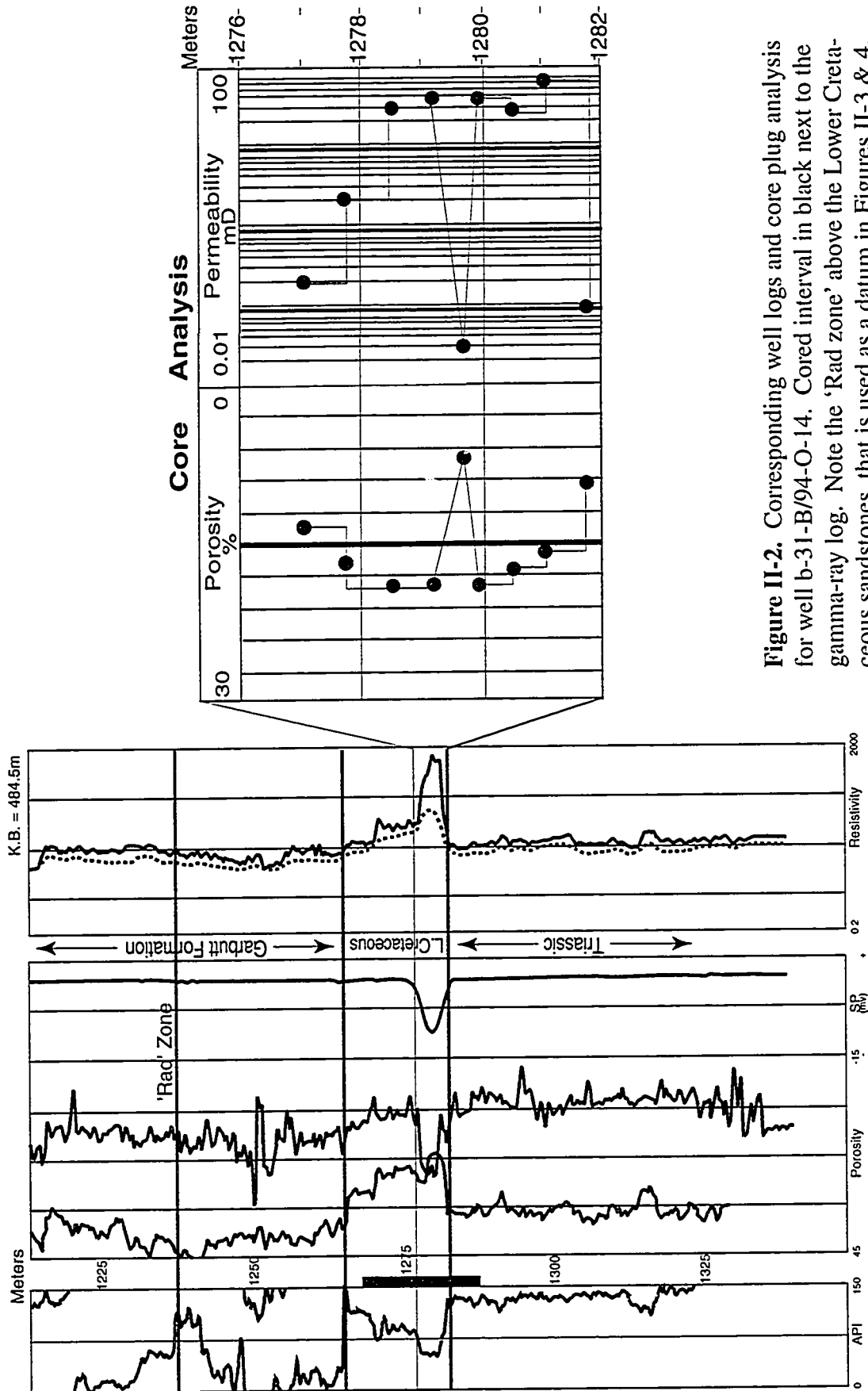


Figure II-2. Corresponding well logs and core plug analysis for well b-31-B/94-O-14. Cored interval in black next to the gamma-ray log. Note the 'Rad zone' above the Lower Cretaceous sandstones, that is used as a datum in Figures II-3 & 4.

bottom seal.

Database and Methodology

The subsurface portion of the study area comprises national topographic system blocks 94-O-11 and 94-O-14 that encompass approximately 1470 km² (see Figure II-1 and Figure II-8). A subsurface database was compiled using data from over 80 wells and over 30 subsurface cores, which penetrate the producing Lower Cretaceous sandstones. Analysis of these cores included the following sedimentological characteristics: grain-size, grain-sorting, lithologic constituents, the nature of unit contacts, thickness of individual units, physical and biogenic sedimentary structures, and the identification and description of macro-fossils.

CROSS-SECTIONS

Two cross sections (Figure II-3 and Figure II-4) are presented, which show the geology within the subsurface at Maxhamish Lake. A high gamma-ray kick within the Garbutt shale was used as a datum. This radioactive zone, or 'rad zone' represents the maximum flooding surface within the Liard Basin during Lower Cretaceous time, and can be traced across the Bovie Fault, proving that the trapping mechanism at Maxhamish is stratigraphic. Williams (1978) has traced the radioactive marker as far west as the Mc Murray Trough, and it was also interpreted to denote the peak of transgression, above which marine shales were deposited during a highstand in sea-level (Leckie and Potocki, 1998).

The dip oriented cross-section has been constructed across the Bovie Fault (Figure II-3). The section displays the entire Lower Cretaceous thinning towards the fault, with subcropping Triassic, Permian and Mississippian strata juxtaposed against the Bovie Fault. The cross-section is consistent with previous workers interpretation, with respect that the "radioactive zone" within the Gabutt shales can be traced across the fault into wells along the footwall of the Bovie Fault (Leckie and Potocki, 1998).

The complexity of the relative sea level changes can be recognized when looking at the interpreted depositional environments. Initially the Lower Cretaceous sandstones were deposited within an energetic shoreface environment, which was well developed parallel to the antecedent topographic high of the Bovie Fault. As sea-level rose offshore

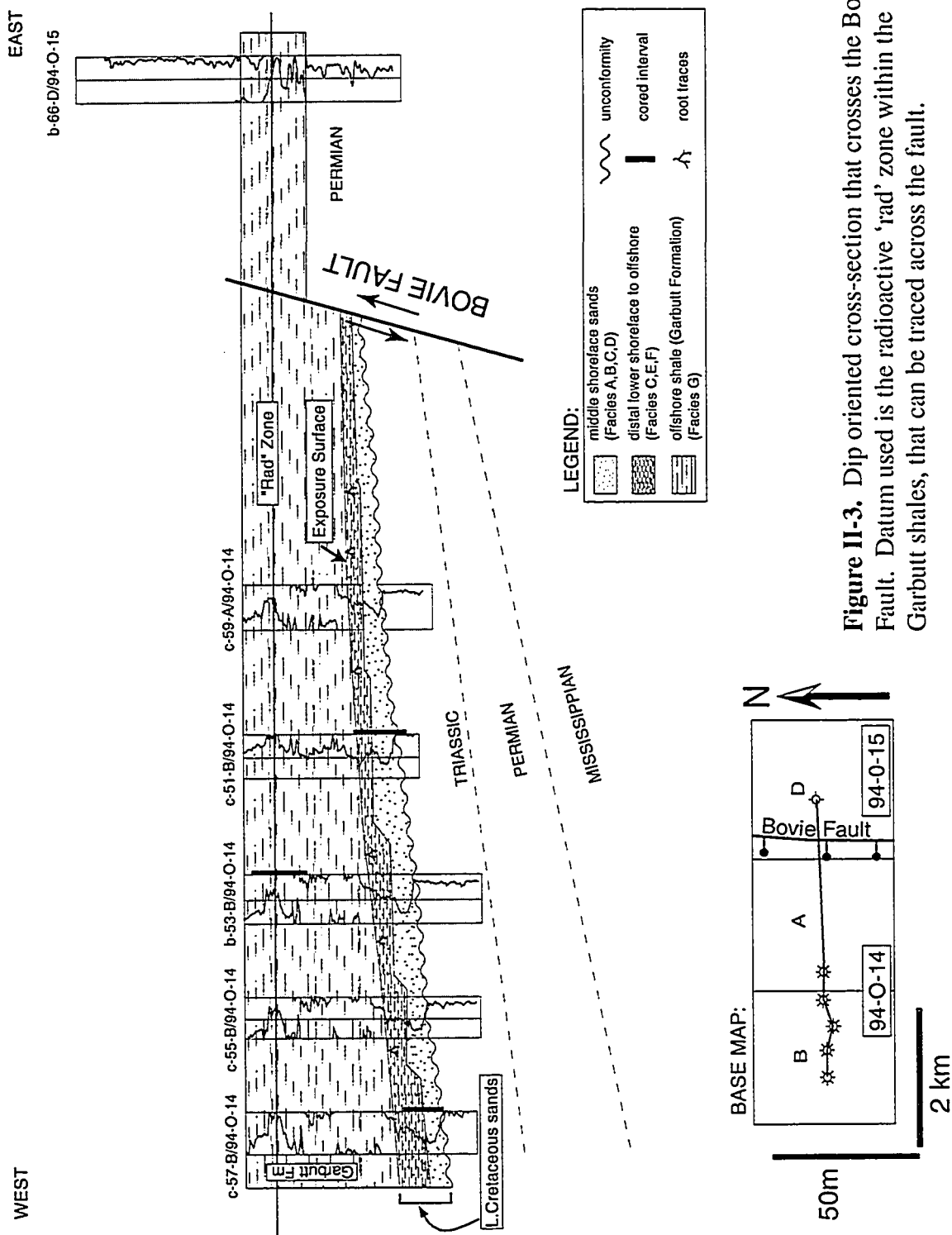


Figure II-3. Dip oriented cross-section that crosses the Bovie Fault. Datum used is the radioactive 'rad' zone within the Garbutt shales, that can be traced across the fault.

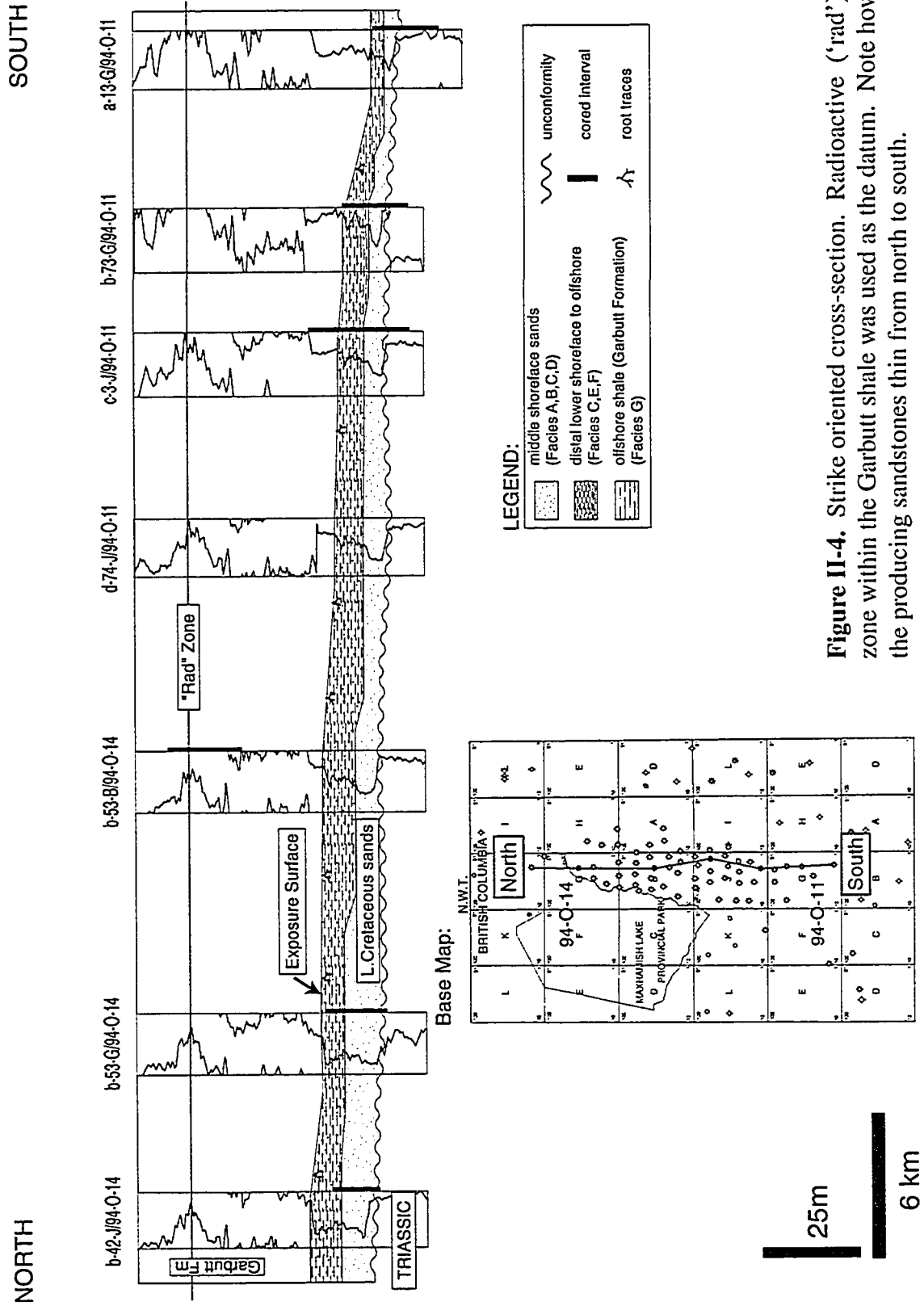


Figure II-4. Strike oriented cross-section. Radioactive ('rad') zone within the Garbutt shale was used as the datum. Note how the producing sandstones thin from north to south.

silts were deposited over the shoreface sandstones. This was accompanied by the drowning of a proximal forrest, as abundant woody debris and fragments were deposited. An extensive burrowed and rooted horizon followed which marks a fall in base level, prior to the maximum flooding event (the radioactive zone in the Garbutt Formation) that blankets the region in marine shales. These episodic sea level changes are a combination of eustatic changes in sea level, and the increased down to the west movement of the Bovie Fault syndepositional with the deposition of the Lower Cretaceous formation. As down to the west movement of the Bovie Fault initiated, accommodation space increased drowning the Bovie Fault parallel shoreline. The rooted and burrowed horizon marks a fall in base level whereby sediments were subaerally exposed, colonized, and rooted prior to the inundation of the deep marine waters.

MAPS

In order to understand the basin in which the Lower Cretaceous sandstones were deposited in, their present day reservoir geometries and prediction of the highest pay zones, a number of maps were created within the study area. In order to approximate the paleotopographic surface on which the Lower Cretaceous sandstones were deposited, a structural contour map was created using the top of the Lower Cretaceous zone (Figure II-5). This pick was consistent from electrical logs within the study area, and utilized with much more accuracy than the Triassic-Cretaceous unconformity at the base of many logs. The map shows dramatic decrease in elevation moving west away from the Bovie Fault, which is highlighted on the eastern edge of all subsurface maps included (see Figures II-5, II-6, and II-7). Another point to note, is the perturbation in contour lines near the western edge of Maxhamish Lake. This deflection, is the Ft. Liard thrust, which has an orientation roughly northeast-southwest. On the surface it passes through the village of Ft. Liard (Stott, 1982), and within the subsurface continues along the eastern edge of Maxhamish Lake intersecting with the Bovie Fault near block I/94-O-11. The Ft. Liard thrust fault occurred late within the Omineca Orogeny, which post-dates the deposition of the Lower Cretaceous sandstones.

An increased understanding of the pre-Cretaceous paleotopography was realized when isopach maps were created from the entire Lower Cretaceous formation. Firstly, total gross thickness was mapped (Figure II-6), which represents the cumulative thickness from the gamma-ray kick corresponding to the burrowed/exposure surface and underlying

Figure II-5. Top of Lower Cretaceous sandstone elevation map. Note dramatic decrease in elevation towards the southwest, as the basin oriented northeast to southwest. Also note the perturbation in contour lines east of Maxhamish Lake. This change in structural elevation is due to the Fort Liard thrust fault that cross-cuts the field (see Figure II-1). Contour interval is 20 meters, and all depths are reported below sea-level. The Bovie Fault is highlighted on the eastern edge of the map.

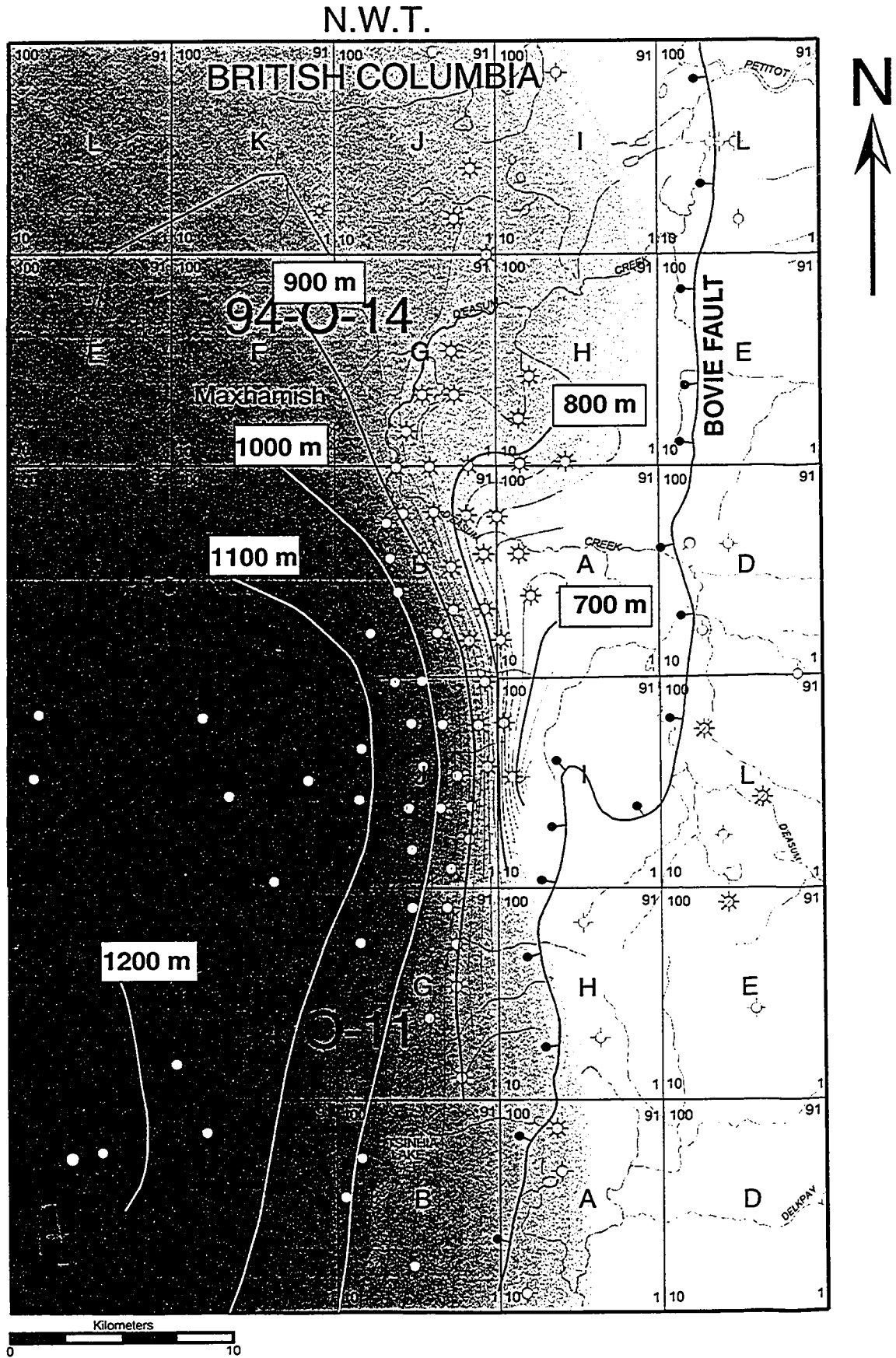


Figure II-6. Total Lower Cretaceous sandstone isopach map. Contour interval is 1 meter, The Bovie Fault is highlighted on the eastern edge of the map.

N.W.T.

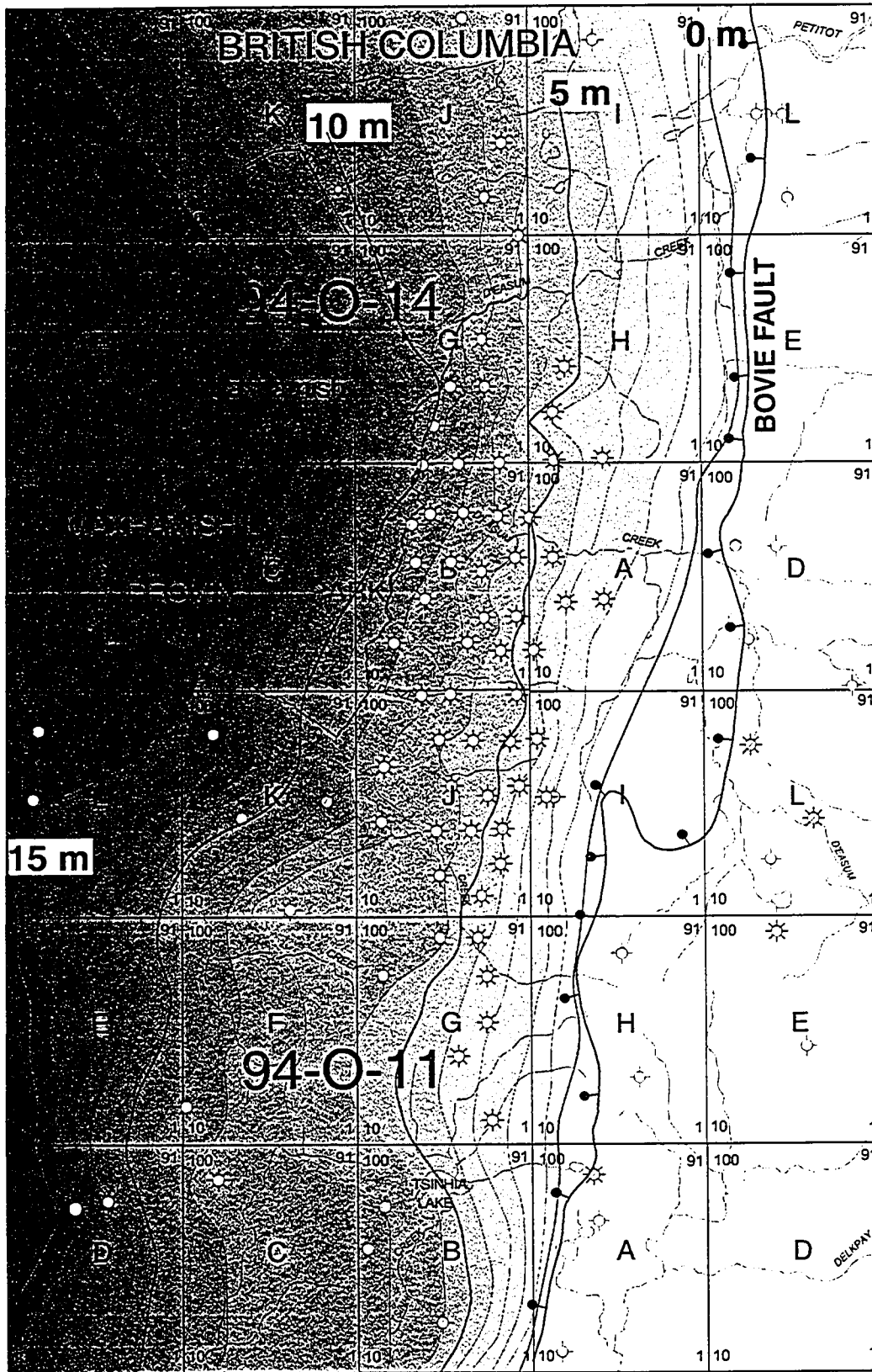
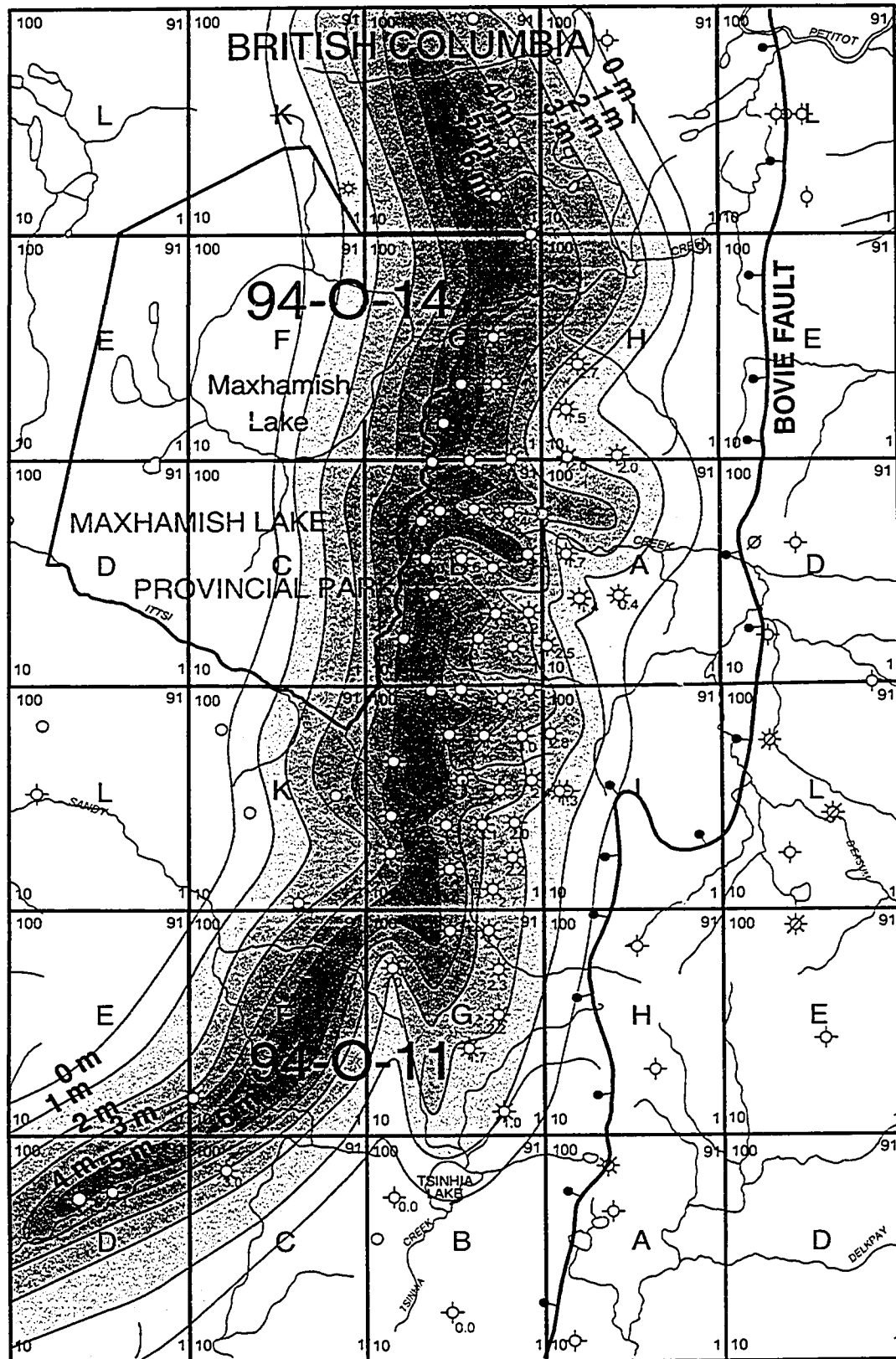


Figure II-7. Net pay map. A porosity cut-off o 10% was used to construct the map. Note the arched orientation of the map in relation to the Bovie Fault. Contour interval is 1 meter, The Bovie Fault is highlighted on the eastern edge of the map.

N.W.T.



N
↑



contact of the Garbutt Formation, to the Triassic-Cretaceous unconformity (see Figures II-10, II-11, and II-12). The map displays the westward increase in the overall thickness of the Lower Cretaceous formation, in response to an increase in accommodation space created by a relative rise in sea-level. The increase in elevation (i.e. depth) towards the west, allowed for an increase in accommodation and hence the increase in overall thickness between Cretaceous Garbutt and Triassic Toad/Liard Formations.

In order to understand reservoir distribution and geometry within the field, net continuous pay was mapped. Electric log signatures were first calibrated to core descriptions and observations. Generally, a clean gamma-ray signature and a corresponding log porosity cut-off of 10% was used to determine net continuous pay thickness. The resulting map (Figure II-7) illustrates an arched pay zone which parallels the Bovie Fault in the central portion of the study area, but curves to the northwest in the north, and curves towards the southwest in the south. This arched pay zone reflects the distribution of middle shoreface sandstones along the eastern margin of the Liard Basin, which have been modified through longshore currents (see discussion).

Facies Descriptions

INTRODUCTION AND OVERVIEW

Seven distinct facies have been identified within the Lower Cretaceous sandstones producing at Maxhamish, which are summarized in Table II-1. These facies are identified based on their physical and biological characteristics observed in core. These features include lithology, grain-size, and physical and biogenic sedimentary structures. Grain size measurements were made by visually comparing the sediments to a grain size card. A number of thin sections were also made and analyzed to determine mineralogy of the sediments and confirm visual observations made from the core.

The facies identified represent the genetic relationship between the environment in which the sandstones were deposited, and the subsequent reworking through physical and biological processes. The relative degree of reworking subsequent to deposition is a product of the environment of deposition. A reconstructed depositional environment is then interpreted based upon analogies with similar facies and successions from both ancient and modern examples.

Lithostratigraphically, facies A represents shale deposits of the Triassic Liard/

Table II-1. Table of facies identified within the subsurface at Maxhamish Lake for the basal Cretaceous sandstones.

Key to abbreviated Ichnofossils:

Pl: *Planolites*, *Pa:* *Palaeophycus*, *Ch:* *Chondrites*, *Th:* *Thalassinoides*, *Te:* *Teichichnus*,
Hel: *Helminthopsis*, *Zo:* *Zoophycos*, *Fu:* *Fugichnia*, *Skol:* *Skolithos*.

Facies	Dominant grain-size and lithology	Ichnofossils	Sedimentary Structures	Interpretation	Stratigraphic Interval
A	Friable to well cemented shales with few silt laminations, often rich in mica.	<i>Pl, Pa, Ch, Th</i>	Generally massive appearing, with occasional silt lamina preserved	Distal offshore to shelf break??	Triassic Toad/Llard Formation
B	Matrix and clast supported conglomerate composed of pebble sized chert clasts with pyritized wood fragments	None observed	None observed	Transgressive lag	Cretaceous Chinkoh Formation
C	Glauconite-rich, fine grained quartz-rich sands.	<i>Ta, Ch, Hel, Pl, Pa, Zo</i> cross-cut by: <i>Th, Tei, Fu</i>	Hummocky and swaley cross-stratified sands with abundant scour surfaces	Distal - Lowershore/face	
D	Fine-grained quartz-rich sands with vaguely discernable bedding. Occasional coral fragments present.	Rare <i>Pa</i>	Leaching of glauconite, has created a massive appearing quartz sandstone reservoir	Lower - Middleshore/face	
E	Silty-shales with fine sand lamination. Abundant pyritized wood fragments, and glauconite throughout.	<i>Ch, Pa, Pl, Hel, Te</i>	Occasional vestigial lamination of fine silt to sand. Mostly obliterated due to intense biogenic reworking	Offshore Marine	
F	Extreme biogenic reworking, results in a massive silt to shale, which is very rich in glauconite.	Glauconite filled <i>Skol</i> overprinted by root traces	None preserved.	Exposure Surface	
G	Fissile shales, occasional bentonite beds preserved.	None Observed	Finely laminated shales	Offshore Marine	Cretaceous Garbutt Formation

Toad Formation, which were deposited in a distal shelf setting. Subsequent hiatus in sedimentation and erosion took place following which, deformation of the Triassic strata produced the angular unconformity on which the Lower Cretaceous sandstones were deposited. Subsequent facies B through F and were deposited in an energetic, wave dominated shoreface environment. Facies G represents the regional transgression of the Garbutt Formation throughout the entire study area. Three detailed core descriptions are included which show the relationship of the abovementioned facies, and how their individual thickness varies across the study area. Their locations are shown in Figure II-8, and Figure II-9 defines the symbols used within each of the detailed well descriptions.

FACIES A: TRIASSIC STRATA

Description

The strata underlying the Cretaceous sandstones at Maxhamish are fine-grained Triassic silts and shales of the Liard/Toad Formation. Generally these shales are highly micaceous and well cemented, with pyrite being common along bedding planes. Since the majority of wells producing at Maxhamish must be stimulated prior to production, this makes an excellent bottom barrier to induced fracturing. Moving west however, the shales become much more friable and cyclical in their depositional nature, with interbeds of silt and very fine-grained sand becoming more common (Figure II-13). These beds are sharp-based, and within individual silt beds grain-size fines upwards with rare migrating ripple laminations. Moving upward through the facies, the relative amount of bioturbation increases. Traces observed include: *Planolites*, *Palaeophycus*, *Chondrites*, and *Thalassinoides*.

The upper contact is very abrupt, sharp and unconformable, where glauconitic Lower Cretaceous sandstone or chert-pebble conglomerate overlies the Triassic shales.

Interpretation

The Triassic silts and shales that unconformably underlie the Lower Cretaceous strata at Maxhamish are interpreted to be distal shelfal deposits. Their monotonously interbedded nature, with sharp based silts which fine-upward at the bed scale that are rarely ripple laminated, coincide with Bouma's (1962) classification of turbidite deposits. These beds and bed sets represent the uppermost C, D, and E divisions within the classification scheme. It is believed that since grain-size and the cyclical nature of the

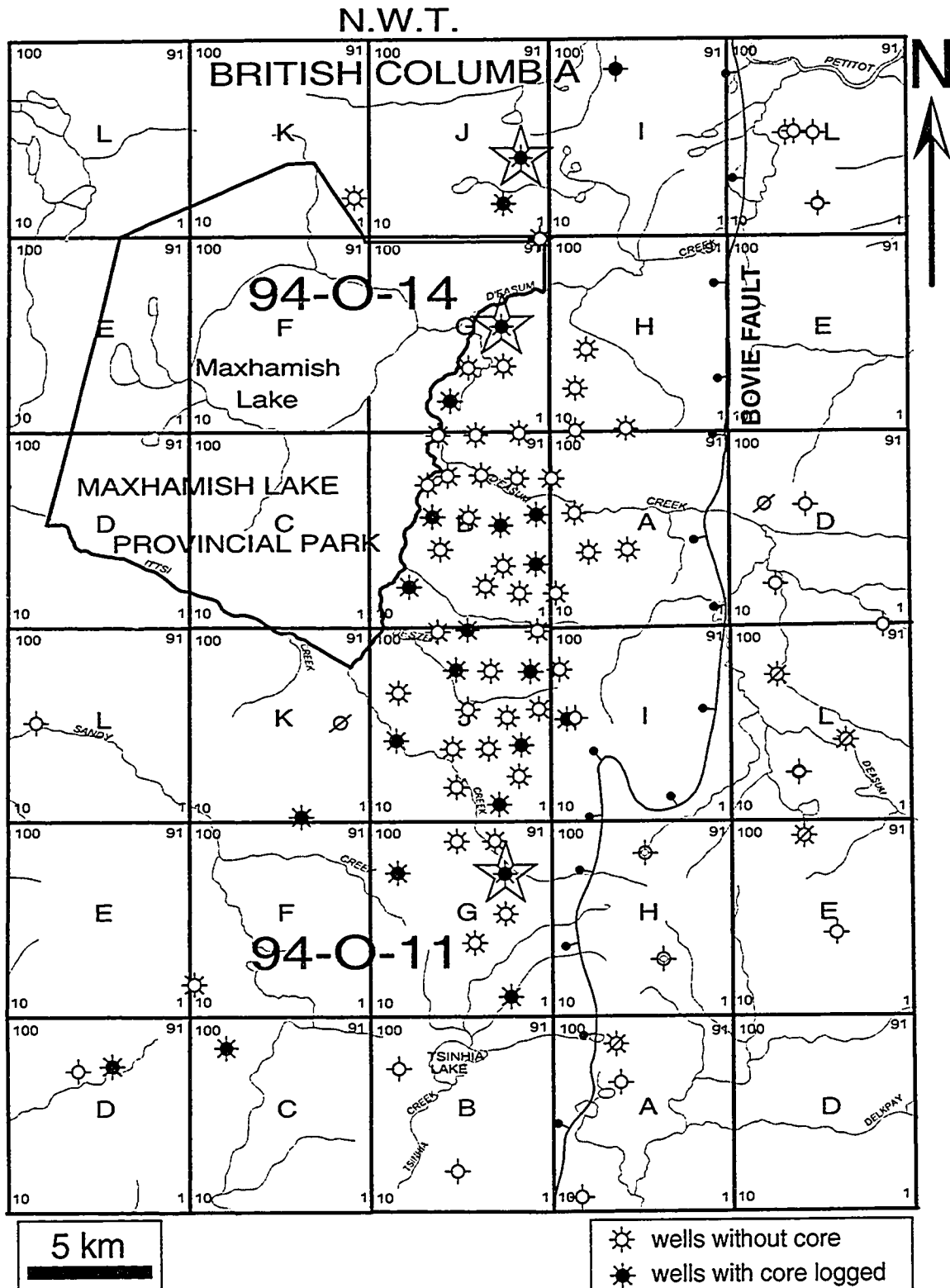


Figure II-8. Well locations within the study area. Stars indicate location of wells with cores described within this chapter (see Figures II-10, II-11, and II-12). The Bovie Fault scarp is traced along the eastern edge of the map.

Lithologic Accessories		Ichnological Symbols		Sedimentary Structures	
	Glauconite		<i>Arenicolites</i>		Synaeresis cracks
	Pyrite		<i>Chondrites</i>		Hummocky cross-strat.
wd	Wood fragments		<i>Cylindrichnus</i>		Cross-stratification
	Coal laminae		<i>Diplocraterion</i>		Soft sediment deformation
	Shale laminae		<i>Fugichnia (Fu)</i>		Planar bedding
	Pebble lag/ conglomerate		<i>Helminthopsis</i>		Ripple Laminations
Contacts				Lithology	
	<i>Glossifungites</i> surface		<i>Palaeophycus (Pa)</i>		Silty shale
	Unconformity		<i>Planolites (Pl)</i>		Sandstone
Burrow Abundance			Root Traces		Shaly sandstone
	Abundant		<i>Skolithos (Sk)</i>		Interbedded sandstone and shale
	Common		<i>Teichichnus (Te)</i>		Shale
	Sparse		<i>Thalassinoides (Th)</i>		Pebbly sandstone
	Absent		<i>Zoophycos (Zo)</i>		Lost core

Figure II-9. Legend of symbols used within litholog descriptions (Figures II-10, II-11, and II-12).

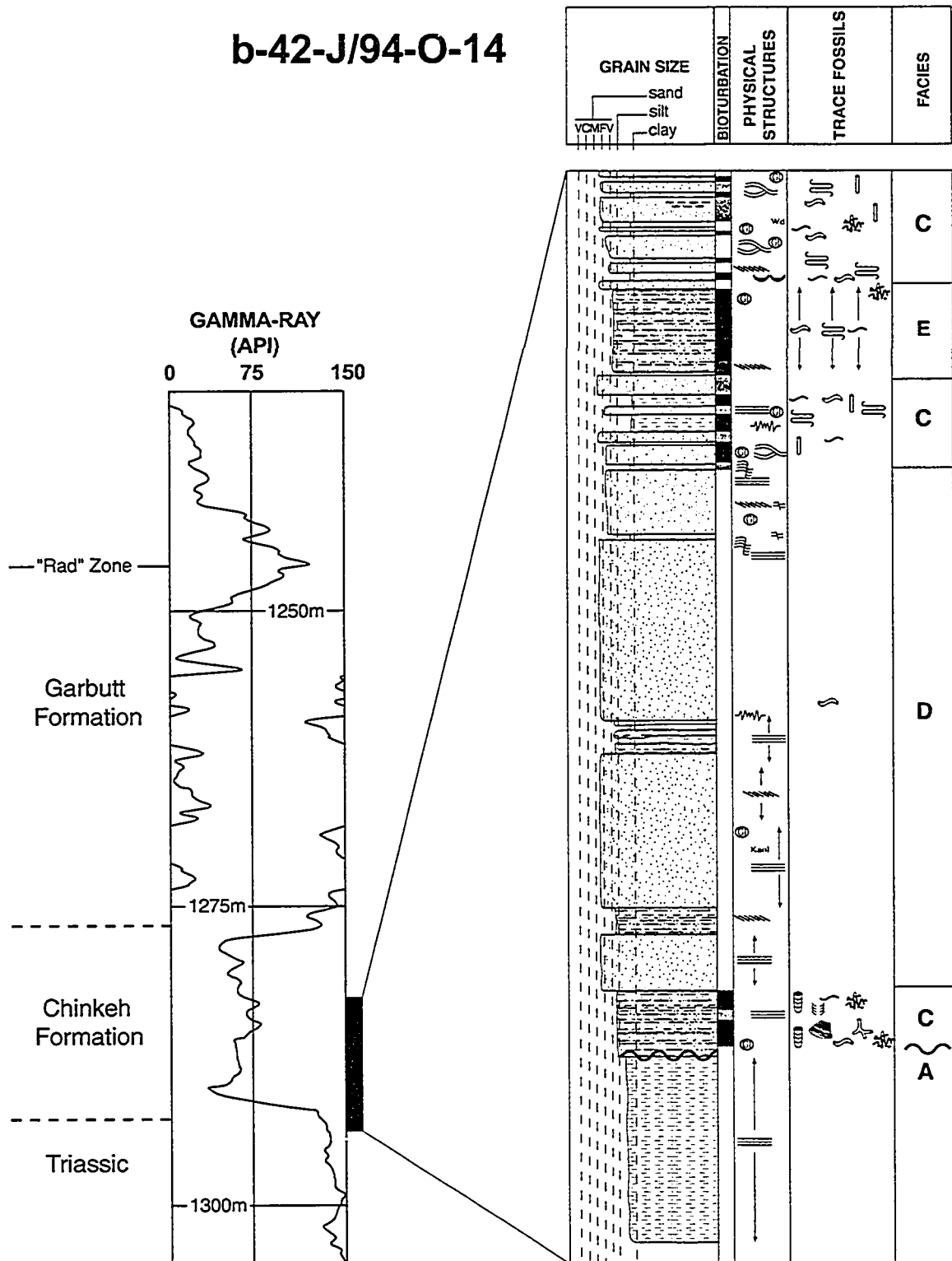
b-42-J/94-O-14

Figure II-10. A typical well (b-42-J/94-O-14) from the northern portion of the subsurface study area. See Figure II-9 for a legend of symbols used. Well location is shown in Figure II-8.

b-53-G/94-O-14

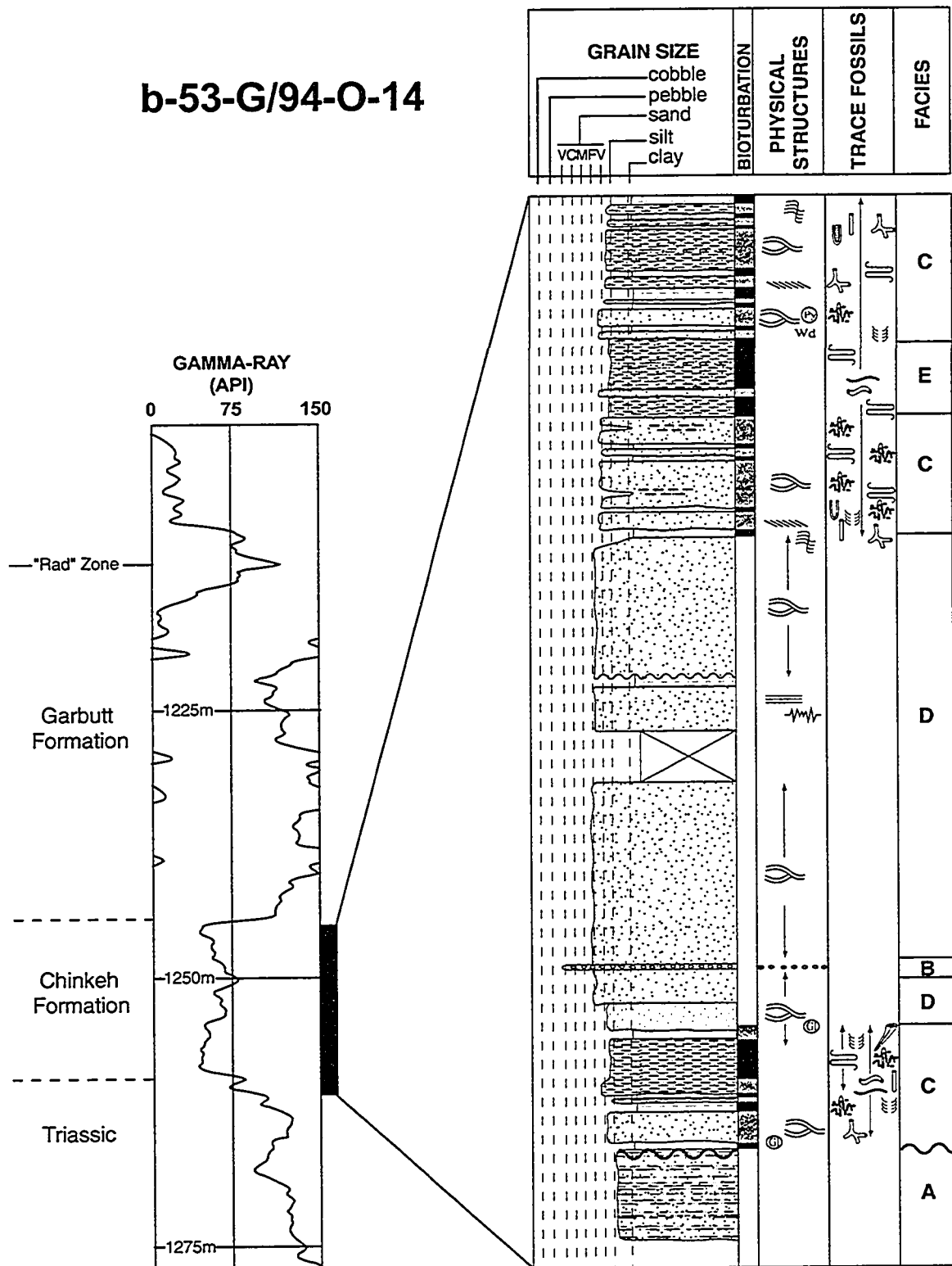


Figure II-11. A typical well (b-53-G/94-O-14) from the central portion of the subsurface study area. See Figure II-9 for a legend of symbols used. Well location is shown in Figure II-8.

b-73-G/94-O-11

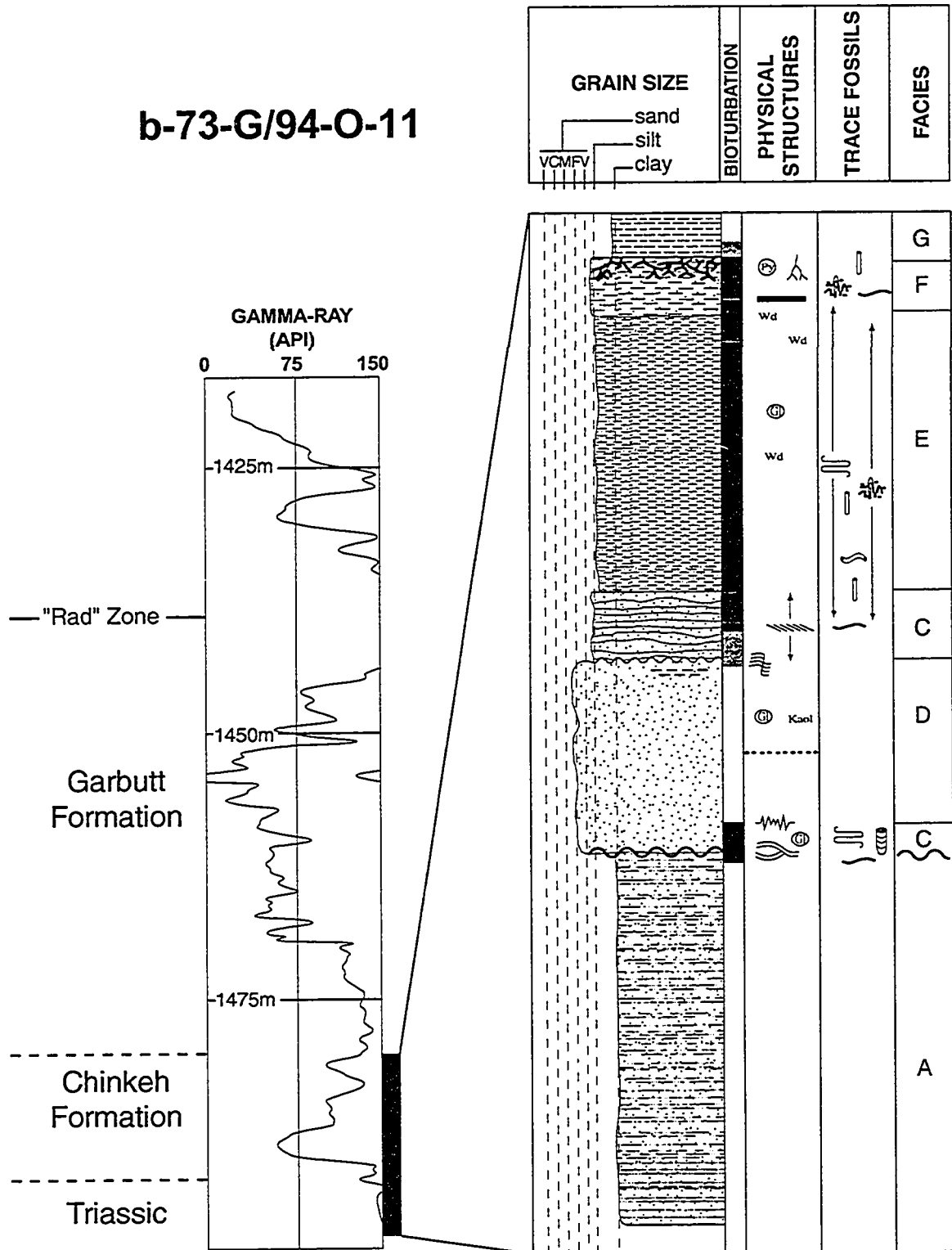


Figure II-12. A typical well (b-73-G/94-O-11) from the southern portion of the subsurface study area. See Figure II-9 for a legend of symbols used. Well location is shown in Figure II-8.

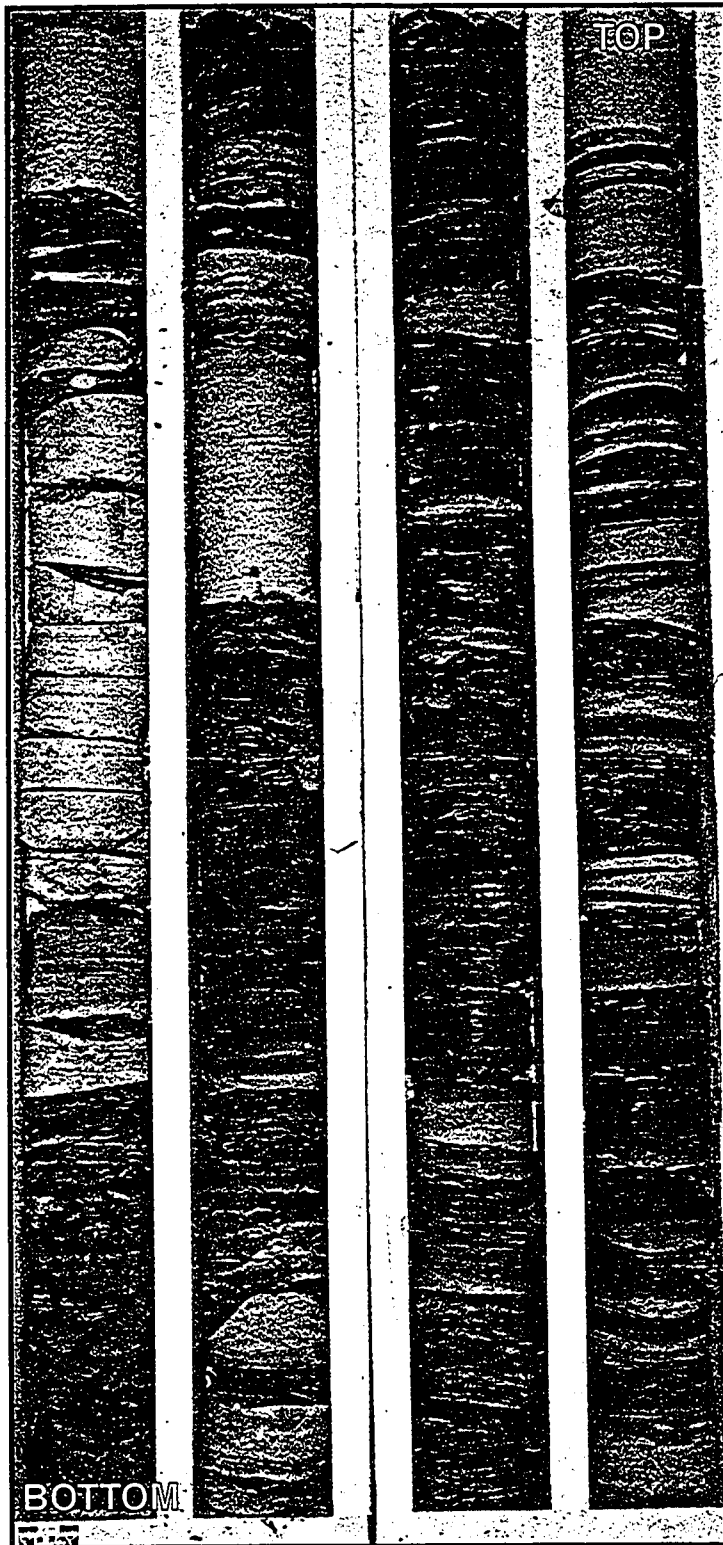


Figure II-13. Typical photo of the Triassic strata at Maxhamish Lake (d-75-D/94-O-11, core #1, boxes 6&7). Note the cyclical nature of the strata, that are well interbedded with silts and shales.

rocks becomes more evident as one moves westward across the study area, that these could be the distal expression turbidites deposited off the continental shelf (Davies, 1997). At Maxhamish there is no production associated with these Triassic beds.

FACIES B: CHERT-PEBBLE CONGLOMERATE

Description

Facies B is composed of two types of conglomerates: matrix and clast supported. Where present, the basal conglomerate represents the first Cretaceous sediments deposited on tilted Triassic shales within the Liard Basin. Conglomerate beds of Facies B do not achieve a thickness of more than 30 cm, and are commonly 10-20 cm thick.

Clasts are dominantly composed of chert and pyritized wood fragments. In general, no imbrication of clasts was noted. Clast size is highly variable, ranging within the same bed from very coarse sand to pebble size, with long axes typically ranging in length from 0.5 cm to 2 cm, and exceptionally large clasts having long axes of greater than 5 cm. The wood fragments noted within these basal conglomerates, are generally small (0.5 cm in length), and in general have long axis orientations which are low in angle or near horizontal. In the case of the clast supported conglomerate, clast size as a whole is smaller, and contains no pyritized wood fragments (Figure II-14).

Where present the matrix within the conglomerate is the same as the overlying sandstones. The matrix is very fine to fine-grained, quartz arenites, glauconite-rich, and well sorted. The overlying contact with facies C is very sharp. There are no biogenic structures associated with facies B.

There is a direct correlation between distance from the Bovie Fault and the nature of the conglomerate preserved at the base of the Cretaceous sandstones at Maxhamish. Where preserved proximal to the fault, matrix supported conglomerates prevail, while cores further from the fault or more basinal, display clast supported conglomerates.

Interpretation

Facies B is interpreted to be a transgressive lag and at Maxhamish, representing the reworking at the Triassic-Cretaceous unconformity. Where present the facies sharply mantles underlying Triassic strata. The presence of well sorted, and well rounded conglomerates indicates that there was considerable winnowing and reworking of these clasts. On occasion facies B appears displaced, and does not sit on top of the Triassic

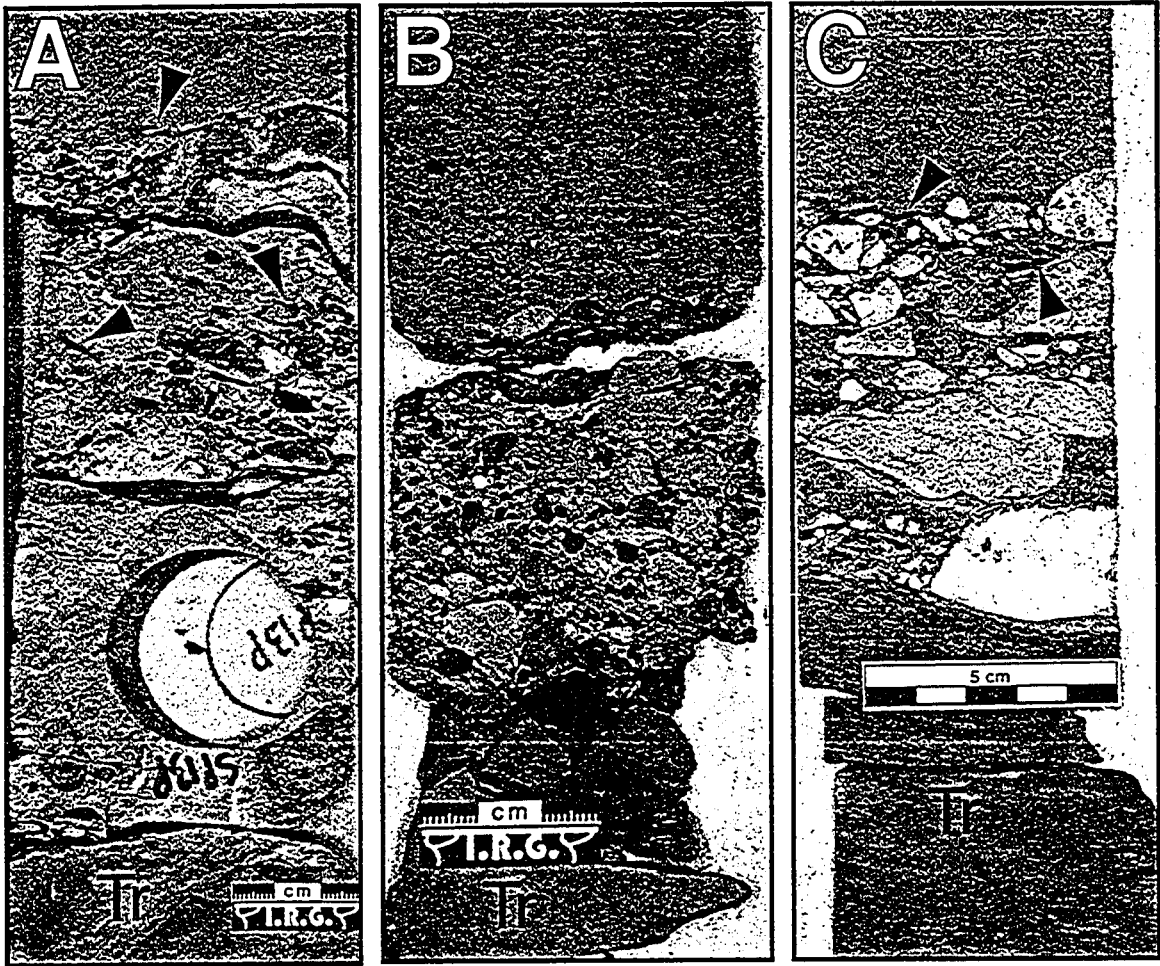


Figure II-14. Examples of Facies B: Matrix and clast-supported chert-pebble conglomerate sitting unconformably on Triassic shales (Tr) along the eastern boundary of the Bovie Fault. Note the sharp upper and lower contacts in all three photos, and the abundant wood fragments (arrows).

Photo A: Bi-modal, matrix supported conglomerate with abundant pyritized wood fragments (arrows).

b-4-K/94-O-11, 1716.0m

Photo B: Well-sorted, sub-rounded to rounded, clast-supported, chert pebble conglomerate. Note the small chert clasts within the overlying sandstone (Facies C), indicating reworking of the conglomerate.

d-76-J/94-O-11, 1553.0m

Photo C: Angular chert clasts with abundant pyritized wood fragments (arrows).

b-88-C/94-O-11, 1678.1m

unconformity (Figure II-11). In these cases, the chert-pebble conglomerate has been reworked, and retransported by wave and storm energies. In essence, the conglomerate which was once found at the base of the lower Cretaceous sandstones, was redistributed by wave energy and exists as pebble stringers within the sandstones of facies C.

The main delivery mechanism for large pebble clasts at the base of the Lower Cretaceous sandstones is fluvial. The antecedent Mississippian cored, topographic high of the Bowie Fault is a likely source area for the delivery of chert-rich clasts into the basin. As base level rose during the deposition of the main shoreface sandstones (Facies D), and marine deposition encroached from the north-west to the north-east (Williams and Stelck, 1975), fluvial processes waned. The pebbles and cobbles once carried into the basin, were now being reworked during the transgression of the Aptian Sea.

The dominance of chert within the conglomerates supports the conclusion that erosion of Permian and Mississippian strata along the Bowie Fault was the source for the cherts at the Triassic-Cretaceous unconformity.

FACIES C: LAMINATED SANDS AND BIOTURBATED SHALES

Description

Well laminated, glauconite-rich quartzose sandstones interbedded with heavily bioturbated silty shales makes up facies C of the Lower Cretaceous sandstones at Maxhamish (Figure II-15). The sandstones of facies C are very finely laminated displaying alternations of glauconite/non-glauconite-rich laminations. Horizontal pebble stringers and rare pyritized wood fragments are common at the base of this facies when overlying facies B. The wood fragments are very well rounded and never exceed 0.5 cm in diameter. Facies C is widespread across the entire study area, and is found both underlying and overlying facies D, which comprises the reservoir facies at Maxhamish. In both instances the change is gradational, moving upwards from facies C to D, or from facies D to C.

Sedimentary structures observed in this facies include: hummocky cross-stratification, swaley cross-stratification, and rare ripple lamination. The bottoms of these bedforms show well developed and distinct scour surfaces, while the upper contacts with shales are bioturbated, obliterating most sedimentary structures. Depths of observed traces penetrating into the underlying well-laminated sandstones are generally 10-20 cm. Overall thickness of these sand units is usually between 10-30 cm thick.

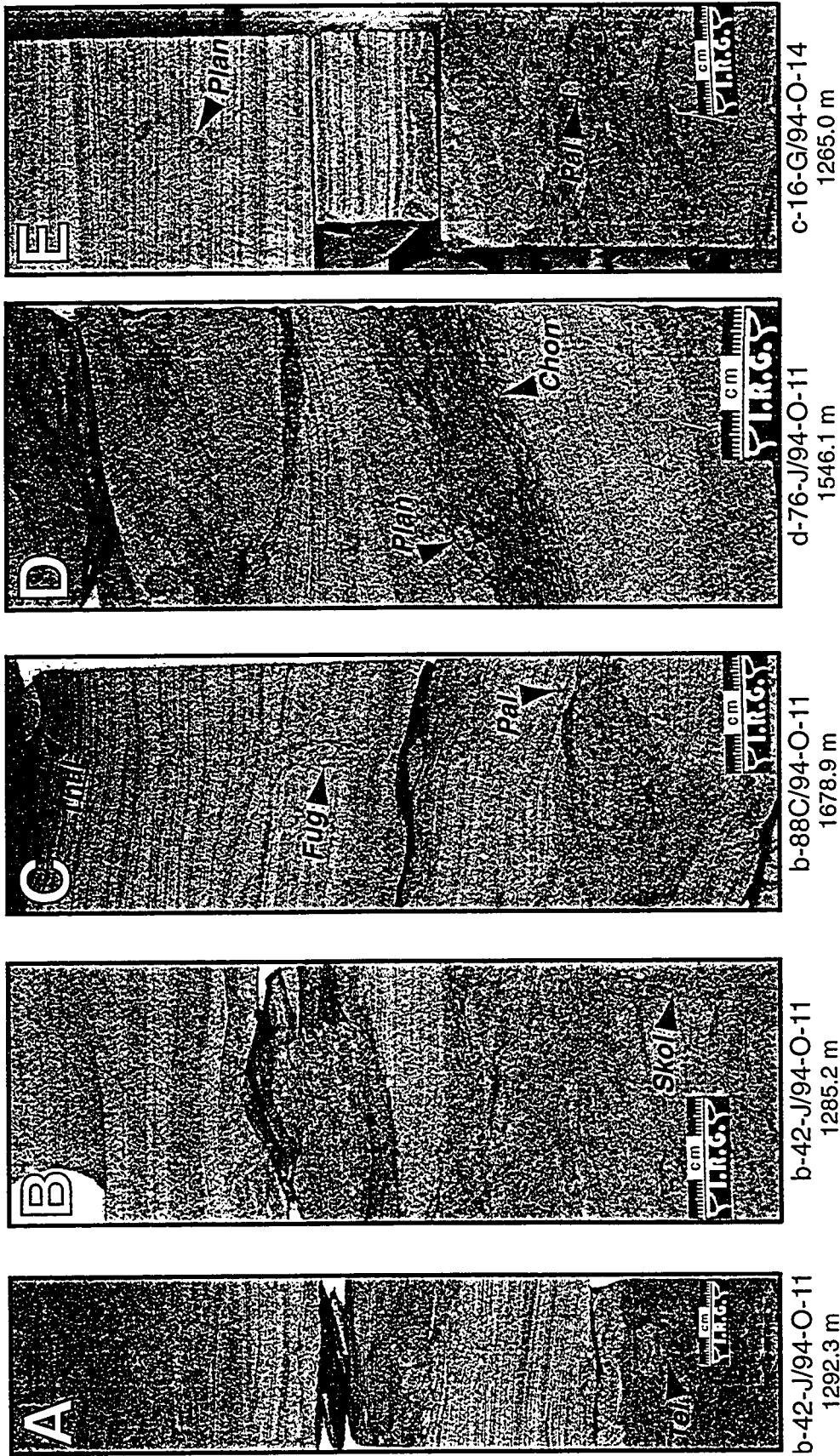


Figure II-14. Core examples of Facies C consisting of fine-grained hummocky cross-stratified sandstone with bioturbated mudstone interbeds (lam-scam). Trace fossils include *Teichichnus* (*Tei*), *Skolithos* (*Skol*), *Thalassinoides* (*Th*), *Paleophycus* (*Pal*), escape traces (*Fug*), *Planolites* (*Plan*) and *Chondrites* (*Chon*). Note the convex-up laminations in photo A (arrowed), and the erosive scours in photos C and D (examples arrowed).

Bioturbation within this facies is characterized two-fold. First are the traces observed within the fine-grained silty shales. These interbeds are highly bioturbated, and where discernible *Chondrites*, *Helminthopsis*, *Planolites*, *Palaeophycus*, and rare *Zoophycus* are observed. These biogenic structures are characteristic horizontal deposit feeding traces of the *Cruziana* ichnofacies. These finer grained bioturbated shale beds do not reach thicknesses of more than 20 cm and are commonly observed to be between 5-10 cm thick.

Secondly, these traces are cross-cut by a subsequent set of biogenic structures, which include: *Skolithos* (up to 15 cm in length), *Thalassinoides*, *Teichichnus*, and escape traces (i.e. Fugichnia). The majority of the biogenic structures within this assemblage show suspension feeding behavior that represents elements of the *Skolithos* ichnofacies. This assemblage of traces is found: (i) within the well-laminated hummocky and swaley cross-stratified sandstones, (ii) cross-cutting primary bedding and traces of the *Cruziana* ichnofacies mentioned above. In some cores it has been observed that portions or complete sections of the bioturbated shales are missing, and only the deeply penetrating vertical burrows remain. In these cases, scours and the preserved vertical traces reveal concealed bed junctions, where portions of traces have been erosionally planed-off during deposition of the overlying bedset.

Interpretation

Facies C is interpreted to be the distal expression of storm deposition within the lower shoreface. The nature of the deposit, with laminated hummocky and swaley cross-stratified glauconite-rich sandstones, interbedded with bioturbated silty shales is indicative of lower shoreface deposits. While the exact mechanism for producing large wavelength bedforms of hummocky and swaley cross-stratification has been debated in the literature (Duke *et al.*, 1991), it is generally agreed that these bedforms form below fair-weather wave base during intense storms (Harms *et al.*, 1975, Dott and Bourgeois, 1982, Hunter and Clifton, 1982). In general, these interbedded lower shoreface deposits have been termed “laminated to burrowed” bedding (Howard, 1972).

Characteristically these laminated to burrowed beds record a transition from quiescent, fairweather conditions to abrupt and rapid sedimentation demarcated by an erosive or scour surface. The abundance of trace fossils within these finer-grained beds, and the ubiquitous cross-cutting relationship, supports slow continuous deposition with little preserved record of storm events (Howard, 1975). This transition zone, within

the lower-middle shorface complex records both storm and fairweather conditions. As a result of rapid deposition of storm beds, escape traces (fugichnia) record the attempt of organisms to burrow up through the tempestite in order to reach the new sediment-water interface (MacEachern and Pemberton, 1992). These recently displaced infaunal organisms have the opportunity to exploit new nutrient rich storm beds. The products of their opportunistic feeding strategy are the cross-cutting relationships observed. In addition, the scouring action of storm deposits preferentially preserves the more deeply penetrating traces (i.e. the *Skolithos* Ichnofacies) above the storm laminated sands, and removes the shallow penetrating traces (i.e. the *Cruziana* Ichnofacies) (Frey and Goldring, 1992, and Pemberton and MacEachern, 1997).

FACIES D: WELL SORTED QUARTZOSE SAND

Description

The clean, well-sorted fine-grained sandstones of Facies D appear massive, with subtle sedimentary structures. Slightly inclined parallel to sub-parallel laminations and moderate amounts of glauconite are noted throughout. Bedding contacts within the facies are generally sharp, and slightly erosive where observable changes in the orientation of lamina sets is observable. Series of stacked beds comprising parallel to sub-parallel lamina are occasionally capped by oscillation and combined flow ripples. The preservation of ripples is low since truncation surfaces are common throughout this facies. The truncation surfaces are demarcated by the low angle intersection ($< 10^\circ$) of parallel to sub-parallel lamina.

There is a lack of bioturbation within the sandstones, with only rare *Palaeophycus* and escape traces are present (Figure II-16). Where the facies becomes more interbedded (near the transition to facies C), the number and abundance of traces increase.

The lower gradational contact of this facies overlies the much more interbedded, bioturbated, and laminated facies C. Occasional pyritized wood fragments, and pebble stingers were observed near the base. An overall grain-size increase throughout these sandstones is noted ranging from lower fine-grained at the base to upper fine-grained near the top of the facies. The thickest continuous sandstones within this facies are no more than 6 m thick, with an average thickness of approximately 3 m.

In addition to the somewhat massive appearing sandstones, *Syringopora* coral fragments have also been observed within the clean quartzose sandstones at Maxhamish

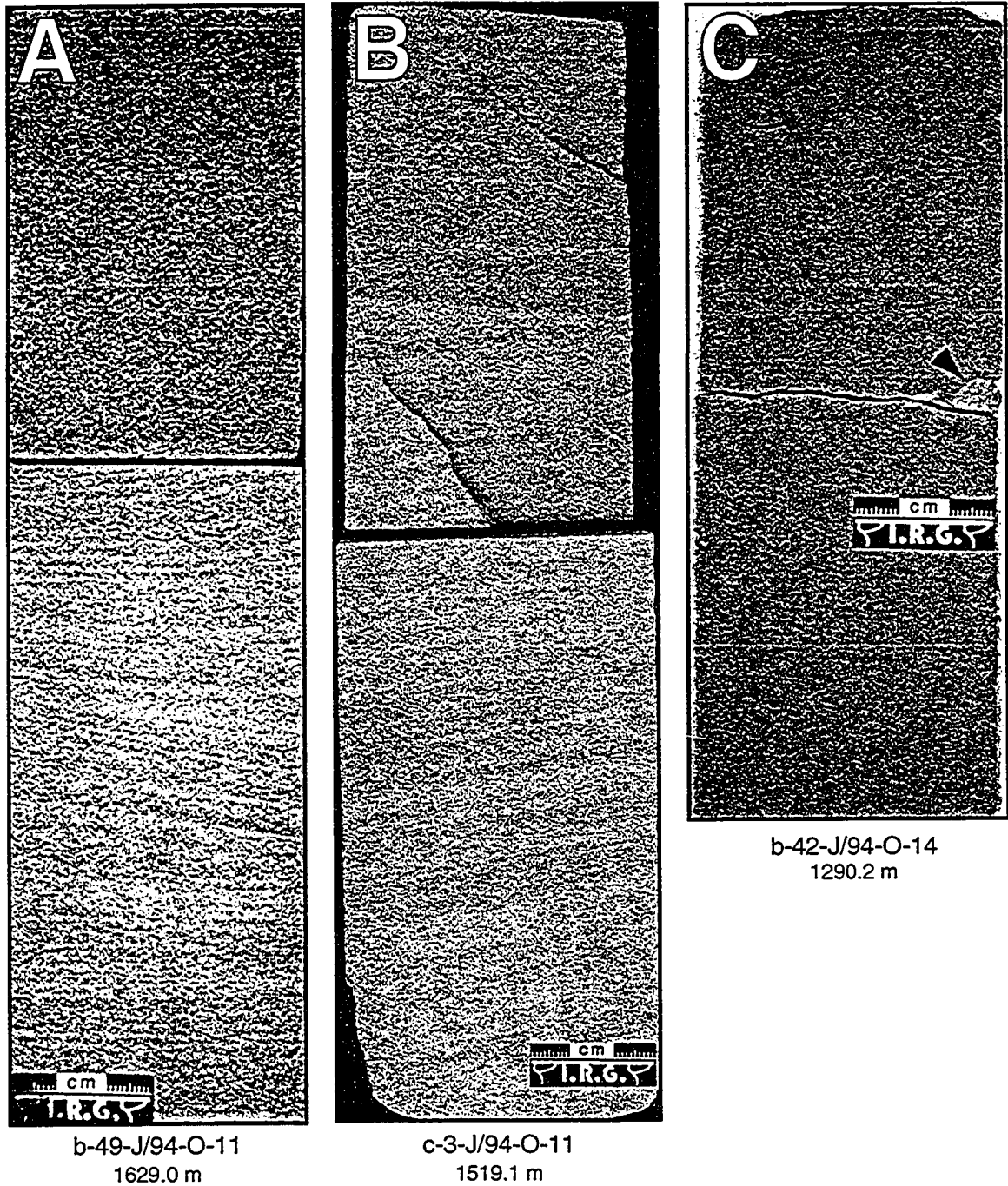


Figure II-16. Core examples of Facies D consisting of fine-to medium grained swaley, cross-stratified glauconitic sandstone. Note the kaolinitized mudstone clast (arrowed) in photo C.

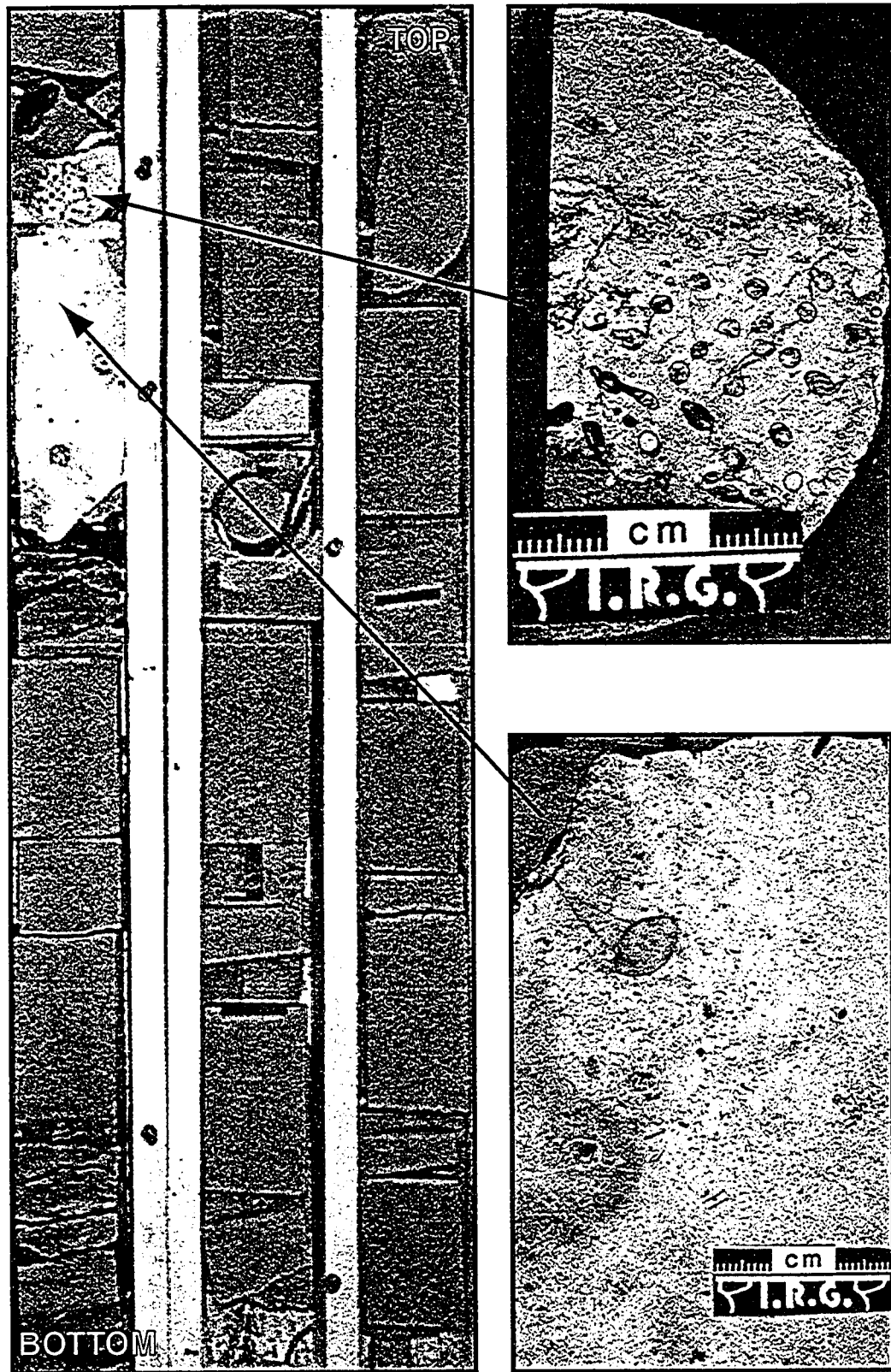


Figure II-17. Detail of carbonate clast within Facies D (c-3-J/94-O-11, 1499.3 m). Note the detail of the columnals of the colonial *Syringopora* in Photos B and C. This genus is Mississippian in age and is eroded from older strata along the Bovie fault scarp.

(Figure II-17).

Through thin-section analysis it has been determined that porosity and permeability at Maxhamish was created through the leaching of glauconite. Thin-section analysis of these sandstones has also indicated that clay content is high. Clay abundances were found to be the following: kaolinite ranging from 5 to 20%, and chlorite ranging from 5-10%. The presence of these hydrophylic clays within reservoir sandstones has complicated reservoir production at Maxhamish, particularly during drilling and completion practices.

The upper contact of this facies is recognized by an increase in interbedded shale beds marking the gradational transition from facies D into facies C.

Interpretation

The quartzose sandstones of the main reservoir unit represent a shoaling upward sequence deposited by storm sedimentation within the proximal lower shoreface. Sedimentary structures within these reservoir sandstones are difficult to observe due to the leaching effect of glauconite, which tends to obliterate most sedimentary structures. However subtle grain-size variations within laminae-sets, and slight mineralogical variation across lamina, do highlight cyclical bedding of amalgamated bed sets. The amalgamation within this facies consists of low angle sub-parallel planar laminations, which are interpreted to represent the amalgamated hummocky cross-stratified (HCS) sandstones. The occurrence of escape traces within the storm beds records the presence of animals entrained within or buried by the storm bed. Their movements through the sediment are preserved in response to regain the new sediment-water interface. The erosional amalgamation of successive tempestites accounts for the lack of biogenic structures within this facies.

The high degree of storm dominance within facies D, makes it difficult to determine lower shoreface from middle shoreface deposits. When preserved, it is the fair-weather trace fossil assemblage which characterizes the two zones (Howard, 1972; 1975). In addition, the greater the storm-dominance, the deeper and further offshore storm-weather wave base is shifted. As a result, lower shoreface deposits may in fact be deposited below fair-weather wave base. In general, the amalgamated nature of these storm deposits makes it impossible to determine where fair-weather wave base deposits were deposited.

As in the underlying facies (Facies C well laminated sandstones and interbedded

bioturbated shales), this facies (Facies D) represents more proximal deposition. The effect of which is the erosion and non-preservation of quiescent, fairweather sedimentation (i.e. the bioturbated shales). They are simply absent from the rock record, and because of the decrease in relative base level, stacked storm sandstones result. Generally, it is not uncommon for middle shoreface sandstones to show little or no burrowing due to shifting substrates, and high water energies (MacEachern and Pemberton, 1992). It is impossible however to determine whether the absence of biogenic structures is due to intense storms (greater erosional amalgamation), or to high frequency of storm events (minimal time for re-establishment of benthic communities). What is evident however, is that variation to the idealized sequence of HCS bedding can lend valuable insight into the proximity of sedimentation within the lower shoreface (Dott, 1983). While Facies C and D appear to be similar and interpreted to have been deposited within the lower shoreface, there are marked differences. Facies C contains a mixed assemblage of *Skolithos-Cruziana* ichnofacies, which are interbedded with HCS sandstones. Within the overlying facies (facies D), a thicker interval of amalgamated HCS sandstones exist, with a much less diverse assemblage of traces (mostly escape traces). Facies D is interpreted in shallow regions of the lower shoreface.

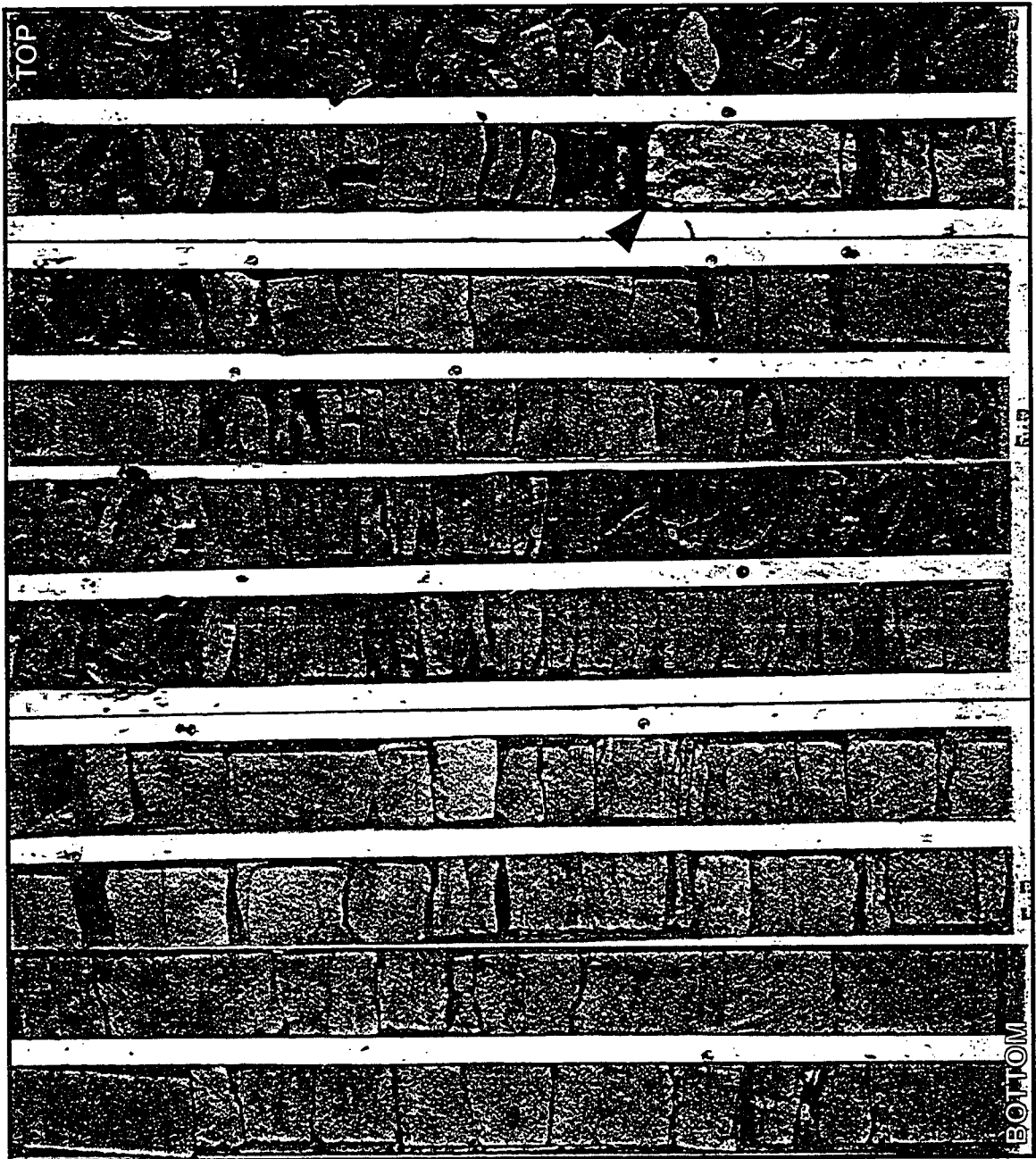
Coral fragments observed within these middle shoreface sandstones are sourced from the paleogeographic high adjacent to the study area. It is believed that these coral fragments are most likely Mississippian in age (C.R. Stelck, *pers. comm.*, 1999), and are reworked deposits from the Bovie Fault, adjacent to the study area. This can be used as evidence for movement of the Bovie Fault syndepositionally to the deposition of Lower Cretaceous sandstones at Maxhamish.

FACIES E: BURROWED SILTS WITH ABUNDANT WOOD FRAGMENTS

Description

Bioturbated silts and shales with abundant pyritized wood fragments characterize Facies E (Figures II-18 and II-19). It consists of fissile, dark coloured shales with variable silt content. Thin (< 3 cm) siltstone and very fine-grained sandstone beds are interspersed throughout the facies. These beds are generally void of any sedimentary structures, however rare ripples and low angle wavy parallel laminations have been observed. Generally, intense biogenic reworking overprints the sedimentary structures

Figure II-18. Gross aspect of Facies E b-73-G/94-O-11, core #1, boxes 1-5). Note the arrowed horizon (1481.1m), consisting of a rooted, *Glossifungites* burrowed surface (see Figure II-20).



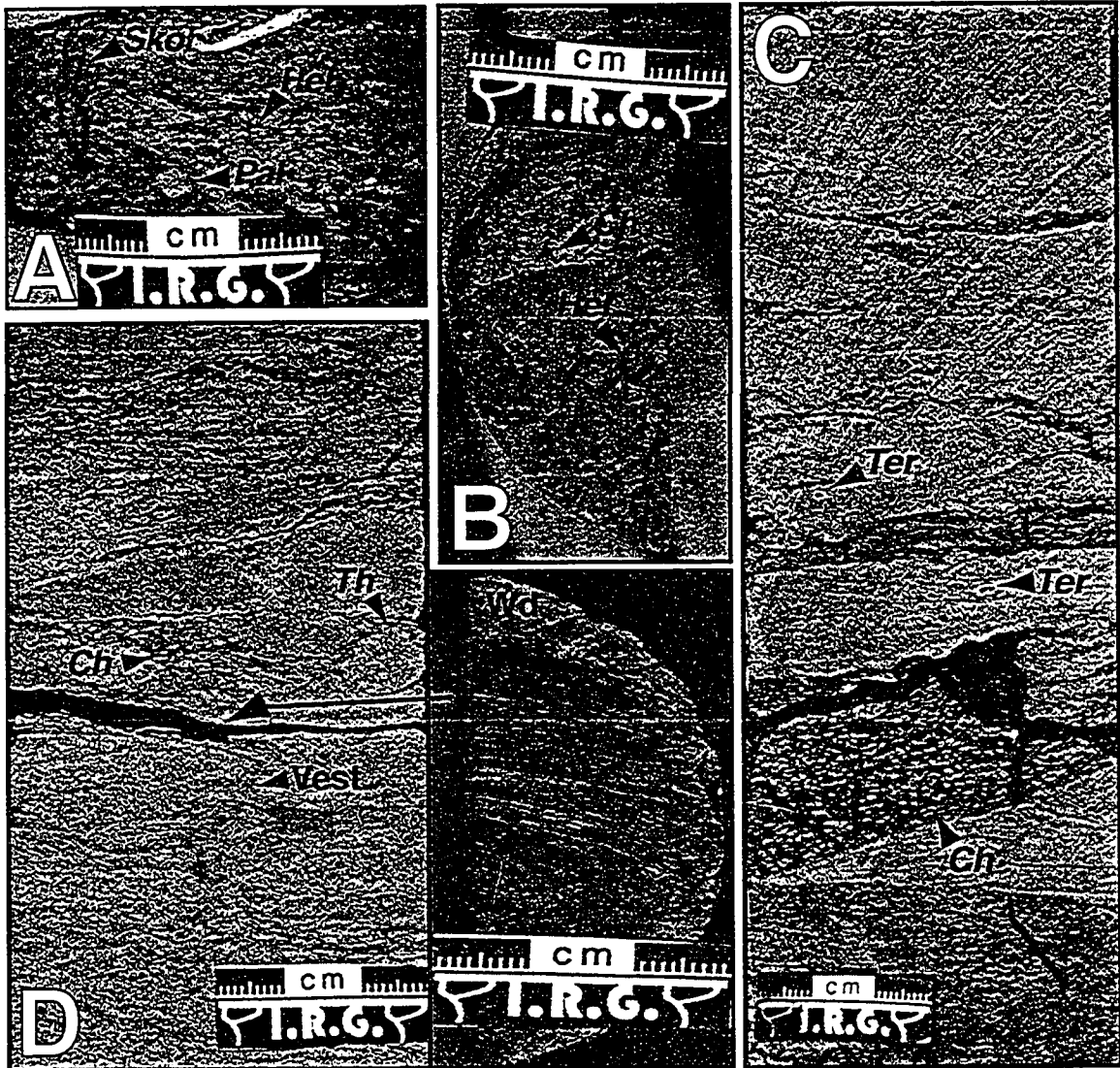


Figure II-19. Detailed photographs of Facies E.

Photo A: Small and diminutive *Skolithos* (*Skol*), *Palaeophycus* (*Pal*), and *Helminthopsis* (*Hel*) (c-3-J/94-O-11, 1494.6 m).

Photo B: Branching *Chondrites* (*Ch*) and *Helminthopsis* (*Hel*) on bedding plane (c-16-G/94-O-14, 1243.0 m)

Photo C: Interbedded lower contact of Facies E with Facies C (d-72-J/94-O-11, 1420 m). Note the well laminated sandstones containing *Terebelina* (*Ter*), interbedded with highly bioturbated shales containing abundant *Chondrites* (*Ch*).

Photo D: Silty vestigial (vest.) laminations interbedded with well bioturbated shale laminations. Traces present include: *Chondrites* (*Ch*), and *Thalassinoides* (*Th*). Arrow indicates location of adjacent photo along bedding plane showing wood (*Wd*) fragments, that are characteristic of Facies E.

within the coarser grained beds. This reworking gives the facies a highly mottled look, where it is difficult to discern physical sedimentary structures. The thin beds do not constitute more than 10% of the facies, and become less common upwards. Facies E grades from facies C (laminated sandstones and bioturbated shales), where the sand content decreases, and the relative amount of bioturbation increases dramatically. The thickness of the facies varies across the study area. In the east it thins to 1.5m along the Bovie Fault, and thickens to over 7m in the west and north (Figure II-3 and II-12). Facies E is sharply overlain by the bioturbated and rooted *Glossifungites* surface F. Mineralogically facies E becomes much more glauconite-rich near the top, at the contact with surface F, and displays a characteristic green colour.

Characteristic of this facies are large pyritized wood fragments that are often larger than the diameter of the core and present on nearly every bedding plane examined within this facies. The wood fragments are very well preserved due to pyritization, where internal lamination of the wood grain can be observed (Figure II-19).

Individual trace fossils are difficult to observe due to the extent of reworking. Where observed, the assemblage consists of: *Palaeophycus*, *Planolites*, *Helminthopsis*, *Chondrites* and in-situ? *Terebelina* (Figure II-19).

Interpretation

The silty shales of facies E are interpreted to be deposited in the offshore, and represent a flooding event due to a rise in relative base level. Relative to the underlying facies C, the characteristics within facies E represent a basinward shift in deposition. The only significant physical sedimentary structures present are remnant parallel laminations and rare ripple laminations. These are interpreted to represent the distal expressions of storm events, transporting coarser-grained sands into the offshore. Since these distal storm beds are deposited well below fair-weather wave base, physical processes during non-storm periods are not competent to modify them, and hence, such beds have a high preservation potential (Dott, 1983, 1988). The combination of slow rates of sedimentation, brief storm events, and long periods of relative quiescence results in an environment dominated by biogenic processes (Howard and Reineck, 1981). Facies E is dominated by a high abundance of grazing/foraging traces, which corresponds to the distal *Cruziana* Ichnofacies.

The presence of abundant wood fragments within this facies is the result of the in place drowning and subsequent basinward transport of woody debris along the margin of

the Liard Basin. With the increase in relative sea-level, the drowning, entrainment and basinward transport and deposition of this debris is plausible.

The northwest thickening of this facies indicates a seaward incursion originating from the northwest. Relative sea-level changes within the encroaching Boreal Sea from the north would be recorded within this basin. In addition tectonic movement syndepositional to the deposition of facies E, would also influence the accommodation space within the Liard Basin. This could be the result of tectonic subsidence in the foreland basin (Cant and Stockmal, 1989), or movement of the Bovie fault, both resulting in a relative rise in sea level.

SURFACE F: GLAUCONITE-RICH, ROOTED AND BURROWED SILTSTONE

Description

Surface F is relatively thin (10-20 cm) and consists of rooted silty shales, which are cross-cut by vertical burrows filled with fine-grained glauconite-rich sand. A distinctive green colour is observed within the burrows, due to the abundance of glauconite, which is characteristic of this surface. This surface is only preserved within the central portion of the study area, and in relative proximity to the Bovie Fault. Where preserved, the surface sharply overlies facies E (offshore shales) and is in turn sharply overlain by deep marine shales of the Garbutt Formation (facies G).

Most primary sedimentary structures have been biogenically reworked, and as a result the surface appears highly mottled. Root traces descending a few centimeters into the bioturbated silts are cross-cut by the vertical, sand-filled burrows (Figure II-20). Occasional vestigial laminations and planar parallel laminations are observed. Abundant wood debris and wood fragments are evident on most bedding surfaces, and range in size from a few centimeters to the full diameter of the core.

Characteristic of this surface is the extensive bioturbation. Long *Skolithos* burrows (up to 15 cm) are preserved and subsequently filled with green glauconitic sand (fine to medium grained), which is much coarser than the surrounding silty matrix.

Interpretation

Surface F represents an amalgamated sequence boundary and marine flooding surface. This surface is demarcated by preserved subaerially exposed rootlets, which are

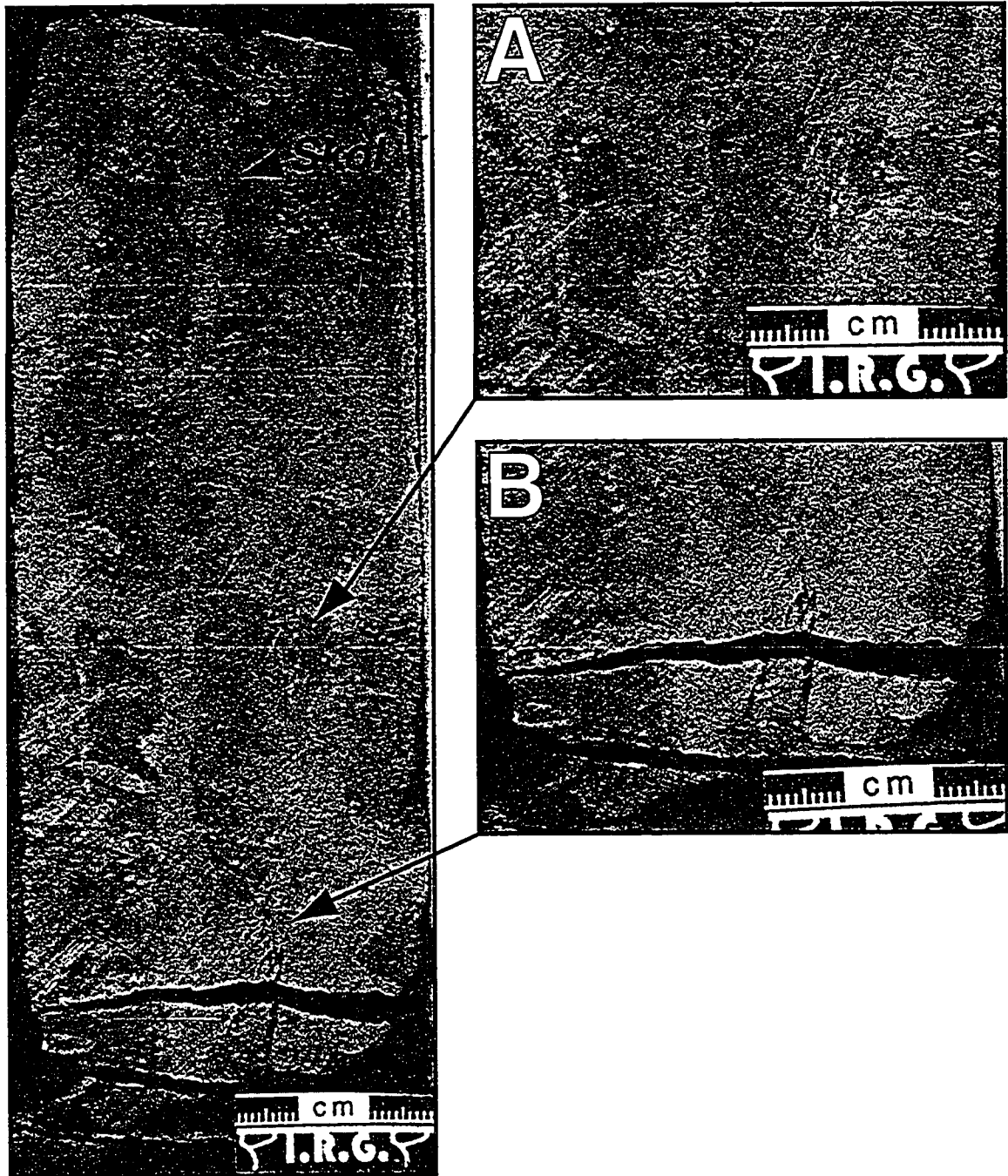


Figure II-20. Detailed photographs of *Glossifungites* surface (overview photo was shown in Figure II-19) (d-73-G/94-O-11, 1418.1 m). The suite consists of large, glauconite-filled *Skolithos* (Skol), cross-cutting a low-angle laminated silty mudstone. The mudstone contains abundant carbonaceous roots (arrowed) suggesting a subaerial exposure surface. The burrows cross-cut this suite and are typically associated with transgression. This horizon is interpreted to represent coeval LSE/TSE.

subsequently burrowed by a *Glossifungites* suite of *Skolithos* and passively in-filled.

The *Glossifungites* ichnofacies consist of robust, unlined and sharp-walled, dominantly vertical dwelling and suspension structures, which are predominantly excavated into erosional exhumed, dewatered and stiff substrates (Pemberton and MacEachern, 1992). The presence of such structures also demonstrates that erosional exhumation of the substrate was not immediately followed by preserved depositional cover; colonization of the exhumed substrate must predate significant depositional cover (Pemberton and Frey, 1985). The stiff nature of the substrate permits the dwelling structures to remain open after they are vacated by the tracemakers and therefore, they are passively filled during the deposition of the next unit.

The surface itself represents a discontinuity associated with a depositional hiatus and the subsequent erosion and passive in-fill associated with transgression. In essence colonization of the exhumed surface post-dates erosive shoreface retreat, but occurs prior to the significant deepening represented by the shales of facies G.

Figure II-20 shows a typical *Glossifungites* suite from Maxhamish. It is evident that there is some degree of stacking to the surface, in that there are multiple cross-cutting relationships between the vertical *Skolithos* and the rootlets. This stacking pattern, although irregular, and not easily discernable does support the interpretation that transgression occurred in pulses, affording multiple generations of *Skolithos* to colonize the substrate.

Regionally it is difficult to quantify the significance of this surface. It is however a surface which demarcates a lowstand surface of erosion and the subsequent transgressive surface or flooding surface. If this surface represents a significant amount of time geologically, it is possible that further basinward shoreface successions would exit coeval to the deposition and colonization of this surface. The passive fine-grained glauconitic burrow fill, does support the interpretation that sand is being transported from the basinward direction on transgression. However, due to the limited number of exploration wells west of the Maxhamish field, this interpretation will be validated with further exploration efforts within the area.

FACIES G: DARK SHALES

Description

This facies is characterized by dark marine shales, which conformably overlie the



Figure II-21. Gross aspect of Facies G (c-3-J/94-O-11, core #1, boxes 4&5), the dark, fissile shales of the Garbutt Formation.

sequence boundary at the top of the Lower Cretaceous sandstones at Maxhamish Lake (Figure II-21). Friable shales and very rare shell fragments dominate the facies. This facies sharply overlies surface F, the *Glossifungites* surface. Facies G is a very thick succession of shale, and at Maxhamish is commonly over 200 m thick. The upper contact of Facies G was never observed in core.

Since this interval does not represent an exploration target few cores exist within the facies. On down-hole geophysical logs, a spike is noted within the gamma-ray logs, and is the datum on which the cross sections in Figure II-3 and II-4 are hung. These shales are fairly nondescript with the exception of thin (3-4 cm) bentonite beds near the spike in the gamma-ray log.

Interpretation

The dark shales that sharply overlie the Lower Cretaceous sandstones at Maxhamish comprise the Garbutt Formation. These shales were deposited in a deep offshore marine setting. Since the Garbutt is not an economic target, very few cores have been cut within this interval. However, down-hole logging tools have collected data through this formation, in a number of locations within the Liard Basin.

The spike in the gamma-ray log represents a maximum marine flooding surface within the Liard Basin. High gamma-ray values, and high organic matter content reflect anoxic bottom water, which are both common during transgressions (Reynolds, 1996). This gamma-ray spike can be traced across the Bovie Fault (Dip Cross-section), and as far east as the Mc Murray trough (Williams, 1978), indicating that this marine incursion was regional in extent.

SUMMARY AND DISCUSSION

The producing Lower Cretaceous sandstones within the Maxhamish gas field of northeastern British Columbia record deposition within storm dominated lower to proximal lower shoreface setting. These sandstones grade upwards into offshore silts and shales, which are overlain by a coeval lowstand surface of erosion and transgressive surface of erosion. Distal offshore marine shales of the Garbutt Formation sharply overlie this surface and continued flooding results in a maximum marine flooding surface traceable well outside of the study area. Figure II-21 shows the interpreted depositional setting for the Lower Cretaceous sandstones within the subsurface at Maxhamish Lake.

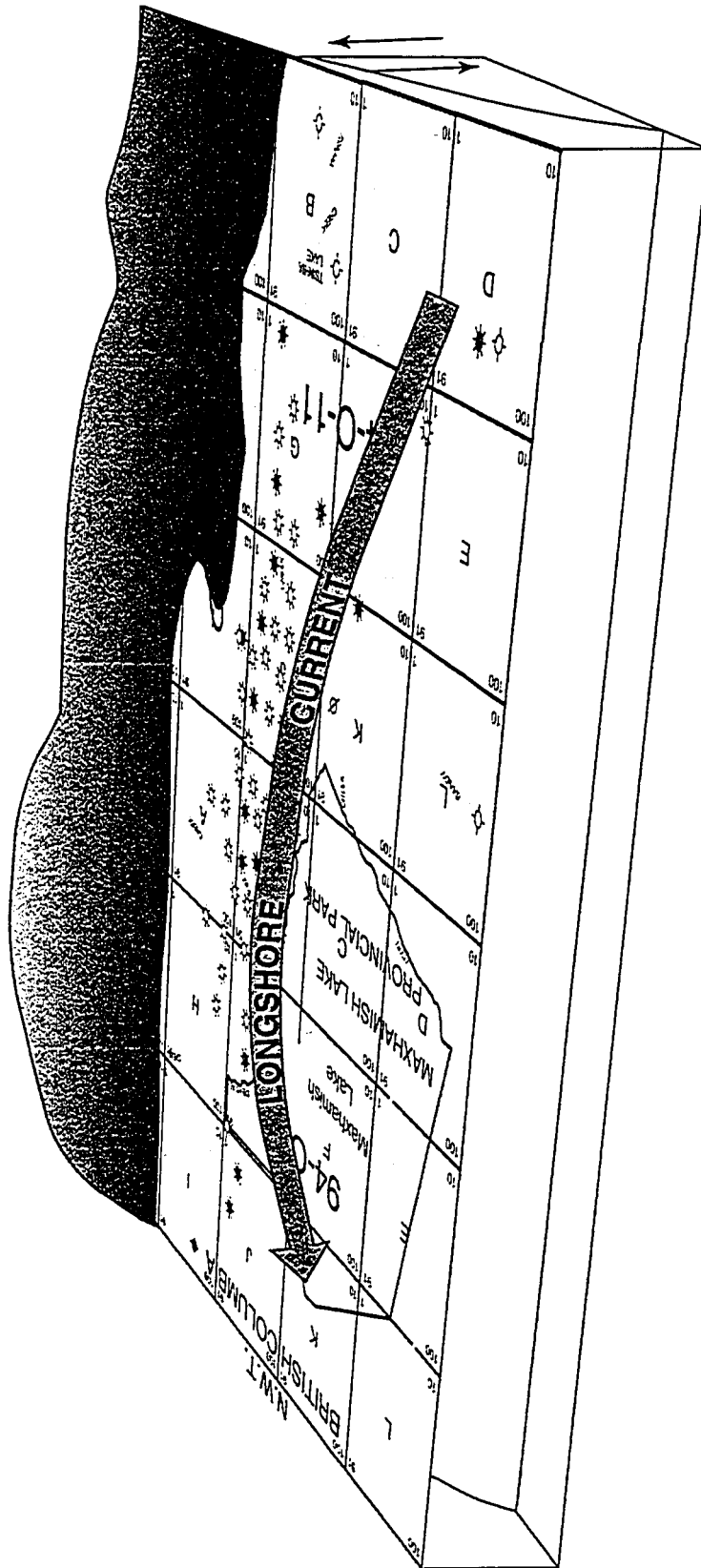


Figure II-22. Generalized schematic diagram illustrating the depositional setting interpreted within the study area for the Lower Cretaceous sandstones. The Bowie Fault is shown as a topographic high during the deposition of the oldest Cretaceous rocks into the Liard Basin. Longshore currents act in a shore parallel direction, distributing reservoir prone facies along the Bowie Fault (see Figure II-7).

While it is somewhat enigmatic in its origin, the Bovie fault has played an important role in the emplacement and localization of sands along its margin. Initially, the Bovie Fault, with Mississippian and Permian strata exposed at surface, acted as a point source for the delivery of coarse pebble-chert conglomerate along the Triassic-Cretaceous unconformity. These coarse sediments were derived by fluvial mechanism off the Bovie high, and transported into the Liard Basin. Upon incursion of the Boreal seaway, these sediments became highly reworked, and preserved as a coarse grained lag that mantles the unconformity surface (Facies B).

As sea level continued to rise, the Bovie fault acted as a barrier to sedimentation from the north and west, resulting in the deposition of a shoreline parallel to the topographic high of the Bovie Fault. Within this shoreline complex a number of reoccurring depositional facies have been identified, and interpreted. In general these grade from the lower shoreface, into more proximal lower shoreface, into the lower shoreface, and finally into the distal lower shoreface. Within these facies, sedimentary and ichnological evidence support the interpretation of an energetic setting. As a whole the biogenic assemblage is not very diverse, where energy stress is causing this lack of diversity. Generally, the ichnofossils of the Lower Cretaceous sandstones consist of horizontal grazing traces, that are cross-cut by the vertical traces of suspension feeders. Horizontal traces are found in the finer-grained sediments which record quiescent deposition within the basin. Intermittently, these episodes are punctuated by highly energetic events, which erode and obliterate most of the quiescent depositional record. The energetic events are marked by erosive bases, and commonly associated with large scale bedforms such as hummocky and swaley-cross stratification. After these storm events wane, and bottom conditions return to ambient conditions, biogenic activity is again observed. Recording again the quiescent moments within an otherwise energetic depositional setting.

Figure II-23 summarizes the depositional facies, surfaces and interpreted relative sea level positions of a typical well within the Maxhamish field. The movement of relative sea-level can be controlled by a number of factors (i.e. glacial isostatic rebound, sedimentation, etc.). Within the study area however, tectonism plays the most important controlling role; in particular the movement of the Bovie fault, and migration of the foredeep in response to the Cordilleran Orogeny. It is not unreasonable then for episodic 'jumps' in sea-level to take place, and be preserved within the rock record.

Further evidence for syndepositional tectonic movement is the presence of

Mississippian coral fragments within shoreface sandstones. During movement of the Bovie Fault, subcropping edges of Mississippian strata were entrained within the energetic shoreface of the Lower Cretaceous. While some reworking is evident (i.e. some rounding), these large clasts have not been transported a great distance. As the Bovie fault was active, these large clasts became entrained within proximal lower shoreface sandstones at Maxhamish. It is also interesting to note that the Mississippian clasts found within a facies directly underlying an interpreted relative rise in sea level, which could be tectonically controlled.

A second, more punctuated inflection of relative sea-level is noted within the *Glossifungites* surface (surface F). Here a substrate is exhumed, eroded, and rooted during a major fall in sea-level. Subsequently, during the initial phases of transgression, this surface is colonized by deeply penetrating *Skolithos*. These burrows remain open, as fine-grained glauconitic sandstones fill-in the burrows, during the subsequent transgressive event and maximum marine transgression of the Garbutt Formation (facies G). The resulting surface is demarcated as a coeval lowstand surface of erosion and transgressive surface of erosion. This surface is interpreted to represent a forced regression within the deposition of the Lower Cretaceous sandstones.

First proposed by Posamentier *et al.* (1992), a forced regression is a basinward movement of a shoreline due to a decrease in relative base level. They can occur with minimal sediment supply to the shoreline, and are prone to creating surfaces rather than depositing sedimentary sequences. Sediments deposited below wave base, prior to the fall in base level, are transposed seaward and deposited disconformably over previously deposited sediments, filling the available accommodation space. Within the Lower Cretaceous sandstones at Maxhamish, this disconformable surface is evident with the presence of the rooted horizon lying directly on top of distal lower shoreface silts. Intuitively, this disconformable surface could be traced basinward, where it would eventually overlie a conformable sequence, the displaced shoreline. Previous workers have identified other forced regressive shorelines (Plint, 1988; Posamentier and Chamberlain, 1993; Posamentier *et al.*, 1992; Walker and Bergman, 1993), where the shoreline trends parallel to depositional strike and shoreline trend.

In general these regressive 'detached' shorelines form when a rapid drop in sea level transports highstand shoreline deposits tens to hundreds of kilometers basinward. Instead of bedload transport, these new shorelines are the result of the drop in relative sea level. The shelf becomes an emergent, non-depositional surface due to the lack of

accommodation space. As the rate of relative sea level fall decreases and begins to rise, these newly transported shorelines are eroded (ravinement surface) and resulted in a sharp-based, shore-parallel sandbody, with an erosional top, which is encased in deeper water sediments.

The evidence for a dramatic drop in sea-level does exist within the Maxhamish Field. It is interpreted to be the result of tectonic activity, which has juxtaposed distal offshore deposits and sub areally exposed rooted surface. While this dramatic relative drop in sea level is the direct result of forming this disconformable surface, a displaced shoreface could exist basinward of the interpreted Maxhamish shoreline. While the limited well penetration precludes direct evidence for this interpretation, the result would result in a new economic target within the Liard Basin.

REFERENCES

- Bouma, A.H. 1962. Sedimentology of some flysch deposits: Amsterdam, Elsevier, 168 p.
- British Columbia Energy and Mines Division 1999, Hydrocarbon and by-product reserves in British Columbia 1999, Ministry of Energy and Mines.
- Cant D.J. and G.S. Stockmal. 1989. The Alberta foreland basin: relationship between stratigraphy and Cordilleran terrane-accretion events: Canadian Journal of Earth Sciences, v. 26, p. 1964-1975.
- Davies, G.R. 1997. The Triassic of the Western Canada Sedimentary Basin: tectonic and stratigraphic framework, paleogeography, paleoclimate and biota: Bulletin of Canadian Petroleum Geology, v. 45, p. 434-460.
- Dott, R.H. 1983. 1982 SEPM presidential address: episodic sedimentation – how normal is average? How rare is rare? Does it matter? Journal of Sedimentary Petrology, v. 53, p. 5-23.
- Dott, R.H. 1988. An episodic view of shallow marine clastic sedimentation. *In*: P.L. de Boer, A. van Gelder and S.D. Nio (eds.). Tide-influenced sedimentary environments and facies. D. Reidel Publishing Company, Boston, p. 3-12.
- Dott, R.H. and J. Bourgeois. 1982. Hummocky stratification: significance of its variable bedding sequences: Geological Society of America Bulletin, v. 93, p. 663-680.
- Duke, W.L., R.W.C. Arnott, and R.J. Cheel. 1991. Shelf sandstones and hummocky cross-stratification: new insights on a stormy debate: Geology, v. 19, p. 625-628.

- Frey, R.W. and A. Seilacher. 1980. Uniformity in marine invertebrate ichnology. *Lethaia* 13: 183-207.
- Frey, R.W., and R. Goldring. 1992. Marine event beds and recolonization surfaces as revealed by trace fossil analysis. *Geology Magazine*, 129: p. 325-335.
- Harms, J.C., J.B. Southard, D.R. Spearing, and R.G. Walker. 1975. Depositional environments as interpreted from primary sedimentary structures and stratification sequences. Society of Economic Paleontologists and Mineralogists Short Course No. 2, Lecture Notes: 161 p.
- Howard, J.D. 1972. Trace fossils as criteria for recognizing shorelines in stratigraphic record. *In*: J.K. Rigby and W.K. Hamblin (eds.), Recognition of ancient sedimentary environments. Society of Economic Paleontologists and Mineralogists Special Publication 16: 215-225.
- Howard, J.D. 1975. The sedimentological significance of trace fossils. *In*: R.W. Frey (ed.), The study of trace fossils. Springer-Verlag, New York, p. 131-146.
- Howard, J.D., and H.-E., Reineck. 1981. Depositional Facies of High-Energy Beach-to-Offshore Sequence: Comparison with Low-Energy Sequence: American Association of Petroleum Geologists, Bulletin, v. 65 p. 807-830.
- Hunter, R.E., and H.E. Clifton. 1982. Cyclic deposits and hummocky cross-stratification of probable storm origin in the Upper Cretaceous of Cape Sebastian area, southwestern Oregon: *Journal of Sedimentary Petrology*, v. 52 p. 127-144.
- Leckie, D.A., D.J., Potocki, and K., Visser. 1991. The Lower Cretaceous Chinkeh Formation: A Frontier-Type Play in the Liard Basin of Western Canada: American Association of Petroleum Geologists, Bulletin, v. 75, p. 1324-1352.
- Leckie, D.A. and D.J. Potocki. 1998. Sedimentology and petrography of marine shelf sandstones of the Cretaceous, Scatter and Garbutt formations, Liard Basin, northern Canada. *Bulletin of Canadian Petroleum Geology*, v. 46, p. 30-50.
- MacEachern, J.A. and S.G. Pemberton. 1992. An integrated ichnological-sedimentological model of Cretaceous shoreface successions and shoreface variability in the Wester Interior Seaway of North America. *In*: S.G. Pemberton (ed.), Applications of ichnology to petroleum exploration - a core workshop. Society of Economic Paleontologists and Mineralogists Core Workshop 17, p. 57-84.

- Pemberton, S.G., and R.W. Frey. 1985. The *Glossifungites* ichnofacies: modern examples from the Georgia Coast, U.S.A. *In*: H.A. Curran (ed.), Biogenic structures: their use in interpreting depositional environments. Society of Economic Paleontologists and Mineralogists, Special Publication 35, p. 237-259.
- Pemberton, S.G., and MacEachern, 1994. The Sequence Stratigraphic Significance of Trace Fossils: Examples from the Cretaceous Foreland Basin of Alberta, Canada. *In*: J.C. Van Wagoner and G. Bertram (eds.), Sequence Stratigraphy of Foreland Basin Deposits - Outcrop and Subsurface Examples from Cretaceous of North America. AAPG Memoir.
- Pemberton, S.G., J.A. MacEachern, and M.J. Ranger. 1992. Integrated Ichnological-Sedimentological Models: Applications to the Sequence Stratigraphic and Paleoenvironmental Interpretation of the Viking and Peasce River Formations, West-Central Alberta. *In*: S.G. Pemberton (ed.), Applications of ichnology to petroleum exploration - a core workshop. Society of Economic Paleontologists and Mineralogists Core Workshop 17, p. 85-117.
- Pemberton, S.G., and J.A. MacEachern. 1997. The Ichnological signature of strom deposits: the use of trace fossils in even stratigraphy. *In*: C.E. Brett, and G.C. Baird (eds.), Paleontological events. Columbia University Press, New York: p. 74-109.
- Plint, A.G, 1988. Sharp-based shoreface sequences and "offshore bars" in the Cardium Formation of Alberta: their relationship to relative changes in sea level. *In*: C.K. Wilgus, B.S. Hastings, C.G.St. C.Kendal, H.W. Posamentier, C.A. Ross and J.C. Van Wagoner (eds.), Sea-level changes: an integrated approach. Society of Paleontologists and Mineralogists, Special Publication 42: p. 357-370.
- Posamentier, H.W. and C.J. Chamberlain. 1991. Sequence stratigraphic analysis of Viking Formation lowstand beach deposits at Joarcam field, Alberta, Canada. *In*: H.W. Posamentier, C.P. Summerhayes, B.U. Haq and G.P. Allen (eds.), Stratigraphy and facies associations in a sequence stratigraphic framework. International Association of Sedimentologists, Special Publication 18: p. 469-485.
- Posamentier, H.W., G.P. Allen, D.P. James and M. Tesson. 1992. Forced regressions in a sequence stratigraphic framework: concepts, examples, and exploration significance. American Association of Petroleum Geologists, Bulletin v. 76, p. 1687-1709.

- Reynolds, A.D, 1996. Paralic Successions. *In*: D. Emery, and K.J. Myers (eds.), Sequence Stratigraphy. Blackwell Scientific Publications, Oxford, pp. 134-177.
- Taylor, G.C., and D.F. Stott, 1968. Maxhamish British Columbia: Geological Survey of Canada paper 68-12, 23 p.
- Stott, D.F., 1982. Late Cretaceous Fort St. John Group and Upper Cretaceous Dunvegan Formation of the Foothills and Plains of Alberta, British Columbia, District of Mackenzie and Yukon Territory. Geological Survey of Canada Bulletin 328, 124p.
- Walker, R.G. and K.M. Bergman. 1993. Shannon Sandstone in Wyoming: a shelf ridge complex reinterpreted as lowstand shoreface deposits. *Journal of Sedimentary Petrology*, v. 63, p. 839-851.
- Williams, G.D., and Stelck, C.R. 1975. Speculations on the Cretaceous palaeogeography of North America. *In*: The Cretaceous System in the Western Interior of North America. W.G.E. Caldwell (ed.). The Geological Association of Canada, Special Paper 13, p. 1-20.
- Williams, G.K., 1977. The Ceibeta structure compared with other basement structures on the flanks of the Tathlina high, District of Mackenzie: Geological Survey of Canada Paper 77-1B, Report of Activities, Part B, p. 301-310.
- Williams, G.K. 1978. An update of Subsurface Information, Cretaceous Rocks, Trout Lake Area, Southern Northwest Territories. *In*: Current Research, Part A; Geological Survey of Canada Paper 78-1A. p. 545-553.

CHAPTER THREE: Outcrop Descriptions and Interpretations

Expansive valleys and meandering streams were the back-drop for the second portion of the study. The goal of the field work season in 1999 was to describe, and interpret the Lower Cretaceous Chinkeh sandstones in outcrop and combine the subsurface core interpretations to form a regional depositional model for these Lower Cretaceous Chinkeh sandstones. By understanding these exposures, a better understanding of the depositional system taking place within the Chinkeh Formation could result, and allow for a clearer predictive model, and possibly new exploration targets.

It was the mandate of the field season to only visit the outcrop exposures of the Lower Cretaceous Chinkeh Formation. However, errors with published maps caused the field party to visit outcrop locations of both Lower Cretaceous Chinkeh and Scatter Formations. Outcrop locations of the Scatter Formation were visited towards the later portions of the field season, and as a result descriptions of two formations were made. This effort was not in vain, as the similarity between the Scatter sandstones in outcrop and the producing sandstones at Maxhamish are very similar, and is the focus of the next chapter.

INTRODUCTION

The investigated field area lies between the Yukon and Northwest Territories borders. It is a landscape whose topography directly mimics the underlying geology consisting of large wavelength folds of anticline and syncline pairs. Synclinal structures display more resistant Paleozoic strata forming ridges, while at their cores Mesozoic strata is preserved. Since the mandate of the field season was to investigate the lowermost Cretaceous Chinkeh Formation, time was spent along the flanks of many of these synclinal structures, where in addition to structural relief, river cuts also aided in exposing the Lower Cretaceous strata.

A total of 10 outcrop localities were visited (Figure III-1), and 16 outcrops were described. Suitable localities were chosen based on their published thickness and relative proximity to the settlement of Ft. Liard, which was used as the helicopter base. All the sites investigated are accessible via helicopter only, and in the aim of saving thesis funds, only sites located closest to one another were described.

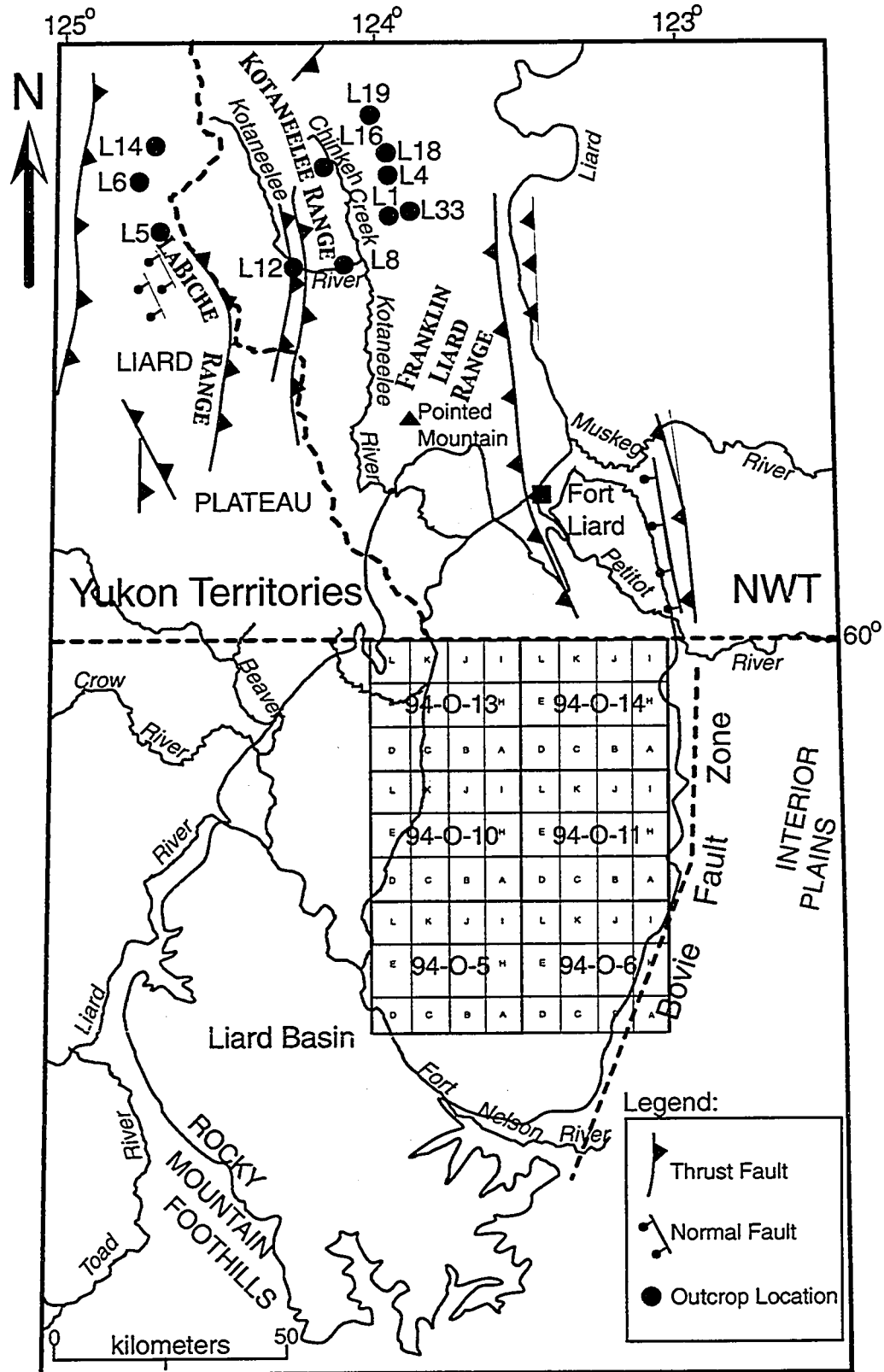


Figure III-1. Outcrop base map displaying locations for measured sections, that include both Chinkeh and Scatter Formations. Note the location of the Bovie Fault, and NTS blocks 94-O-14 and 94-O-11 (approximate location of the Maxhamish gas field).

The main objectives of this chapter are threefold. First, describe the outcrop exposures of the Lower Cretaceous Chinkeh and Scatter Formations. Secondly, give depositional environments for the outcrops described, and thirdly interpret a depositional model for the study area. A detailed discussion relating the outcrop descriptions of the Scatter Formation and interpretations within the subsurface will be investigated within the next chapter of the thesis.

METHODOLOGY

All the exposures described are accessible by helicopter only. Using published reports as a guide, landing locations were chosen off of airphotos. Generally camp could be constructed relatively close to outcrop exposures, however on occasion a considerable hike was in order to access the investigated outcrop sites. On subsequent camp moves, the helicopter en-route from Ft.Liard, would replenish the field party with fresh supplies, and transport samples back to the helicopter base in Ft.Liard.

All the exposures measured were accessible via creek cuts, and often many of the lithologs included in the descriptions are amalgamations of a number of locations along a given creek. It was possible to describe a complete section by simply following the creeks, since the dip of the bedding was steeper than the dip of the creek beds. Once a desirable base of section had been determined, outcrop thickness was determined via the use of the time honored pogo stick. A litholog was created by describing the following: grain-size, nature of contacts, lithology, sedimentary structures, lateral variability within the exposure, trace fossils (identification of individual forms, and relative abundance), and any body fossils present. Most of these pertinent observations were also photographed where possible. Fist sized samples were also collected at every one meter interval of the exposure for thin-section analysis and biostratigraphic identification.

Finally, a hand-held scintillometer was used to measure naturally occurring gamma-ray emissions from the outcrop exposure. Five measurements were taken every two seconds for every half meter of measured outcrop. The highest and lowest values collected were then disregarded and the mean calculated for the remaining data in that interval. The average of these three values was then plotted along side the measure litholog for each exposure measured. Where time permitted, a spectral gamma radiation analysis was also conducted in order to determine which radiogenic species (K, U, or Th) was emitting highest radiation amounts, and contributing to the total gamma-radiation

counts. For any one given radiogenic species, three counts were taken every two seconds at each half meter of measured outcrop. These results were not plotted along with the litholog, however raw data is recorded within the appendix of this thesis. A number of workers have also shown the usefulness of using the gamma-ray tool on outcrop exposures (Slatt *et al.*, 1992, Aitken and Howell, 1996, Davies and Elliott, 1996).

Upon returning from the field, these observations and measurements were redrafted, and compiled (see Figures III-2 to 11). It must be stated, that although a good portion of these outcrop localities had been described previously (Leckie *et al.*, 1991), an increase in measured thickness and geological detail has been recorded at each outcrop location. In addition, four key outcrop localities have been described in error, either grouping them into the incorrect geological formation (locations Murky Creek-L1, and Kotaneelee River-L8) or were simply not present (L12, L16, and possibly Tika Creek-L6).






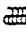





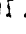













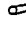
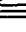




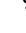




Outcrop Descriptions

INTRODUCTION















This chapter is organized in the following manner. A brief overview is provided for each of the measured sections. This includes a photo-mosaic for each locality, a litholog, outcrop based gamma-ray log, orientation, and UTM location (see Figures III-2 to 11). The purpose of the brief description is to draw attention to details within each outcrop locality, not otherwise seen within the lithologic or facies descriptions. Subsequently, a detailed analysis of each facies will be presented, in which detailed descriptions and interpretations will be given. Following the outcrop descriptions and interpretations a detailed discussion of the interpreted depositional setting will follow, that will tie outcrop descriptions and interpretations to the more regional interpretation of the Chinkeh Formation. For reference, Figure III-1 shows each outcrop locality, and their relation to the Liard Basin. Table III-1 is a legend or symbols used in the outcrop descriptions.

The Chinkeh Formation as seen in outcrop, is composed of quartz-rich sandstones, which rest unconformably on Permian strata (See figure III-12). While many of the described sections are expansive in their exposure (i.e. Otter Slide-L4, and Burnt Timber-L19), they are not located in close proximity to one another. Closest distances between outcrop locations are between 5 and 10 kilometers, with distances reaching over 50 kilometers for outcrops at the extreme corners of the study area (i.e. Six Bald Point-L5



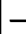


Ichnofossil Symbols

 Arenicolites (Ar)	 Ophiomorpha (Op)
 Asterosoma (As)	 Palaeophycus (Pa)
 bivalve adjustment trace	 Phycosiphon (Ph)
 bivalve resting trace	 Planolites (Pl)
 Chondrites (Ch)	 Rhizocorallium (Rh)
 Conichnus/Bergaueria (Co)	 Root Traces/Casts
 Cruziana (Cr)	 Roselia
 Cylindrichnus (Cy)	 Scalarituba (Sc)
 Diplocraterion (Di)	 Siphonites (Si)
 feeding pit (FP)	 Skolithos (Sk)
 Fugichnia (Fu)	 Spongelliomorpha (Sp)
 Gyrolithes (Gy)	 Teichichnus (Te)
 Gyrochorte (Gyr)	 Terebelina (Ter)
 Helminthopsis/Helminthoida (He)	 Thalassinoides (Th)
 Lockeia (Lo)	 Treptichnus (Tre)
 Lingulichnus (Li)	 Trichichnus (Tri)
 Macaraonichnus (Ma)	 Undifferentiated Bioturb.
 Monocraterion (Mo)	 Zoophycos (Zo)




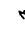



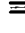

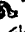




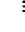










Fossil Symbols

 Conodont
 Gastropod
 Bivalved pelecypod
 Crinoid debris
 Echinoid debris
 Spiriferid Brachiopod
 Terebratulid Brachiopod
 Lingulid Brachiopod
 Rugose Coral
 Vertebrate skeletal elements
 Ammonoid
 Wood and leaves
 Bioclastic debris
 Cryptalgal laminae

Contacts

 Unconformity
 Erosional/Disconformity
 Scoured/Storm event
 Sharp
 Gradational

Physical Sedimentary Structures

 Synaeresis cracks	 Flaser Bedding	 Hummocky cross-strat.
 Tool marks	 Lenticular Bedding	 Planar cross-stratification
 Soft sediment faulting	 Tidal Couplets	 Trough cross-stratification
 Soft sediment deformation	 Wavy bedding (heterolithic)	 Over steepened cross-strat.
 Dewatering structure	 Wavy bedding (homogeneous)	 Planar bedding
 Convolute lamination	 Ripple Laminations (wave)	 Scour and Fill
 Shrinkage cracks	 Ripple Laminations (current)	 Imbricated clasts
 Pedogenic slickensides	 Climbing Ripples	
 Load casts	 Low angle cross-stratification	

Extras
















 Rip-up clasts	 Graded Bedding	 Photo Available
 Mud clasts	 Glauconite	 Sample collected
 Pebble lag	 Stylolite	 Glossifungites surface
 Carbonaceous matter	 Pyrite	
 Carbonaceous laminae	 Phosphate	
 Shale laminae	 Siderite	

Table III-1. Legend of symbols used within outcrop lithologs and summaries.

and Burnt Timber-L19).

In general the Chinkeh Formation can be described as a coarsening upwards, quartz-arenite, well sorted sandstone. It is dominated by large-scale bedforms, and with the exception of a few facies, relatively few biogenic structures. Thickness of the Chinkeh Formation varies, ranging from 5.5 meters at its western most extreme (Tika Creek-L6) to 22 meters in the northeast (Burnt Timber-L19). Most outcrop exposures do not emit high gamma-ray counts, never averaging more than 40 counts per second. All exposures of the Lower Cretaceous Chinkeh Formation are sharply overlain by the shales of the Garbutt Formation.

The Scatter Formation (more precisely the Bulwell Member of the Scatter Formation) as observed in outcrop, consists of fine to medium-grained, glauconite-rich, quartz-rich sandstones. These glauconite-rich exposures are found directly overlying shales of the Garbutt Formation and underlying the Wildhorn shale member of the Scatter Formation. Exposures are recessive in nature, and highly interbedded with bioturbated shale beds. Outcrop exposures ranged in thickness from 9 meters (Murky Creek-L1), (where the base of section was not observed), to 11 meters (Kotaneelee River-L8). These exposures are fairly radioactive, and gamma-ray counts averaged never less than 50 counts per second.

At all outcrop locations, the Lower Cretaceous Chinkeh Formation sat unconformably on Permian strata. In general this contact was very sharp, and demarcated by a grain-size increase, and an undulatory contact.

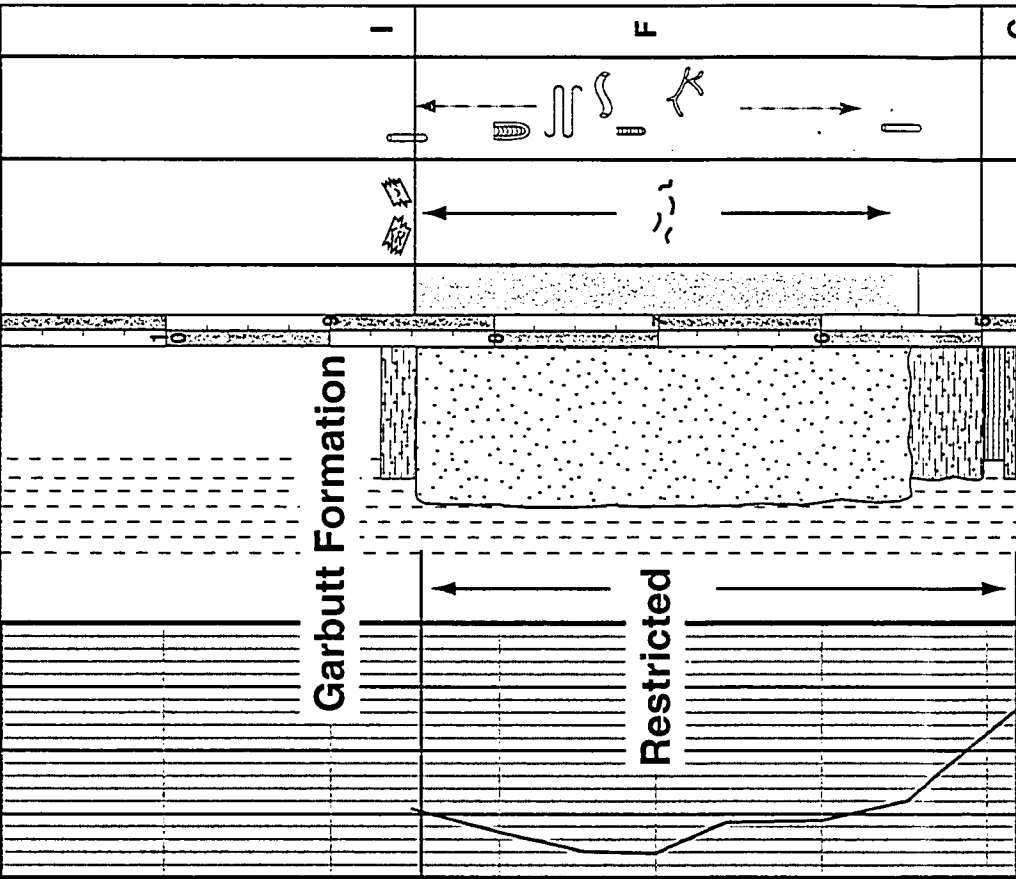
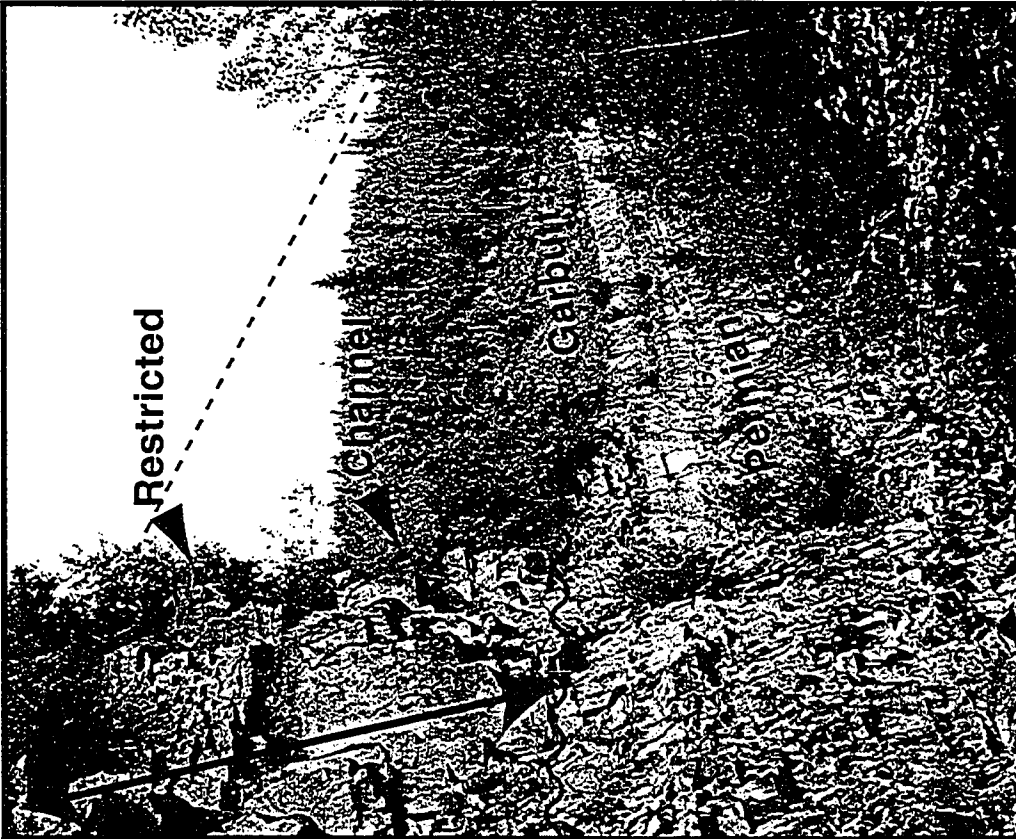
LOWER CRETACEOUS CHINKEH FORMATION

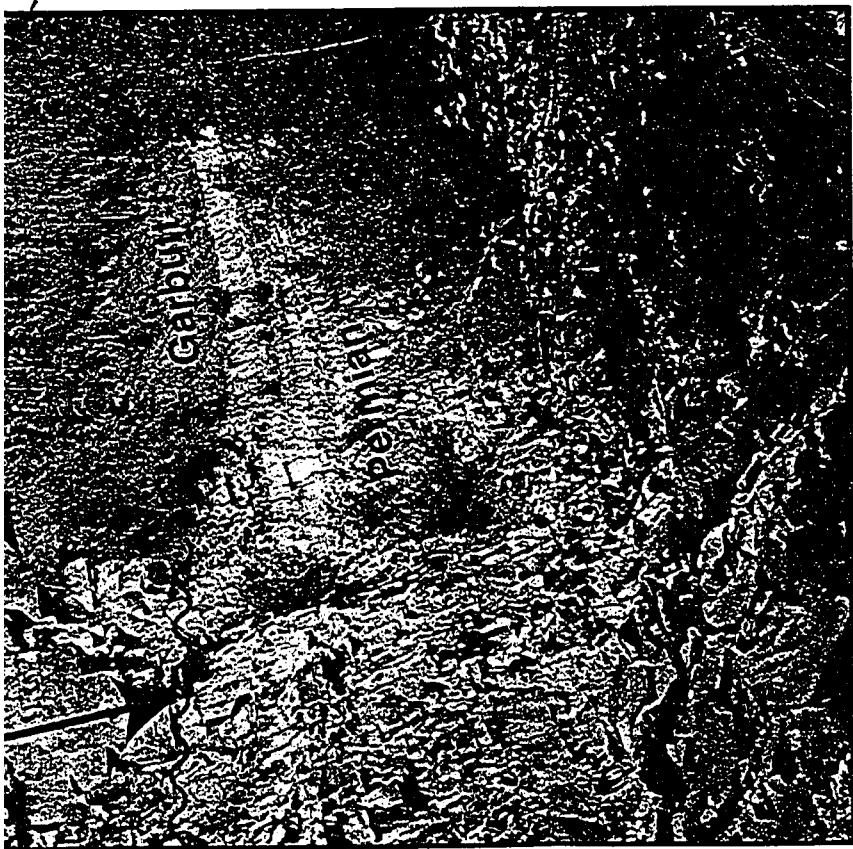
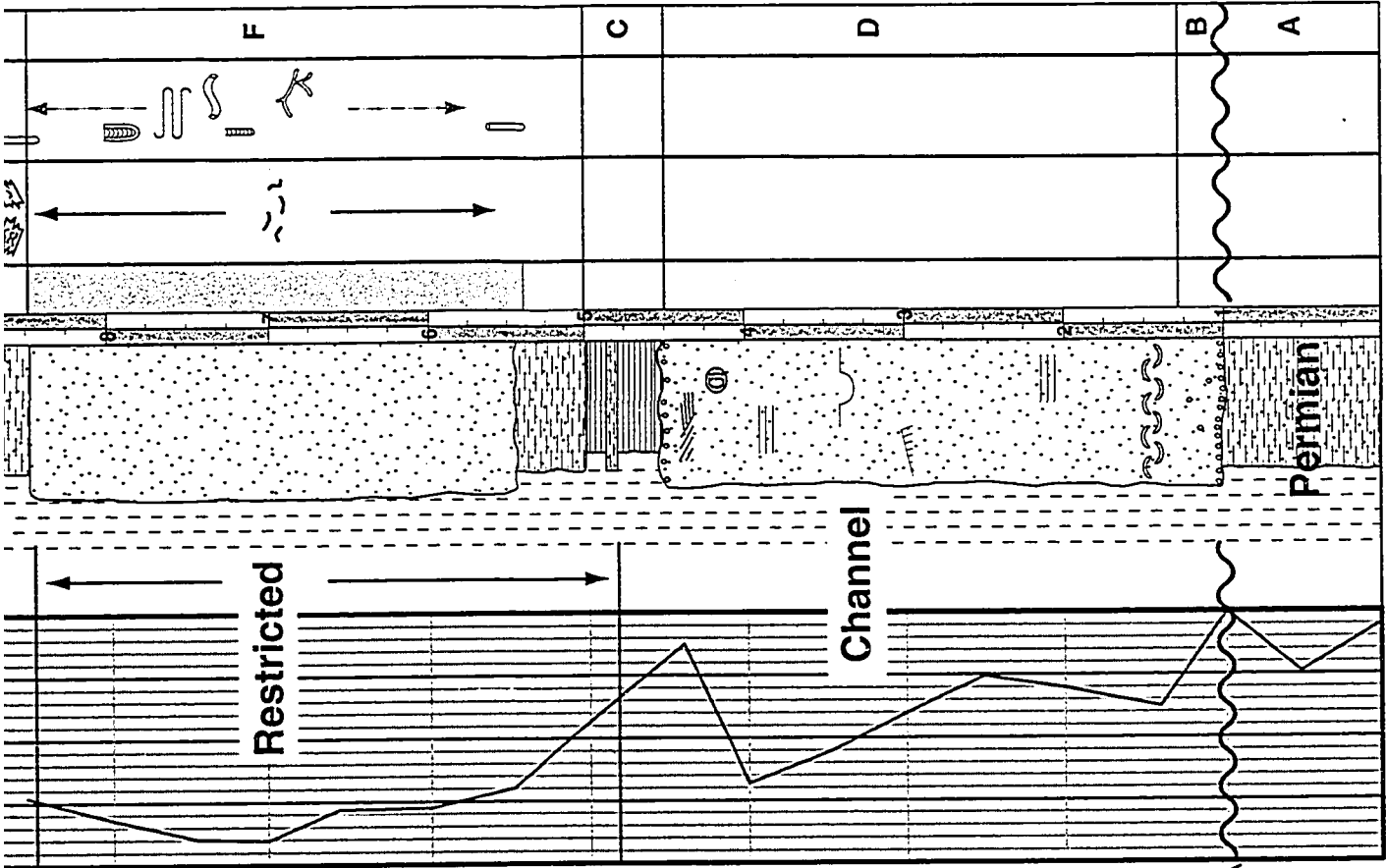
OUTCROP MURKY CREEK (L18)

The exposure of the Chinkeh Formation along the upper sections of Murky Creek was expansive (Figure III-2). The creek itself had eroded down through the Garbutt, Chinkeh and Permian Mattson Formations, giving continuous vertical and lateral exposure through these units of rock (30 meters of vertical exposure). Approximately 500 meters of continuous lateral section was observed from this location, and showed some significant lateral changes through the Chinkeh Formation (see Figure III-29). In

Location: L18 - Murky Creek (0445826E 6735349N +/- 73m)			
Outcrop Interval: 0-8.65m	Date: Aug. 14, 1999		
Formation: K Chinkeh	Orientation: 150°/ 025°		
Logged by: Jason & Murray	Comments:		

Gamma Ray (CPS)	GRAIN SIZE	DEPTH	BIOTURBATION	PHYSICAL STRUCTURES	TRACE FOSSILS	FACIES
30 40 50	<div> <div>sand</div> <div>silt</div> <div>clay</div> <div>vcmfv</div> </div>					





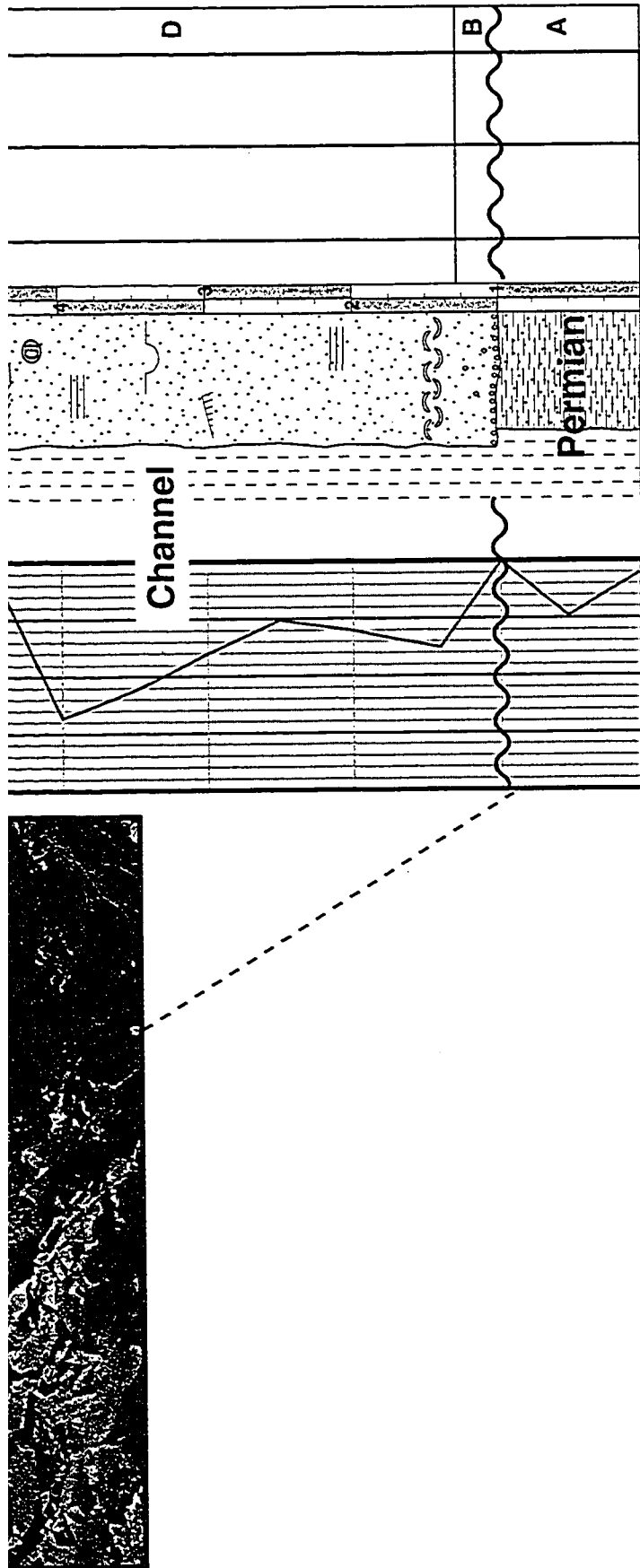


Figure III-2. Photomosaic, outcrop lithology, and gamma-ray data for the Chinkeh Formation at the Murky Creek (L18) exposure. Note the blocky appearance of the lowermost sands resting unconformably on Permian strata, that becomes much more interbedded near the top contact with the Garbutt Formation (see Figure III-29 for a view of the outcrop from across the canyon). The arrow represents approximate base and top of the measured section. Outcrop location is shown in Figure III-1, and symbols used are defined in Table III-1.

particular, the lowermost sand package thinned dramatically in an east to west orientation. Outcrop thickness at this location was measured at 8.5 meters.

OUTCROP BURNT TIMBER-L19

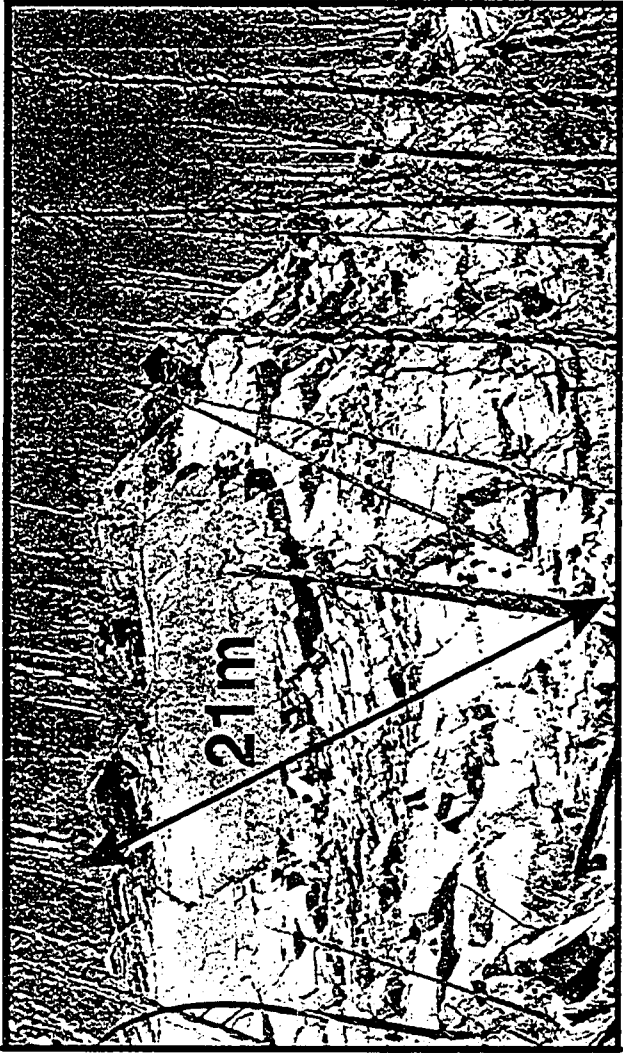
With over 40 meters of section, this locality represents the thickest Chinkeh outcrop exposure observed. It lies the farthest north and east within the study area (see Figure III-1), and is also shows the highest diversity in terms of interpreted facies. This outcrop lies on the flank of a large synform, and is believed that the thickness observed is the result of shallow thrusting, and doubling the preserved Chinkeh Formation. While no direct evidence was found (i.e. shallow slickenslides, or observable bed offset), the dramatic thickness difference compared with the other outcrops within the study, and the repeated facies within both facies suggests that this outcrop has been tectonically modified, in effect doubling the observed Chinkeh Formation. Two outcrop lithologs were created from this outcrop location (Figures III-3 and III-4). The first started at the Permian-Cretaceous unconformity, base of section. Working up stratigraphically, a large unconsolidated section was encountered 18 meters above the base of section. A total of 4 meters of missing section was recorded over this interval. The second litholog continues from the top of the unconsolidated section, keeping the original base of section as reference. This unconsolidated section between the two lithologs is where the shallow thrust faults are interpreted to cut through the Chinkeh Formation. The total thickness of Chinkeh Formation measured at this location was 43.25 meters.

Discussions and interpretations with the Burnt Timber outcrop will include the fully exposed section, however only half of the doubly exposed section will be included within discussions of Chinkeh Formation thickness within the Liard Basin.

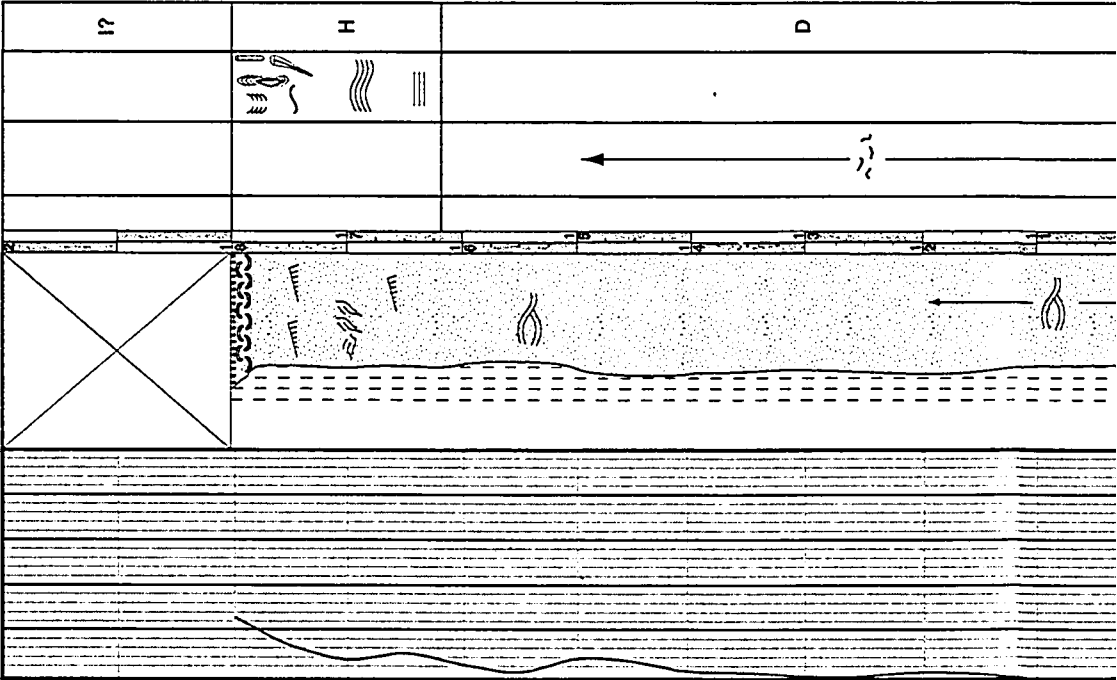
OUTCROP L5 – SIX BALD POINT

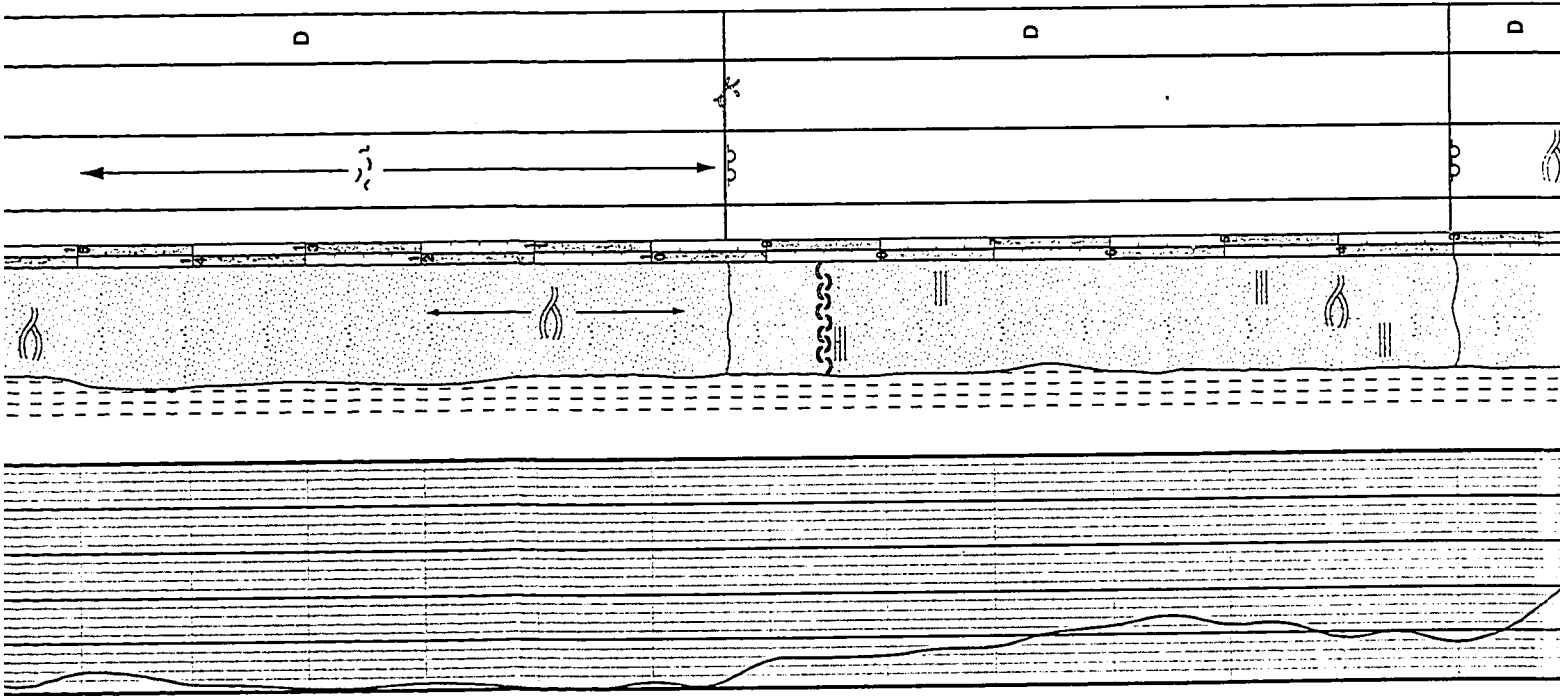
The outcrop location along the LaBiche River, exposed excellent outcrop of the Chinkeh Formation. While the lower contact of the Chinkeh was never observed, the location did give an excellent opportunity to observe the upper contact with the Garbutt Formation. Since the outcrop faces observed at this location were steep, and in many places overhanging, walking the section out down stream allowed for the creation of a complete section (Figure III-5). It should also be noted that the sandstones observed

Location: L19 Burnt Timber (442425E 6742556N)	
Outcrop Interval: 0-43.25m	Date: Aug. 11, 1999
Formation: K Chinkah & Perm	
Orientation: 169°/ 025°	
Logged by: Jason & Murray	
Comments: Part I	



Gamma Ray (CPS)	GRAIN SIZE			DEPTH	BIOTURBATION	PHYSICAL STRUCTURES	TRACE FOSSILS	FACIES
	40	60	80	100				





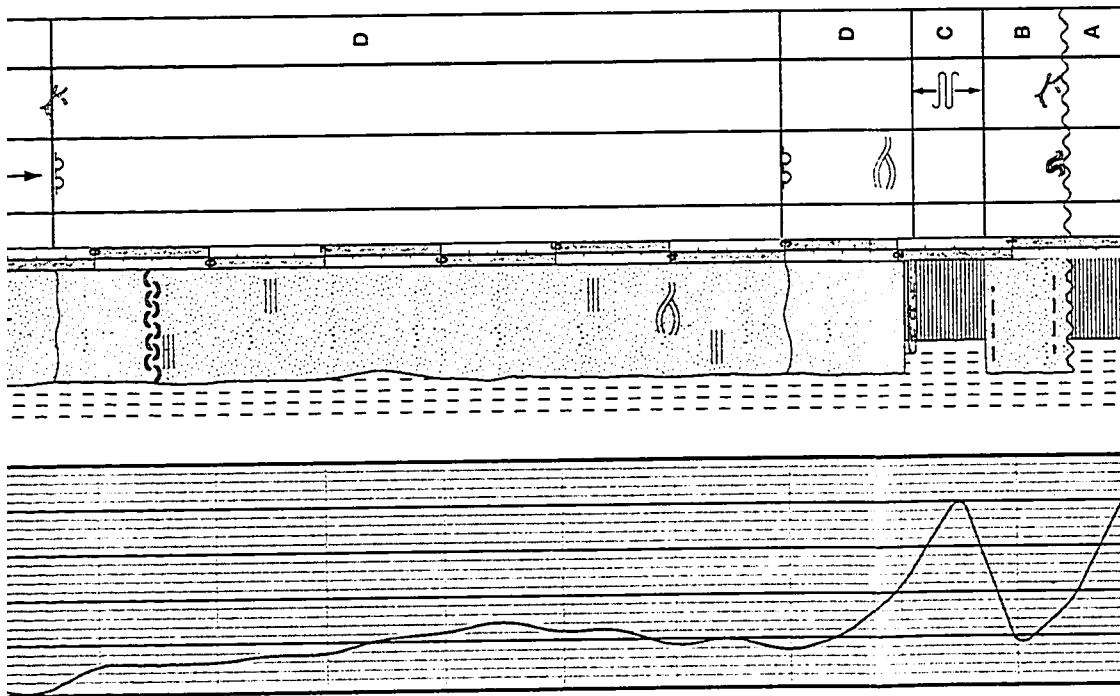
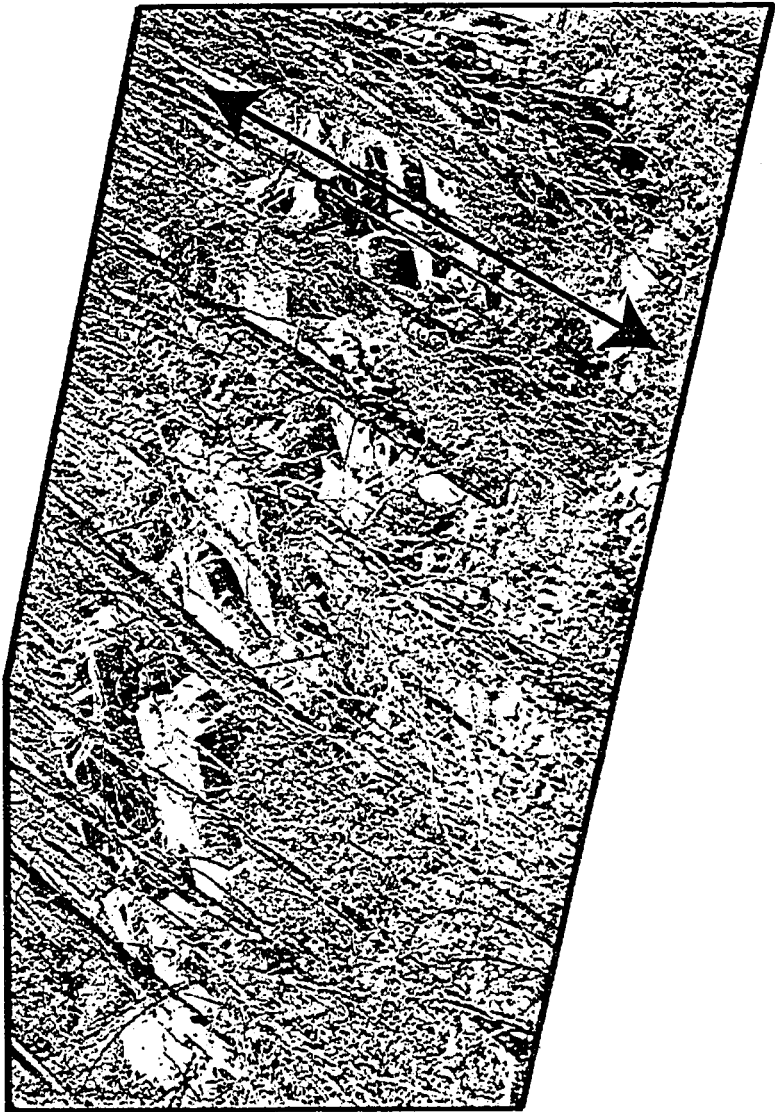
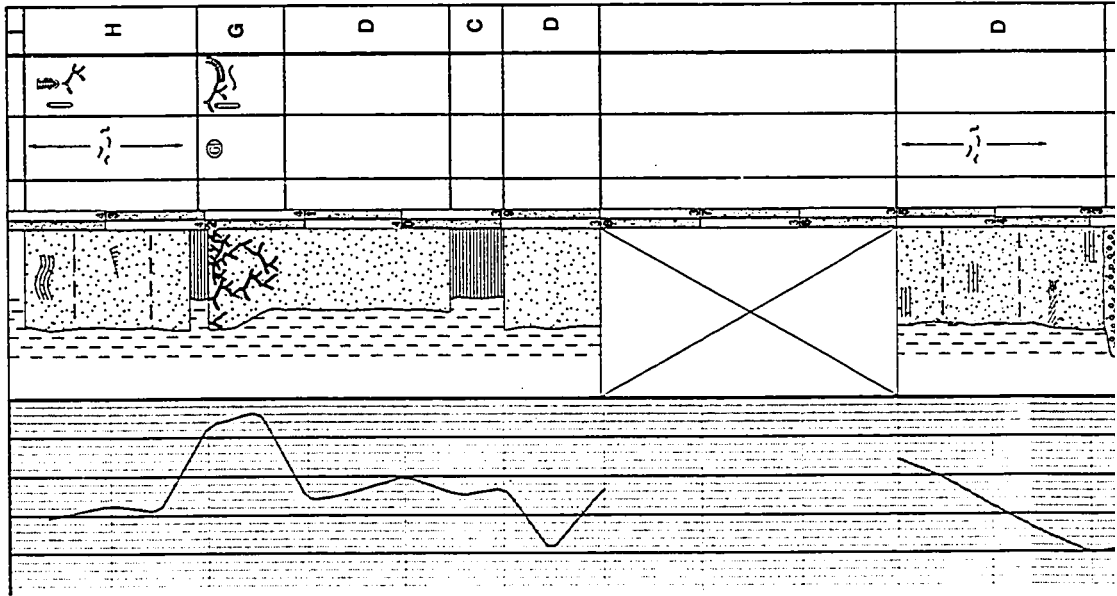


Figure III-3. Photomosaic, outcrop litholog and recorded gamma-ray data for the Clinch Formation at the Burnt Timber (L19) exposure. This section represents half of the total measured section observed at this locality, the second half is presented in Figure III-4. Arrow denotes the approximate base and top of the measured section. Outcrop location is shown in Figure III-1, and symbols used are defined in Table III-1.

Location: L19 Burnt Timber (442425E 6742556N)	
Outcrop Interval: 0-43.25m	Date: Aug. 11, 1999
Formation: K Chinkah & Perm	Orientation: 169/ 025°
Logged by: Jason & Murray	Comments: Part II



Gamma Ray (CPS)	DEPTH	GRAIN SIZE	BIOTURBATION	PHYSICAL STRUCTURES	TRACE FOSSILS	FACIES
30						
40						
50						
60						



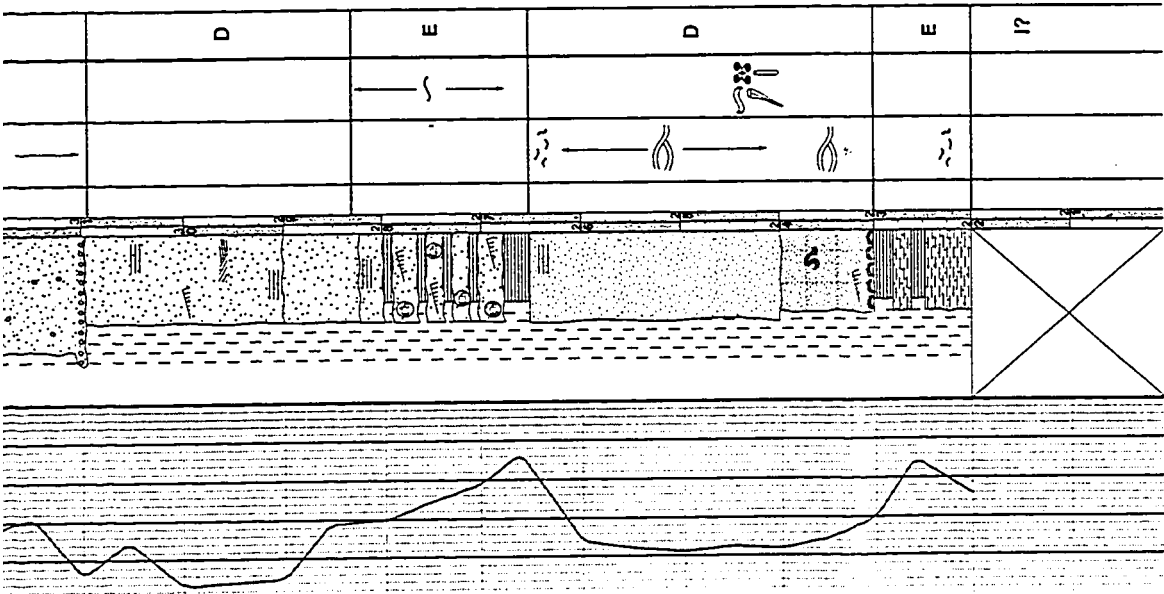
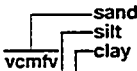


Figure III-4. Photomosaic, outcrop litholog and recorded gamma-ray data for the Chinkeh Formation at the Burnt Timber (L19) exposure. This section represents half of the total measured section observed at this locality, the first half is presented in Figure III-3. Arrow denotes approximate base and top of measured section. Outcrop location is shown in Figure III-1, and symbols used are defined in Table III-1.

Gamma Ray (CPS) 5 10 15 20	GRAIN SIZE 	DEPTH	FACIES	PHYSICAL STRUCTURES	TRACE FOSSILS	Location: L5 - 6 Ball Point (404407E 6720692N)	
						Outcrop Interval: 0-13m	Date: Aug. 7, 1999
						Formation: K Chinkeh	Orientation: 113°/003°
						Logged by: Jason & Mark	Comments:

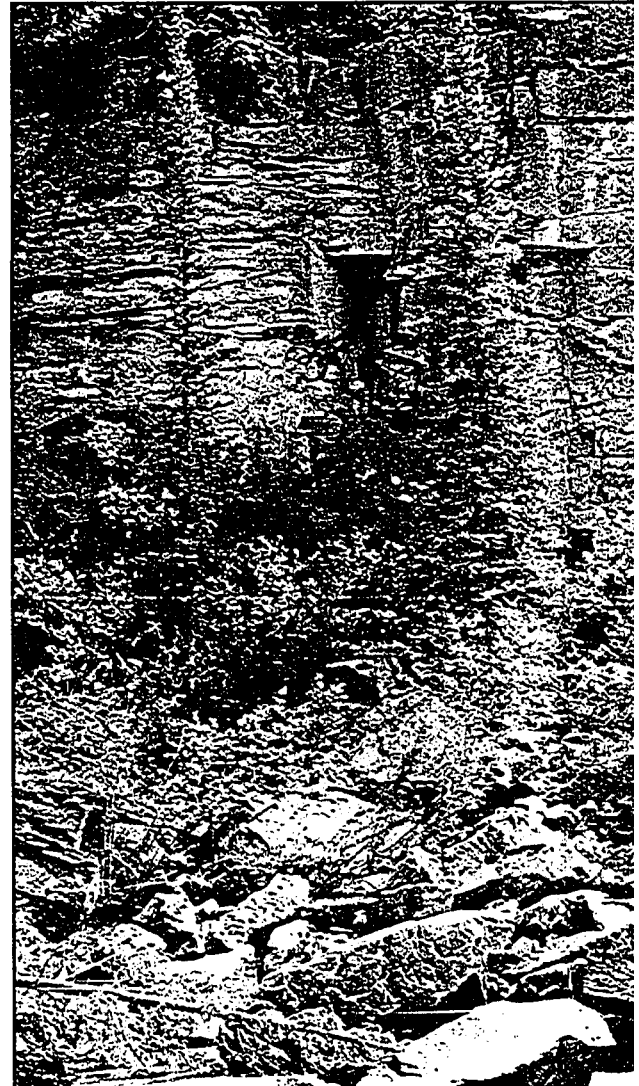
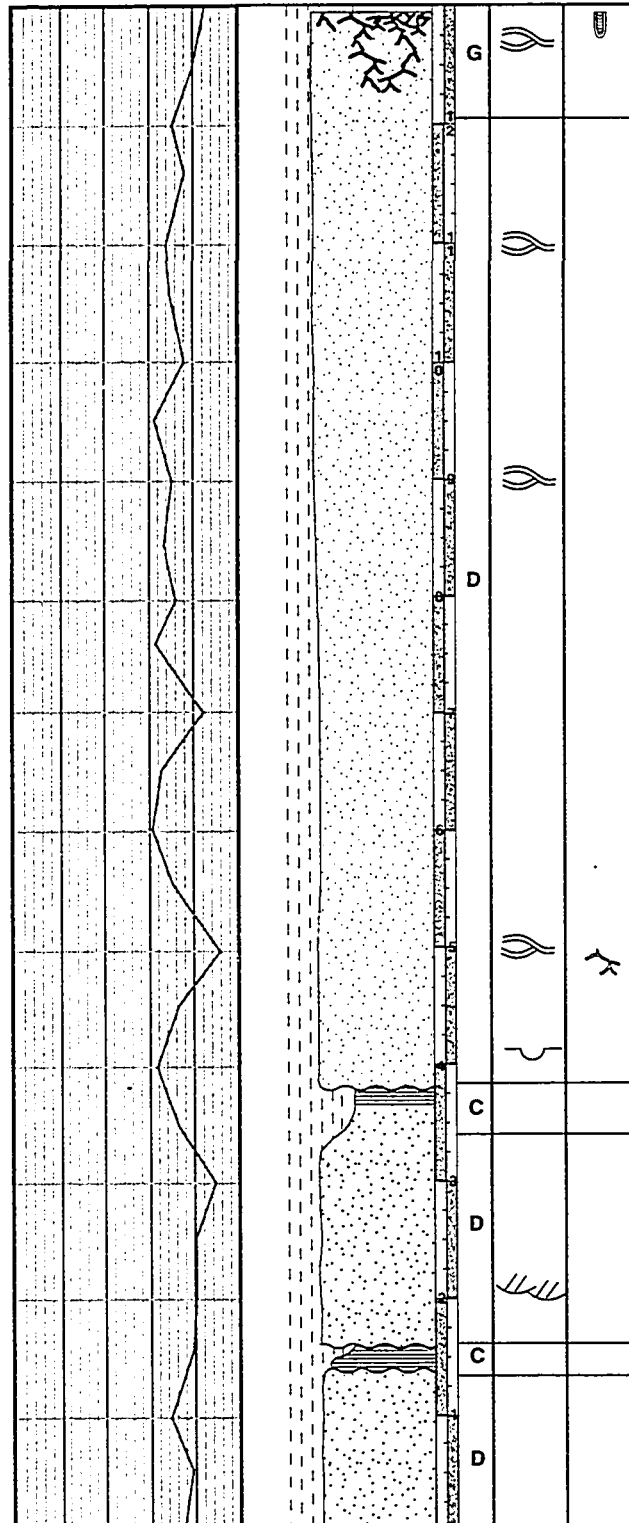
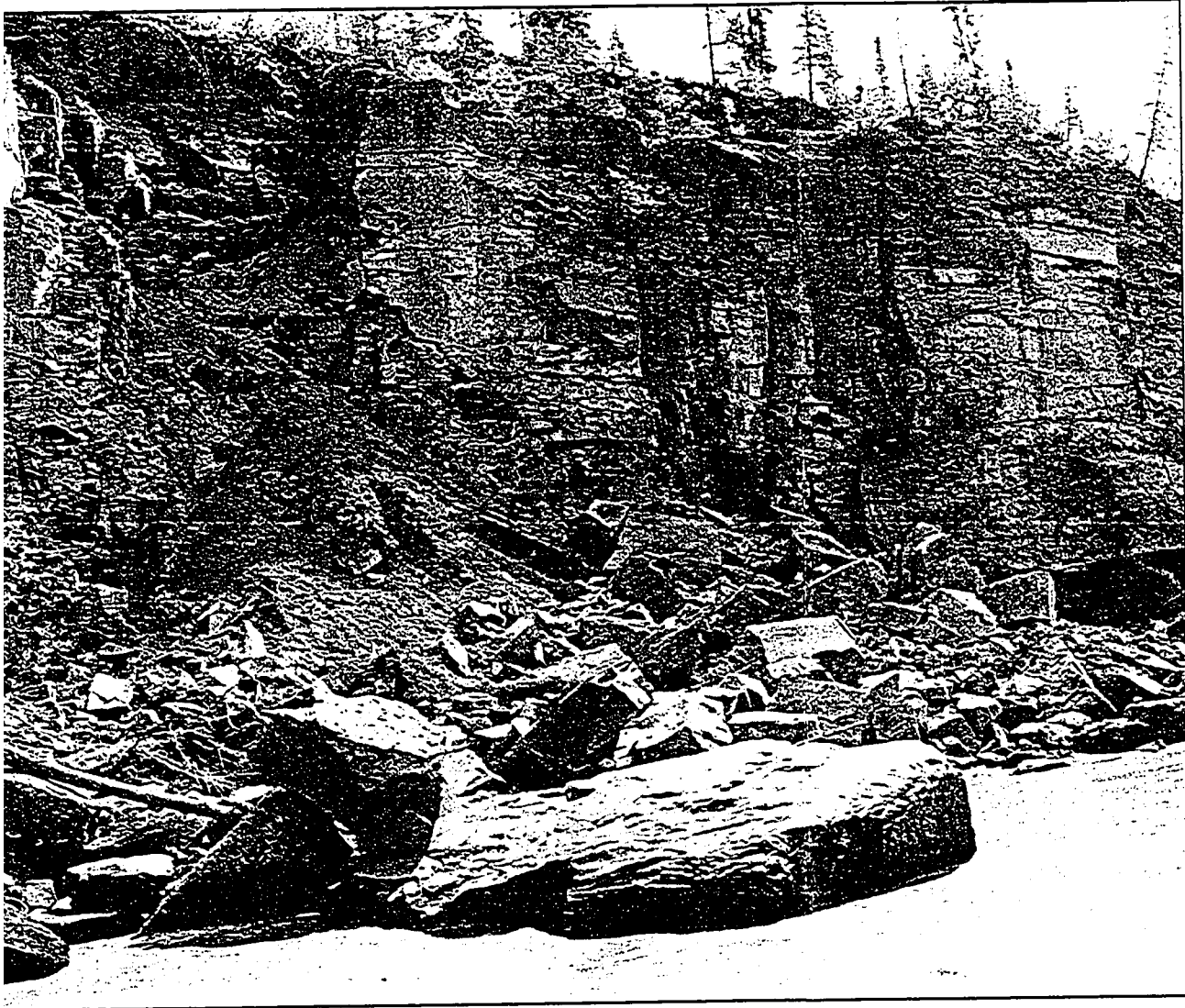


Figure III-5. Photomosaic, of exposure. Based on visual estimates of outcrop exposures visited. Not shown in Figure III-1, and syn

Location: L5 - 6 Ball Point (404407E 6720692N)	
Outcrop Interval: 0-13m	Date: Aug. 7, 1999
Formation: K Chinkeh	Orientation: 113°/003°
Logged by: Jason & Mark	Comments:



Figure III-5. Photomosaic, outcrop litholog and recorded gamma-ray data for the Chinkeh Formation a exposure. Based on visual estimates of porosity and permeability, this exposure displays the best reserv outcrop exposures visited. Note that lower contact with Permian strata was not exposed along the LaBic shown in Figure III-1, and symbols used are defined in Table III-1.



p litholog and recorded gamma-ray data for the Chinkeh Formation at the Six Bald Point (L5) es of porosity and permeability, this exposure displays the best reservoir characteristics of all at lower contact with Permian strata was not exposed along the LaBiche River. Outcrop location is s used are defined in Table III-1.

at this location were the most homogenous and continuous of all the outcrop locations visited. They also displayed the most favourable reservoir characteristics (i.e. porosity and permeability), based on visual estimates. Thickness of Chinkeh Formation at this locality was 13 meters.

OUTCROP L33 – SULLY CREEK

The Sully Creek outcrop location showed good exposure of the Lower Cretaceous Chinkeh Formation. A complete vertical succession could be observed, and lateral exposures were on the order of 100 meters. Both upper and lower contacts were observed, and a total of 13 meters of Chinkeh was recorded. Two distinctive styles of bedding were observed; the lower more thinly interbedded, and the upper a more massive, blocky appearance (Figure III-6). These distinct facies will be discussed in further detail, within the subsequent facies descriptions.

OUTCROP L4 – OTTER SLIDE

At this location a narrow slot canyon afforded excellent exposures of the Chinkeh Formation. In a lateral extent, the outcrop did not extend very far, though it did give a complete vertical section (Figure III-7). Thickness of the Chinkeh Formation at this location was measured at 14 meters.

OUTCROP L14 – SLIP-ROCK CREEK

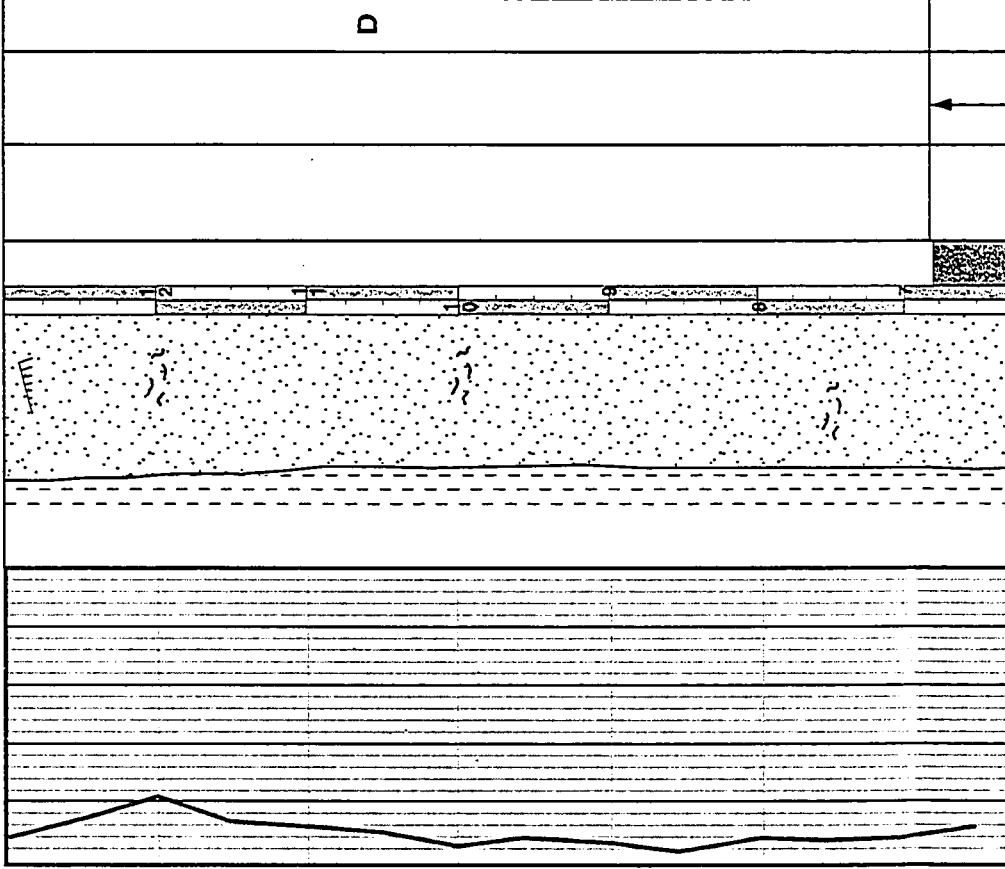
This outcrop locality was not very accessible; logging outcrops along the tributary created a composite section. Previously described as the ‘type-section’ of the Chinkeh (Leckie *et al.*, 1991) this outcrop displays the second highest variability of any exposures observed within the study area. A complete section was observed, from the lower contact with the Permian to the upper contact with the Garbutt Formation (Figure III-8). A total of 18.5 meters of Chinkeh Formation was observed at this location.

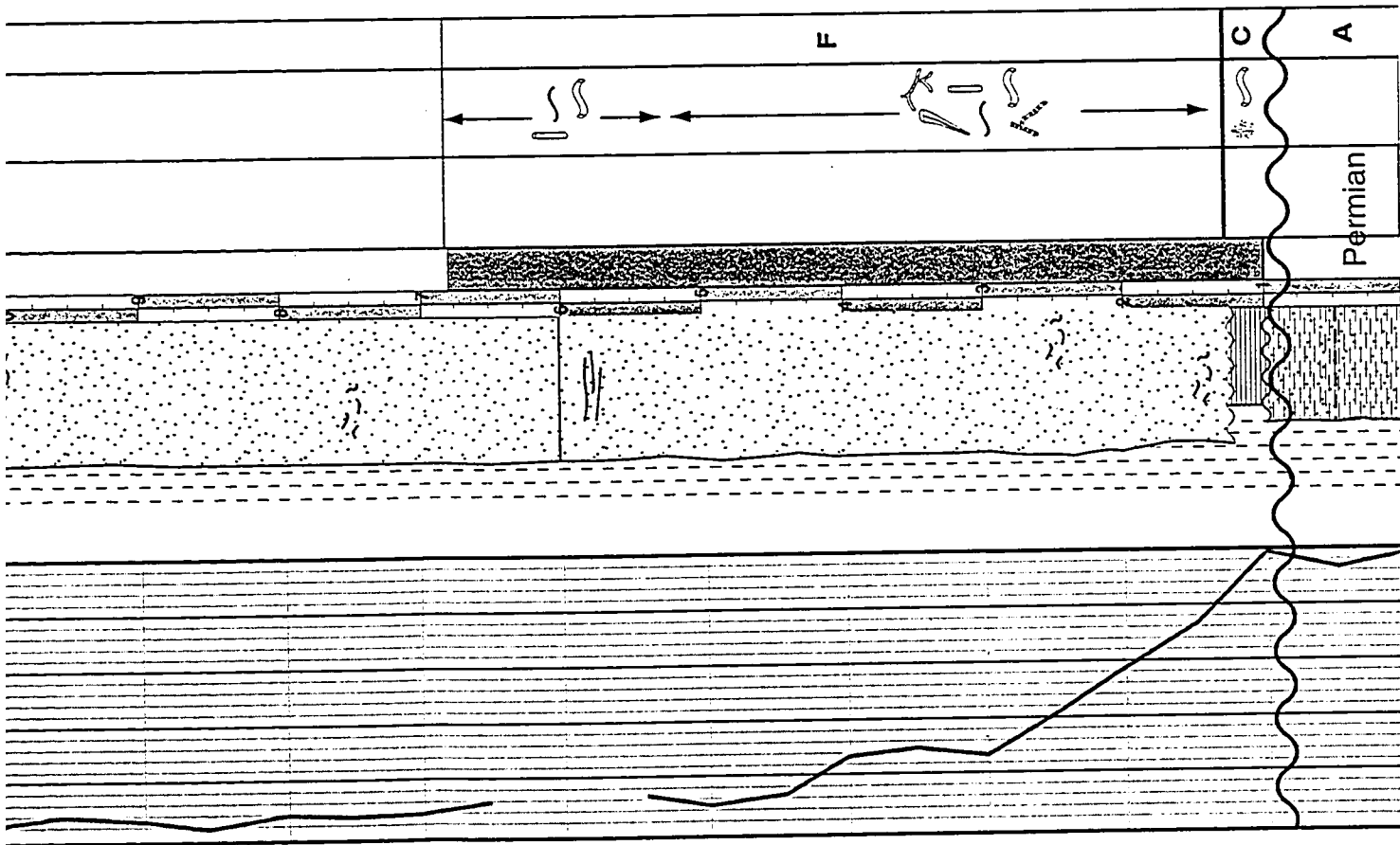
OUTCROP L6 – TIKA CREEK

There is conjecture surrounding the validity of this location. It was very

Location: L33 - (0449362E 6726440N +/- 91m)	
Outcrop Interval: 0-13m	Date: Aug. 16, 1999
Formation: K Chinkeh	Orientation: 117°/ 024°
Logged by: Jason & Murray	
Comments:	

Gamma Ray (CPS)	DEPTH	GRAIN SIZE	BIOTURBATION	PHYSICAL STRUCTURES	TRACE FOSSILS	FACIES
20 30 40 50		sand silt clay vcmfv				





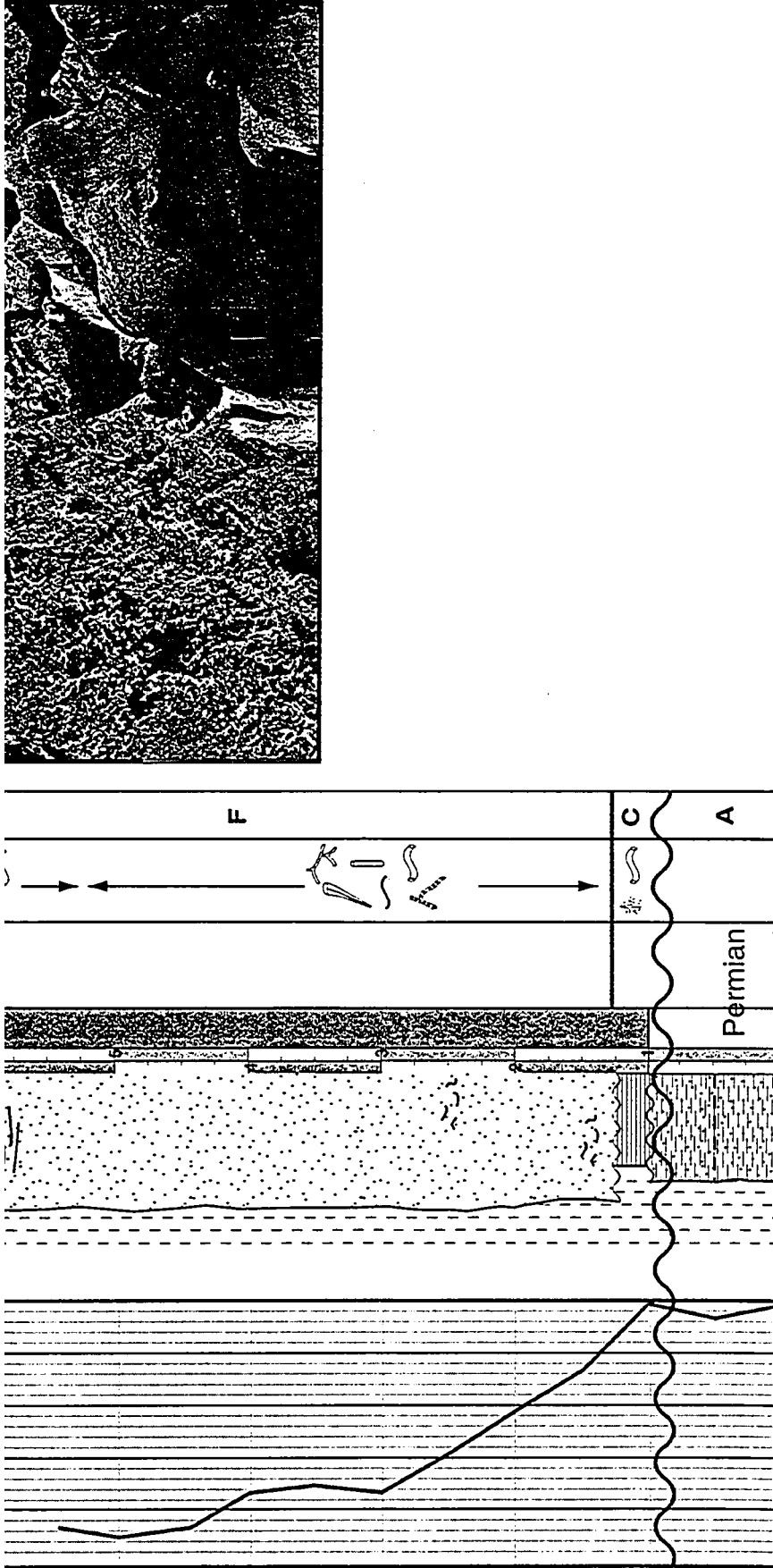
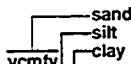


Figure III-6. Photomosaic, outcrop litholog and recorded gamma-ray data for the Chinkeh Formation at the Sully Creek (L33) exposure. Note the interbedded nature of the Chinkeh Formation directly overlying the Permian strata, that becomes much more blocky towards the upper contact with the Garbutt Formation. Gamma-ray counts were omitted at 6 meters above base of section because of inaccessibility. Outcrop location is shown in Figure III-1, and symbols used are defined in Table III-1.

Gamma Ray (CPS)	GRAIN SIZE 	DEPTH	FACIES	PHYSICAL STRUCTURES	TRACE FOSSILS	Location: L4 - (0446383E 6733983N +/- 51m)	
						Outcrop Interval: 0-14m	Date: Aug. 13, 1999
						Formation: K Chinkeh	Orientation: 163°/ 022°
						Logged by: Jason & Murray	Comments:

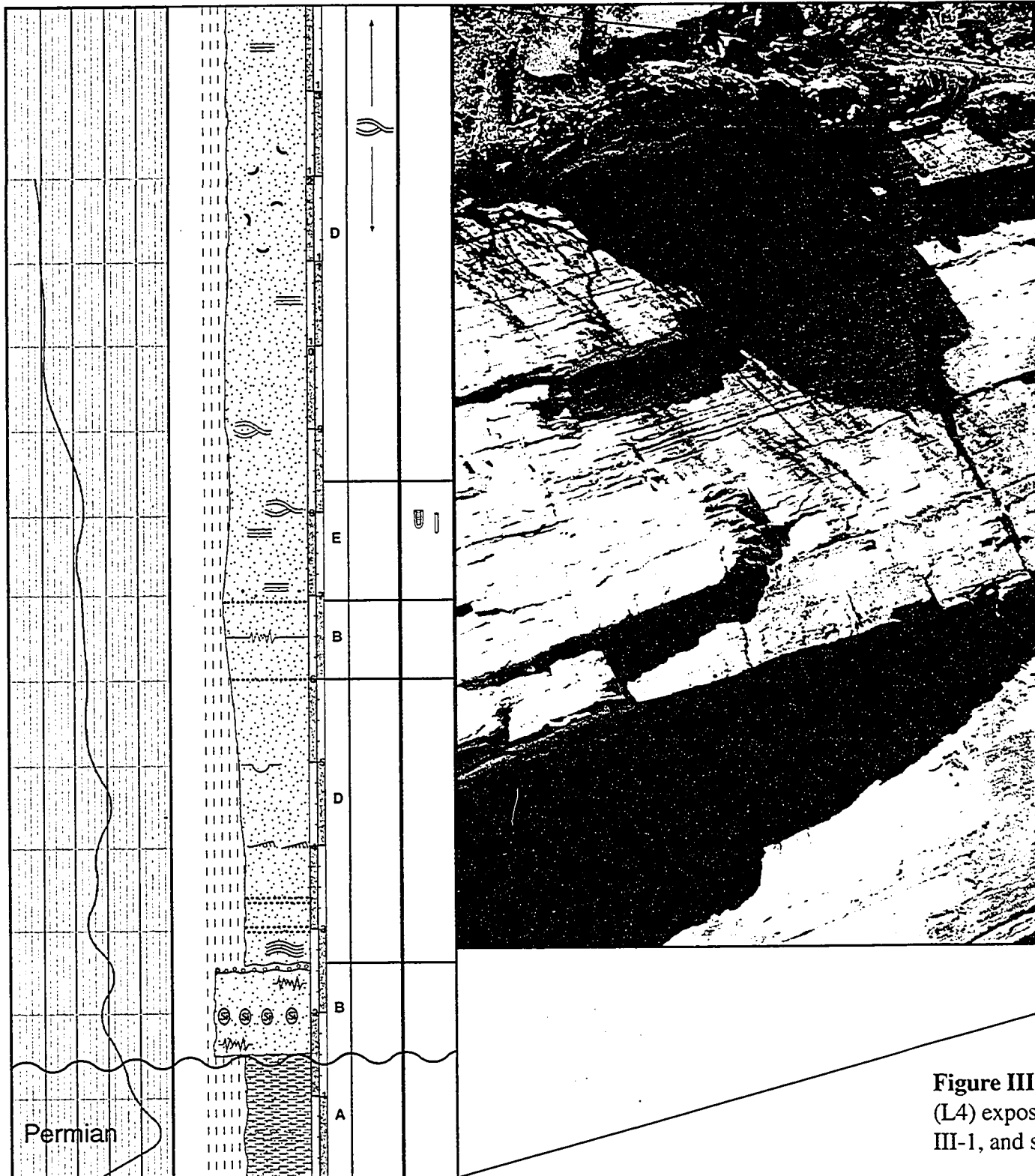


Figure III.
(L4) expos
III-1, and s

- (0446383E 6733983N +/- 51m)	
Interval: 0-14m	Date: Aug. 13, 1999
Location: Chinkeh	Orientation: 163°/ 022°
Geologists: Jason & Murray	Comments:



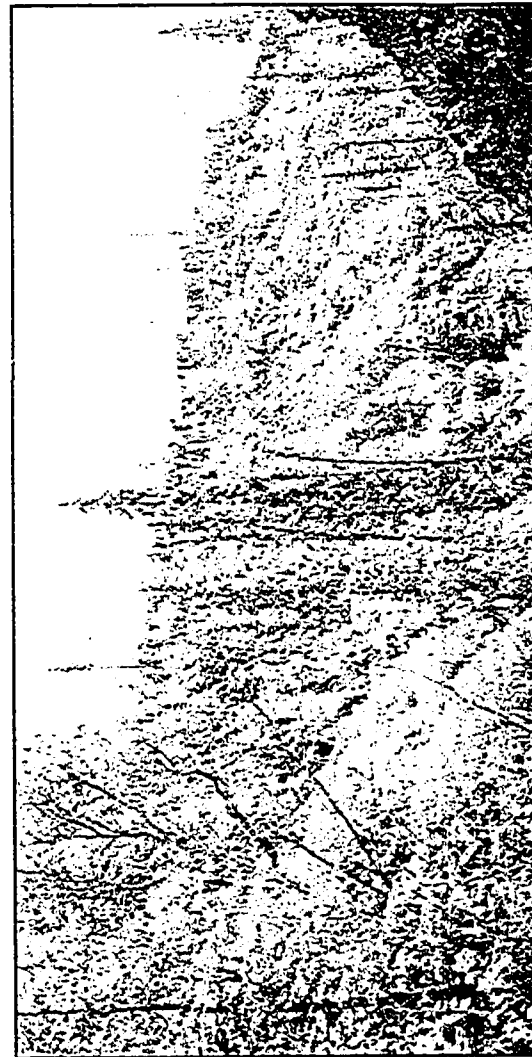
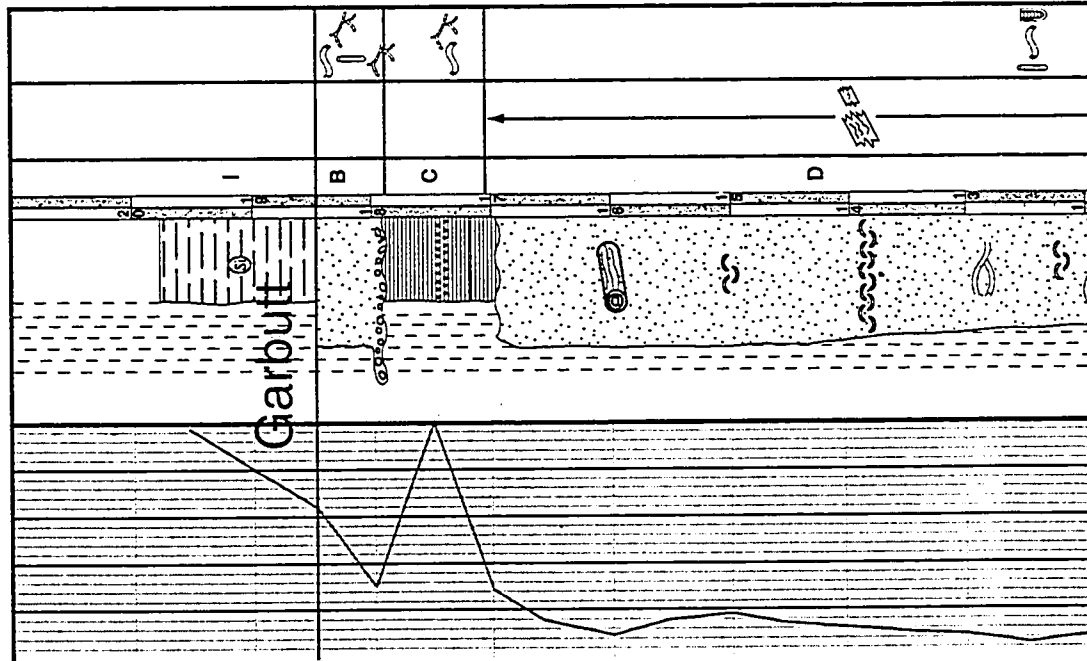
Figure III-7. Photomosaic, outcrop litholog and recorded gamma-ray data for the (L4) exposure. Arrow denotes approximate base and top of measured section. O III-1, and symbols used are defined in Table III-1.



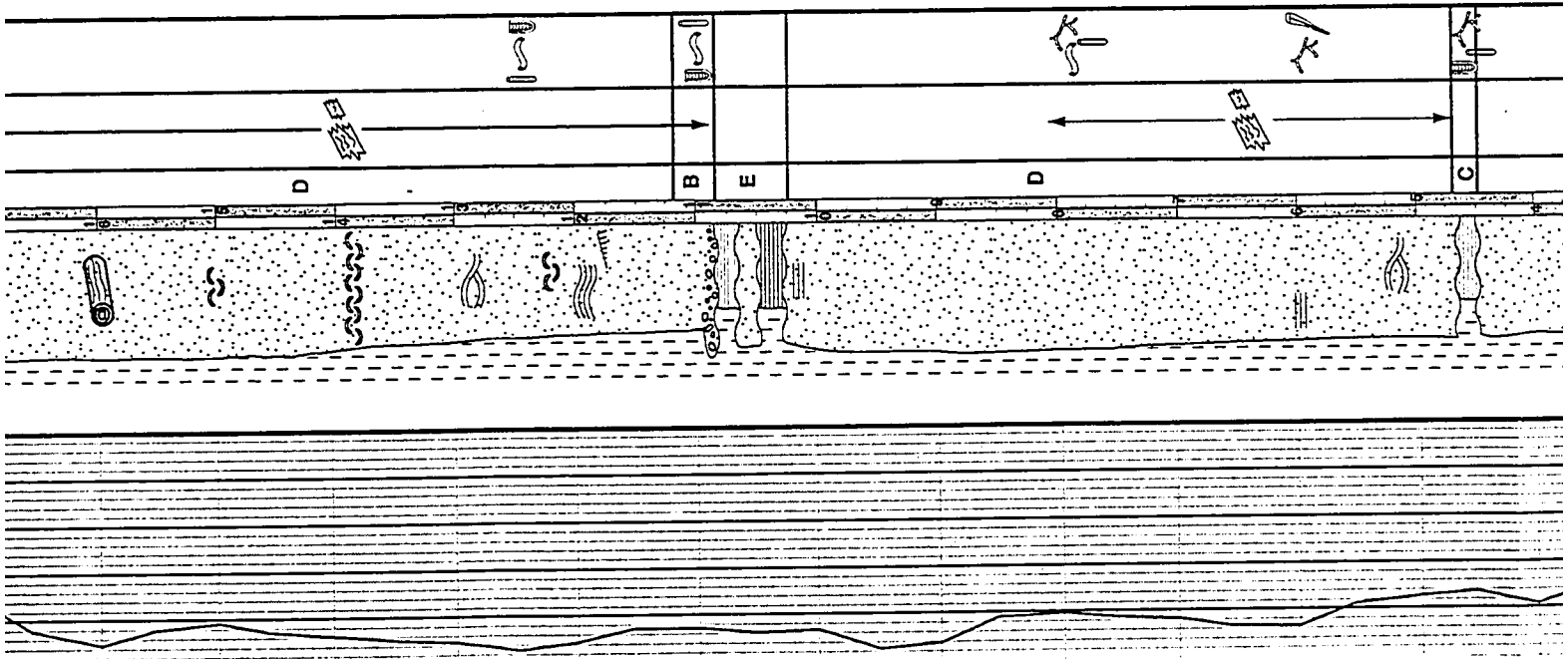
II-7. Photomosaic, outcrop litholog and recorded gamma-ray data for the Chinkeh Formation at the Otter Slide exposure. Arrow denotes approximate base and top of measured section. Outcrop location is shown in Figure I-1. Symbols used are defined in Table III-1.

Location: Slip-Rock Creek - L14 - (411355E 6739859N)	
Outcrop Interval: 0-18.5m	Date: Aug. 5, 1999
Formation: K Chinkeh & Perm	Orientation: 169°/ 025°
Logged by: Jason & Murray	Comments: Type Section

Gamma Ray (CPS)	GRAIN SIZE	DEPTH	FACIES	PHYSICAL STRUCTURES	TRACE FOSSILS
20 30 40 50	<div> <div>sand</div> <div>silt</div> <div>clay</div> </div> <div> <div>very fine</div> <div>fine</div> <div>medium</div> <div>coarse</div> </div>				



Chinken Permian



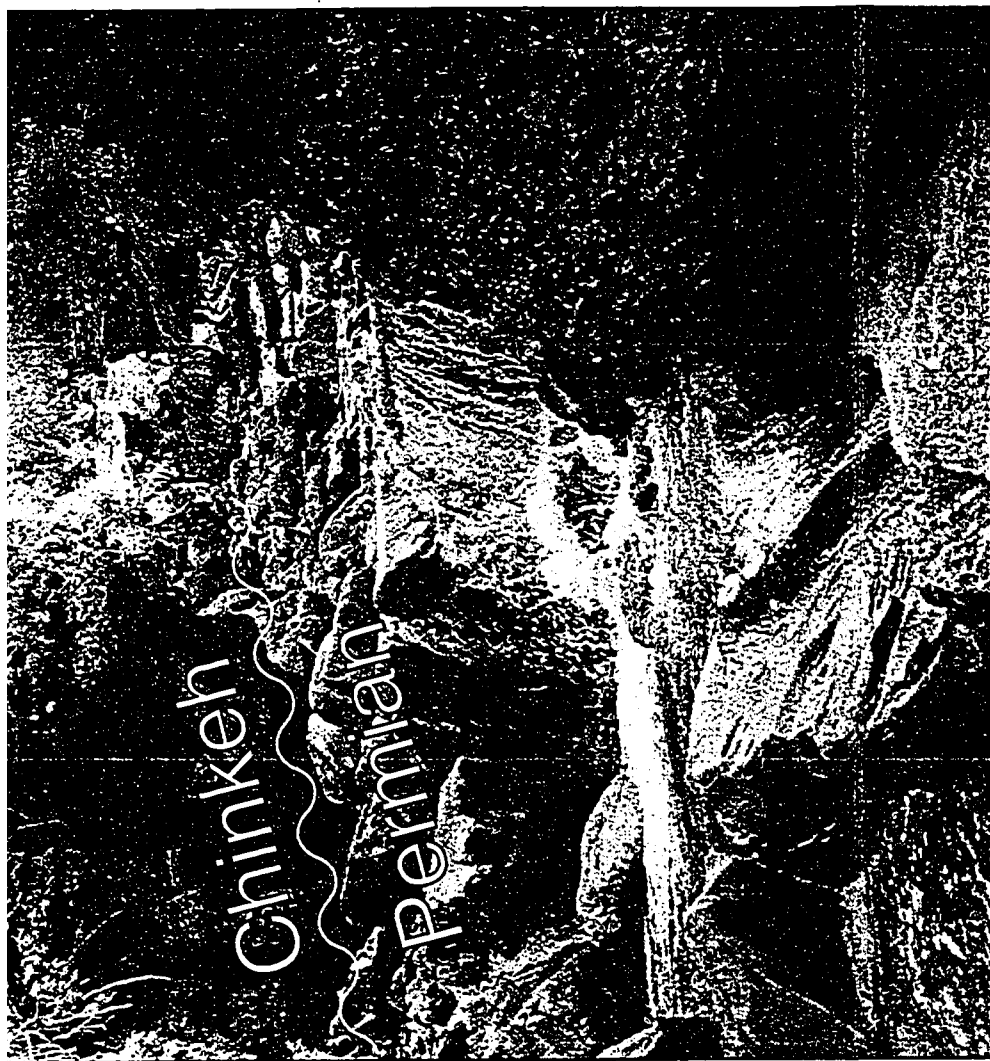
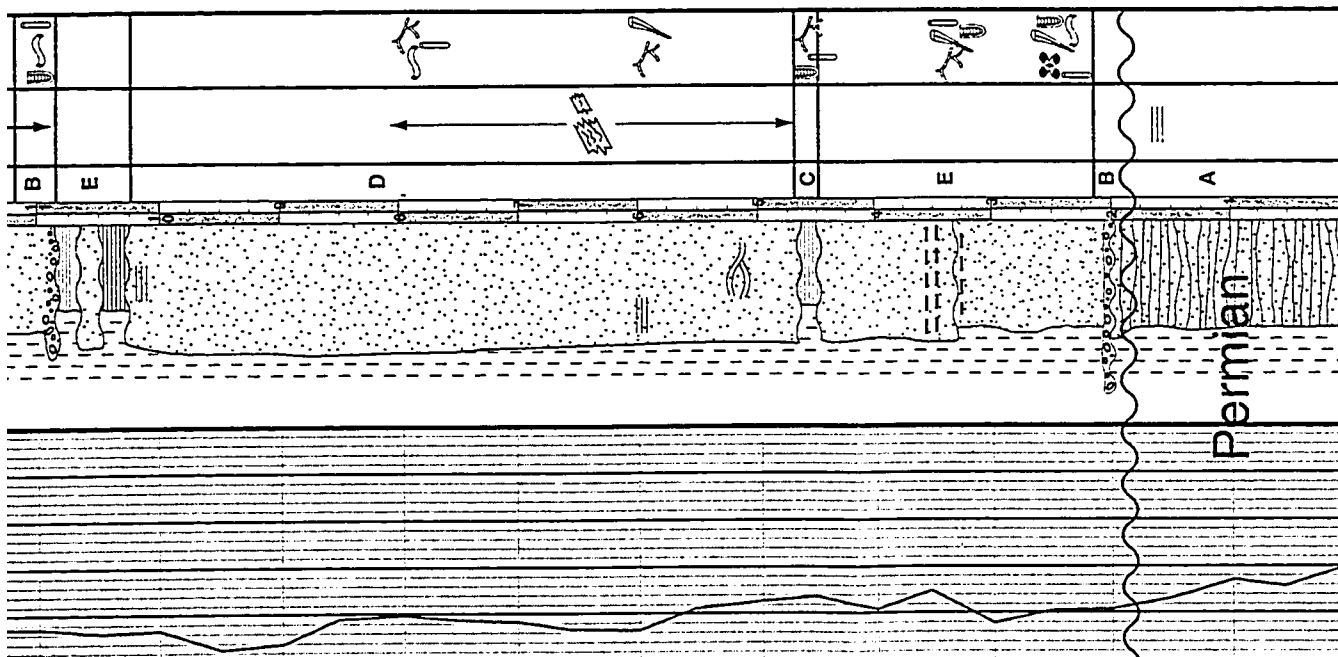


Figure III-8. Photomosaic, outcrop litholog and recorded gamma-ray data for the Chinkh Formation along the Slip Rock Creek (L14) exposure. Approximate base of section is shown on the photomosaic. Outcrop location is shown in Figure III-1, and symbols used are defined in Table III-1.



difficult to determine where in the stratigraphy this section was located. Located in a tightly folded canyon, this exposure was extremely contorted. Only 100 meters along dip, bedding in the underlying stratigraphy was vertical, and appeared in stacked shallow thrusts. The descriptions from this location have been omitted from the facies descriptions and interpretations. However as a matter of completeness, its photomosaic and litholog are included here (Figure III-9). Thickness observed at this location is 13 meters.

LOWER CRETACEOUS SCATTER FORMATION

The two outcrop localities visited that investigated the Bulwell Member of the Scatter Formation, display very similar depositional facies. In general the outcrop exposures were composed of highly interbedded sandstones and intensely bioturbated shales. Sands were well laminated with alternating glauconite-rich and non-glauconite laminations. These sandstones were also dominated by high wavelength bedforms, that on occasion amalgamated to form 50 centimeter thick beds.

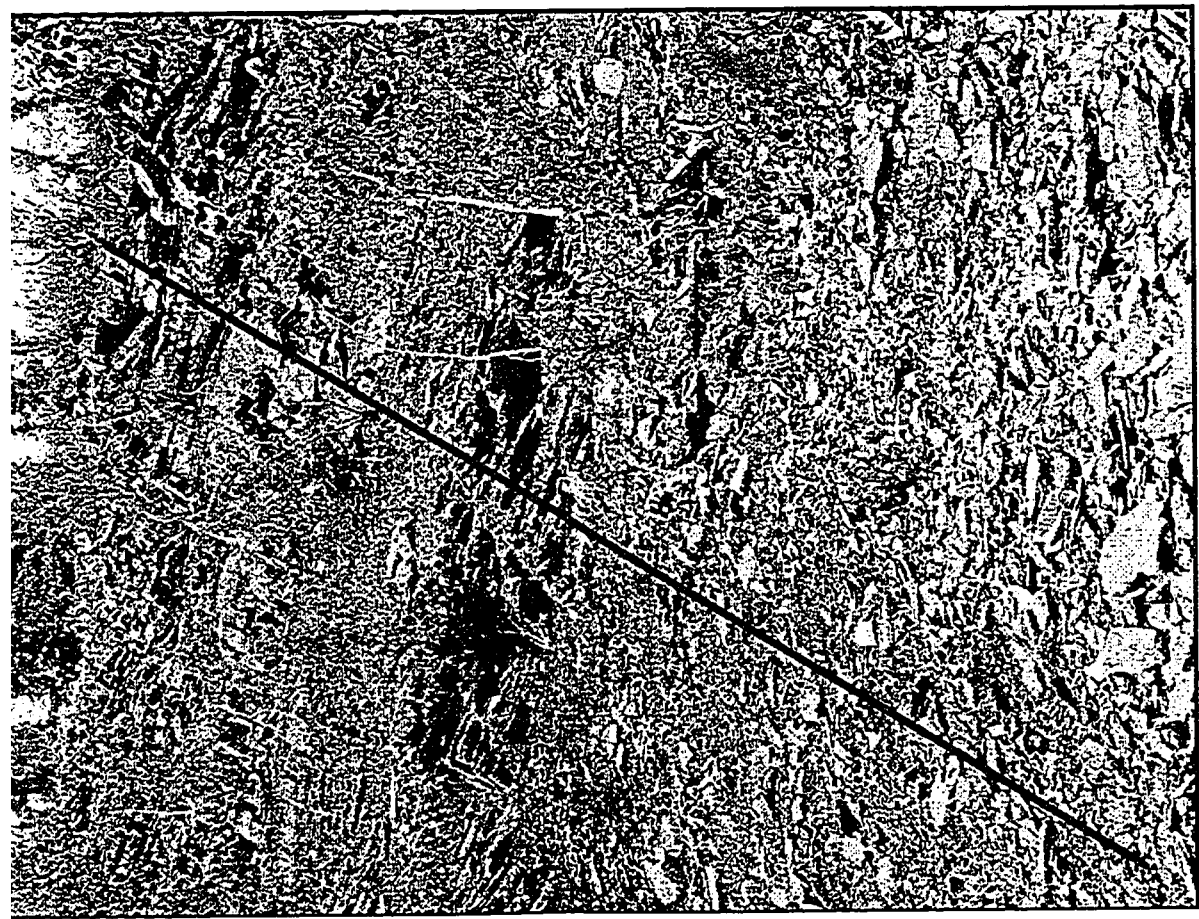
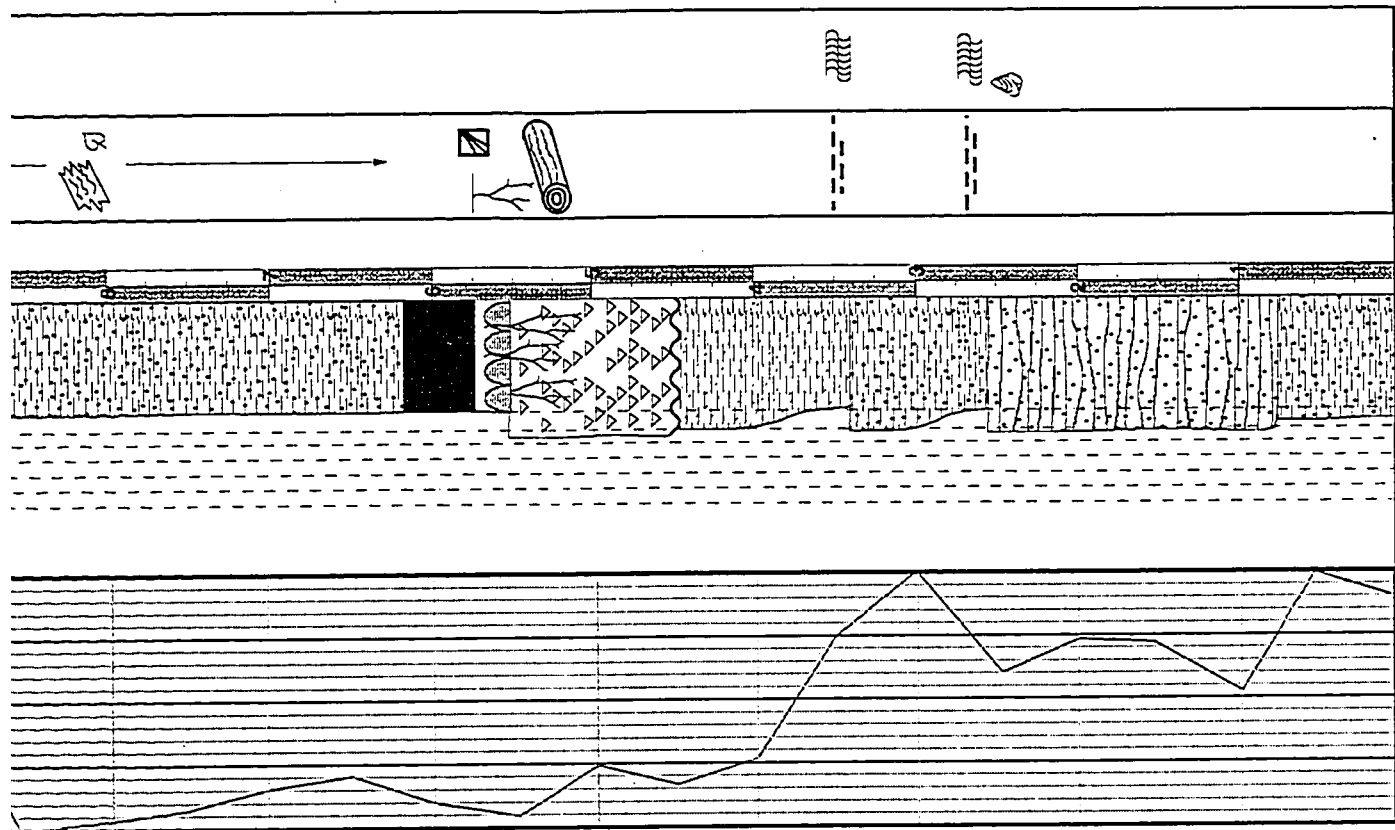
Within the context of this thesis, the Bulwell Member is defined as the first occurrence of glauconite-rich sand above the shales of the Garbutt Formation. A much more rigorous investigation of the Scatter Formation is dealt with in the following chapter.

OUTCROP L8 – KOTANEELEE RIVER

The exposures along the Kotaneelee River gave good opportunity to observe the glauconite-rich sandstones of the Scatter Formation. Base of section was taken from the first occurrence of sand above the Garbutt Formation shales. Top of section was defined based on the last occurrence of sand, and marks the contact with the shales of the Wildhorn Member of the Scatter Formation. The thickness of glauconitic sandstones of the Bulwell Member is 11 meters (Figure III-10). Lower contact with shales of the Garbutt Formation was not exposed at this location.

OUTCROP L1

This outcrop like L33 lies on the Sully Creek, and so it was possible to walk to the contact between the Chinkeh, Garbutt and lower two members of the Scatter Formations.



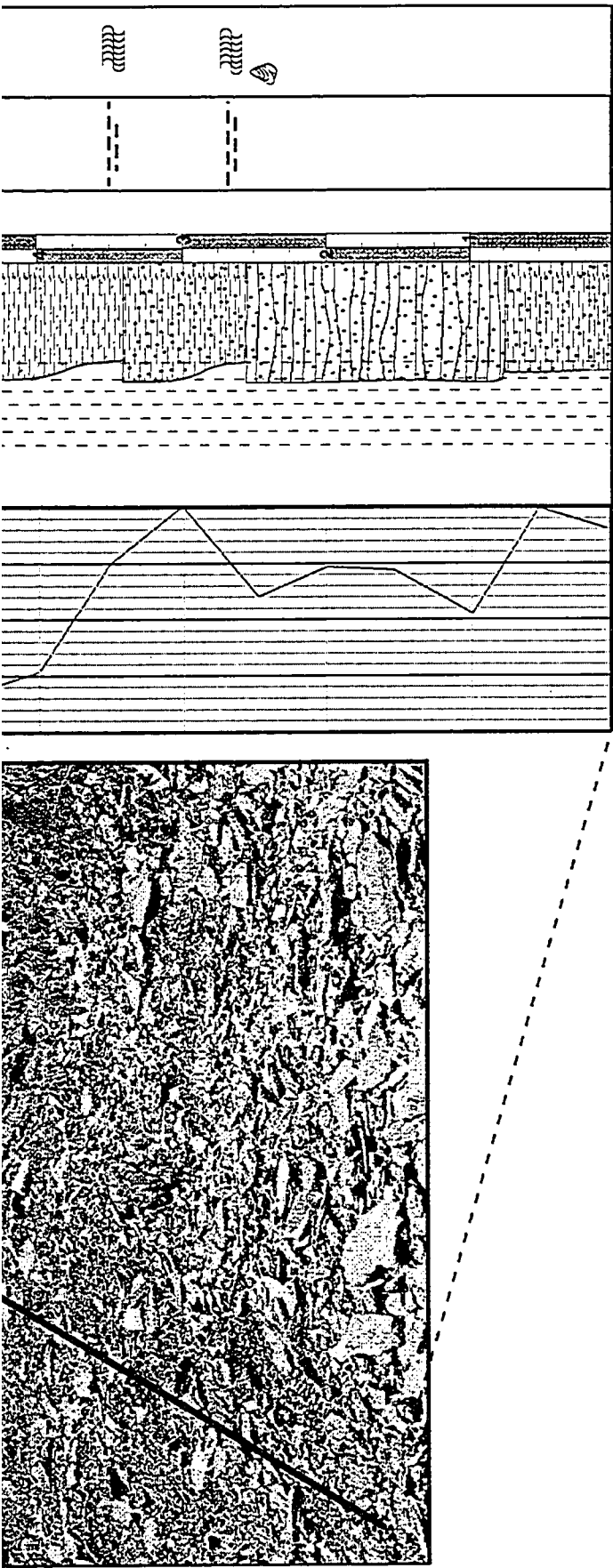


Figure III-9. Photomosaic, outcrop litholog and recorded gamma-ray data for the Chinkoh Formation along Tika Creek (L6). Approximate line of section is shown on the photomosaic. Outcrop location is shown in Figure III-1, and symbols used are defined in Table III-1.

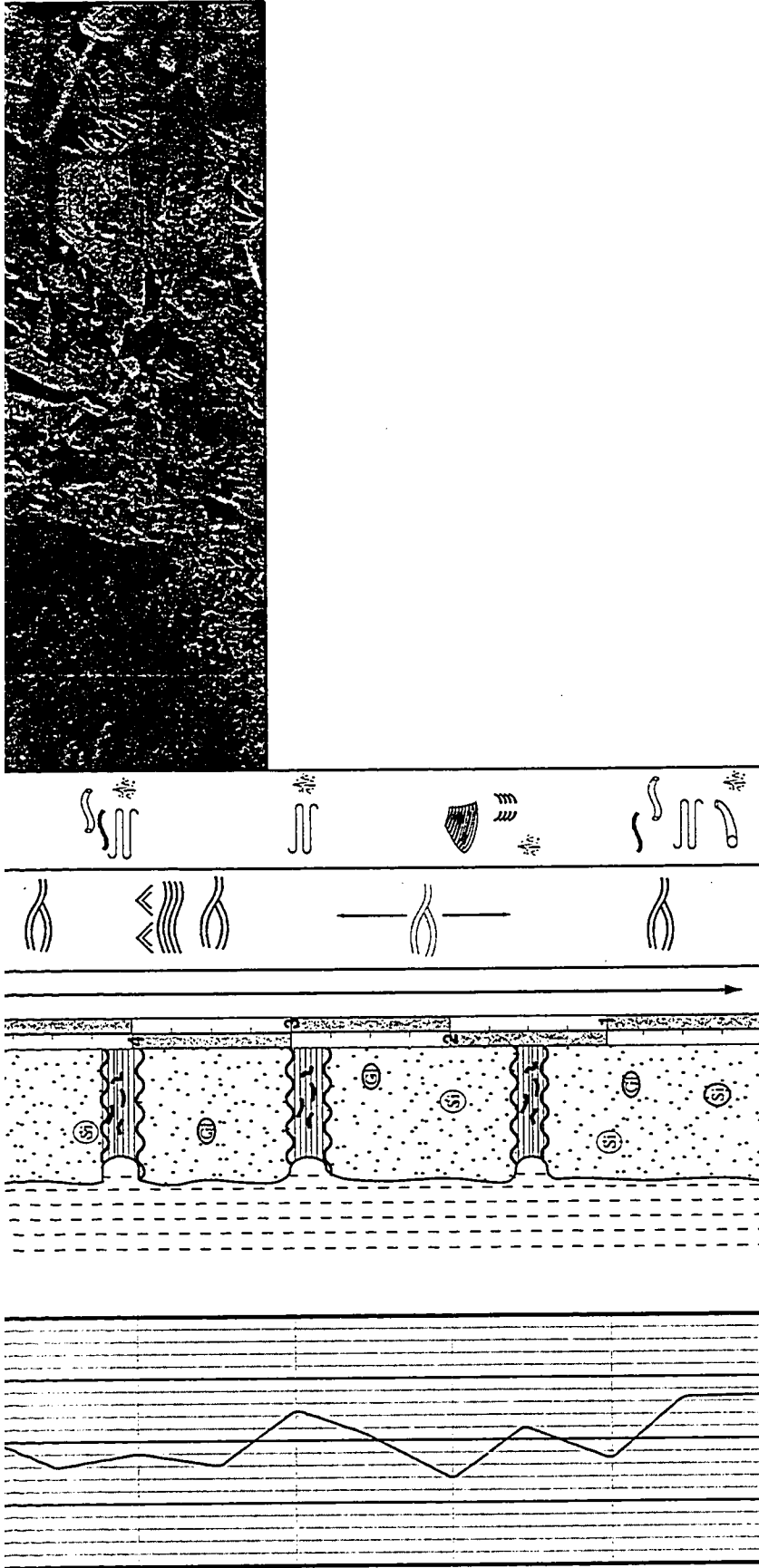


Figure III-10. Photomosaic, outcrop litholog and recorded gamma-ray data for the lowermost member of the Scatter Formation along the Kotaneelee River (L8). Note the highly interbedded nature of the exposure, consisting entirely of Facies E. Outcrop location is shown in Figure III-1, and symbols used are defined in Table III-1.

The thickness and gamma-ray data was collected for the stratigraphic distance between the two formations. These results are summarized in Figures III-27 and III-28. As was the case for the previous Scatter outcrop (Kotaneelee River-L8), base of section was defined based on the first occurrence of sandstone above the Garbutt Formation. Top of section was defined on the last occurrence of sandstone, below the Wilhorn Member shales. Observed thickness of the Bulwell member is 9.5 meters (Figure III-11).

Facies Descriptions

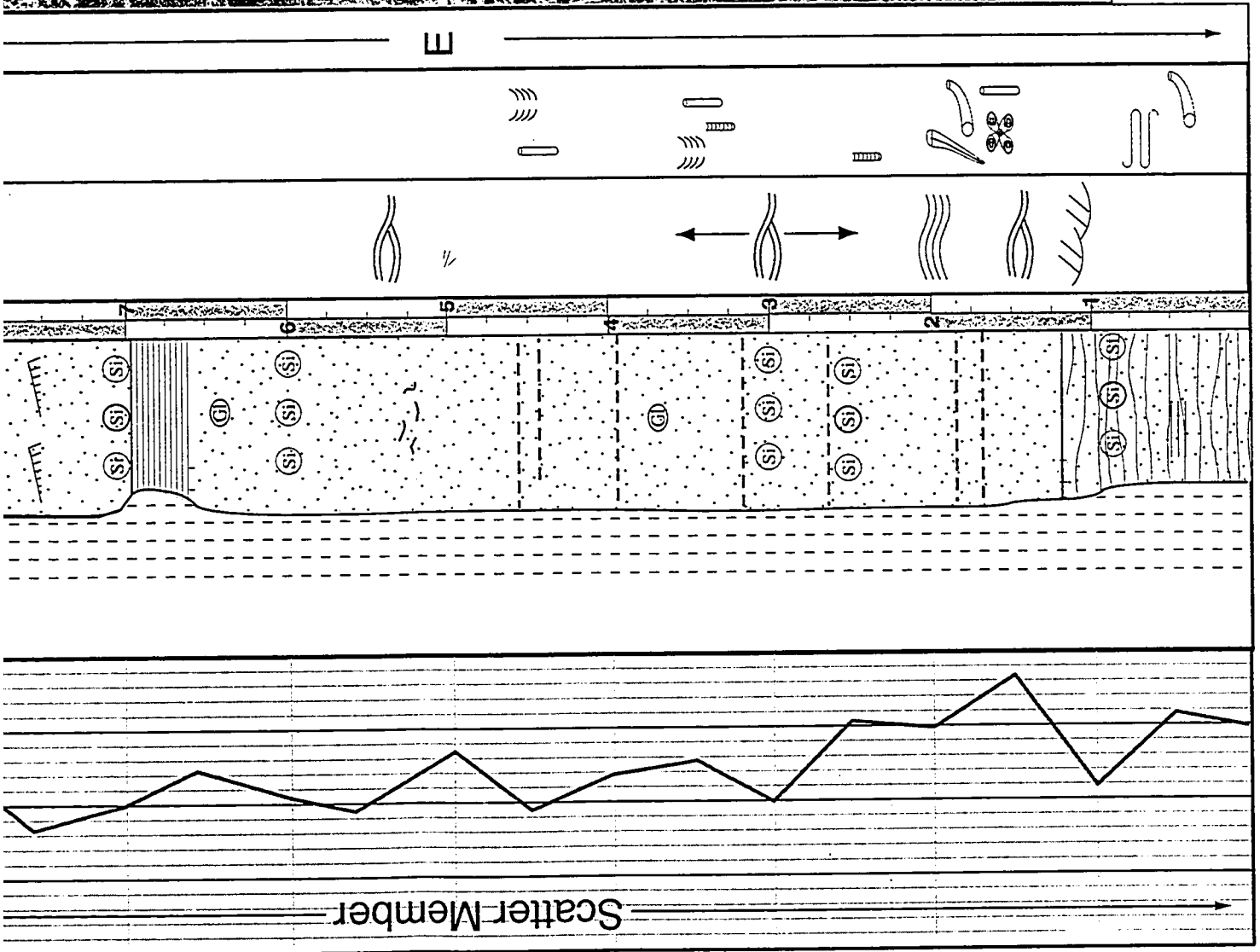
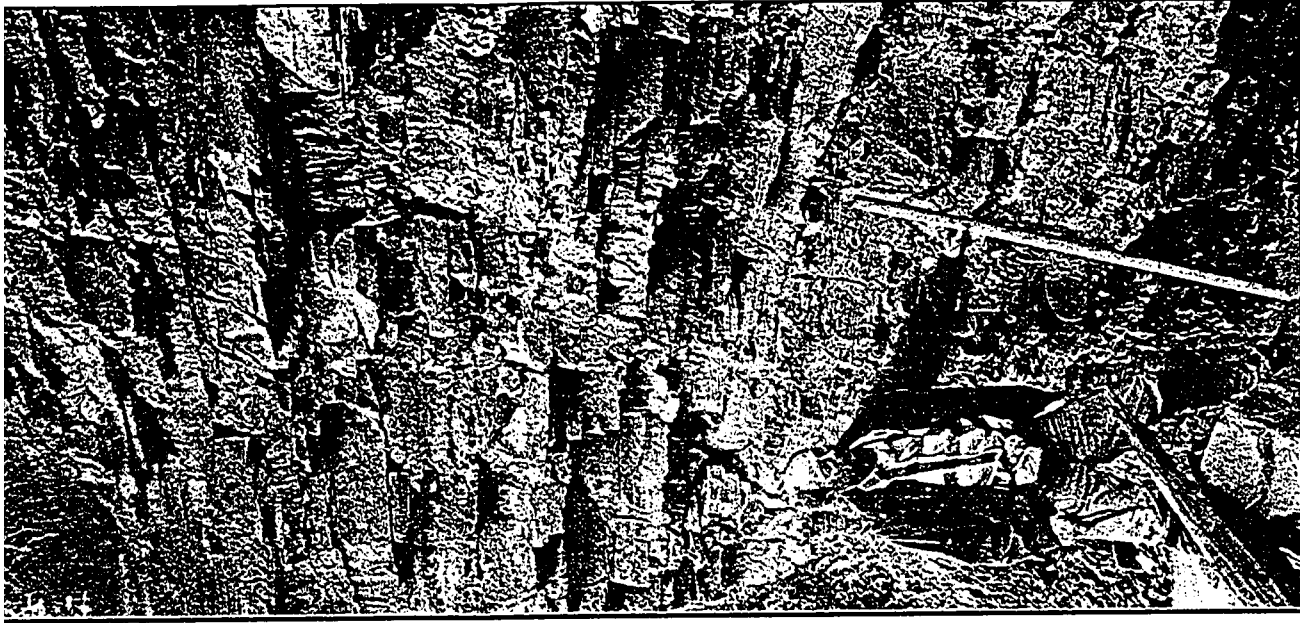
Nine distinct facies were recognized in the outcrop exposures examined within the Liard Basin. These are summarized within Table III-2. These facies are identified based on their physical and biological characteristics observed at the outcrop-scale. These features include lithology, grain-size, and physical and biogenic sedimentary structures. Grain size measurements were made by visually comparing the sediments to a grain size card. The facies identified represent the genetic relationship between the environment in which the sandstones were deposited, and the subsequent reworking through physical and biological processes. The relative degree of reworking subsequent to deposition is a product of the environment of deposition. A reconstructed depositional environment is then interpreted based upon analogies with similar facies and successions from both ancient and modern examples.

FACIES A: PERMIAN STRATA

Description

The Permian strata, which underlies the outcrop exposures of the Lower Cretaceous Chinkeh Formation is highly variable. At some outcrop localities, interbedded silts and shales were observed (Figure III-12 A&B), however a fine- to medium-grained sand was also observed (Figure-12 C). Here large wavelength swaley-cross stratified sandstones were observed, within white coloured, quartzose sandstones. The upper contact of the Permian with the Lower Cretaceous Chinkeh Formation is always sharp, and often is accompanied with a coarse-grained, chert-pebble conglomerate (Facies B). Locally, the Permian strata display deformational structures, especially where overlain by coarse-grained clasts of Facies B.

The observed ichnology within the Permian strata is remarkable. The morphology



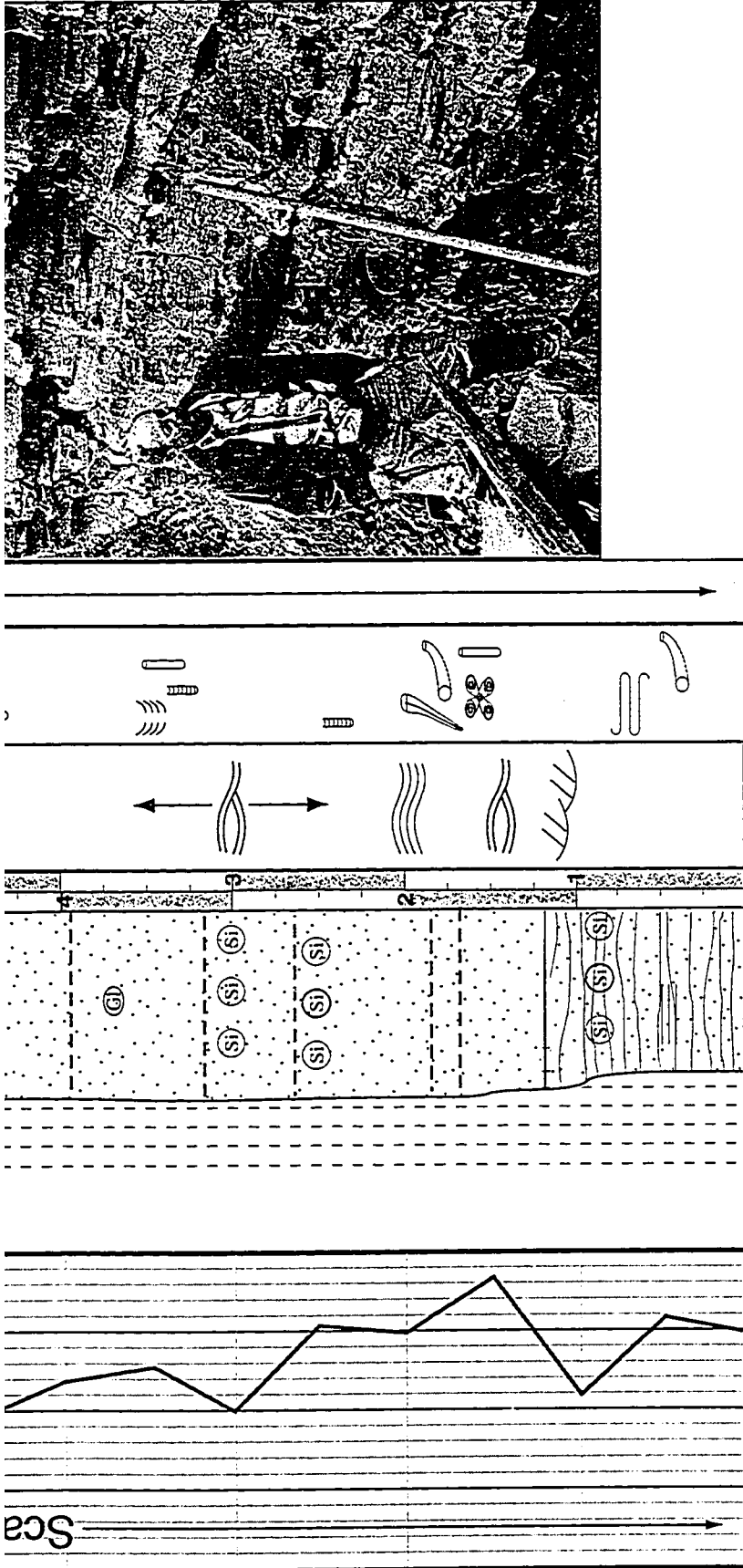


Figure III-11. Photomosaic, outcrop litholog and recorded gamma-ray data for the lowermost member of the Scatter Formation along Sully Creek. Author's father holding pogo stick (1.5 m in length) at base of section for scale. Note the highly interbedded nature of the exposure, consisting entirely of Facies E. Outcrop location is shown in Figure III-1, and symbols used are defined in Table III-1.

Facies	Dominant grain-size and lithology	Ichnofossils	Sedimentary Structures	Interpretation	Stratigraphic Interval	
A	Interbedded silts and shales OR fine-grained quartz-rich sands.	None Observed	Planar parallel laminations in finer-grained strata, while coarser-grained strata contained HCS and SCS	Shelfal??	Permian Mattson Formation	
B	Matrix and clast supported chert-pebble conglomerate, and coarse grained quartzose sands	Rare <i>Thal.</i>	Siderite nodules and stylolites	Transgressive lag & Lowstand incision events	Cretaceous Chinkeh Formation	
C	At outcrop scale, continuous shale beds	<i>Ch.</i> and <i>Pl.</i>	Bedding on centimeter-scale	Distal - Lowershoreface Flooding Surface		
D	Fine- to medium-grained quartz sandstone. Minor wood fragments, and shell fragments present locally.	Rare <i>Thal.</i> , <i>Skol.</i> , and <i>Ophs.</i>	HCS/SCS sands, loaded mega ripples, rare tool marks.	Reworked Lower - Middleshoreface		
E	Interbedded fine-grained quartzose sands and bioturbated shales. Scatter Formation - these sands are glauconite-rich	<i>Thal.</i> , <i>Skol.</i> , and <i>Diplo</i> cross-cutting <i>Ch.</i> , <i>Pa.</i> , <i>Pl.</i> , <i>Hel.</i> , <i>Te.</i>	Sharp-based HCS/SCS sands, with rare ripple laminations.	Lower shoreface - Offshore transition		Cretaceous Scatter (Bulwell Member) Formation
F	Carbonaceous-rich quartz sandstone. Minor shell fragments, and wood debris locally.	<i>Thal.</i> , <i>Plan.</i> , <i>Paleo.</i> , <i>Cyl.</i> , <i>Skol.</i> , <i>Diplo.</i> , <i>Hel.</i> , <i>Te.</i> , <i>Ophs.</i>	Cross-laminated sands, with minor trough cross-bedding grading upwards into ripple and wavy laminations	Prodelta sediments, embayment		
G	Fine- to medium-grained sands, subtended by vertical burrows filled with galuconite-rich sands.	<i>Diplocraterion</i> , <i>Habiche.</i> , <i>Rhizo.</i> , <i>Skol.</i> , and <i>Thal</i>	None preserved	Transgressive surface of erosion		
H	Quartzose sands dominated dominated by woody debris.	<i>Cyl.</i> , <i>Skol.</i> , and rare escape traces	Wavy to lenticular sands, ripple laminated capped by shell hash layer	Intertidal deposits		
I	Dark fissile shales, sideritized nodules forming bedding planes.	None observed	Bedded on centimeter scale	Distal offshore deposits	Cretaceous Garbutt Formation	

Table III-2. Table of facies identified in Lower Cretaceous outcrop exposures within the Liard Basin.

Key to abbreviated Ichnogenera:

Thal.: *Thalassinoides*, *Ch.*: *Chondrites*, *Pl.*: *Planolites*, *Pa.*: *Palaeophycus*, *Skol.*: *Skolithos*, *Ophs.*: *Ophiomorpha*, *Diplo.*: *Diplocraterion*, *Hel.*: *Helminthopsis*, *Te.*: *Teichichnus*, *Cyl.*: *Cylindrichnus*, *Rhizo.*: *Rhizocorallium*.

Key to abbreviated sedimentary structures:

HCS: Hummocky cross-stratification, SCS: Swaley cross-stratification

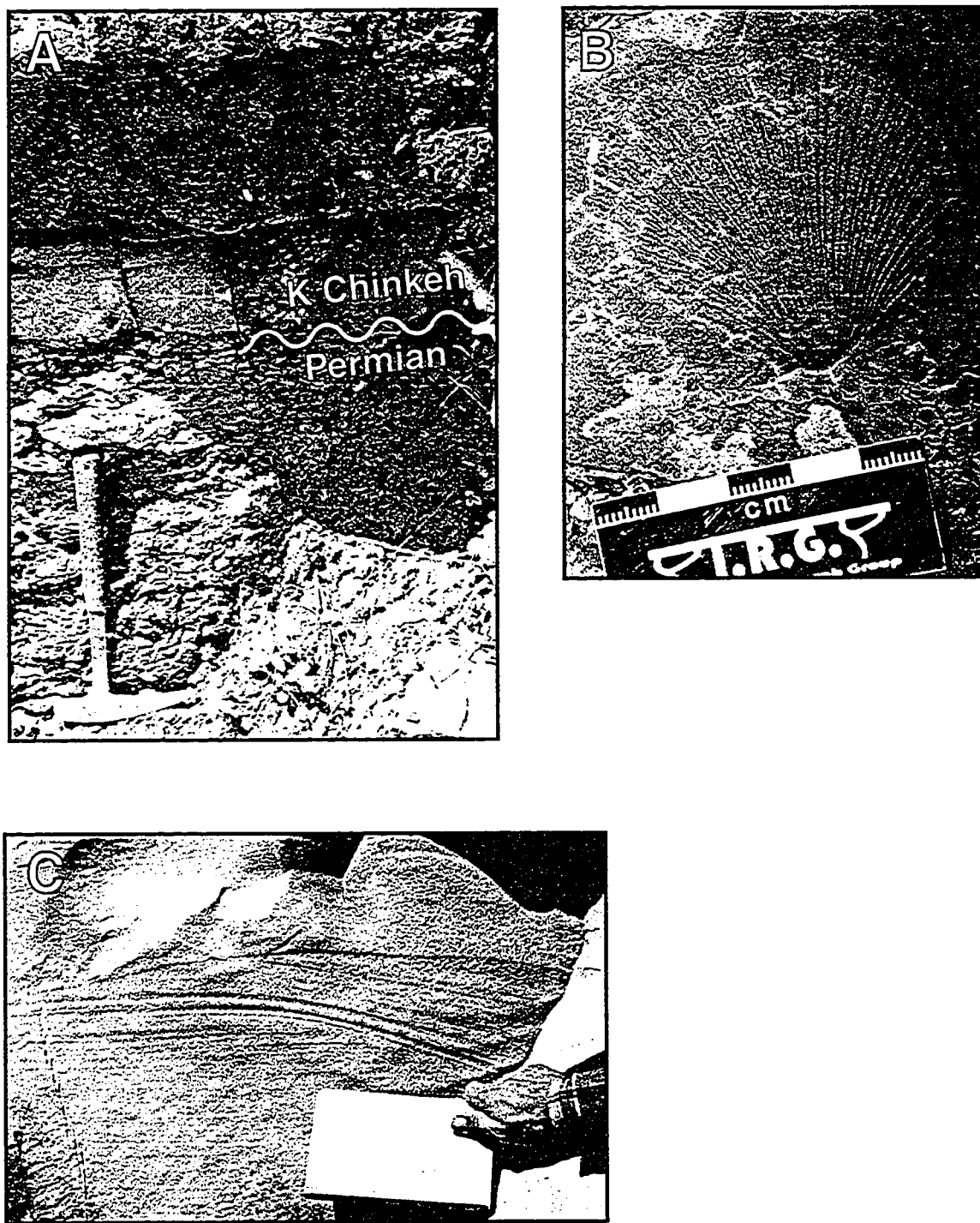


Figure III-12. Variability in grain-size within the underlying Permian strata. Photo A: Base of Burnt Timber (L19) section. Note the dramatic grain-size difference. Photo B: Pecten mold found within fine-grained Permian strata (base of section - Burnt Timber exposure). Photo C: Fine to medium-grained, swaley cross-stratified Permian sandstones below base of section at Sully Creek (L18).

of traces are larger, and much more robust than the morphologies observed within the Cretaceous sections examined. While no detailed investigation has been completed on these biogenic structures at these localities, it would be imperative in determining the deposition environment of these sandstones.

Interpretation

While it is beyond the scope of this project to comment on the depositional setting of the Permian strata, it should be noted that these sandstones were deposited under marine conditions.

FACIES B: CHERT-PEBBLE TO COBBLE CONGLOMERATE AND COARSE GRAINED-SANDS

Description

Facies B is easily recognized as it comprises the coarsest-grained sediments within the Chinkeh Formation. It is comprised of clast and matrix supported chert conglomerate and coarse-grained sand. While the grain-size does not vary locally, outcrop exposures containing Facies B show considerable variation in grain-size. Clasts within the conglomerate can range from pebble to cobble size. These clasts are composed entirely of chert clasts, subrounded to rounded, which show no imbrication. Facies B is commonly found sharply and erosively overlying Permian strata. The most spectacular example of this facies was found at the Murky Creek (L18) outcrop. Here cobble-sized, rounded chert clasts sit unconformably over fine-grained sandstones of the Permian Mattson Formation (Figure III-13). While this is the most extreme example of grain-size variation across this contact, generally most other outcrop exposures exhibit a similar chert-pebble conglomerate at the base of section. Grading upward, the facies contains common chert pebble stringers floating in quartz arenite sandstone, which can be observed along bedding surfaces within the facies. Sedimentary structures are difficult to discern within this facies, and generally it appears massive, and structureless. Bedding planes become more abundant towards the upper contact of the facies.

The chert-pebble conglomerate of Facies B can be observed interformationally within the Chinkeh, conformably overlying finer-grained sandstones. Within this context, the conglomerate is comprised of matrix-supported pebble- to gravel-sized chert clasts with a scoured, undulatory lower contact (Figure III-14). Floating chert clasts are also

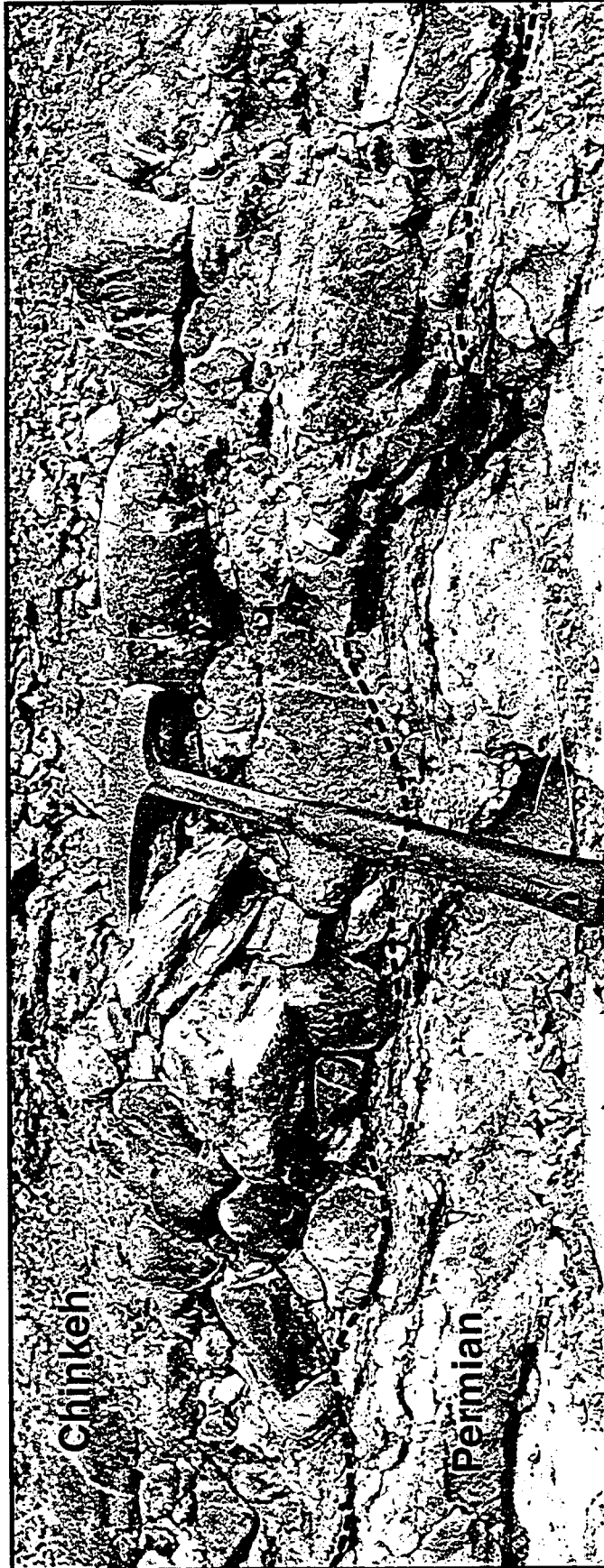


Figure III-13. Coarse-grained cobble conglomerate of Facies B at base of Murky Creek (L18) section. Undulatory, unconformable contact is highlighted (dashed line), where fine-grained Permian strata is overlain by Facies B of the Chinkeh Formation.



Figure III-14. Intraformational conglomerates of Facies B, within swaley cross-stratified sandstones. Note the abundance of chert clasts (arrows) entrained within the large wavelength bedforms. 35.1 m above base of section at the Burnt Timber (L19) exposure.

observed above these undulatory scours, that are entrained along large-scale swales within the overlying medium-grained sandstones. Swales have a wavelength of 1 to 2 meters, and the chert clasts are found along sedimentary bedform boundaries. In total these interformational coarser-grained floating chert-clast conglomerates are no thicker than 2 meters. They fine-upwards into fine- to medium-grained sandstones, more characteristic of the Chinkeh Formation.

The thickness of Facies B ranges from 10 centimeters to 2 meters. It is overlain gradationally by fine to medium-grained quartz sandstones (Facies D) that are typical of the Chinkeh Formation. More rarely it is sharply overlain by shales of Facies C, displaying a distinct 'break' at the outcrop scale. In addition, stylolites, and siderite nodules (up to 5 centimeters in diameter) have been observed within this facies.

Laterally, this Facies B is quite sporadic in its distribution within the study area. The coarsest clasts are found at the base of section at the Murky Creek (18), Burnt Timber (L19), Otter Slide (L4) and Slip Rock Creek (L14). Intraformationally, Facies B is also well developed at Burnt Timber (L19), Slip Rock Creek (L14) and Otter Slide (L4).

The facies is devoid of any trace makers, however where overlying sandstones become more sorted, traces are observed.

Interpretation

The coarse-grained chert conglomerate found at the base of the Chinkeh Formation represents a transgressive lag deposit. This lag is the result of reworking deposits along the Permian/Cretaceous unconformity. The presence of well-rounded and generally well-sorted conglomerates indicates that there was considerable winnowing and reworking at the unconformity. As indicated, these clasts grade upwards into coarse-grained sandstones, that contain 'floating' chert clasts. In this case, chert clasts have been reworked and retransported by wave and storm processes. It is evident that these 'floating' chert clasts are of the same composition, and relatively the same grain-size of those sitting at the base of section.

The provenance for the chert-clasts sitting above the Permian/Cretaceous unconformity is the Paleozoic strata now exposed on the flanks of broad structural highs within the Liard Basin. As marine conditions ensued within the early Cretaceous, topographically high regions were drained into the newly encroaching boreal seaway. Within this drainage network were entrained chert clasts from uplifted Cordilleran structures, which drained into the Liard Basin. As the seaway entered, these

coarser-grained clasts become reworked and dispersed along the Permian/Cretaceous unconformity. As punctuated flooding events continued reworking the unconformity, coarse-grained chert clasts also become entrained and reworked, and deposited further above the unconformity.

Chert clasts found well within the Chinkeh Formation, are also sourced from Paleozoic strata, however these clasts were entrained through a much different manner. Clasts found within the central portions of the outcrop are due to erosional events caused by relative drops in sea level. This drop in base level caused the fluvial channels (still supplying sediment to the Liard Basin) to incise and increase their sediment load to the basin. Eventually as sea level rose once more, these coarser deposits became reworked through more basinal wave processes.

As mentioned above, the distribution of Facies B within the study area is quite sporadic. The coarse-grained conglomerates at the base of section are not present at every exposure of the Chinkeh Formation. This suggests that the distribution of coarse clastic material at the time of transgression was not uniform and/or the mechanism of reworking was also not equal across the study area.

The intraformational conglomerates of Facies B show a more consistent pattern in their distribution. Where Facies B is observed intraformationally, adjacent exposures along depositional strike do not contain Facies B. These adjacent exposures display the reworked, more amalgamated bedding styles of Facies D and F, that represent the laterally equivalent point source sandstones redistributed in shore parallel directions (see depositional synopsis).

FACIES C: LATERALLY CONTINUOUS SHALE BEDS

Description

Facies C is very recognizable at the outcrop-scale, and is characterized by a continuous horizon of dark shale. Within these continuous shale horizons sedimentary structures consists entirely of planar laminated shales (Figure III-15). These shales are bedded on the centimeters scale. Some biogenic reworking is evident, with observable *Chondrites* and *Planolites*.

Facies C never reaches a thickness more than 50 centimeters. It gradationally overlies Facies D, and is overlain sharply by either Facies B, D or F.



Figure III-15. Oblique view of the dark, laterally continuous, fissile shales of Facies C. Note the sharp contact between sandstones below (white arrow), and above (black arrow). Sully Creek (L18) outcrop, 4.5 - 5.5 meters above base of section.

Interpretation

Facies C was deposited in a distal offshore setting. The dark and planar laminated nature of the shales, suggest that they were deposited well below storm wave base. In addition the continuous nature of the facies also suggests a quiescent depositional environment. The stacking pattern, and continuous nature of the facies implies that these shale horizons are marine flooding surfaces. Where present they can be traced across the entire outcrop exposure, and indicate offshore marine conditions. Comparing outcrops from north to south suggests that the preservation of Facies C is limited to the northernmost exposures, where basin depth and therefore accommodation space was the greatest.

The preservation of Facies C represents the flooding surface capping cyclic progradational sequences from the north, and represent the overall southward transport of sediments into the Liard Basin. Three cycles are observed in the northernmost outcrops (i.e. Burnt Timber-L19 and Six Bald Point-L5), while only two are observed further towards the south (Sully Creek-L33 and Otter Slide-L4). The preservation of these small scale flooding surfaces demonstrates the allocyclic controls on sedimentation in the northern, deeper portions of the basin. While towards the south, autocyclic sedimentation dominates and overprints any eustatically controlled sedimentation.

FACIES D: LARGE WAVELENGTH BEDFORM SANDSTONES

Description

Facies D represents the most common facies within the Chinkeh Formation, and it is also the thickest. Characteristic of this facies is the homogenous nature of the sandstones, and the large wavelength bedforms, which dominate the exposure sections. Generally these outcrop exposures are also very 'blocky' in appearance, whose exposures weather vertically. Lithologically the facies consists of quartz arenites, that grade upwards from fine to medium-grained sandstones. The sandstone occurs in beds that are between 10 to 60 centimeters in thickness, but are more typically erosional amalgamated. Generally the sandstones are well-sorted, with organic debris and wood fragments becoming more common towards the top of the facies. These wood fragments range in size from 2 to 3 centimeters in length, to a maximum observed length of 30 centimeters. Facies D observed at outcrop L14 (Slip Rock Creek) showed a recessively weathered tree trunk mold with a diameter of 30 centimeters and a length of 1.25 meters

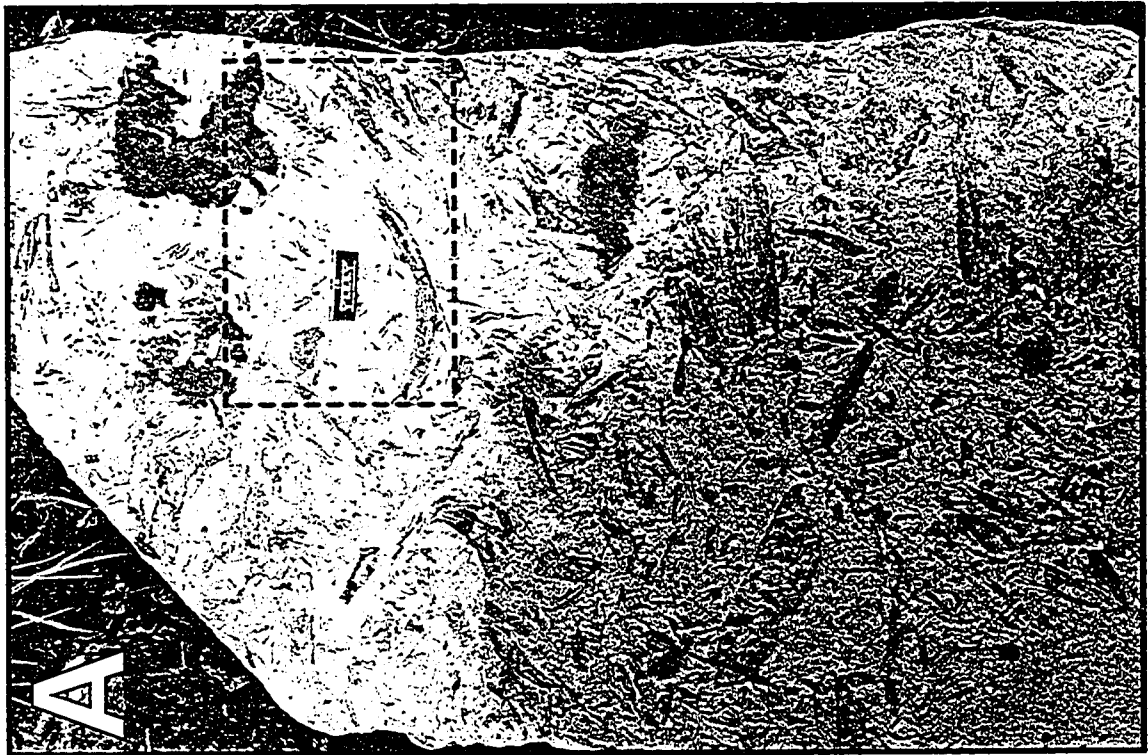
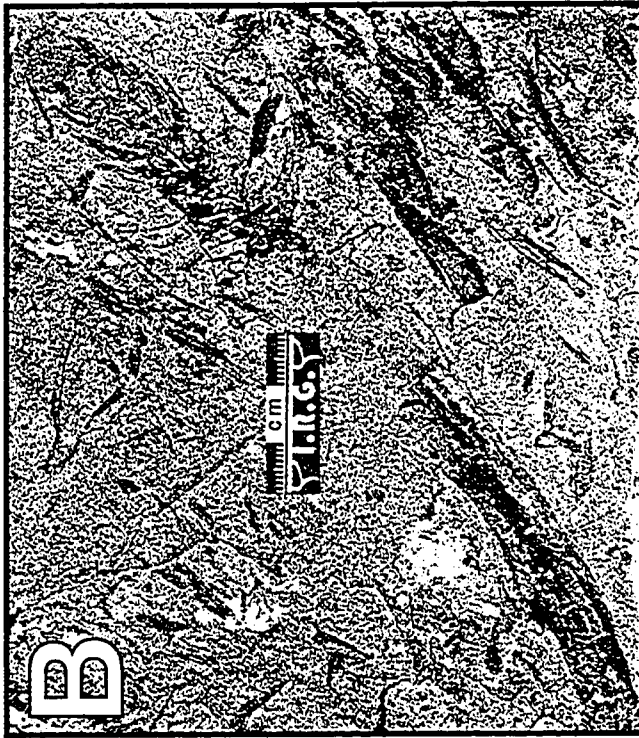


Figure III-16. Bedding plane view of abundant organic debris of Facies D. Photo A: Gross aspect view of bedding plane showing enlarged area of photo B. Six Bald Point (L-5), 12.5 m above base of section.

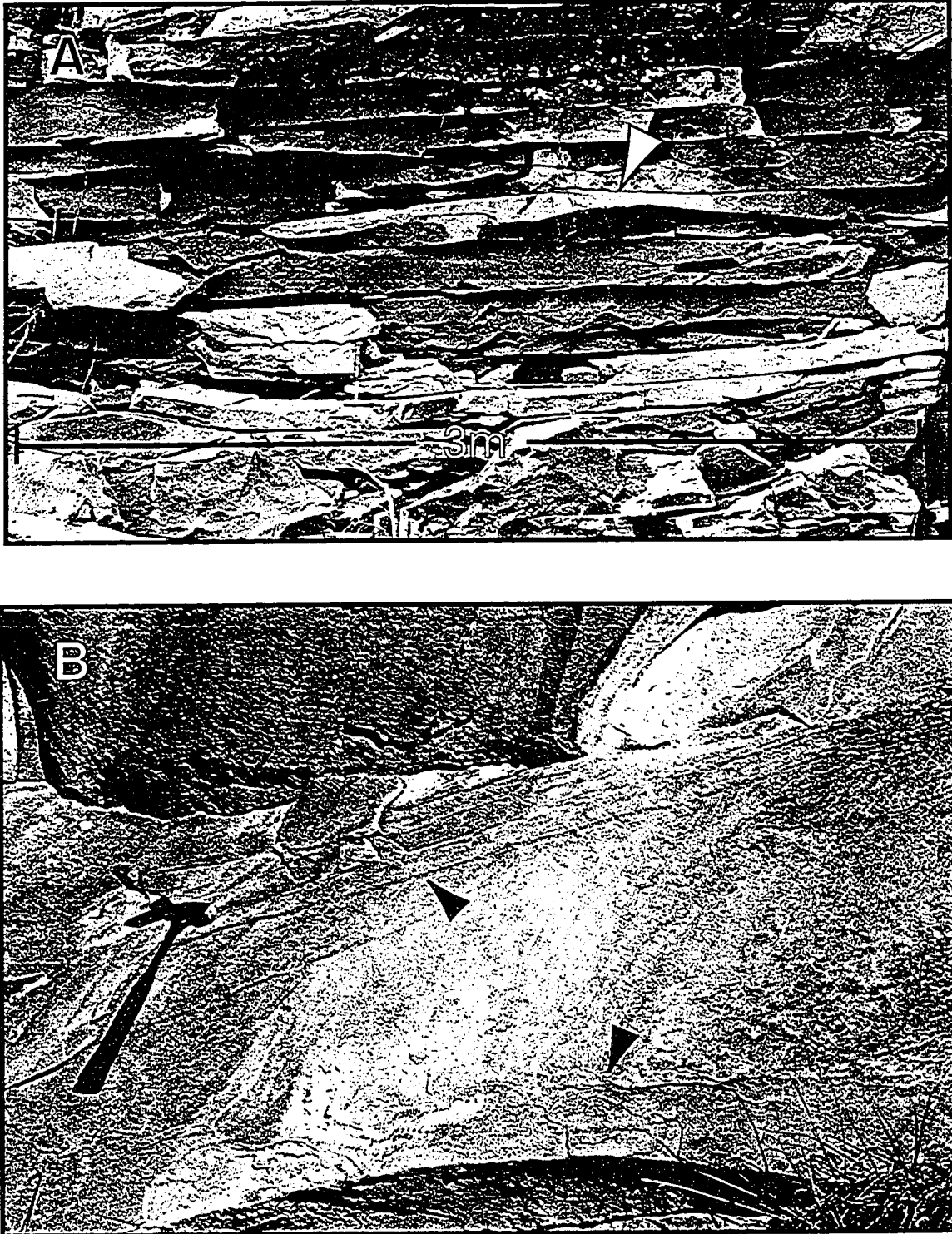


Figure III-17. Amalgamated large wavelength bedforms of Facies D. Photo A: Hummocky cross-stratified sandstones with a wavelength of over 3 m. Hammer is sitting on concave up bedform, while white arrow denotes convex up bedform. Six Bald Point (L5) 8m above base of section. Photo B: Swaley cross-stratified sandstones (arrows denote the swales). Burnt Timber (L19) 25 m above base of section.

(Figure III-16).

The sandstone beds are sharp-based and bounded by truncation surfaces. Hummocky and swaley cross-stratification are abundant within the lower portions of the facies, with wavelengths recorded up to 3 meters (Figure III-17). These bedforms are amalgamated to form amalgamated bedsets of well laminated sandstones that may reach well over 10 meters in thickness.

On a local scale, molds of shells were observed on bedding planes within the sandstones. The shell molds were of uniform size, and were found in hydrodynamically stable positions (i.e. convex upward) (Figure III-18 A). In addition thin (3 to 5 centimeter) disarticulated shell layers were also observed on a local scale within upper most portions of Facies D (Figure III-18 B).

Sedimentary structures within this facies are quite varied. As mentioned above, the lowermost portions of the facies is dominated by large wavelength bedforms of hummocky and swaley cross-stratification. Moving upwards from these amalgamated bedsets, trough cross-stratified sandstones become increasingly more abundant (Figure III-19 B). Steep dipping lamination of foresets and bottom sets are evident. As well, loaded mega ripples of 5 to 10 centimeters of vertical relief were observed within the middle to upper portions of the facies (Figure III-19 A). Towards to the top of the facies, combined flow ripples (Figure III-19 C) and planar parallel laminations dominate the outcrop exposures.

Overall, the facies starts at the base with hummocky and swaley cross-stratification, moving up to trough and ripple lamination and represents an overall increase in grain-size.

The ichnological record of Facies D is poorly recorded in outcrop exposures. Burrowing is typically of low intensity at the base of the facies, with biogenically reworked zones separated by thick intervals of unburrowed, erosionally amalgamated laminated sandstones. Moving upwards however the degree of reworking increases, in both amount and diversity.

The trace fossil assemblage observed at the base of the facies consists mainly of rare deeply penetrating *Skolithos*, that are truncated by amalgamated bedding (Figure III-20 A&B). Moving upwards rare *Ophiomorpha*, *Thalassinoides*, *Cylindrichnus*, *Skolithos*, and *Diplocraterion* (?) are observed (Figure III-20 C). Here to traces become truncated by overlying sandstone beds, and only the deeply penetrating burrows are preserved.

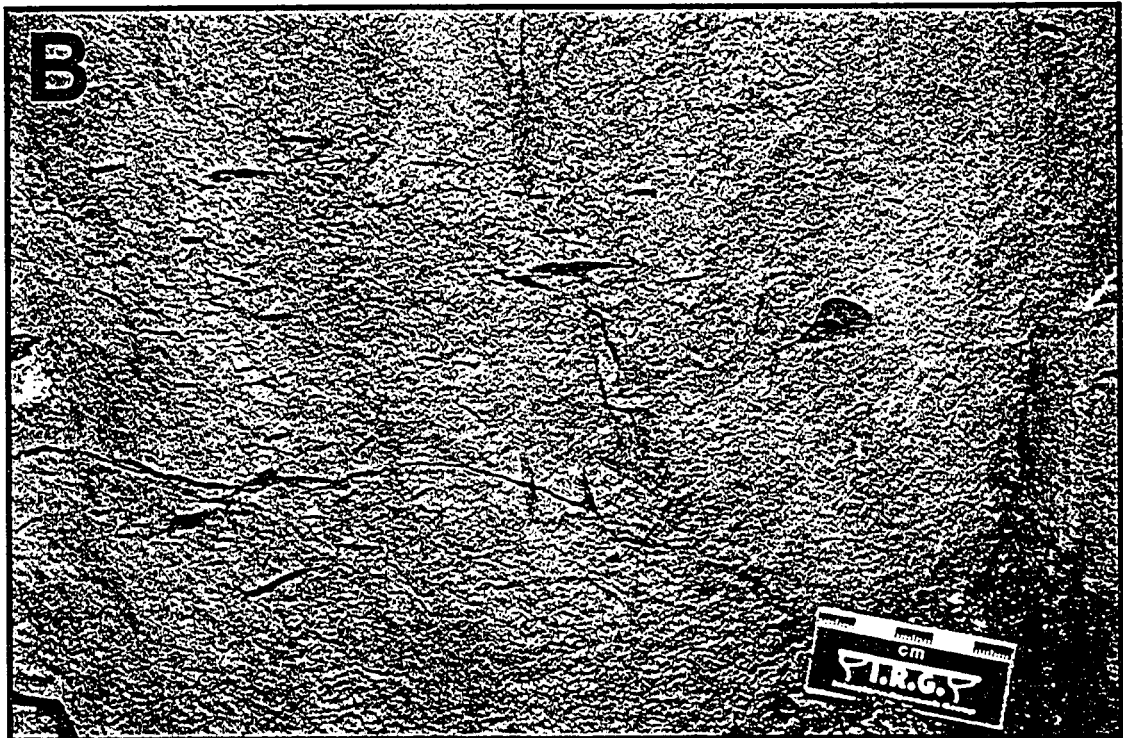


Figure III-18. Shell Fragments within Facies D. Photo A: bedding plane view of shells oriented with the majority in a concave up position. Burnt Timber (L19) 23 m above base of section. Photo B: leached disarticulated shell fragments, highlighting bedding planes. Slip Rock Creek (L14), 14 m above base of section.

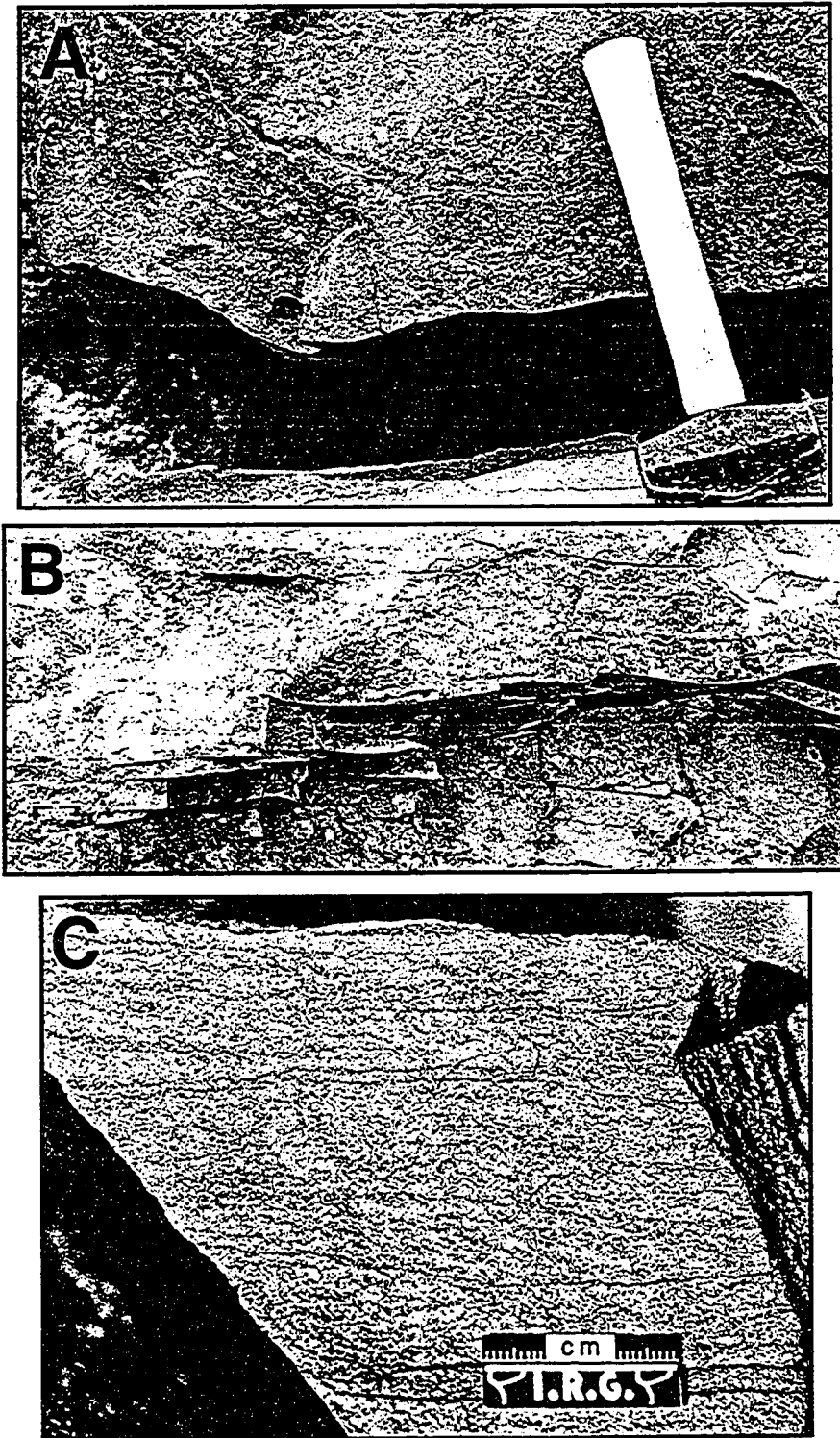


Figure III-19. Sedimentary structures observed within the middle to upper portions of Facies D. Photo A: loaded flute casts with 5 cm of vertical relief at the base of hummocky bed. Six Bald Point (L5), 5 m above base of section. Photo B: trough cross-bedding along the base of beds. Note scale bar in lower left hand corner. Six Bald Point, 2.5 m above base of section. Photo C: combined flow ripples. Otter Slide (L4), 12.5 m above base of section.

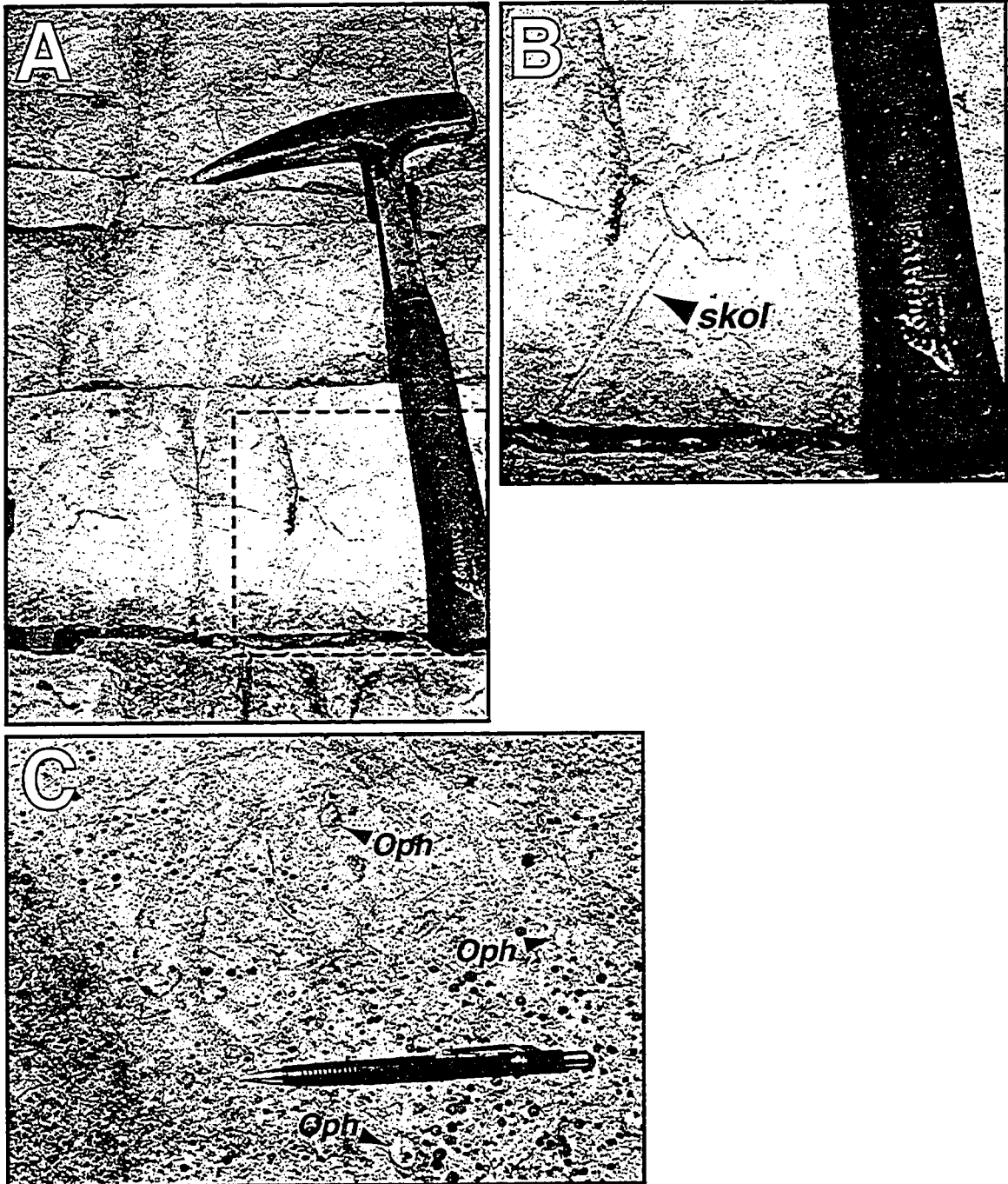


Figure III-20. Typical Ichnology of Facies D. Photo A: Gross view of swaley cross-stratified sandstones (swale at tip of hammer), showing enlarged area of photo B. Sully Creek (L18), 6 m above base of section. Photo B: truncated *Skolithos* (*Skol*) within swaley cross-stratified sandstones. Photo C: bedding plane view of rare *Ophiomorpha* (*Oph*). Otter Slide (L4), 12 m above base of section.

Facies D ranges in thickness from 3.5 to over 11 meters in thickness. It sharply overlies Facies B and F, while gradationally overlying Facies E. It is overlain gradationally by Facies G and sharply by Facies B, F, or I.

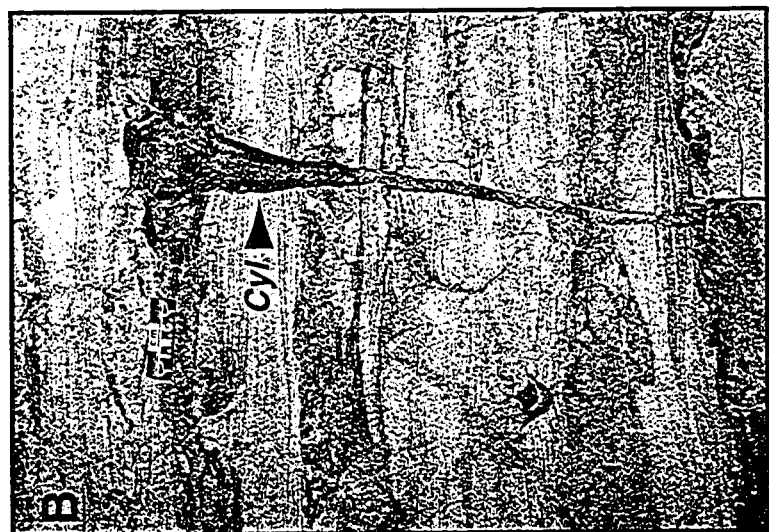
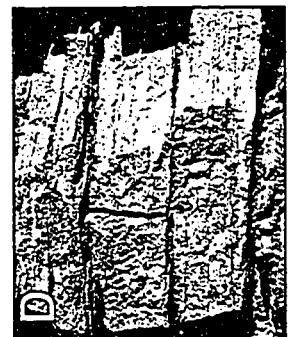
Interpretation

The lowermost portions of Facies D are interpreted to reflect tempestite accumulation within a lower to middle shoreface setting, that prograded southward into the Liard Basin. Hummocky to swaley cross-stratification found at the base of the section were deposited at and above storm weather wave base. The erosional amalgamation of successive tempestites accounts for the lack of biogenic structures within the investigated outcrop sections. Only the remnants of deeply penetrating *Skolithos* are preserved. These burrows are the result of the opportunistic feeding traces of the resident fair-weather suite (Pemberton and Frey, 1984).

Moving upwards, deposition is interpreted as more proximal middle to upper shoreface, than the lower portions of the facies. Here medium-grained trough cross-stratified sandstones become more common, which is interpreted to represent deposition within the middle to upper shoreface. Modern studies of the shoreface have identified that virtually all subenvironments within the upper shoreface are characterized by trough and current ripple cross-bedding (e.g. Clifton *et al.*, 1971, and Howard and Reineck, 1981).

As mentioned above, the coarse-grained pebble to cobble conglomerates of Facies B is laterally equivalent to Facies D. The well-sorted, amalgamated sandstones of Facies D represent the shoreward expression of these coarser-grained point sources. The zones of greatest grain-size correspond with apices of major fan delta complexes and there is a corresponding fining of grain-size away from major sediment sources (Kirk, 1980). In addition sediments become better sorted in the direction of transport (McLearen and Bowles, 1985). Disarticulated bivalve shells in the concave down position are also indicative of current processes (Middleton, 1967; Emery, 1968), which were taking place alongshore. Thus the outcrop exposures containing intraformational conglomerates of Facies B lie proximal to major point sources. While outcrop exposures located further from the fluvial point sources contain finer-grained, better sorted shoreface deposits (see depositional synopsis).

Figure III-21. Characteristics typical of Facies E. Photo A: Large wavelength hummocks within Bulwell Member of the Scatter Formation. Murky Creek (L1), 3 m above base of section. Photo B: Lam-scam style deposition within the Bulwell Member of the Scatter Formation. Note the truncated *Cylindrichnus* (*Cyl*) indicating a stable sediment-water interface prior to truncation by a subsequent storm event. Murky Creek (L1), 2 m above base of section. Photo C: bedding plane view of *Chondrites* within shales separating glauconite-rich, swaley cross-stratified sandstones of the Scatter Formation. Kotaneelee River (L8), 3 m above base of section. Photo D: interbedded sandstones and bioturbated shales of Facies E as observed within the Chinkeh Formation. Burnt Timber (L19), 26-27 m above base of section.



FACIES E: INTERBEDDED SHARP-BASED SANDS AND BIOTURBATED SHALES

Description

At the outcrop scale, Facies E consists of blocky, dominant sandstones with are interbedded with recessive bioturbated shales (Figure III-21). The bases of the fine-grained sandstones are very sharp and undulatory. Sedimentary structures present within the sandstones are hummocky and swaley cross-stratification, that grade upwards into rare planar laminations or ripple lamination. The swales and hummocks have wavelengths from 1 to 2 meters (see Figure III-21 A&B). The thickness of these dominant sand beds is between 30 and 40 centimeters. The uppermost exposed portion of these sandstones shows the greatest amount of bioturbation, while the sandstones dominated by large-scale bedforms are devoid of any traces. Rare escape traces (i.e. fugichnia), *Thalassinoides*, *Diplocraterion*, *Cylindrichnus*, and *Skolithos* were observed at the tops of the sand beds ascending towards the overlying shale beds (see Figure III-21 C). Chert concretions were also common within the sandstones. They ranged in size from 5 to 20 centimeters in diameter, and were always observed within the upper 10 centimeters of the sand beds. The sandstones were sharply overlain by intensely bioturbated dark shales.

The shales that characterize Facies E were difficult to observe. They weathered recessively, such that an identification of individual traces was difficult. However, their mottled and non-planar appearance suggests that their degree of reworking is quite high. Individual traces observed within the shales include *Planolites*, *Palaeophycus*, *Chondrites*, and rare *Helminthopsis* and *Teichichnus* (see Figure III-21 D). The shale beds range in thickness from 10 to 20 centimeters, which are overlain by sharply and erosively by a subsequent large bedform, fine-grained sandstones.

In general Facies E is observed to be between 1 and 2 meters thick. The facies is gradationally overlain by Facies D, which becomes much more blocky and continuous upwards. The characteristics that define Facies E are common among both the Chinkeh and the Scatter outcrops, and is the only facies which is common to both formations at the outcrop-scale.

Interpretation

The interbedded sandstones and bioturbated shales of Facies E are distal expressions of storm deposition within the lower shoreface. The interbedded nature of

the deposits are indicative of lower shoreface deposits and have been termed “laminated to burrowed” bedding (Howard, 1972). Within this facies the shales record quiescence within the depositional setting. Horizontal grazing traces of the *Cruziana* ichnofacies found within the shales, imply that the deposition was between storm and fairweather wave base. Erosively cut into these shales are fine-grained sandstones containing large wavelength hummocky and swaley cross-stratification. Even though the mechanism for producing these sedimentary bedforms is a topic of much debate (Duke et al., 1991), there is consensus that they form below fair-weather wave base during intense storms (Harms *et al.*, 1975, Dott and Bourgeois, 1982, Hunter and Clifton, 1982).

Characteristically these laminated to burrowed beds record a transition from quiescent, fairweather conditions to abrupt and rapid sedimentation demarcated by an erosive or scour surface. The abundance of trace fossils within these finer-grained beds, and the ubiquitous cross-cutting relationship, supports slow continuous deposition with little preserved record of storm events (Howard, 1975). This transition zone, within the lower-middle shoreface complex records both storm and fairweather conditions. As a result of rapid deposition of storm beds, escape traces (fugichnia) record the attempt of organisms to burrow up through the tempestite in order to reach the new sediment-water interface (MacEachern and Pemberton, 1992). In addition, the scouring action of storm deposits preferentially preserves the more deeply penetrating traces (i.e. the *Skolithos* Ichnofacies) above the storm laminated sandstones, and removes the shallow penetrating traces (i.e. the *Cruziana* Ichnofacies) (Frey and Goldring, 1992, and Pemberton and MacEachern, 1997).

FACIES F: CARBONACEOUS-RICH BIOTURBATED SANDSTONES

Description

Characteristic of Facies F is its mottled appearance. At the outcrop-scale the facies is bedded on the centimeter-scale, with bed partings present every 0.5 to 0.75 meters. This makes Facies F readily identifiable compared with blocky exposures of the more typical Chinkeh Formation. The facies consists almost entirely of lower fine-grained to medium-grained sandstones, with thin (less than 2 centimeter) organic-rich interbeds. The shale interbeds are sharply overlain by sandstones, that often contain abundant wood debris. These shale interbeds are not a major component of the facies, and are more common at the base, where it sharply overlies Facies C or gradationally overlies Facies

D. Most sedimentary structures are completely obliterated due to biogenic activity. Typical vestigial laminations are the only remnant of non-biogenic structures within the sandstones. On occasion combined flow ripples and oscillation ripples were noted. Sharply overlying Facies F are thick marine shales of the Garbutt Formation (Facies I). This contact also marks a dramatic increase in the content of wood fragments, which were observed up to 6 centimeters in diameter and 10's of centimeters in length. In addition the woody material had a crude north-south orientation. Wood fragments were also observed within the lower 50 centimeters of Facies I.

The ichnological record of Facies F is difficult to discern. While the overall appearance of the facies suggests a high degree of biogenic reworking, individual traces are difficult to identify. *Palaeophycus*, *Thalassinoides*, *Teichichnus*, and rare *Helminthopsis*, *Diplocraterion*, and *Skolithos* were identified within the facies (Figure III-22). As well traces were generally smaller in size than within other facies of the Chinkeh Formation.

Interpretation

Facies F reflects deposition within the middle to lower shoreface positions of a delta front. The ichnology recorded in Facies F shows colonization by opportunistic organisms under marine to brackish influenced conditions, while the amount of suspension feeding traces found is characteristically low. The low diversity and abundance of robust trace fossils suggest deposition within a stressed environment. Stresses within the deposition of Facies F include brackish water, high sedimentation rates, turbidity and high water energy. It is believed that higher than normal water turbidity, as is common in delta front settings, may be responsible for the decrease in suspension feeding organisms (Rhoads and Young, 1971). In addition, sediments deposited in stressed environmental settings are known to contain low diversity and diminutive trace fossil assemblages when compared to fully marine environments (Howard and Frey, 1973; Pemberton and Wightman, 1992).

Organic material present within Facies F is detrital and occurs as transported fragments from the coastal plain. These fragments are incorporated into Facies F and reworked into shore parallel oriented wood or plant fragments by wave energy.

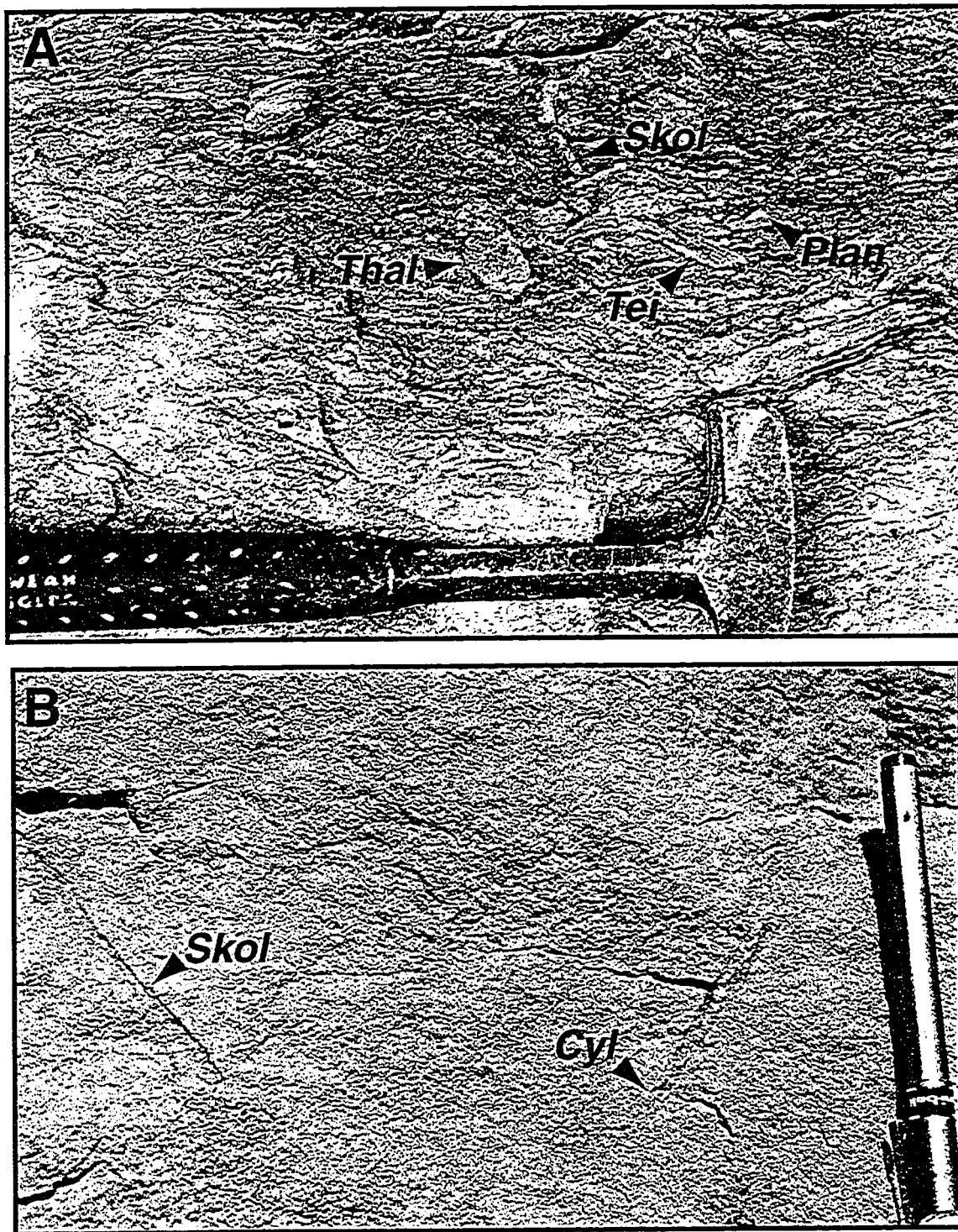


Figure III-22. Carbonaceous-rich, highly bioturbated sandstones of Facies F. Photo A: *Skolithos* (*Skol*), *Teichichnus* (*Tei*), *Planolites* (*Plan*), and *Thalassinoides* (*Thal*). Sully Creek (L18), 3 m above base of section. Photo B: *Skolithos* (*Skol*), and *Cylindrichnus* (*Cyl*) within mottled sandstones. Sully Creek (L33), 3.5 m above base of section.

FACIES G: VERTICAL BURROWS FILLED WITH GLAUCONITE-RICH SANDS

Description

The burrows of Facies G descend into the shoreface sandstones of Facies D. It has a thickness of between two and four meters and has been observed at two outcrop locations (Six Bald Point-L5, and Burnt Timber L-19). It is distinct in its appearance, in that it contains burrows that are filled with green glauconitic sandstones. These burrows have been observed to descend into the underlying sandstones up to 2 meters. Sharply overlying this facies are the dark organic-rich shales of the Garbutt Formation.

Individual traced burrows within the facies include: *Diplocraterion habiche*, *Skolithos*, *Rhizocorallium*, *Thalassinoides*, and *Palaeophycus*. Outcrop Six Bald Point contained only traces of *Diplocraterion habiche* (Figure III-23). These traces were closely spaced, with one burrow every three to five centimeters, which descend vertically between 1.5 and 2 meters into quartz-rich shoreface sandstones of Facies D. This facies was observed to exist throughout a large area around the measured outcrop location, being noted over one kilometer upstream on the LaBiche River from the actual measured outcrop location. At the Burnt Timber outcrop, the ichnogenera were more diverse, containing *Skolithos*, *Rhizocorallium*, *Thalassinoides*, and *Palaeophycus* (Figure III-24). These traces descended one meter into underlying shoreface sandstones, and like burrows at Six Bald Point were completely in-filled with glauconite.

Interpretation

The vertical burrows infilled with glauconite form a *Glossifungites* surface of Facies G. As defined by Frey and Seilacher 1980, these burrows are associated with semilithified or firm substrates. The substrates typically consist of dewatered, cohesive muds, due either to subareal exposure, or burial and subsequent exhumation (Pemberton and Frey, 1985). In general the dwelling burrows are emplaced into a firm substrates, which negates the need for a lining. When the organisms who produced the burrow vacates, the burrow remains open allowing the material from the succeeding depositional event to passively fill the open structure (MacEachern *et al.*, 1992). The observed population density observed at Six Bald Point is typical of opportunistic assemblages observed at similar boundaries in the rock record (Levinton, 1970; MacEachern *et al.*, 1992; Pemberton and Frey, 1984).

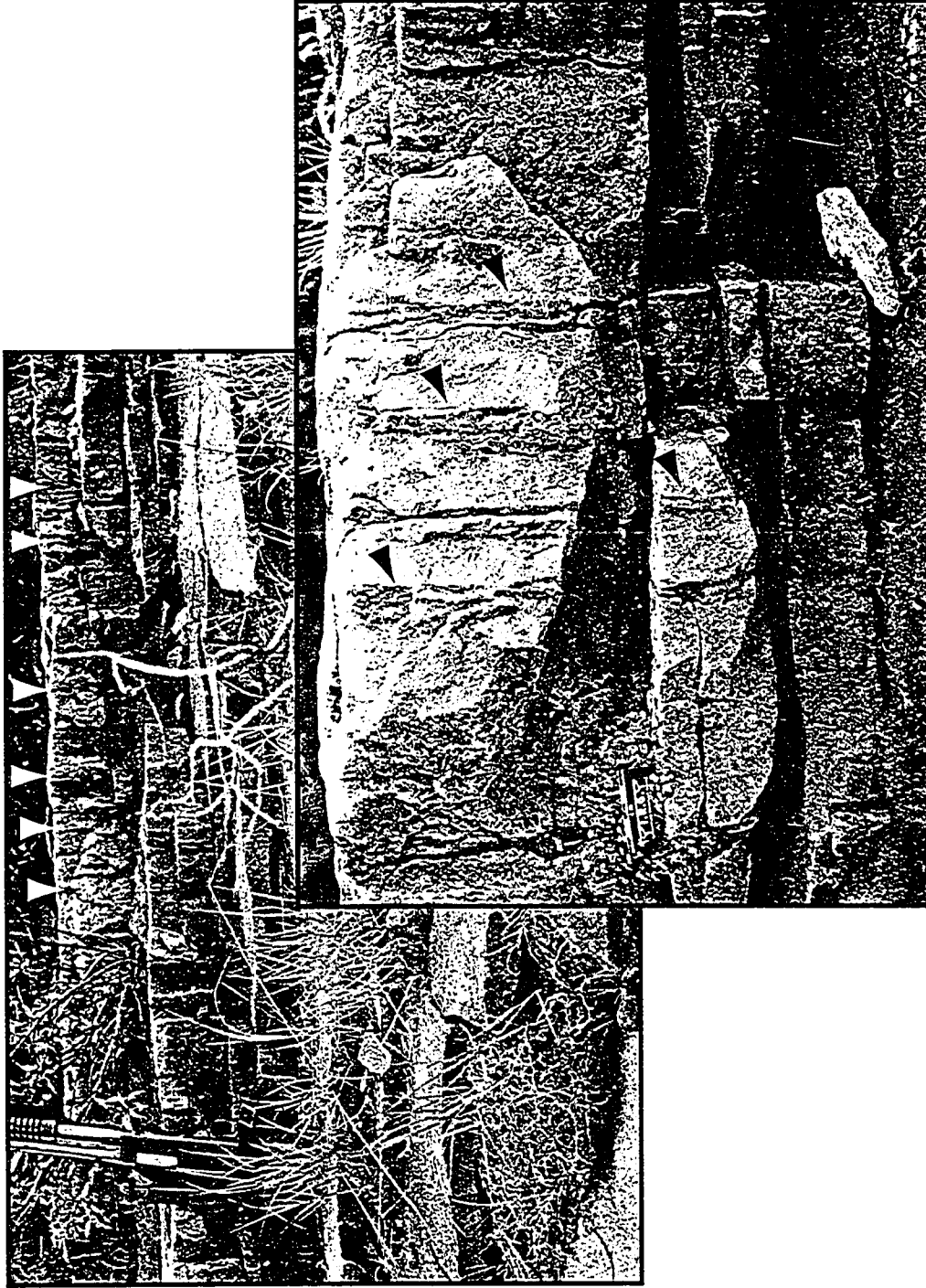
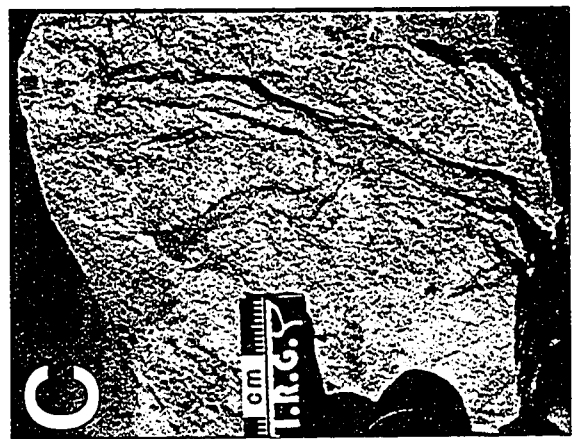
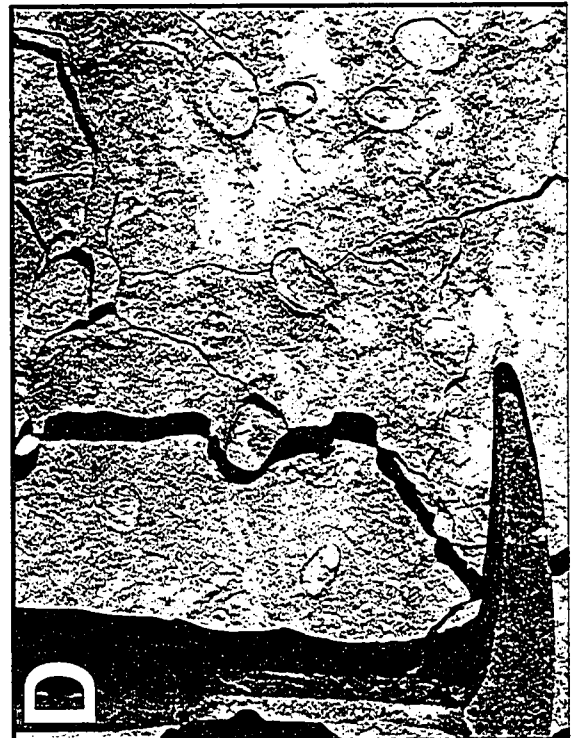


Figure III-23. Facies G observed at Six Bald Point (L5), top of section. Background photo shows burrow density (each white arrow denotes a single *Diplocraterion habbiche*). Penetration depth is up to 30 centimeters. Note gun for scale. Inset photo shows glauconite filled burrows descending from the upper contact with the Garbutt Formation.

Figure III-24. Facies G observed at Burnt Timber (L19), 42 m above base of section. Photo A: Gross aspect of underlying interbedded sandstones. Note hammer for scale along left hand side. Photo B: *Rhizocorallium* filled with glauconite descending into underlying interbedded sandstones and shales (photo A). Photo B: branching *Thalassinoides* filled with glauconite. Photo D: Bedding plane view of glauconite filled, *Skolithos* 'buttons' vertically descending into underlying sandstones.



FACIES H: WAVY TO LENTICULAR SANDS CAPPED BY SHELL MATERIAL

Description:

Facies H represents a unique set of sedimentary and biogenic structures within the Lower Cretaceous Chinkeh Formation, as it is only observed at the Burnt Timber (L19) outcrop. It sharply overlies planar-laminated shales of Facies C, and is 2 meters thick (Figure III-25). The facies is characterized by wavy to lenticular bedding grading upwards into ripple- to planar-laminated fine-grained sandstones (Figure III-26). In turn, a 20 cm thick disarticulated shell layer caps these fine-grained sandstones. Abundant organic debris and occasional migration ripples are also present, whose orientation is to the west. Facies H is overlain by dark, fissile shales of the Garbutt Formation (Facies I).

Biogenic structures are common to rare, with readjustment and escape traces (i.e. *Fugichnia*), and shifting *Cylindrichnus*, and *Skolithos* being the most observable (Figure III-26 A&C). These biogenic structures are small in size, never reaching more than a few centimeters in length, or width. Sedimentary structures are well preserved, with small scour and fill structures being the most predominant throughout the facies. The scours themselves do not penetrate deeply into the underlying sediment, only 0.25 to 0.5 centimeters. However they are common, and can be observed repeatedly along any given bedding plane (Figure III-26 D).

Interpretation

The wavy to lenticular sandstones of facies H were deposited within a sandy intertidal setting. The low diversity of trace fossil assemblage is a consequence of numerous stresses such as fluctuating currents, salinity, periodic desiccation (in the upper intertidal zone), and sporadic deposition (Weimer *et al.*, 1982). The presence of sand interbedded with shale, low-relief scours, migrating ripples, abundant organics, and shells with limited amounts of burrowing suggests deposition within a sediment-rich, shifting substrate depositional environment. Localized small-scale scour surfaces are related to associated tidal runoff creeks.

While this facies is restricted to only one outcrop exposure, it does give insight into the overall Lower Cretaceous depositional system. Laterally adjacent outcrop exposures show numerous point sources debouching and reworking deposits into the Liard Basin. At the Burnt Timber exposure, a large, low relief sandy tidal flat existed

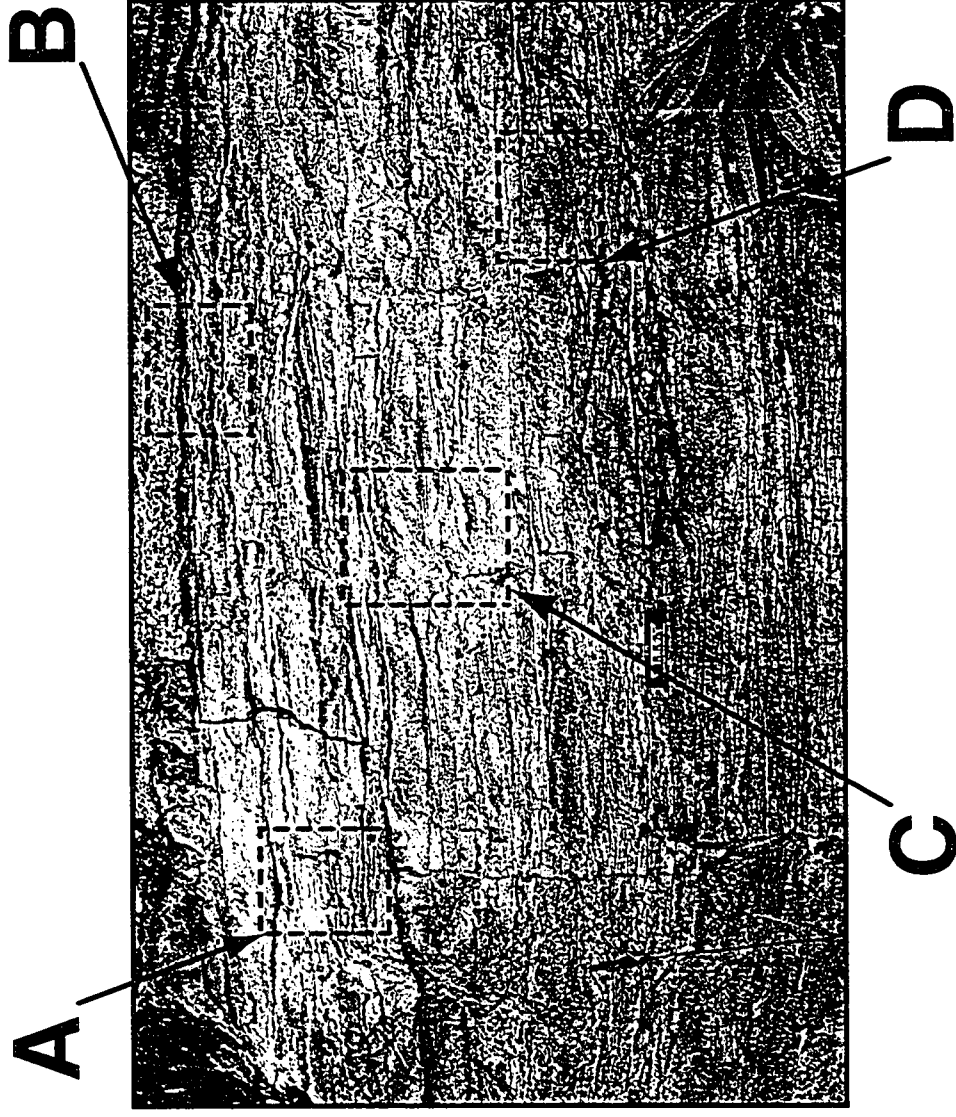


Figure III-25. Gross aspect overview of wavy to lenticular bedding of Facies H observed at Burnt Timber (L19), 42 m above the base of section. Note approximate location of detailed photographs in Figure III-26 are outlined here. Photo A: Shifting *Cylindrichnus*, moving from right to left, due to tidal currents. Photo B: Capping shell hash layer, approximately 3 to 5 cm thick. Photo C: *Skolithos* (*Skol*) and escape trace (Fug) in lenticular to wavy bedded, silty sandstones. Photo D: Migrating ripple (moving basinward (i.e. towards the East) and low relief scour surface (arrowed), that is interpreted as tidal runoff channel.

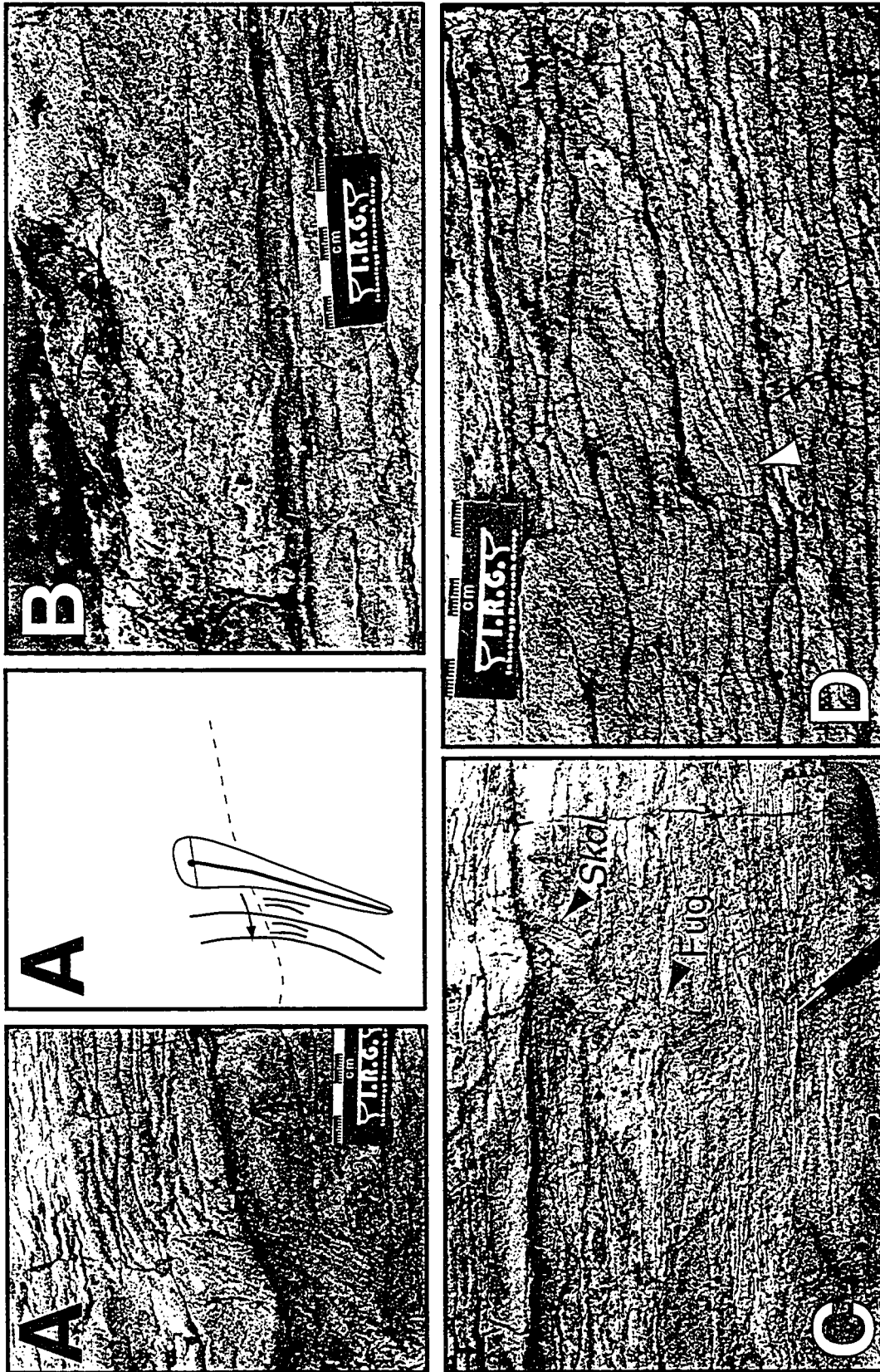


Figure III-26. Details of Facies H as observed at the Burnt Timber (L19) outcrop, 42 m above base of section.

in an embayment adjacent to one of these point sources. The genesis of the tidal flat can be debated; either caused by abandonment of a distributary lobe, or relative sea level outpacing sedimentation. Irrespective, its presence does support a large embayment in the northeast corner of the study area (see Figure III-29).

FACIES I: THINLY BEDDED, DARK FISSILE SHALES

Description

Facies I consists entirely of dark, fissile shales containing beds of sideritized nodules. The shales are among the most noticeable geological formation when entering the Liard Basin. They are extremely thick, some exposures are well over 150 meters. These shales belong to the Garbutt Formation, and sharply overlie the quartzose sandstones of the Lower Cretaceous Chinkeh Formation.

The shales are bedded on the centimeter-scale, which are void of any biogenic traces. The siderite nodules within the shales can reach diameters of up to 20 centimeters. These nodules form along the same bedding surface at the outcrop scale, and can be traced laterally for hundreds of meters. These shales emit gamma-rays at between 60 and 70 counts per second, with counts as high as 100 counts per second being observed (Figure III-27).

Grading upwards, these shales become interbedded with the glauconitic sandstones of the Bulwell member. The distance between the two sand bearing formations (i.e. Chinkeh and Bulwell) has been measured along Sully Creek. Here, the creek has eroded through the Lower Cretaceous, giving the opportunity to measure the complete stratigraphic interval with continuous exposure. The thickness relationship between the two formations will be discussed further within the chapter.

Interpretation

The dark fissile shales of Facies I were deposited in general quiescence, within a deep offshore environment. These shales were deposited during marine transgression of the Liard Basin, where the entire northern portion of the depressed foredeep was filled with shale (Stott, 1982). Both high gamma-ray values, and high organic matter content reflect anoxic bottom water, that are common during transgressions (Reynolds, 1996). While it is not clear at exactly clear to which gamma-ray spike this correlates to within the subsurface, it should be noted that this spike lies approximately 20 meters above the

Chinkeh Formation.

RELATIONSHIP BETWEEN THE CHINKEH AND SCATTER FORMATIONS

Towards the later portions of the field season, two outcrop locations came into question. Sections along the Kotaneelee River (L8) and Sully Creek (L1) were determined to contain sandstones of the Scatter Formation, rather than Chinkeh Formation. While only Scatter Formation was found along the Kotaneelee river, the outcrop exposures along the Sully Creek presented a good opportunity to observe the relationships between the two formations. This section is only intended to prove the stratigraphic relationship between the two formations. The depositional context of the Scatter formation will be dealt with in greater detail in the following chapter.

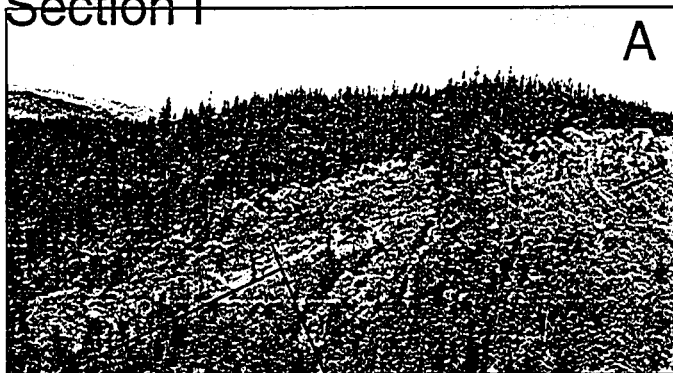
As mentioned above, it was possible to directly observe the relationship between the Chinkeh, Garbutt and Scatter Formations. By walking out the contacts along the Sully Creek, it was possible to measure the thickness of each formation, and determine the stratigraphic relationship to each other (see Figure III-27).

Initially, the published paper by Leckie (1991) had grouped both outcrops L1 and L33 as part of the Chinkeh Formation. Since the mandate for the field season was to describe as many Chinkeh outcrop sections as possible, with fewest possible camp moves, Sully Creek was an ideal location. Camp was set at the terminus of the creek, and since the dip of the strata exceeded dip of the creek, it was possible to walk the entire section out.

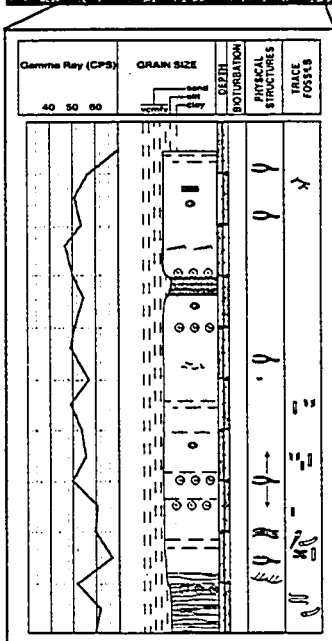
Walking upstream, the first sandstone encountered was the Bulwell member of the Scatter Formation. These sandstones differed greatly from other outcrop locations visited up until that time. Lithologically, these sandstones contained abundant amounts of glauconite (up to 80%), and the overall sand content was much lower than previous outcrop sections. In general, the outcrop contained interbedded sandstones and intensely bioturbated shales (detailed facies description and interpretations are given under Facies E). The amount of bioturbation was also unusual in comparison to previous Chinkeh outcrops visited. A total of 9.5 meters was measured from the first occurrence of sandstone to the last occurrence of sandstone. Gamma-ray data collected also indicated much higher counts than previously observed within the Chinkeh Formation.

Working upstream (down stratigraphic section), thick shales of the Garbutt

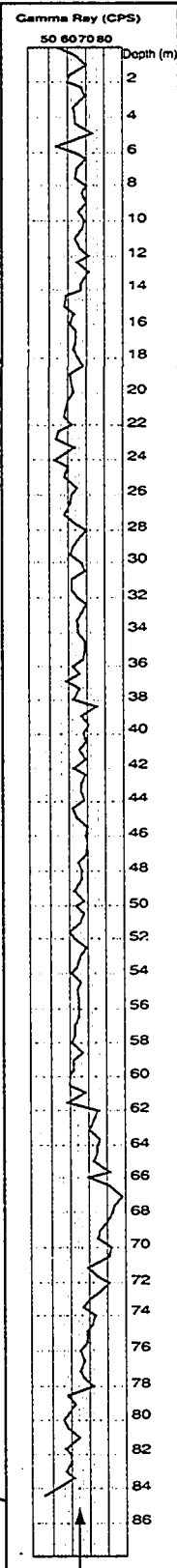
Section I



A



B



Missing Section

Section II



A

Figure III-27. Montana Figure III-1 for location overview of the Bulwer and gamma-ray data. Formation, and associated was collected to river level the Chinkeh Formation (note field partner hole). Outcrop overview looking where the Chinkeh Formation represents the top of the

Section II

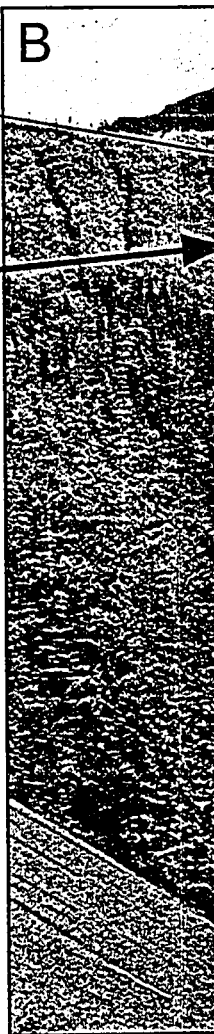
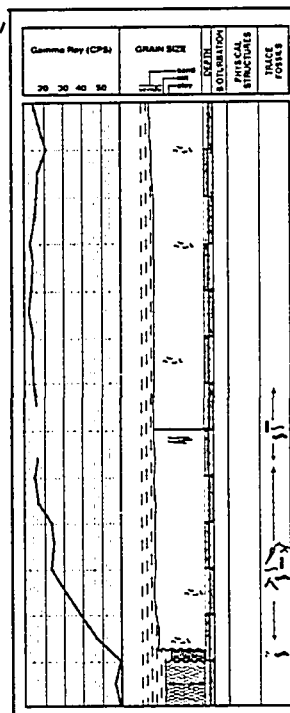
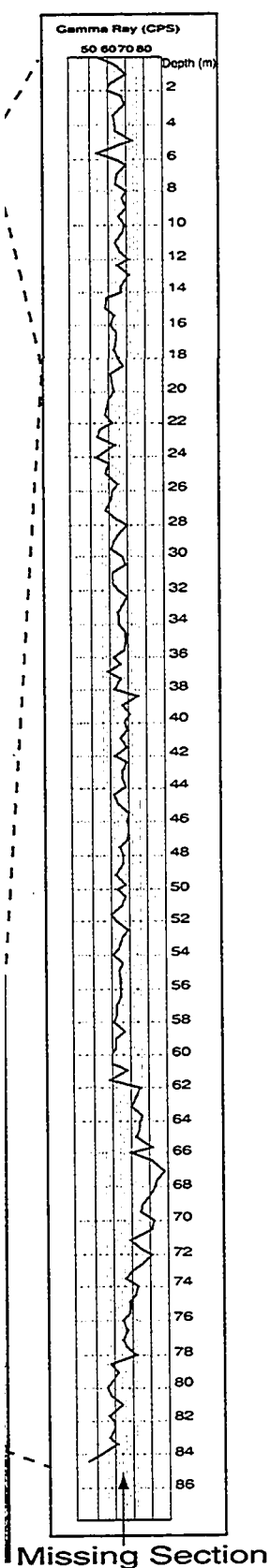
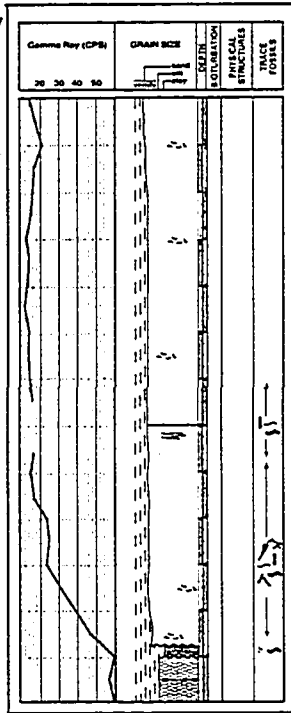


Figure III-27. Montage of outcrop exposures along the Sully Creek (see Figure III-1 for location of outcrops). Section I: Photo A: Outcrop overview of the Bulwell Member (Outcrop L1), and associated litholog and gamma-ray data. Photo B: Outcrop overview of the Garbutt Formation, and associated gamma-ray log. Thickness and gamma-ray data was collected to river level. Section II: Photo A: Outcrop overview of the Chinkeh Formation (L33), and associated litholog and gamma-ray data (note field partner holding 1.5 m long pogo stick for scale). Photo B: Outcrop overview looking East from the Garbutt shales towards the canyon where the Chinkeh Formation is exposed. The "treed" surface (arrowed), represents the top of the Chinkeh Formation.



outcrop exposures along the Sully Creek (see outcrops). Section I: Photo A: Outcrop member (Outcrop L1), and associated lithology and gamma-ray log. Thickness and gamma-ray data are shown. Section II: Photo A: Outcrop overview of the Garbutt (Outcrop L2), and associated lithology and gamma-ray data (1.5 m long pogo stick for scale). Photo B: Outcrop overview of the Garbutt shales towards the canyon. The "treed" surface (arrowed), which is exposed, is the Garbutt Formation.

Formation were encountered (see Figure III-27). These shales were dark in colour, containing abundant sideritized nodules (up to 20 cm in diameter), which formed distinctive bedding horizons. The shales were extremely fissile, and contained no bioturbation (detailed descriptions and interpretations are given under Facies I). To determine thickness of the Garbutt shales, a suitable continuous section was chosen where the Bulwell sandstones outcropped at the top of section and exposure was continuous to creek level. Top of Garbutt section was taken to be the last occurrence of glauconitic sand. Since some section was covered between the lowermost Garbutt and the Chinkeh Formation, a calculation had to be used to estimate the amount of covered section (Figure III-28). A total 105 meters of Garbutt shales (84.3 meters of measured section, and 20.7 meters of covered section) was determined for the thickness between Bulwell and Chinkeh sandstones (Figure III-28 for details of the calculations).

Finally, the Chinkeh Formation was encountered at the headwaters of the Sully Creek. Here a slot canyon exposed the much more typical sandstones previously encountered in the field season. Quartz-rich, non-glauconitic, blocky sandstones of the Chinkeh formed steep canyon walls within the canyon. These sandstones were moderately bioturbated at the base, with lower average gamma-ray counts (approximately 20 counts per second near the top of section).

The exposures along Sully Creek afforded a great opportunity to observe and measure the relationships between the lowermost glauconite-rich, highly interbedded sandstone member of Scatter Formation, the dark shales of the Garbutt Formation, and the quartz-rich, blocky sandstones of the Chinkeh Formation.

MURKY CREEK CHANNEL SECTION

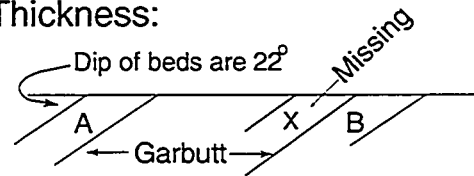
Description

As mentioned above, the outcrop exposures along the Murky Creek were very vast in lateral extent, and showed significant lateral changes. Two main sand bodies are immediately observed above massive Permian sandstone cliffs at the outcrop scale (Figure III-29). On further investigation, it was noted that these sandstones pinch-out laterally, further up and down stream. At the most downstream extent (outcrop L18B), the lower sand package contained a boulder sized chert conglomerate (Facies B) sitting on Permian strata (see Figure III-13). This facies graded laterally upstream to sandstones of Facies D consisting of load casts, disarticulated shell fragments, rare ripple laminations, and planar

A) Actual Thickness:

Scatter	A	9.5m
Garbutt		84.5m
Chinkeh	B	13m
		X (missing)

B) Apparent Thickness:

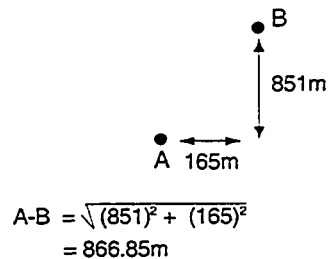


$$\sin 22^\circ = 9.5/A \quad A = 25.36m$$

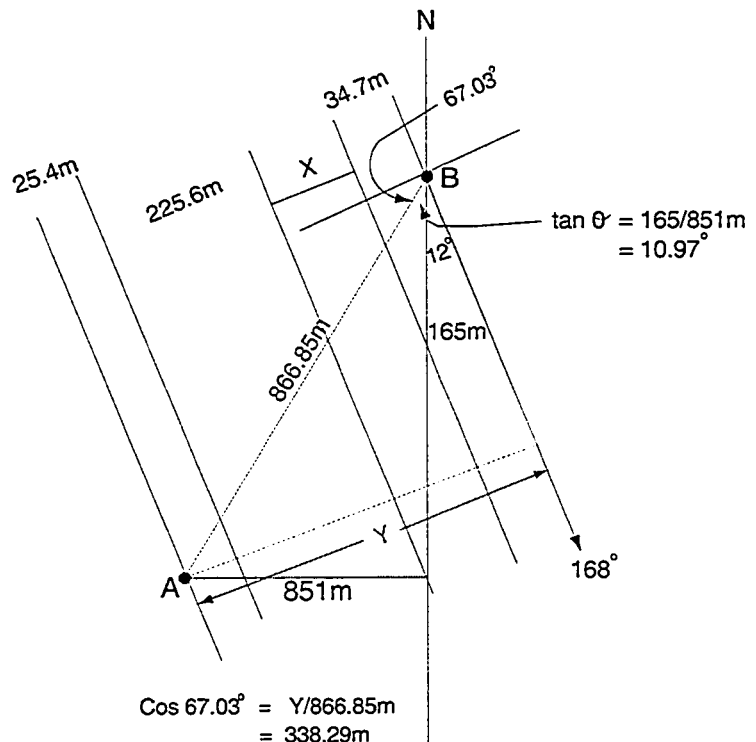
$$\sin 22^\circ = 13/B \quad B = 34.7m$$

$$\sin 22^\circ = 84.5/\text{Shale} \quad \text{Garbutt} = 225.6m$$

C) Distance Between outcrops A&B:



D) Calculation of missing Garbutt Section:



$$(\sin 22^\circ)Y = 126.72m \quad (\text{True Thickness})$$

$$X = Y - (9.5m + 84.5m + 13m) = 20.72m \quad \text{Missing Section} \sim 20.7m$$

Figure III-28. Detailed calculations for non-outcropping section between base of Garbutt Formation and top of the Chinkeh Formation.

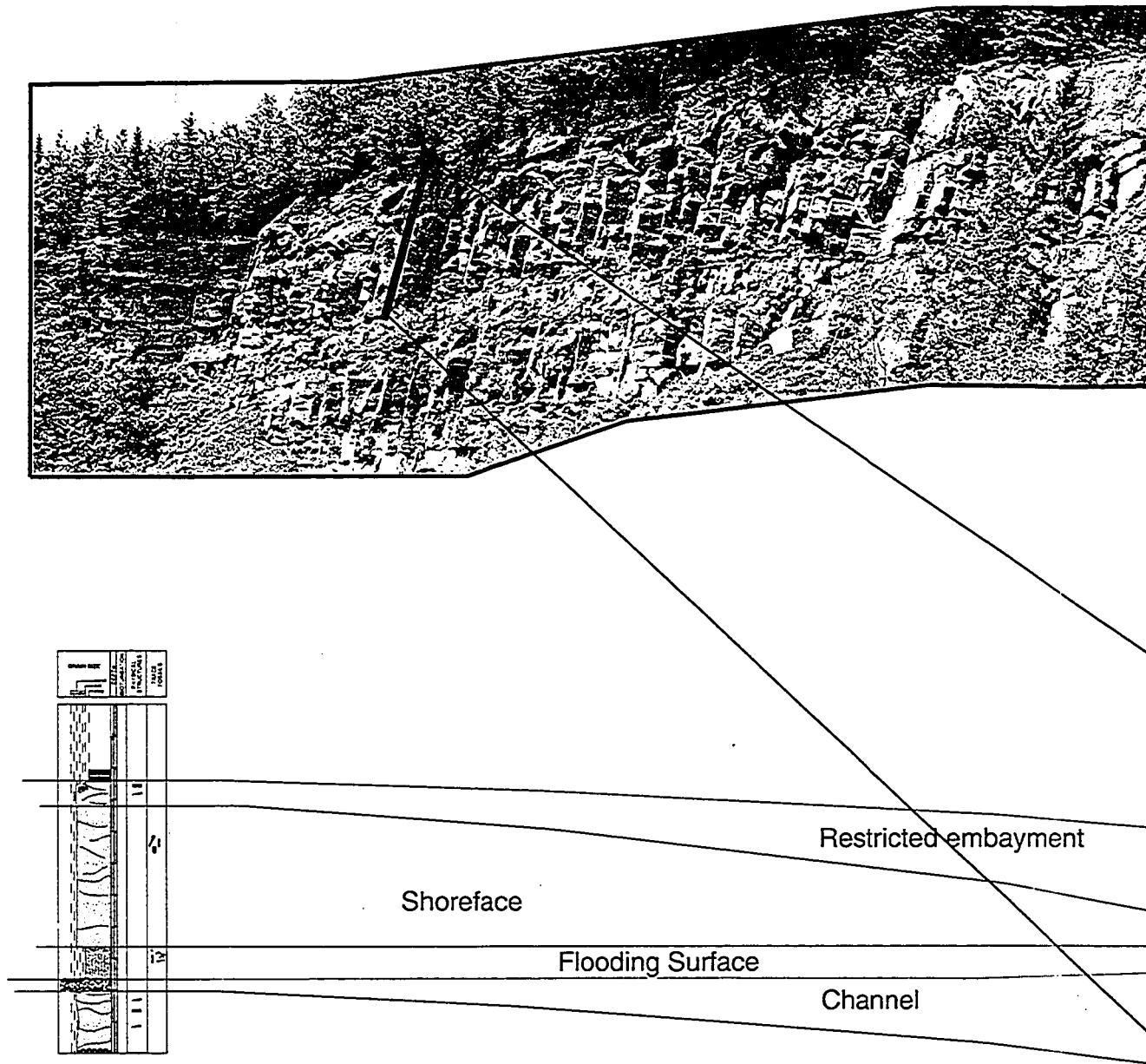
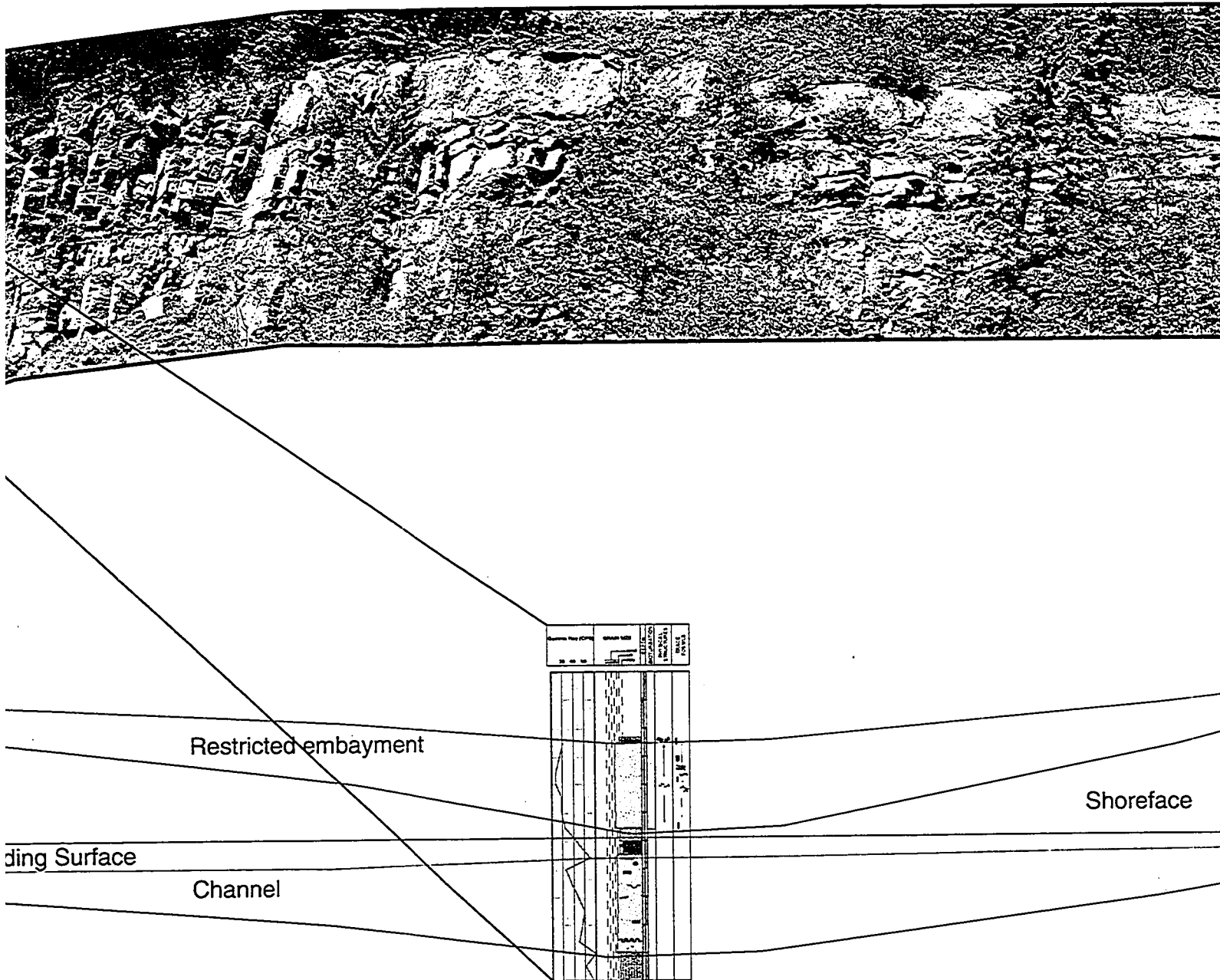
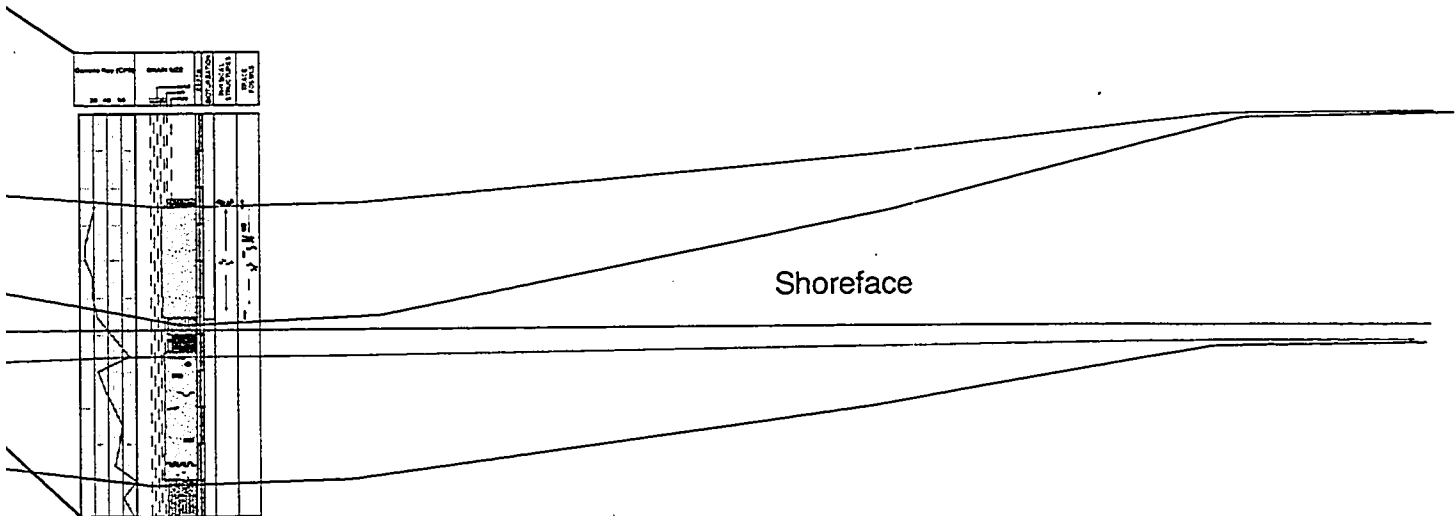


Figure III-29. Murky Creek channel section. An outcrop photomosaic is shown at the top of the figure, while the second litholog was described further downstream. Two distinct sand packages: lowermost is interpreted to be an active distributory channel, while the upper is a restricted embayment



A topographic photograph of a riverbank is shown at the top of the figure, while below is their interpreted depositional environment. The location of the photograph is further downstream. Two distinct sand packages are observed along the Murky Creek. Both display channel-like morphology. The lower package is a channel, while the upper is a restricted embayment forming after the abandonment of active channel deposition.



, while below is their interpreted depositional environment. The location of the first litholog is shown on the map of the study area. Both display channel-like morphologies, that pinch out laterally. The formation is interpreted as a channel deposit, formed after the abandonment of active channel deposition.

parallel laminations near the top. These sandstones appeared massive, with very few bed partings or interbeds. Overlying these massive sandstones, was a continuous bed of shale approximately 0.5 meters in thickness. This shale bed of Facies C could be traced across the entire outcrop and was devoid of any traces except at the extreme downstream location (L18B) where *Skolithos*, *Palaeophycus*, *Thalassinoides*, and rare *Chondrites* were found.

Sharply above the shale horizon another sand package was encountered. At the outcrop scale these sandstones appeared much more interbedded, with bed partings on the decimeter scale. Hummocky and swaley cross-stratified sandstones of Facies D were observed throughout the downstream outcrop (L18B), however they became much less common to absent upstream. At the upstream location, these sandstones (3 meters thick) consisted entirely of Facies F, containing abundant carbonaceous debris, and a much more diverse group of traces. Facies F was also observed downstream, however only 1 meter was observed sharply overlying Facies D sandstones. Finally, dark shales of Facies I (the Garbutt Formation) were found sharply overlying the sandstones along Murky Creek.

Discussion

The exposure along Murky Creek shows good evidence for point source deposition and subsequent reworking during Lower Cretaceous Chinkeh deposition. The first sand package is interpreted to be a distributary channel, that is observed to erode into the underlying Permian strata. The channel morphology is seen to pinch out upstream and downstream, where the chert boulder conglomerate (Facies B) exists at its margins. These shoreface sediments of Facies D only exist at the downstream extreme, where they are also subsequently eroded into by a subsequent sand with a channel-like morphology. Unlike the first, the sediments here are much more interbedded and contain much diverse set of traces, and organic debris. The second package of sand (Facies F) which erodes into Facies D downstream is interpreted as an abandoned distributary channel and restricted embayment.

The lateral facies changes seen along the creek indicate that complex channel deposition and subsequent abandonment were the dominant processes along the eastern boundary of the Liard Basin during Chinkeh deposition. Here distributary channels delivering clastic material into the basin, were being reworked along shore into shoreface sandstones. Subsequently, as the channels switched orientations, some of the shoreface material became eroded, while the older channels become filled with finer-grained,

bioturbated, sediments.

DEPOSITIONAL SYNOPSIS

Discussion

The Chinkeh Formation as examined in outcrop, consists of upward coarsening, quartz arenite sandstones that are moderately to poorly bioturbated. The interpreted depositional model consists of a shoreface complex with punctuated point sources, strandplanes, and embayments along either side (Figure III-30).

The interpreted depositional environment for the Lower Cretaceous Chinkeh Formation is a south-east prograding shoreface complex. A horseshoe shaped embayment with greatest width in the north, was the basin configuration at the time of Lowermost Chinkeh deposition. The seaway interpreted for these outcrops was at least 125 km in width (no amount of structural shortening has been taken into account). The two roughly parallel shoreline trends delineated, were punctuated by river systems carrying quartz-rich sediments, that flowed both from the west and east into the embayment. On the western edge these fluvial systems carried clastic material from the west into the boreal seaway. While on the eastern margin of the seaway, streams emptied their depositional load into the basin from the east along the eastern margin. Strandplains developed adjacent to these perturbations of the shoreline. Where more proximal to point sources, these deposits are characterized by less intense bioturbation, and much more abundant carbonaceous debris on bedding planes. Where distal from these point sources, deposits are characterized by the amalgamation of high energy bedforms, the preservation of only deeply penetrating traces, and a much cleaner sedimentary package. Here depending on the location of the main distributary arms of the point sources, material became reworked and remigrated along shore due to incipient wave energy moving this material along shore. The strong overprint of high energy systems on the outcrops and their overall bed migration directions gives evidence for this process. Longshore currents carried point source material in shore parallel directions, in general towards the southeast, the direction of overall progradation.

In general there is a repetition to these deposits, with three repeated parasequences being observed in the northern most outcrops, and two in the south. This directly reflects progradation reflecting in the phased advances of the Boreal sea from the north.

In a localized outcrop section, intertidal deposits were found capping the shoreface

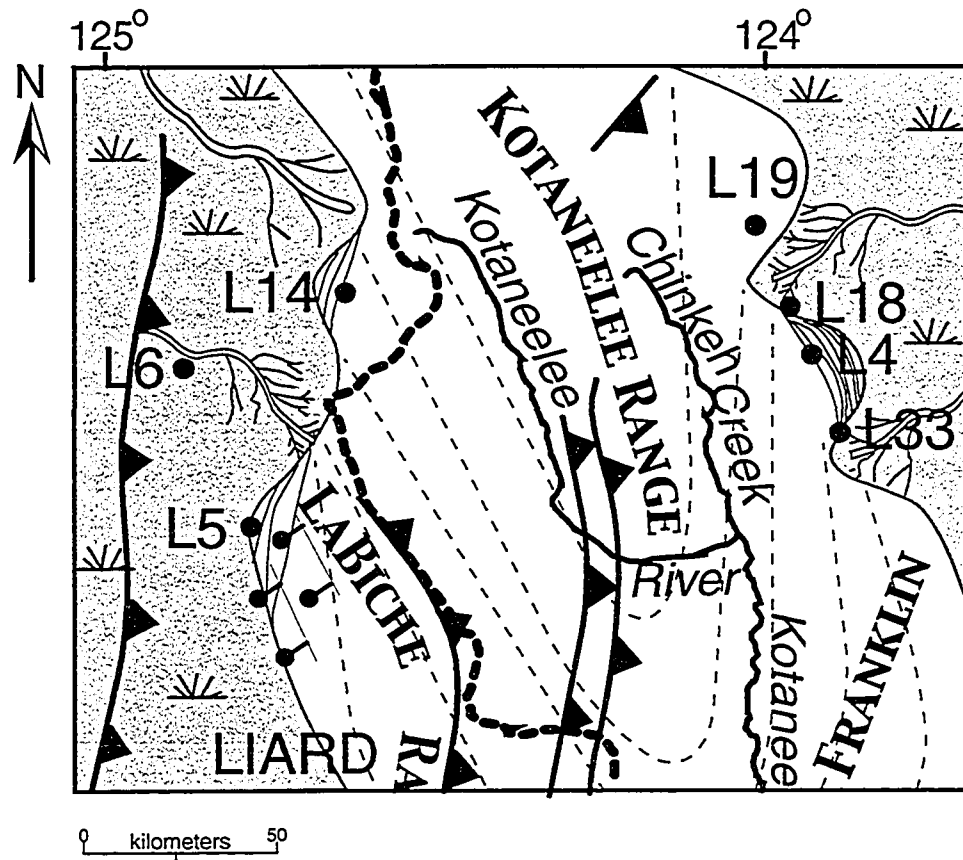


Figure III-30. Interpreted depositional environment for the Lower Cretaceous Chinkeh Formation. A narrow basin is envisioned, having point sources entering the Liard Basin from both eastern and western sides. These build out, and create protuberances of the shoreline, adjacent to which embayments and strandplains form. Longshore currents constantly rework these deposits and transport material along the paleo shoreline. Overall direction of progradation is towards the southeast.

sequences. Characterized by runoff channels, shell fragments, muddy sedimentation, and diminutive bioturbation, these deposits represent the infill of embayments adjacent to main distributary arms. While not ubiquitous throughout the study area, these tidal indicators suggest that in select depositional environments, tidal processes were invoking controls on sedimentation, at least on a local scale.

References:

- Aitken, J.F., and J.A. Howell. 1996. High Resolution sequence stratigraphy: innovations, applications and future prospects. *In*: J.A. Howell, and J.A. Aitken, eds., Geological Society Special Publication 104, p. 1-9.
- Clifton, H.E., R.E. Hunter, and R.L. Phillips. 1971. Depositional structures and processes in the non-bar high energy nearshore. *Journal of Sedimentary Petrology*, 41: p. 651-670.
- Davies, S.J., and T. Elliott. 1996. Spectral gamma ray characterization of high resolution sequence stratigraphy: examples from Upper Carboniferous fluvio-deltaic systems, Country Claire, Ireland. *In*: J.A. Howell, and J.A. Aitken, eds., Geological Society Special Publication 104, p. 25-35.
- Dott, R.H. and J. Bourgeois. 1982. Hummocky stratification: significance of its variable bedding sequences. *Bulletin of the Geological Society of America*, 93, p. 663-680.
- Duke, W.L., R.W.C. Arnott, and R.J. Cheel. 1991. Shelf sandstones and hummocky cross-stratification: new insights on a stormy debate: *Geology*, v. 19, p. 625-628.
- Emery, K.O. 1968. Positions of empty pelecypod valves on the continental shelf. *Journal of Sedimentary Petrology*, v. 38, p. 1264-1269.
- Frey, R.W., and R. Goldring. 1992. Marine event beds and recolonization surfaces as revealed by trace fossil analysis. *Geology Magazine*, 129: p. 325-335.
- Harms, J.C., J.B. Southard, D.R. Spearing, and R.G. Walker. 1975. Depositional environments as interpreted from primary sedimentary structures and stratification sequences. *Society of Economic Paleontologists and Mineralogists Short Course No. 2, Lecture Notes*: 161 p.
- Howard, J.D. 1972. Trace fossils as criteria for recognizing shorelines in stratigraphic record. *In*: Recognition of ancient sedimentary environments. J.K. Rigby and W.K. Hamblin (eds.). *Society of Economic Paleontologists and Mineralogists*

Special Publication 16: 215-225.

- Howard, J.D. 1975. The sedimentological significance of trace fossils. *In*: R.W. Frey (ed.), The study of trace fossils. Springer-Verlag, New York, p. 131-146.
- Howard, J.D. and R.W. Frey. 1973. Characteristic physical and biogenic sedimentary structures in Georgia estuaries. *American Association of Petroleum Geologists Bulletin*, v. 57, p.1169-1184.
- Howard, J.D. and H.E. Reineck. 1981. Depositional facies of a high energy beach-to-offshore sequence: comparison with low-energy sequence. *American Association of Petroleum Geologists, Bulletin*, v. 65 p. 807-830.
- Hunter, R.E., and H.E. Clifton. 1982. Cyclic deposits and hummocky cross-stratification of probable storm origin in the Upper Cretaceous of Cape Sebastian area, southwestern Oregon: *Journal of Sedimentary Petrology*, v. 52 p. 127-144.
- Kirk, R.M. 1980. Mixed sand and gravel beaches: morphology, processes and sediments. *Progress in Physical Geography*, v. 4 p. 189-210.
- Leckie, D.A., D.J., Potocki, and K., Visser. 1991. The Lower Cretaceous Chinkeh Formation: A Frontier-Type Play in the Liard Basin of Western Canada: *American Association of Petroleum Geologists, Bulletin*, v. 75, p. 1324-1352.
- Levinton, J.S. 1970. The Paleocological significance of opportunistic species. *Lethaia*, 3, p. 69-78.
- MacEachern, J.A. and S.G. Pemberton. 1992. An integrated ichnological-sedimentological model of Cretaceous shoreface successions and shoreface variability in the Western Interior Seaway of North America. *In*: S.G. Pemberton (ed.), Applications of ichnology to petroleum exploration - a core workshop. *Society of Economic Paleontologists and Mineralogists Core Workshop 17*, p. 57-84.
- MacEachern, J.A., I. Raychaudhuri, and S.G. Pemberton. 1992. Stratigraphic applications of the *Glossifungites* Ichnofacies: Delineating discontinuities in the rock record. *In*: Applications of ichnology to petroleum exploration – a core workshop. S.G. Pemberton (ed.). *Society of Economic Paleontologists and Mineralogists Core Workshop 17*, p. 169-198.
- McLaren, P. and D. Bowles. 1985. The effects of sediment transport on sediment grain-size distributions. *Journal of Sedimentary Petrology*, v. 55, p. 457-470.

- Middleton, G.V. 1967. The orientation of concavo-convex particles deposited from experimental turbidity currents. *Journal of Sedimentary Petrology*, v. 37, p. 229-232.
- Pemberton, S.G., and J.A. MacEachern. 1997. The Ichnological signature of storm deposits: the use of trace fossils in even stratigraphy. *In*: C.E. Brett, and G.C. Baird (eds.), *Paleontological events*. Columbia University Press, New York: p. 74-109.
- Pemberton, S.G. and D.M. Wightman. 1992. Ichnological characteristics of brackish water deposits. *In*: *Applications of ichnology to petroleum exploration – a core workshop*. S.G. Pemberton (ed.). Society of Economic Paleontologists and Mineralogists Core Workshop 17, p. 401-421.
- Pemberton, S.G. and R.W. Frey. 1984. Ichnology of storm-influenced shallow marine sequence: Cardium Formation (Upper Cretaceous) at Seebee, Alberta. *In*: D.F. Stott and D.J. Glass, eds., *The Mesozoic of middle North America*. Canadian Society of Petroleum Geologists Memoir 9, p. 281-304.
- Pemberton, S.G. and R.W. Frey. 1985. The *Glossifungites* ichnofacies: modern examples from the Georgia Coast, U.S.A. *In*: H.A. Curran, ed., *Biogenic structures: their use in interpreting depositional environments*. Society of Economic Paleontologists and Mineralogists, Special Publication, 35, p. 237-259.
- Reynolds, A.D., 1996. Paralic Successions. *In*: D. Emery, and K.J. Myers (eds.), *Sequence Stratigraphy*. Blackwell Scientific Publications, Oxford, pp. 134-177.
- Rhoads, D.C., and D.K. Young. 1978. Animal-sediment relations in Cape Cod Bay, Massachusetts. II. Reworking by *Molpadia oolitica* (Holothuroidea). *Marine Biology*, v. 11, p. 193-240.
- Stott, D.F., 1982. Late Cretaceous Fort St. John Group and Upper Cretaceous Dunvegan Formation of the Foothills and Plains of Alberta, British Columbia, District of Mackenzie and Yukon Territory. *Geological Survey of Canada Bulletin* 328, 124p.
- Slatt, R.M., and D.W. Jordan, A.E. D'agostino, and R.H. Gilespe. 1992. Outcrop gamma-ray logging to improve understanding of subsurface well log correlations. *In*: H. A. Griffiths, and C.M. Worthington, eds., *Geological applications of wireline logs II: Geological Society Special Publication* 65, p. 3-19.
- Weimer, R.J., J.D. Howard, and D.R. Lindsay. 1982. Tidal Flats. *In*: *Sandstone Depositional Environments*. P.A. Scholle and D. Spearing (eds.). American Association of Petroleum Geologists, Memoir 31, p. 191-246.

CHAPTER FOUR: Depositional relationships of the Lower Cretaceous Scatter and Chinkeh Formations

INTRODUCTION

Outcrop work done on exposures of the Scatter and Chinkeh Formations, have shown that although their environments of deposition are similar, their lithology, physical appearance, and distribution within the Liard Basin are very different. More significantly, the Bulwell Member sandstones examined in outcrop exposures closely resemble producing sandstones within the subsurface at Maxhamish Lake. Based on the data gathered, the Lower Cretaceous sandstones in production at Maxhamish belong to the Bulwell Member of the Scatter Formation, and not of the Chinkeh Formation as originally thought. Figure IV-1 is a stratigraphic table for the study area and southern equivalents.

OBJECTIVES

The objective of this chapter will be stated quite emphatically, that the sandstones producing at Maxhamish Lake are part of the lowermost member of the Scatter Formation, and not the Chinkeh Formation. To achieve this aim, the following will be addressed: 1) The outcrop thickness and distribution, 2) Lithological similarities between the Scatter Formation and the producing lower Cretaceous sandstones, and 3) Present a depositional model for the Lower Cretaceous within the study area, illustrating two very different depositional systems; the Chinkeh Formation and the Bulwell Member of the Scatter Formation.

OUTCROP THICKNESS AND DISTRIBUTION OF THE LOWERMOST MEMBER WITHIN THE SCATTER FORMATION

DEFINITION

The Scatter Formation was first described by Kindle in 1944. His descriptions along the banks of the Scatter River consisted of two major sandstone members separated by a

thick shale member. In general Kindle described the Scatter Formation as follows:

The succession of sandstones and shales that overlie the Garbutt Formation have been named the Scatter Formation, the type locality being along the Scatter River where the beds are exposed for over ten miles, commencing at a point one and a half miles west of the Liard.

Stott (1982), further defined the three members of the Scatter Formation as follows:

The basal sandstone of the Scatter Formation in type section of the formation occurring about 2.4 km upstream on the Scatter River above its junction with the Liard River, is defined as the Bulwell Member, the name being derived from Bulwell Creek map-sheet (94 N/11).

A thick succession of mudstone, occurring between the two resistant sandstone members of the Scatter Formation, is defined as the Wildwood Member. The name is taken from the Wildhorn Creek, a tributary of Scatter River.

The upper sandstone unit of the Scatter Formation is named the Tussock Member, and the type section is that of the sequence of beds found in the Scatter Formation on Scatter River. The member is underlain by mudstones of the Wildhorn Member, and is overlain by mudstones of the Lepine Formation.

Since this study is chiefly concerned with the lowermost member of the Scatter Formation, the middle and upper members will not be discussed in any great detail. Although the Bulwell Member is not well dated, it overlies the Garbutt Formation that contains microfauna of Early to Middle Albian age, and appears to occupy a stratigraphic position largely equivalent to that of the Gates Formation at Peace River (Stott, 1982).

DISTRIBUTION AND THICKNESS

Stott (1982) showed that the thickness at the type section totaled 347 meters, with the lower sandstone being more than 122 m; the middle shale approximately 137 m; and the upper sandstone member being 76 m thick. The Bulwell sandstone extends southward from the type locality to the junction of the Toad and Liard Rivers but becomes indistinct about 3.2 km farther south and is not mappable (Stott, 1982).

The sandstones investigated by the author along the Kotaneelee River (L8) and Sully Creek (L1), match the descriptions of the basal Scatter sandstone. The measured thickness of these outcrop exposures is 11 m and 9.5 m respectively. A sandstone isopach

map illustrating the thickness of the Bulwell Member within the Liard Basin is shown in Figure IV-2. The map was created using the outcrop descriptions from Stott (1982), outcrop descriptions from this study, and well control within the Maxhamish field (see Figure II-5).

MINERALOGY

Outcrop exposures of the Bulwell Member of the Scatter Formation and the subsurface cores retrieved within the Maxhamish Lake gas field, display striking similarities. Most obvious is that both contain high amounts of glauconite, and show a similar diagnostic green colour. Secondly, both subsurface and outcrop samples are quartz-rich and contain minor amounts of carbonate.

In the original descriptions of the Scatter Formation, both Kindle (1944), and Stott (1982), noted the abundance of glauconite within the Scatter Formation.

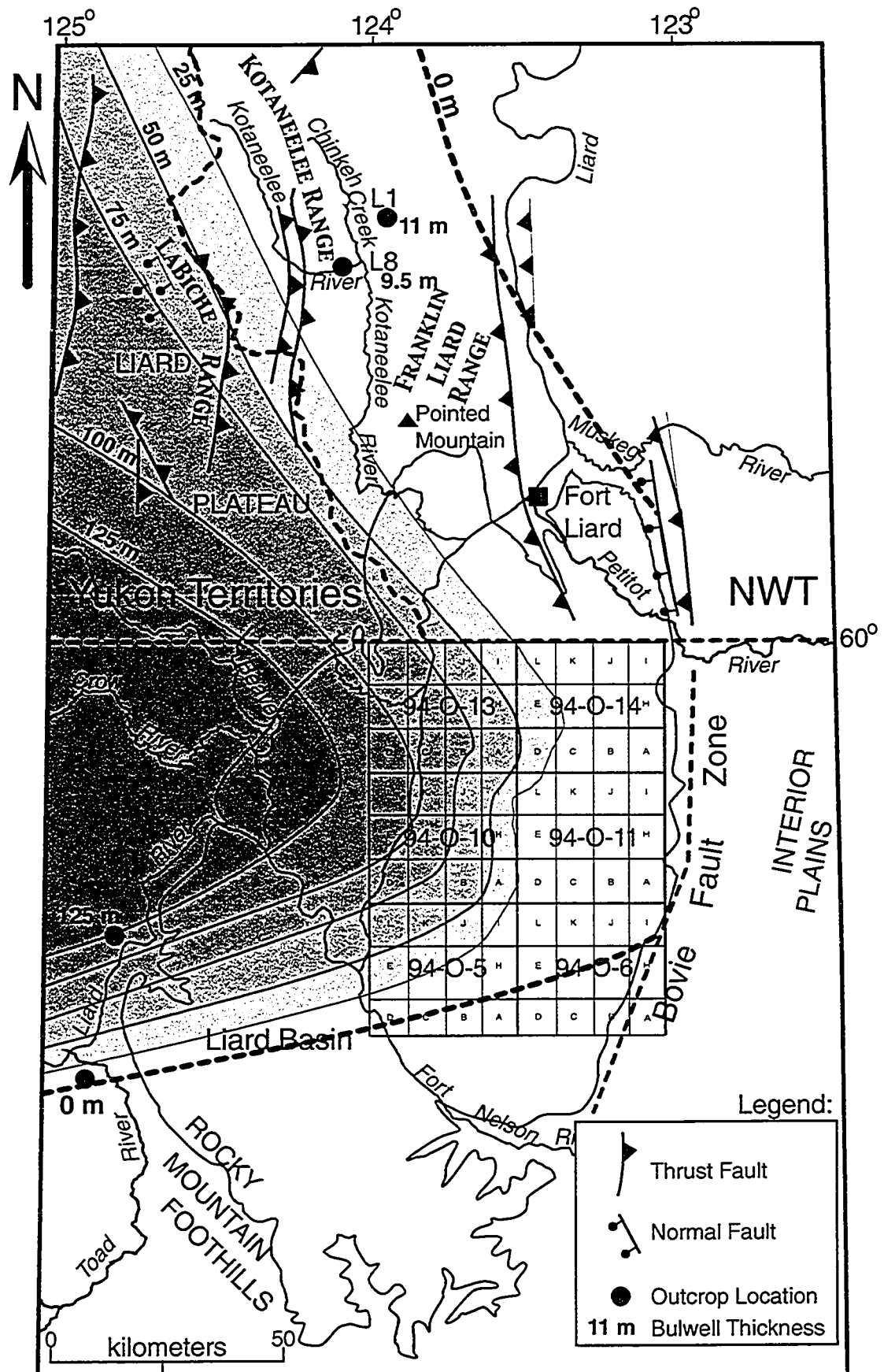
Glauconite is extremely abundant throughout and several beds, 2.5 – 10 cm thick, are present. Glauconite gives a very distinct green colour to the rock. It occurs as discrete grains and also as patches and irregularly shaped masses surrounding sand grains (Stott, 1982).

Outcrop thin sections examined show that between 1 to 20 percent, and locally 50 percent of the sandstone is comprised of glauconite (Leckie and Potocki, 1998). Thin section descriptions taken from subsurface cores also indicate high glauconite content, that ranges from 40 to 60 percent, with localized content being as high as 80 percent.

Glauconite is thought to form in open marine conditions with active bottom currents and minimal detrital deposition (Odin and Matter, 1981; Amorosi, 1995). Within shallow marine conditions glauconite formation is unfavourable, since conditions are more turbulent and well oxygenated. Favourable conditions for the formation of glauconite are inferred during the deposition of the Scatter sandstones, since the abundance of the mineral is high and widespread. Glauconite forms in areas of low sedimentation and active currents, where precursor grains lying on the sea floor (clay-rich fecal pellets or inorganic clay-peloids) can be transformed into glauconite (Logvinenko *et al.*, 1975). These sediments are then transported and concentrated by storm events into the bedforms observed within the outcrop and subsurface. Here laminations are defined based on subtle differences in glauconite content, and alternate between glauconite-rich and non-glauconite. In general, a glauconite-rich source area lying outside of the present

BLANK PAGE

Figure IV-2. Bulwell Member isopach map. The map was constructed using both outcrop data (this study and Stott, 1981), and subsurface data (see Figure II-5). Contour interval is 25 meters. The zero edge is highlighted, and parallels the Bovie Fault towards the east.



day Liard Basin is interpreted, whereby storm events subsequently rework and distribute the glauconite-rich sediments across the basin.

In comparison, the outcrop exposures investigated of the Chinkeh Formation did not contain any glauconite. In general the samples from the Chinkeh contained less feldspar and less lithic material, suggesting that the Scatter sandstones were sourced from different areas (Leckie and Potocki, 1998).

Depositional Model for the Lower Cretaceous Bulwell Member within the Liard Basin

INTRODUCTION

The Lower Cretaceous Bulwell Member of the Scatter Formation was deposited in a highly wave dominated shelfal setting. Using isopach maps, mineralogy, regional cross-sections and outcrop interpretations it has been determined that Bulwell sandstones originated from the west, and prograded across the Liard Basin towards the east. Here wave processes, combined with localized fault movement, contributed to create a wave dominated setting parallel to the Bovie Fault.

REGIONAL CROSS-SECTIONS

Two regional cross-sections were created to illustrate the Lower Cretaceous stratigraphy within the Liard Basin (Figure IV-3 for section locations). In particular these sections were created to illustrate the surface to subsurface correlations. A regional datum was chosen within the Middle Cretaceous Lepine Formation, well above the Scatter Formation, that is readily identified on subsurface logs.

The west-east section (Figure IV-4) was created using the outcrop descriptions of Stott (1982) at the westernmost extreme. Here outcrop descriptions from along tributaries of the Liard River were compiled, and placed in a stick section. Starting at the base, shales of the Garbutt Formation rest unconformably on Permian strata. The first identifiable sandstone within the section is the Bulwell Member of the Scatter Formation. This lowermost sandstone has been correlated across the Liard Basin, where at well location a-75-D/94-O-11 it onlaps onto Triassic strata, the southernmost extreme of the Maxhamish gas field. The Bulwell sandstones encounter the steep gradient of the

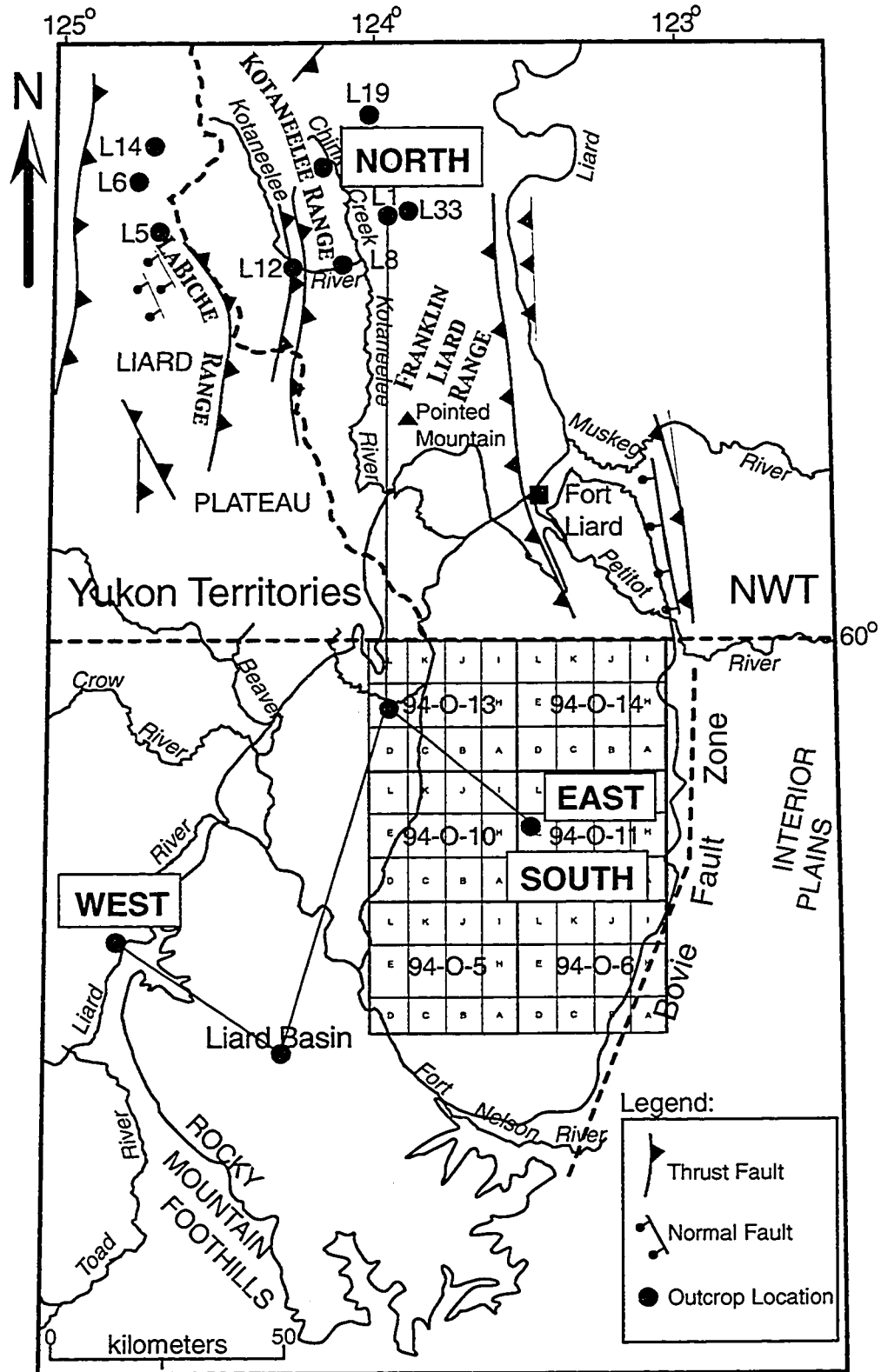


Figure IV-3. Locations of cross-sections (Figures IV-4 & 5), that combine both outcrop and subsurface data. Note the data for the western most outcrop was acquired from Stott, 1981.

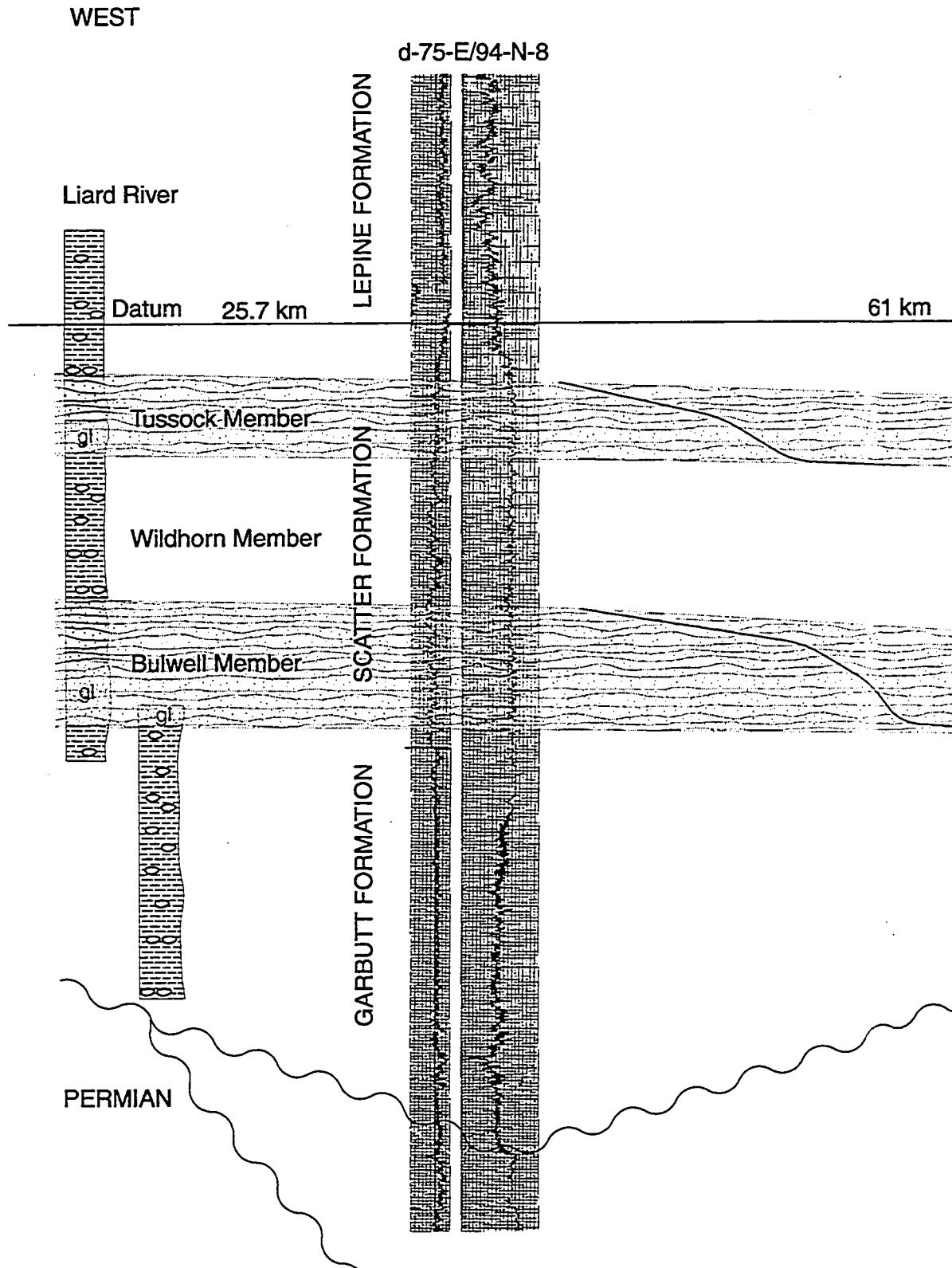
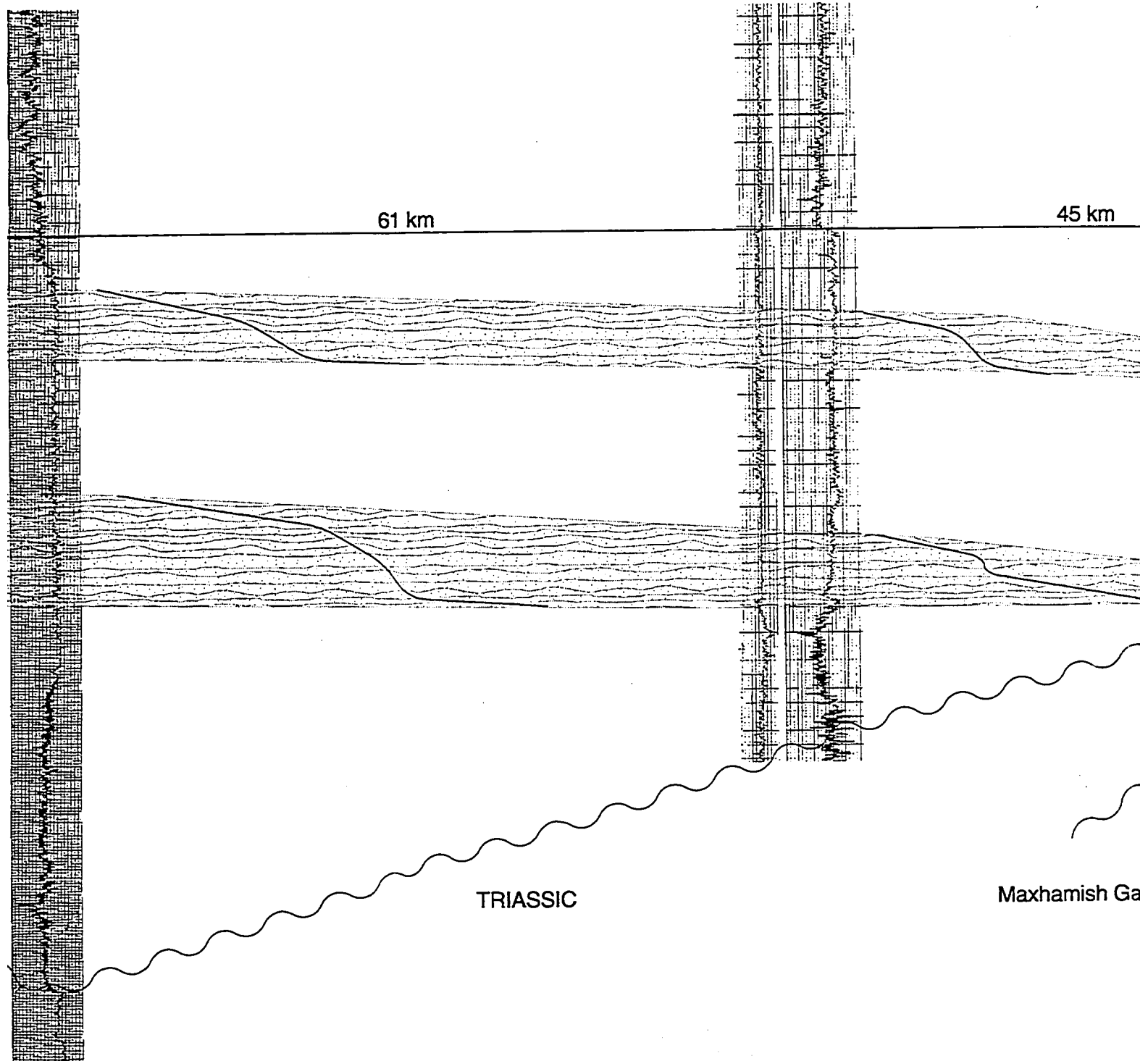


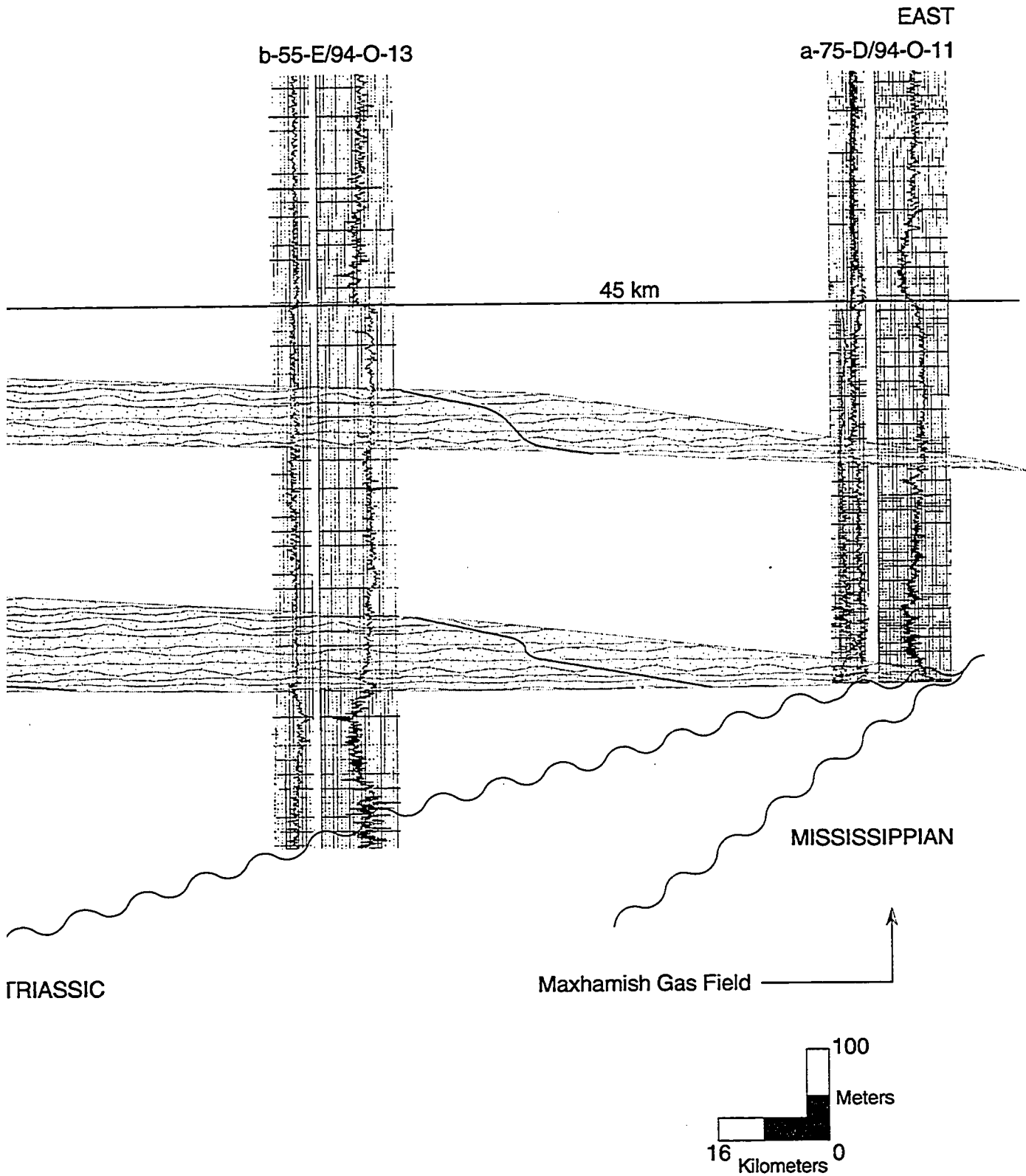
Figure IV-4. West to East cross-section across the Liard Basin (see Figure IV-3 for location). Sandstone onlaps onto Triassic strata along the eastern margin of the Liard Basin, where current production from exposures along this line of section. Outcrop data used along the Liard River from Stott, 1981.

E/94-N-8

b-55-E/94-O-13



Liard Basin (see Figure IV-3 for location). Sandstone members of the Scatter Formation prograde eastward into the Liard basin of the Liard Basin, where current production from the Maxhamish gas field exists. Note the Chinkeh Formation isn't preserved along the Liard River from Stott, 1981.



Members of the Scatter Formation prograde eastward into the Liard basin. The lowermost Bulwell Member of the Maxhamish gas field exists. Note the Chinkeh Formation isn't present in any well penetrations or outcrop

Bovie Fault, which halts progradation. The second sandstone unit encountered within the Scatter Formation, the Tussock Member, can also be traced across the Liard Basin. It is believed that the sandstones of the Tussock continue eastward across the Bovie Fault (Figure IV-7). The cross-section identifies the western extreme as a point source for sedimentation, which progrades towards the east.

The second regional cross-section is constructed from north to south, using the same two subsurface locations (Figure IV-5). The northernmost outcrop location is along Murky Creek, where the author had good control over the thickness, and stratigraphic relationship to the sandstones being investigated. The stick section represents measured outcrop exposures of the Chinkeh, Garbutt and Scatter Formation. Here the Lower Cretaceous Chinkeh Formation has a thickness of 13 m, and is shown prograding towards the south into the basin. However, the Chinkeh sandstones do not prograde far into the Liard basin, as they onlap Triassic strata before well b-55-E/94-O-13 penetrates the stratigraphic section. Sands of the Bulwell and Tussock are shown as static features on the cross-section, as the line of section has intersected them in a strike direction. Again, the Bulwell sandstones onlap unconformably onto Triassic strata in the vicinity of the Maxhamish gas field.

OUTCROP DESCRIPTIONS

At the type locality, Stott (1982) noted that the Bulwell Member was characterized by two major parts; a lower unit containing thick bedded, fine-grained cross-bedded and channel filled sandstone, and an upper unit containing interbedded silty mudstone and argillaceous sandstone. Subsequent workers visiting the site identified hummocky cross-stratification, symmetrical wave ripples, combined flow ripples, and rare climbing ripples within the Bulwell Member (Leckie and Potocki, 1998). In addition large soft sediment deformation structures were described (Stott, 1982) within the Garbutt Formation at Scatter River, that indicate high sedimentation rates near a point source.

The previous chapter described the two outcrop exposures along the Kotaneelee River (L8) and Sully Creek (L1). The outcrop exposures consisted entirely of one dominant facies, well laminated, glauconite-rich sandstones, interbedded with highly bioturbated shales (Facies E described in Chapter #3). These outcrops are interpreted as being deposited within a storm dominated, distal lower shoreface environment. While these outcrop exposures are over 100 km northwest of the Maxhamish Lake gas field, their depositional environment coincides with subsurface interpretations. The outcrop

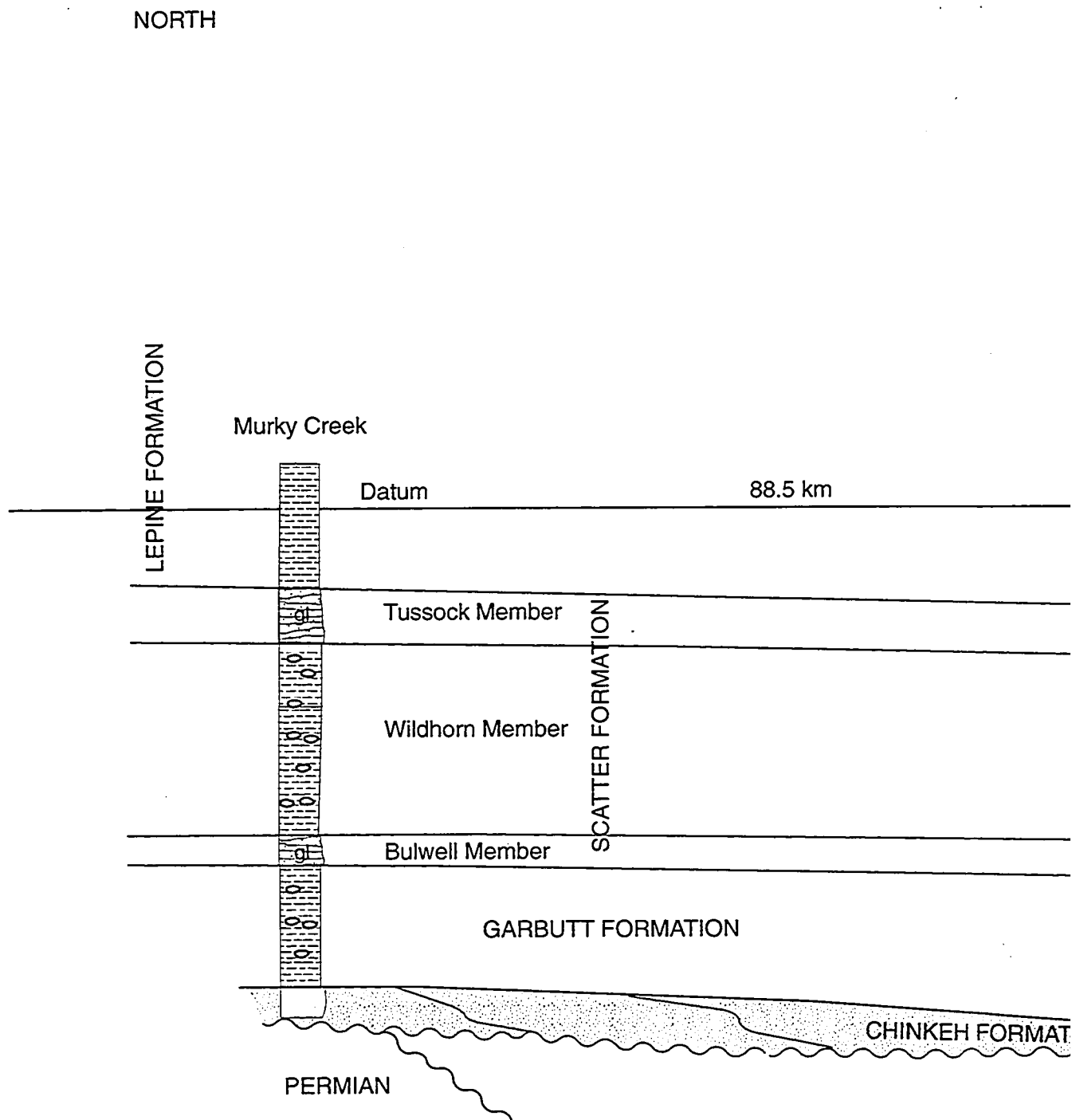
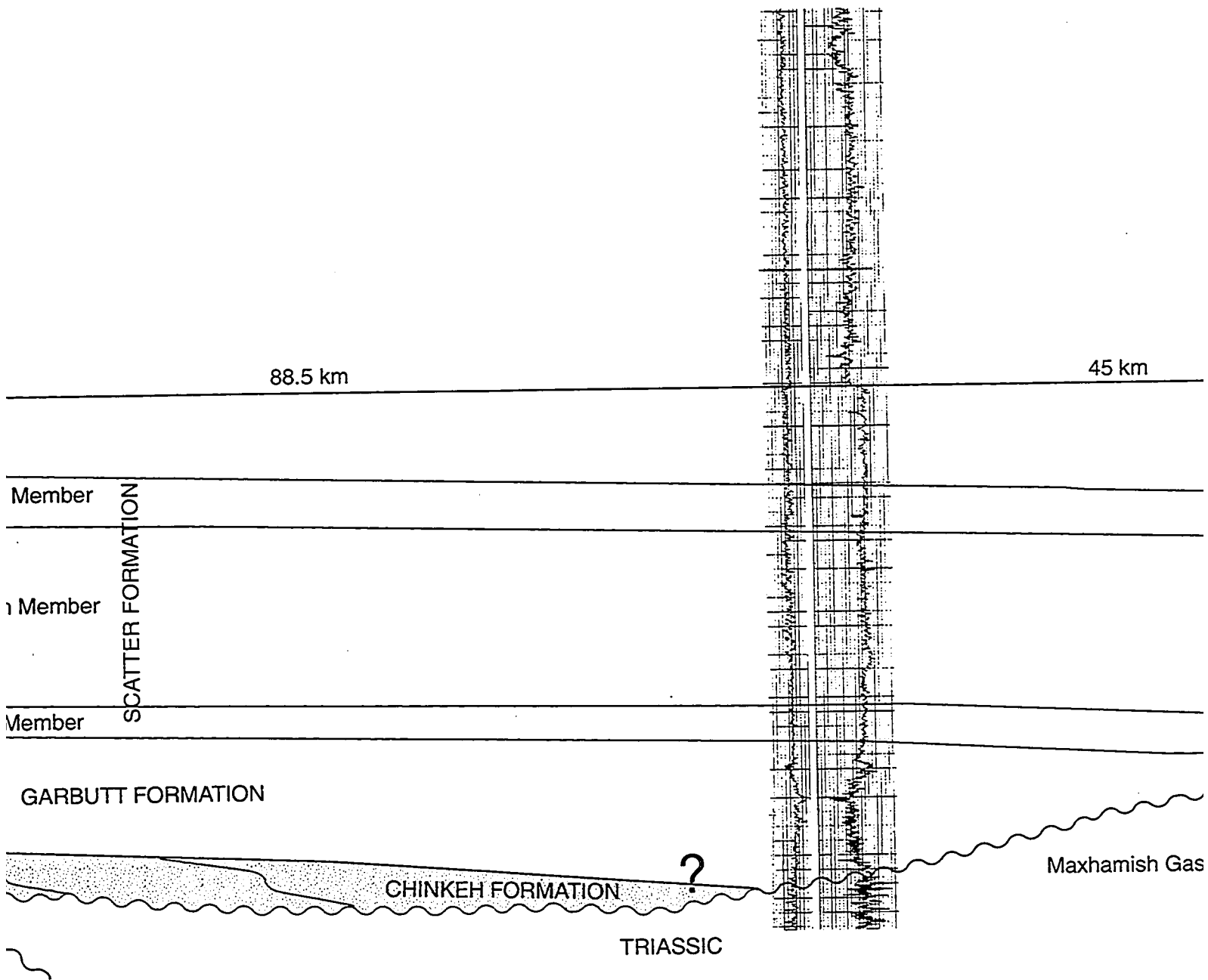


Figure IV-5. North-south cross-section constructed from Murky creek outcrop to the Maxhamish gas field to the south. It overlies Triassic strata before being penetrated by the b-55-E/94-O-13 well. The Bulwell Member is the producing reservoir, not the Chinkeh Formation.

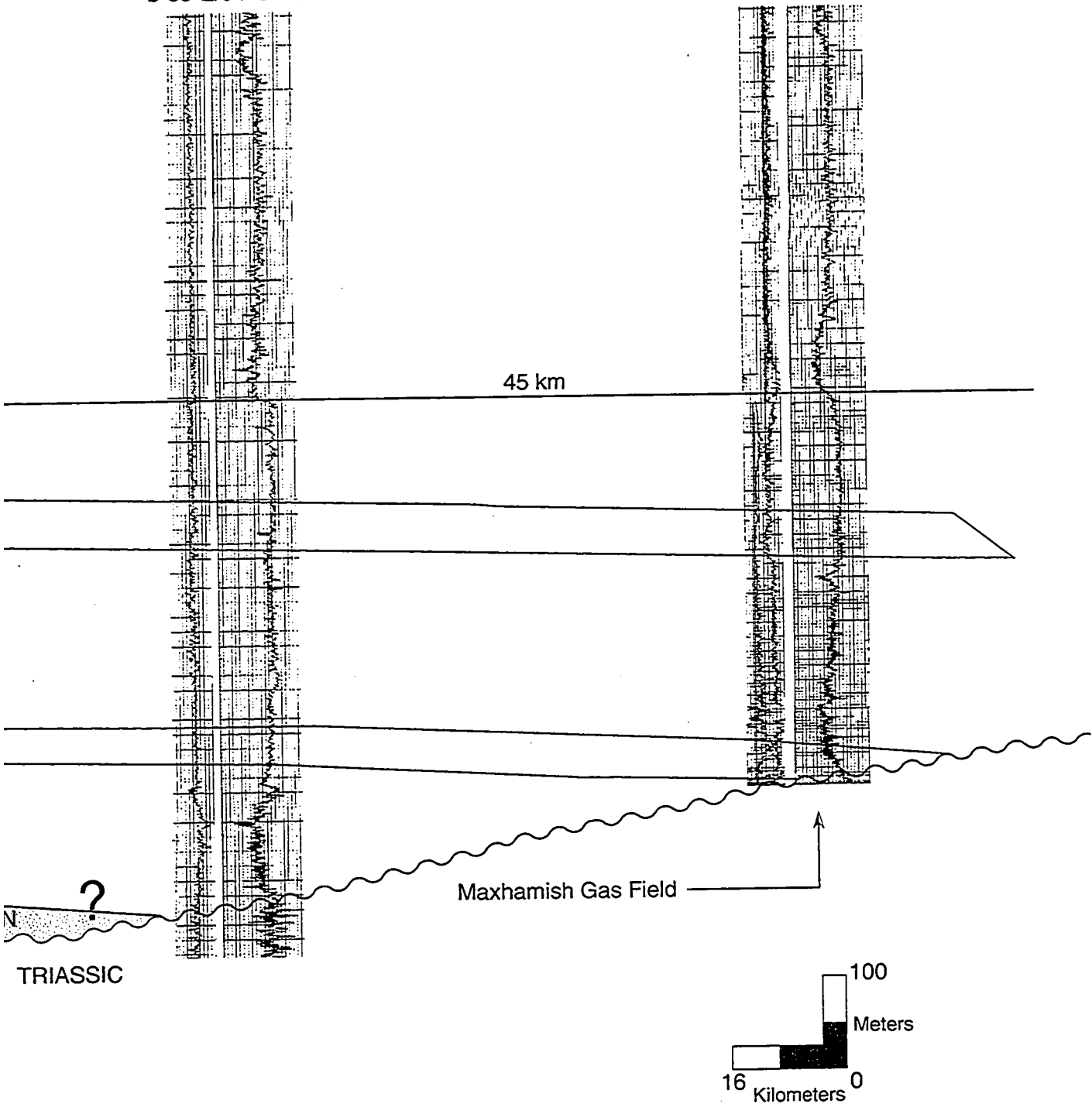
b-55-E/94-O-13



constructed from Murky creek outcrop to the Maxhamish gas field (see Figure IV-3 for location). The Chinkeh Formation is in
ing penetrated by the b-55-E/94-O-13 well. The Bulwell Member of the Scatter Formation onlaps Triassic strata at the Max
Chinkeh Formation.

b-55-E/94-O-13

a-77-D/94-O-11



1 (see Figure IV-3 for location). The Chinkeh Formation is interpreted to prograde from the north towards the south. The Scatter Formation onlaps Triassic strata at the Maxhamish Lake gas field, and the former

exposures are only 30-40 km basinward of the interpreted paleoshoreline along the Bovie fault. Thus, it is reasonable to find distally equivalent facies basinward.

In outcrop exposures of the lowermost member of the Scatter Formation, highly interbedded sandstones and bioturbated shales were noted (Facies E of the previous chapter). These descriptions match those of facies C within subsurface descriptions. Both consist of well laminated, glauconite-rich sandstones that are interbedded by highly bioturbated shales (Figure IV-6). Additionally, both of these facies have been interpreted as being deposited in a distal lower shoreface to offshore transitional zone.

SUMMARY AND CONCLUSIONS

This final chapter describes a sand member of the Scatter Formation and its relation to the Lower Cretaceous Chinkeh Formation. Although there were only two outcrops measured and described, the similarity between the cores taken within the subsurface and the above mentioned outcrop locations are striking. It leaves the author with no other conclusion but to state that the producing sandstones at Maxhamish are part of the lowermost sandstone member of the Scatter Formation, not Chinkeh Formation.

Both the outcrop and subsurface cores are dominated by lower shoreface to offshore sedimentation and traces. Eastward prograding sandstones of the Scatter Formation have been shown to move across the Liard Basin. This progradation was halted at the topographic high of the Bovie Fault scarp (whose orientation is nearly perpendicular to depositional dip of the Scatter Formation). It was against the western edge of the fault scarp that these sandstones became reworked, and formed a linear shoreface where current day production exists (see Chapter #2 for the subsurface descriptions and maps). Figure IV-7 summarizes the the relationship between the Chinkeh and the Bulwell Member of the Scatter Formations within the Liard Basin.

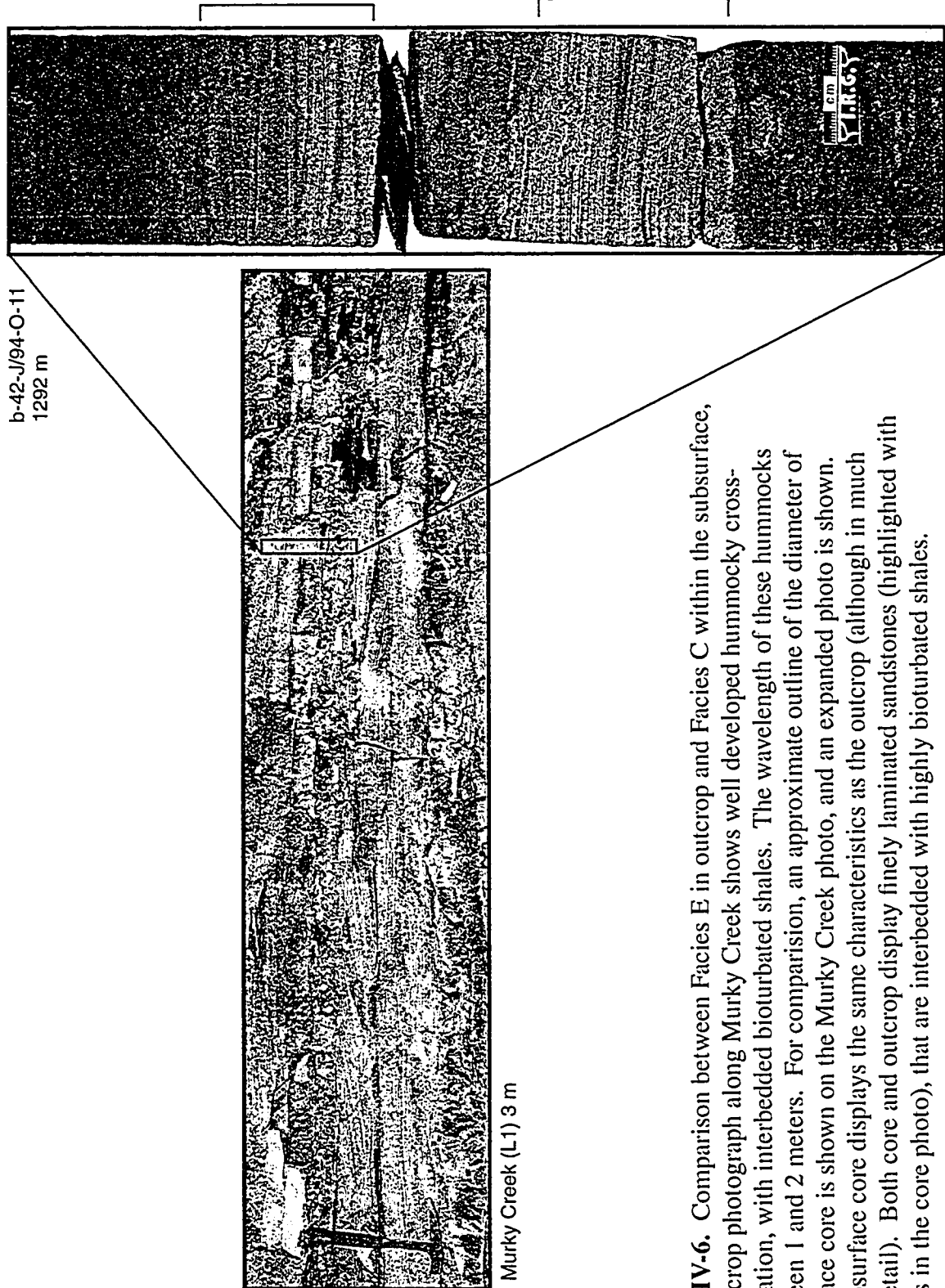


Figure IV-6. Comparison between Facies E in outcrop and Facies C within the subsurface. The outcrop photograph along Murky Creek shows well developed hummocky cross-stratification, with interbedded bioturbated shales. The wavelength of these hummocks is between 1 and 2 meters. For comparison, an approximate outline of the diameter of subsurface core is shown on the Murky Creek photo, and an expanded photo is shown. The subsurface core displays the same characteristics as the outcrop (although in much more detail). Both core and outcrop display finely laminated sandstones (highlighted with brackets in the core photo), that are interbedded with highly bioturbated shales.

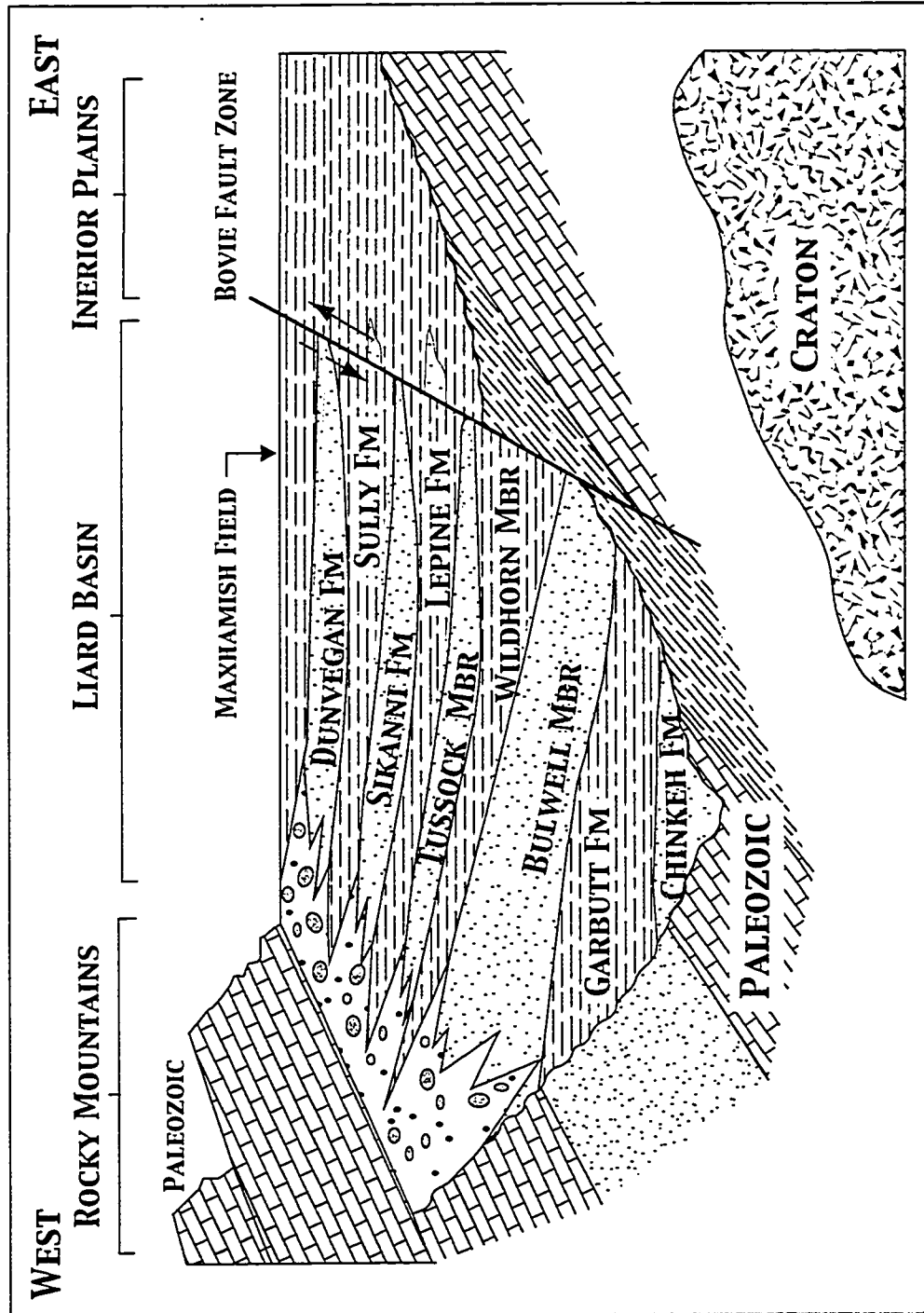


Figure IV-7. Schematic depositional summary within the Liard Basin (modified from Leckie *et al.*, 1991). Eastward prograding sandstones of the Scatter Formation thin dramatically across the Liard Basin. The lowermost Bulwell member, sits directly on Triassic strata adjacent to the Bovie Fault in the vicinity of the Maxhamish Lake gas field. The Chinkah Formation prograded from the North is not present at Maxhamish Lake.

REFERENCES

- Amorosi, A. 1995. Glaucony and sequence stratigraphy: a conceptual framework of distribution in siliciclastic sequences. *Journal of Sedimentary Research*, v. B65, p. 419-425.
- Kindle, E.D. 1944. Geological reconnaissance along Fort Nelson, Liard and Beaver Rivers, northeastern British Columbia and southeastern Yukon; Geological Survey of Canada, Paper 44-16, 19 p.
- Leckie, D.A., and Potocki, D.J. 1998. Sedimentology and petrography of marine shelf sandstones of the Cretaceous, Scatter and Garbutt Formations, Liard Basin, northern Canada. *Bulletin of Canadian Petroleum Geology*, v. 46, p. 30-50.
- Leckie, D.A., Potocki, D.J., and Visser, K. 1991. The Lower Cretaceous Chinkeh Formation: a frontier-type play in the Liard Basin of Western Canada. *American Association of Petroleum Geologists Bulletin*, v. 74, p. 1324-1352.
- Logvinenko, N.V., Volkov, I.I., and Rozanov A.G. 1975. Genesis of the Glauconite in the sediments of the Pacific Ocean. *Lithology and Mineral Resources*, v. 2, p. 145-153.
- Odin, G.S. and Matter, A. 1981. De glauconarium origins. *Sedimentology*, v. 28, p. 70-75.
- Smith, D.G. 1994. Paleogeographic evolution of the Western Canada Foreland Basin. *In: Geological Atlas of the Western Canada Sedimentary Basin*. G.D. Mossop and I. Shetson (comps.). Canadian Society of Petroleum Geologists and Alberta Research Council, p. 277-296.
- Stott, D.F. 1982. Late Cretaceous Fort St. John Group and Upper Cretaceous Dunvegan Formation of the Foothills and Plains of Alberta, Britishcolumbia, District of Mackenzie and Yukon Territory. *Geological Survey of Canada, Bulletin 328*, 124 p.

CHAPTER FIVE: Conclusions

1. Lower Cretaceous sandstones producing at Maxhamish are part of the lowermost Bulwell Member of the Scatter Formation.
2. Regional cross-sections, isopach maps and outcrop descriptions show that source areas for the Bulwell were to the west, along the present day Liard River. These sandstones prograded east and onlap Triassic strata adjacent to the Bovie Fault, where wave and storm processes further reworked the sediments parallel to the Bovie Fault scarp.
3. The Lower Cretaceous Chinkeh was deposited in a restricted, wave dominated basin with point sources to the east and west. This system prograded towards the south into the Liard Basin.
4. Two petroleum exploration plays exists within the Liard Basin:
 - a. A basinward extension of the Maxhamish Lake gas field play, targeting Bulwell Member sandstones (note the Scatter Formation has tested gas to surface).
 - b. The Lowermost Cretaceous Chinkeh Formation in the extreme northern portions of the Liard Basin.

APPENDIX I - Scintillometer Data

[illegible]

Date:	Aug. 11, 1999						Logged By:	Jason/Murray					
Location:	Burnt Timber (L19)						Interval Logged:	0 - 43.5m					
Page 1 of 3													
	Measurement	tc2 - 1sec.						K		U		Th	
	from bottom	Raw data					Ave.	Raw data	Ave.	Raw data	Ave.	Raw data	Ave.
	0.00	113	116	84	92	95	100.0						
	0.50	59	54	58	57	60	58.0						
	1.00	38	34	33	37	29	34.7						
	1.50	96	111	127	120	111	114.0						
	2.00	62	64	57	62	64	62.7						
	2.50	41	48	39	42	42	41.7						
	3.00	38	28	34	35	35	34.7						
	3.50	45	43	39	33	42	41.3						
	4.00	37	35	46	27	41	37.7						
	4.50	56	48	48	43	39	46.3						
	5.00	45	45	42	45	42	44.0						
	5.50	45	51	44	48	54	48.0						
	6.00	42	40	49	49	41	44.0						
	6.50	41	45	38	49	35	41.3						
	7.00	28	35	36	35	38	35.3						
	7.50	33	35	37	37	28	35.0						
	8.00	34	32	36	30	31	32.3						
	8.50	30	35	36	24	31	32.0						
	9.00	33	32	33	35	25	32.7						
	9.50	16	21	22	17	19	19.0						
	10.00	19	22	27	21	29	23.3						
	10.50	16	21	17	20	21	19.3						
	11.00	13	24	17	16	18	17.0						
	11.50	23	25	24	20	20	22.3						
	12.00	22	23	24	25	20	23.0						
	12.50	23	19	22	19	22	21.0						
	13.00	25	23	15	19	21	21.0						
	13.50	22	21	22	22	26	22.0						
	14.00	22	21	22	22	26	22.0						
	14.50	25	30	32	23	27	27.3						
	15.00	30	29	28	27	22	28.0						
	15.50	21	21	24	25	17	22.0						
	16.00	26	29	24	19	24	24.7						
	16.50	31	36	31	27	33	31.7						
	17.00	26	24	21	29	28	26.0						
	17.50	37	36	31	27	33	33.3						
	18.00	48	45	42	47	46	46.0						
	18.50	Covered											
	19.00												
	19.50												
	20.00												
	20.50												
	21.00												

Date:	Aug. 11, 1999					Logged By:	Jason/Murray
Location:	Burnt Timber (L19)					Interval Logged:	0 - 43.5m
Page 2 of 3							
Measurement	tc2 - 1sec.						
from bottom	Raw data						Ave.
	Covered						
21.50							
22.00	49	55	45	44	43		46.0
22.50	54	59	49	60	51		54.7
23.00	41	36	42	42	38		40.3
23.50	33	38	41	34	33		35.0
24.00	33	34	28	35	30		32.3
24.50	36	33	34	31	32		33.0
25.00	31	35	33	31	29		31.7
25.50	33	32	28	34	32		32.3
26.00	27	43	40	29	34		34.3
26.50	57	55	59	62	54		57.0
27.00	54	48	46	52	45		48.7
27.50	48	43	42	47	44		44.7
28.00	43	38	39	39	42		40.0
28.50	38	43	37	31	47		39.3
29.00	26	28	26	23	20		25.0
29.50	26	23	26	23	20		24.0
30.00	18	22	25	33	24		23.7
30.50	33	31	38	35	37		35.0
31.00	25	26	23	29	29		26.7
31.50	38	39	40	45	47		41.3
32.00	38	34	38	42	36		37.3
32.50	32	30	36	33	32		32.3
33.00	21	30	31	35	30		30.3
33.50	39	37	31	32	39		36.0
34.00	44	41	46	36	42		42.3
34.50	52	50	47	44	53		49.7
35.00	56	59	54	53	49		54.3
35.50	Covered						
36.00							
36.50							
37.00							
37.50							
38.00	46	45	48	48	50		47.3
38.50	37	32	30	27	30		30.7
39.00	45	47	53	46	50		47.7
39.50	44	53	46	46	30		45.3
40.00	48	50	54	47	53		50.3
40.50	48	42	44	46	55		46.0
41.00	42	46	43	44	45		44.0
41.50	61	71	73	65	64	4.0	66.7
42.00	72	51	54	64	70	9.0	62.7
42.50	48	36	45	32	43		41.3
43.00	43	41	50	40	43		42.3

[illegible]

[illegible]

Date:	Sept. 3, 1999						Logged By:	Jason/Heinz					
Location:	L 1(Garbutt Shales)						Interval Logged:	0 - 85.0m					
Page 1 of 4													
Measurement	tc2 - 1sec.						K		U		Th		
from bottom	Raw data						Ave.	Raw data	Ave.	Raw data	Ave.	Raw data	Ave.
0.00	51	56	49	65	58	55.0						(Base of	
0.50	63	73	66	64	62	64.3						Scatter Sands)	
1.00	70	74	68	72	69	70.3							
1.50	65	75	67	51	49	61.0							
2.00	61	50	57	71	63	60.3							
2.50	64	79	62	73	64	67.0							
3.00	72	68	69	69	69	69.0							
3.50	60	62	67	73	61	63.3							
4.00	66	61	70	60	65	64.0							
4.50	64	68	62	58	66	64.0							
5.00	70	76	73	75	65	72.7							
5.50	52	52	50	59	60	54.3							
6.00	62	62	65	65	67	64.0							
6.50	68	74	68	73	66	69.7							
7.00	65	66	58	68	64	65.0							
7.50	64	58	65	62	69	63.7							
8.00	67	79	65	78	65	70.0							
8.50	61	64	84	69	70	67.7							
9.00	73	64	80	69	69	70.3							
9.50	75	57	62	69	67	66.0							
10.00	76	69	71	66	66	68.7							
10.50	79	69	62	69	65	67.7							
11.00	63	68	61	69	53	64.0							
11.50	60	64	73	69	65	66.0							
12.00	65	72	75	73	69	71.3							
12.50	64	64	67	63	66	64.7							
13.00	73	67	75	72	62	70.7							
13.50	74	81	81	85	77	79.7							
14.00	67	69	64	66	70	67.3							
14.50	73	63	65	67	69	67.0							
15.00	59	63	56	54	61	58.7							
15.50	60	53	74	61	51	58.0							
16.00	55	66	66	63	54	61.3							
16.50	63	57	65	64	64	63.7							
17.00	66	62	75	64	61	64.0							
17.50	61	59	67	62	73	63.3							
18.00	68	65	63	69	55	65.3							
18.50	60	79	66	64	74	68.0							
19.00	58	57	63	63	69	61.3							
19.50	63	58	62	62	66	62.3							
20.00	56	68	81	58	63	63.0							
20.50	60	52	63	64	56	59.7							
21.00	70	56	56	61	59	58.7							

Date:	Sept. 3, 1999									Logged By:			Jason/Heinz			
Location:	L 1(Garbutt Shales)									Interval Logged:			0 - 85.0m			
Page 2 of 4																
Measurement	tc2 - 1sec.							K			U			Th		
from bottom	Raw data					Ave.	Raw data	Ave.	Raw data	Ave.	Raw data	Ave.	Raw data	Ave.		
21.50	85	58	51	61	61	60.0										
22.00	61	51	62	67	64	62.3										
22.50	58	62	51	55	53	55.3										
23.00	56	54	56	43	52	54.0										
23.50	63	65	66	55	62	63.3										
24.00	52	47	52	56	58	53.3										
24.50	69	66	55	58	51	59.7										
25.00	60	63	64	55	57	60.0										
25.50	65	54	52	60	60	58.0										
26.00	63	72	69	62	54	64.7										
26.50	64	61	62	60	65	62.3										
27.00	73	57	56	56	66	59.7										
27.50	53	61	54	59	64	58.0										
28.00	64	63	80	61	66	64.3										
28.50	71	70	66	69	77	70.0										
29.00	63	71	55	65	70	66.0										
29.50	71	59	59	56	69	62.3										
30.00	55	65	62	64	58	61.3										
30.50	70	68	65	68	64	67.0										
31.00	74	75	69	63	64	69.0										
31.50	63	57	60	77	64	62.3										
32.00	62	59	67	69	66	65.0										
32.50	73	69	71	70	64	70.0										
33.00	70	62	65	67	68	66.7										
33.50	63	58	68	67	65	65.0										
34.00	74	65	60	70	60	65.0										
34.50	67	72	67	80	67	68.7										
35.00	69	70	73	67	67	68.7										
35.50	66	64	75	63	74	68.0										
36.00	60	60	64	73	64	62.7										
36.50	68	56	64	65	71	65.7										
37.00	59	60	54	64	57	58.7										
37.50	70	67	65	65	57	65.7										
38.00	64	65	61	61	63	62.7										
38.50	75	62	74	77	75	74.7										
39.00	66	68	66	68	57	66.7										
39.50	71	73	69	77	67	71.0										
40.00	75	69	71	63	58	67.7										
40.50	57	63	75	69	74	68.7										
41.00	61	68	66	74	65	66.3										
41.50	63	70	64	73	73	69.0										
42.00	61	67	60	62	65	62.7										
42.50	68	70	70	73	67	69.3										
43.00	63	73	68	71	61	67.3										

Date:	Aug. 3, 1999					Logged By:	Jason/Heinz
Location:	L 1(Garbutt Shales)					Interval Logged:	0 - 85.0m

Page 3 of 4

Measurement		tc2 - 1sec.						K			U			Th		
from bottom		Raw data					Ave.	Raw data		Ave.	Raw data		Ave.	Raw data		Ave.
	43.50	57	72	67	61	72	66.7									
	44.00	72	69	68	58	66	67.7									
	44.50	64	46	67	60	61	61.7									
	45.00	59	66	64	63	64	63.7									
	45.50	67	74	68	58	69	68.0									
	46.00	73	73	52	75	60	68.7									
	46.50	72	66	65	73	72	70.0									
	47.00	65	64	77	70	72	69.0									
	47.50	62	65	67	69	51	64.7									
	48.00	60	63	62	75	78	66.7									
	48.50	67	63	69	65	71	67.0									
	49.00	66	62	52	62	65	63.0									
	49.50	71	65	74	61	64	66.7									
	50.00	61	64	70	68	61	64.3									
	50.50	71	68	65	72	62	68.0									
	51.00	62	66	69	67	64	65.7									
	51.50	60	59	62	59	73	60.3									
	52.00	66	72	60	58	63	63.0									
	52.50	73	77	67	64	52	68.0									
	53.00	73	58	63	67	67	65.7									
	53.50	72	67	62	64	62	64.3									
	54.00	66	58	60	73	57	61.3									
	54.50	66	74	57	70	62	66.0									
	55.00	64	54	71	64	65	64.3									
	55.50	64	56	73	62	69	65.0									
	56.00	68	65	64	62	66	65.0									
	56.50	58	66	68	72	62	65.3									
	57.00	61	63	63	65	62	62.7									
	57.50	63	63	66	65	62	63.7									
	58.00	59	60	62	60	64	60.7									
	58.50	68	66	63	68	67	67.0									
	59.00	58	62	50	66	70	62.0									
	59.50	64	56	57	67	64	61.7									
	60.00	67	55	57	61	63	60.3									
	60.50	60	59	62	56	66	60.3									
	61.00	72	66	71	56	68	68.3									
	61.50	66	57	63	54	57	59.0									
	62.00	79	86	70	68	75	74.7									
	62.50	64	93	68	75	76	73.0									
	63.00	63	73	71	67	79	70.3									
	63.50	72	75	82	77	77	76.3									
	64.00	81	70	73	65	82	74.7									
	64.50	76	74	65	76	80	75.3									
	65.00	71	70	76	73	83	73.3									

Date:	Aug. 3, 1999							Logged By:	Jason/Heinz				
Location:	L 1(Garbutt Shales)							Interval Logged:	0 - 85.0m				
Page 4 of 4													
Measurement	tc2 - 1sec.							K		U		Th	
from bottom	Raw data						Ave.	Raw data	Ave.	Raw data	Ave.	Raw data	Ave.
65.50	88	74	80	74	91	80.7							
66.00	71	70	60	69	73	70.0							
66.50	87	85	77	71	81	81.0							
67.00	88	101	83	91	86	88.3							
67.50	89	71	85	77	87	83.0							
68.00	79	72	91	81	88	82.7							
68.50	74	81	81	85	77	79.7							
69.00	75	75	83	76	78	76.3							
69.50	70	75	75	83	75	75.0							
70.00	80	69	89	78	92	82.3							
70.50	87	76	81	85	77	81.0							
71.00	70	74	76	68	70	71.3							
71.50	78	62	73	78	73	74.7							
72.00	75	73	87	85	84	81.3							
72.50	77	72	76	81	74	75.7							
73.00	63	66	71	72	73	69.7							
73.50	69	63	76	64	68	67.0							
74.00	69	77	62	74	75	72.7							
74.50	73	67	76	75	67	71.7							
75.00	65	67	71	69	76	69.0							
75.50	77	61	68	63	67	66.0							
76.00	66	67	67	62	61	65.0							
76.50	69	65	67	70	63	67.0							
77.00	64	64	65	67	75	65.3							
77.50	70	69	63	71	61	67.3							
78.00	69	65	72	75	74	71.7							
78.50	58	56	69	56	59	57.7							
79.00	62	69	67	57	58	62.3							
79.50	55	62	57	61	63	60.0							
80.00	57	55	56	59	46	56.0							
80.50	64	55	57	62	56	58.3							
81.00	70	56	62	63	66	63.7							
81.50	68	49	53	64	54	57.0							
82.00	54	59	50	64	76	59.0							
82.50	66	63	63	55	55	60.3							
83.00	63	57	61	55	55	57.7							
83.50	63	52	66	61	59	61.0							
84.00	57	59	46	50	48	51.7							
84.50	64	93	68	75	76	73.0							
85.00	50	42	46	51	39	46.0							

[illegible]

[illegible]

Date:	Aug. 13, 1999							Logged By:	Jason/Murray										
Location:	Otter Slide (L4)							Interval Logged:	0 - 12.0m										
	Measurement	tc2 - 1sec.					K			U			Th						
	from bottom	Raw data					Ave.	Raw data		Ave.	Raw data		Ave.	Raw data		Ave.			
	0.00	42	33	44	34	35	37.0												
	0.50	72	68	53	62	59	63.0												
	1.00	43	47	48	47	52	47.3												
	1.50	48	45	42	58	39	45.0												
	2.00	35	36	34	36	37	35.7	3	2	1	2.0	3	1	2	2.0	0	0	0	0.0
	2.50	47	41	50	46	43	45.3	3	1	3	2.3	2	3	3	2.7	0	0	2	0.7
	3.00	27	35	33	31	31	31.7	3	3	2	2.7	1	2	1	1.3	1	1	0	0.7
	3.50	40	38	36	45	35	38.0												
	4.00	32	37	37	31	36	35.0												
	4.50	48	37	45	45	43	44.3												
	5.00	36	37	32	36	33	35.0												
	5.50	33	34	35	33	31	33.3												
	6.00	26	37	29	37	39	34.3	2	1	2	1.7								
	6.50	33	34	35	33	31	33.3												
	7.00	34	34	31	30	37	33.0												
	7.50	26	35	30	31	30	30.3												
	8.00	37	26	31	35	40	34.3												
	8.50	35	29	34	31	26	31.3												
	9.00	26	26	27	26	21	26.0												
	9.50	20	21	31	19	21	20.7												
	10.00	20	26	17	23	20	21.0												
	10.50	19	24	21	24	18	21.3												
	11.00	19	17	23	25	16	19.7												
	11.50	20	19	21	20	22	20.3												
	12.00	15	24	18	19	18	18.3												
	12.50																		
	13.00																		
	13.50																		
	14.00																		
	14.50																		
	15.00																		
	15.50																		
	16.00																		
	16.50																		
	17.00																		
	17.50																		
	18.00																		
	18.50																		
	19.00																		
	19.50																		
	20.00																		
	20.50																		
	21.00																		

P/K u/c

Date:	Aug. 5, 1999							Logged By:	Jason/Murray											
Location:	Slip Rock Creek (L14)							Interval Logged:	0 - 19.5m											
	Measurement	tc2 - 1sec.						K			U			Th						
	from bottom	Raw data						Ave.	Raw data		Ave.	Raw data		Ave.	Raw data		Ave.			
	0.00	26	30	34	30	30	30.0	1	2	2	1.7	1	3	4	2.7	1	1	0	0.7	
	0.50	21	28	28	27	25	26.7	1	1	3	1.7	2	2	1	1.7	0	1	0	0.3	
	1.00	25	25	33	28	30	27.7	2	2	2	2.0	2	1	1	1.3	2	0	0	0.7	
	1.50	22	16	22	28	27	23.7	1	2	1	1.3	1	2	5	2.7	0	1	0	0.3	
	2.00	22	24	20	14	20	20.7	1	1	2	1.3	1	1	2	1.3	0	2	0	0.7	
	2.50	26	18	22	17	22	20.7	1	1	3	1.7	2	1	1	1.3	1	0	1	0.7	P/K u/c
	3.00	18	19	16	17	21	18.0	1	1	0	0.7	1	2	1	1.3	0	2	0	0.7	
	3.50	26	27	21	22	29	25.0	4	2	1	2.3	3	0	2	1.7	0	1	1	0.7	
	4.00	19	22	22	18	21	20.7													
	4.50	20	31	28	22	23	24.3													
	5.00	23	25	24	23	23	23.3													
	5.50	26	31	17	19	19	21.3													
	6.00	18	17	17	16	15	16.7													
	6.50	18	16	17	19	13	17.0													
	7.00	14	18	18	19	20	18.3													
	7.50	22	19	18	18	19	18.7													
	8.00	20	20	20	19	17	19.7													
	8.50	19	19	19	13	20	19.0													
	9.00	16	16	12	13	13	14.0													
	9.50	14	17	10	10	14	12.7													
	10.00	20	20	15	13	16	17.0													
	10.50	15	19	18	15	16	16.3													
	11.00	21	15	15	13	21	17.0													
	11.50	14	16	12	21	21	17.0													
	12.00	15	10	13	15	15	14.3													
	12.50	17	13	13	11	13	13.0													
	13.00	16	11	15	16	12	14.3													
	13.50	14	20	14	17	16	15.7													
	14.00	18	20	15	10	16	16.3													
	14.50	18	17	17	20	18	17.7													
	15.00	20	14	22	22	16	19.3													
	15.50	20	15	17	22	17	18.0													
	16.00	17	20	13	12	13	14.3													
	16.50	17	22	21	16	13	18.0													
	17.00	23	32	28	23	20	24.7	2	3	2	2.3	1	2	2	1.7	1	1	0	0.7	
	17.50	69	64	65	55	65	64.7	3	5	5	4.3	3	4	3	3.3	2	1	1	1.3	
	18.00	27	20	23	26	29	25.3	2	2	2	2.0	1	1	3	1.7	1	0	0	0.3	
	18.50	36	46	44	45	35	41.7	5	3	3	3.7	3	2	2	2.3	1	0	0	0.3	Chin./Garbutt
	19.00	45	49	53	55	48	50.0	3	3	4	3.3	3	3	4	3.3	2	0	1	1.0	
	19.50	62	56	67	46	60	59.3	3	5	6	4.7	5	3	4	4.0	2	0	1	1.0	
	20.00																			
	20.50																			
	21.00																			

P/K u/c

Chin./Garbutt

Date:	Aug. 10, 1999							Logged By:	Jason/Murray								
Location:	Tika Creek (L6)							Interval Logged:	0 - 11.0m								
	Measurement	tc2 - 1sec.						K			U			Th			
	from bottom	Raw data					Ave.	Raw data	Ave.	Raw data	Ave.	Raw data	Ave.				
	0.00	50	58	53	60	56	55.7										
	0.50	66	56	57	56	66	59.7										
	1.00	36	46	40	38	46	41.3										
	1.50	49	51	58	47	44	49.0										
	2.00	45	56	53	50	41	49.3										
	2.50	49	42	43	48	43	44.7										
	3.00	67	64	68	64	58	65.0										
	3.50	51	41	57	44	55	50.0										
	4.00	29	26	37	32	33	31.3										
	4.50	27	35	29	27	25	27.7										
	5.00	34	35	29	27	25	30.0										
	5.50	24	22	20	21	24	22.3										
	6.00	22	21	26	25	29	24.3										
	6.50	30	29	26	26	30	28.3										
	7.00	28	25	30	26	21	26.3										
	7.50	24	21	32	24	22	23.3										
	8.00	20	25	21	24	18	21.7										
	8.50	19	22	20	22	16	20.3										
	9.00	44	42	37	43	35	40.7										
	9.50	31	39	38	42	36	37.7										
	10.00	30	32	27	31	33	31.0										
	10.50	26	31	35	31	24	29.3										
	11.00	30	36	24	24	33	29.0										
	11.50																
	12.00																
	12.50																
	13.00																
	13.50																
	14.00																
	14.50																
	15.00																
	15.50																
	16.00																
	16.50																
	17.00																
	17.50																
	18.00																
	18.50																
	19.00																
	19.50																
	20.00																
	20.50																
	21.00																

Date:	Aug. 17, 1999					Logged By:	Jason/Murray									
Location:	Kotaneelee River (L8)					Interval Logged:	0 - 12.0m									
	Measurement	tc2 - 1sec.						K			U			Th		
	from bottom	Raw data					Ave.	Raw data	Ave.	Raw data	Ave.	Raw data	Ave.			
	0.00	44	51	46	39	54	47.0									
	0.50	43	48	49	41	53	46.7									
	1.00	44	34	33	41	36	37.0									
	1.50	43	41	33	45	43	42.3									
	2.00	35	33	35	33	33	33.7									
	2.50	44	37	37	43	42	40.7									
	3.00	42	53	45	48	38	45.0									
	3.50	30	39	37	33	44	36.3									
	4.00	38	36	40	47	35	38.0									
	4.50	43	31	35	32	40	35.7									
	5.00	32	41	44	37	50	40.7									
	5.50	48	48	42	36	43	44.3									
	6.00	41	41	39	37	36	39.0									
	6.50	41	30	34	38	39	37.0									
	7.00	44	44	45	46	44	44.3									
	7.50	37	43	40	36	41	39.3									
	8.00	44	39	33	34	34	35.7									
	8.50	51	56	46	53	56	53.3									
	9.00	62	64	53	62	66	62.7									
	9.50	62	58	60	76	57	60.0									
	10.00	58	52	17	23	20	31.7									
	10.50	60	58	56	51	64	58.0									
	11.00	60	54	59	57	58	58.0									
	11.50	57	52	53	55	58	55.0									
	12.00	56	43	49	42	54	48.7									
	12.50															
	13.00															
	13.50															
	14.00															
	14.50															
	15.00															
	15.50															
	16.00															
	16.50															
	17.00															
	17.50															
	18.00															
	18.50															
	19.00															
	19.50															
	20.00															
	20.50															
	21.00															